Bull Trout Performance During Passage Over a Horizontal Flat Plate Screen

Final Report

20 July 2002

Larval Fish Laboratory Contribution Number 128

Bull Trout Performance in a Horizontal Flat Plate Screen

Final Report to:

Brent Mefford and Kathy Frizell

U. S. Bureau of Reclamation
Water Resources Research Laboratory Group
Denver, Colorado 80225-0007

Prepared by:

Dr. Daniel W. Beyers, and Dr. Kevin R. Bestgen

Larval Fish Laboratory
Department of Fishery and Wildlife Biology
Colorado State University, Fort Collins, CO 80523
T: (970) 491-5475; F: (970) 491-5091; E: danb@lamar.colostate.edu
T: (970) 491-1848; F: (970) 491-5091; E: kbestgen@lamar.colostate.edu

20 July 2002

Contribution 123, Larval Fish Laboratory, Department of Fishery and Wildlife Biology,
Colorado State University, Fort Collins, CO 80523, U.S.A.

Acknowledgments

We gratefully acknowledge the contributions of other individuals who provided assistance in this investigation. Kathy Frizell, Brent Mefford, and Bill Baca facilitated our use of testing facilities at the Water Resources Research Laboratory. Don Edsall (Creston National Fish Hatchery, Kalispell, Montana) provided bull trout for this investigation and also offered advice about culture techniques. Nick Bezzerides, Diane Miller, Emily Plampin, Sean Seal, Tasha Sorensen, and Cameron Walford provided assistance in the laboratory. This study was funded by the U. S. Bureau of Reclamation.

Table of Contents

Acknowledgments ii

List of Tables iv

List of Figures v

Executive Summary vi

Introduction 1

Materials and Methods 3

Results 12

Discussion 28

References 30

List of Tables

Table 1. Summary of discharge (m3/sec) and velocity (m/sec) conditions over a horizontal flat plate screen at two sweeping velocities……..…5

Table 2. Summary of bull trout total lengths (mm) for three life stages studied.....7

Table 3. Summary of elapsed times (s) for passage of individual bull trout over a horizontal flat plate screen at two sweeping velocities.....15

Table 4. Summary of elapsed times (s) for passage of batches of 10 bull trout over a horizontal flat plate screen at two sweeping velocities.....16

Table 5. Summary of condition of 25 28-mm individual bull trout assessed after handling (C) or after passage over a horizontal flat plate screen (T) at a sweeping velocity of 1.2 m/sec 17

Table 6. Summary of condition of 25 28-mm individual bull trout assessed after handling (C) or after passage over a horizontal flat plate screen (T) at a sweeping velocity of 0.6 m/sec 18

Table 7. Summary of condition of 25 37-mm individual bull trout assessed after handling (C) or after passage over a horizontal flat plate screen (T) at a sweeping velocity of 1.2 m/sec 19

Table 8. Summary of condition of 25 37-mm individual bull trout assessed after handling (C) or after passage over a horizontal flat plate screen (T) at a sweeping velocity of 0.6 m/sec 20

Table 9. Summary of condition of 25 58-mm individual bull trout assessed after handling (C) or after passage over a horizontal flat plate screen (T) at a sweeping velocity of 1.2 m/sec 21

Table 10. Summary of condition of 25 58-mm individual bull trout assessed after handling (C) or after passage over a horizontal flat plate screen (T) at a sweeping velocity of 0.6 m/sec 22

Table 11. Summary of 24-h survival for batches of 10 bull trout after passage over a horizontal flat plate screen at two sweeping velocities.....26

Table 12. Summary of 96-h survival for batches of 10 bull trout after passage over a horizontal flat plate screen at two sweeping velocities.....27

List of Figures

Figure 1. Picture and plan view of horizontal flat plate screen testing area.....2

Figure 2. General areas (shaded) on a horizontal flat plate screen occupied by 58-mm bull trout for long periods of time.....13

Executive Summary

This investigation was conducted to the describe effects of passage of bull trout Salvelinus confluentus over a horizontal flat plate screen. Experimental releases were conducted with three sizes of bull trout that averaged 28, 37, and 58 mm total length (TL). Fish were released individually and in batches to: (1) describe general behavior near and on the screen; (2) estimate physical condition and survival of fish after passage; and (3) estimate entrainment and impingement rates.

Consistent negative effects from passage of bull trout over a horizontal flat plate screen were not observed. Potential entrainment was ≤ 3.5% for 28-mm fish, and was never observed for larger fish. Impingement never occurred. Passage times increased with fish size and ranged from 4 sec to more than 10 min. Physical damage to eyes, fins, and integument was either rare (eyes) or less frequent in fish that passed over the screen than in control fish. Fish that passed over the screen did contact the bottom more frequently than control fish, but no immediate mortality occurred from screen passage. Survival at 24 h was ≤ 1.5% lower for fish that passed over the screen compared to controls. At 96 h after passage, survival was reduced, but was not consistently lower for fish that passed over the screen compared to controls. Thus, physical effects of screen passage were at, or near the level of background effects induced by fish culture, handling, transport, and testing.

Water depth and orientation of bull trout changed with fish size and age despite the use of a standardized release methodology. Larger fish were more frequently observed near the bottom and more frequently oriented upstream than smaller fish. The tendency to occupy deeper water

increased the likelihood that fish contacted the horizontal flat plate screen. It also increased the likelihood that fish discovered attractive hydraulic properties of the screen. We observed several 58-mm fish that appeared to be maintaining position by using downward pressure generated by water approaching the screen. This behavior was the main factor responsible for increased passage time for larger fish. Thus, we did observe that certain hydraulic conditions of the horizontal flat plate screen used in this investigation attracted fish and delayed their movement over the screen.

Introduction

Bull trout Salvelinus confluentus is an endangered char that occurs in cool-water streams in northwestern North America (Lee et al. 1980). Presence of water diversion structures for irrigation in that area have the potential to influence movement and survival of bull trout. Horizontal flat plate screens are potentially useful to reduce negative effects of diversion structures on bull trout because rate of horizontal movement of water across the screen (sweeping velocity) is higher than the rate of movement of water through the screen (approach velocity). This characteristic enhances self cleaning and reduces the likelihood of impingement and entrainment of organisms. An evaluation of hydraulic characteristics and operation of horizontal flat plate screens was conducted with a working model constructed at the U.S. Bureau of Reclamation, Water Resources Research Laboratory, Denver, Colorado (Figure 1). A detailed description of the model is available (Frizell and Mefford 2001) and it is useful for establishing design criteria for horizontal flat plate screens deployed in the field.

Another important aspect of development of design criteria for horizontal flat plate screens is an evaluation of potential effects on resident fish. During passage through screened structures, fish may become impinged on the screen or entrained into diversions. Fish may also avoid or be attracted to physical or hydraulic characteristics of screened structures which can influence natural movement and migration. To investigate the potential effects of passage on

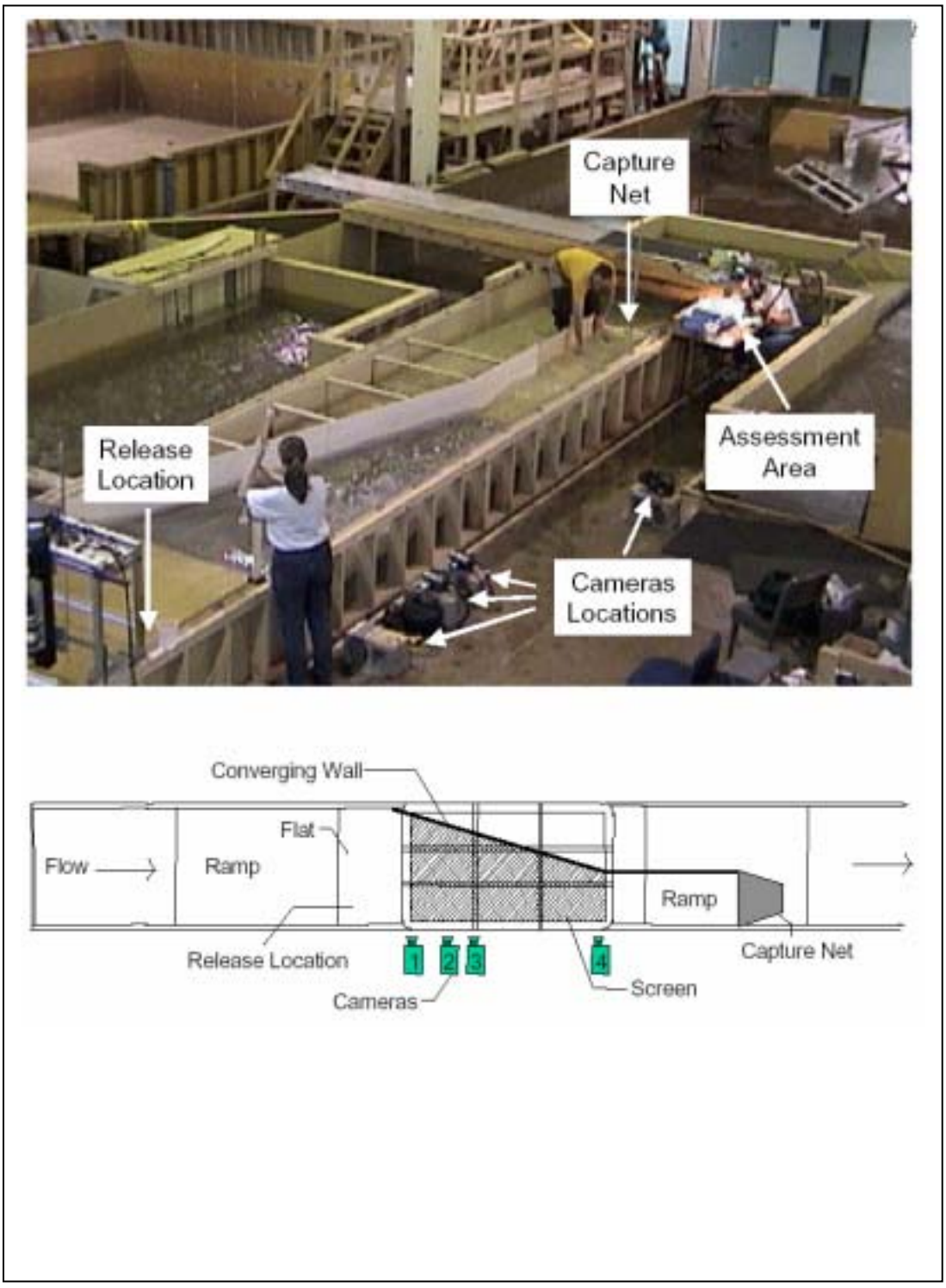

Figure 1. Picture and plan view of horizontal flat plate screen testing area.

bull trout, we conducted experimental releases with three early life stages of bull trout using the model horizontal flat plate screen at the Water Resources Research Laboratory. Fish were released individually and in batches to address three study objectives: (1) describe general behavior of fish near and on the screen; (2) estimate physical condition and survival of fish after passage over the screen; and (3) estimate entrainment and impingement rates of bull trout. Results describe bull trout behavior and effects of passage at two sweeping velocities.

Materials and Methods

Horizontal Flat Plate Screen and Testing Characteristics

The horizontal flat plate screen was 1.8×3.6-m-long with 2.4-mm (3/32 inch) perforations. The screen had a vertical 15° converging wall on one side and a vertical transparent plexiglass wall on the other side (Figure 1). The bypass entrance was 0.744-m-wide. Water for the screen was recirculated by a pump from an underground reservoir. Discharge rates were manipulated to produce the two sweeping velocities studied in this investigation: 0.6 m/s (2 ft/s) or 1.2 m/s (4 ft/s). Flow conditions over the screen were subcritical at 0.6 m/s and supercritical at 1.2 m/s. Water depth under both conditions was 13 cm. Descriptions of corresponding approach velocities and testing conditions are summarized in Table 1 and detailed elsewhere (Frizell and Mefford 2001).

Fish movements during passage over the screen were recorded using four video cameras (Figure 1). Cameras 1, 2, and 3 were positioned sequentially at the upstream end of the screen and camera 4 was positioned at the downstream end of the screen. Collectively, video cameras recorded fish passage over one-half (1.8 m) of the screen.

Fish were introduced onto the screen using release tubes constructed of 19- or 38-mm (inside diameter) PVC pipe. The 19-mm diameter release tube was used for the smallest life stage studied; the 38-mm, for the other two life stages. In preparation for a release, fish and holding water were transferred to a release tube and a rubber stopper prevented fish from escaping. The release tube was positioned on the floor of the screen structure, at the beginning of the flat, 1.2 m upstream of the screen and 0.3 m from the plexiglass wall. A release was accomplished by removing the rubber stopper and opening a valve that allowed water and fish to exit the tube. The release tube was designed so that fish emerged from the screen near the bottom of the water column, oriented in an upstream direction.

After a release, fish were recaptured using a drift net mounted 2.4 m downstream of the screen. Dimensions of the 363-µm mesh net were 40 × 80 × 86-cm long. The net sampled the entire bypass discharge from the screen. Following capture, the cod end of the net was opened and fish were rinsed into a pan for assessment.

Fish Culture, Acclimation, and Handling

Bull trout embryos were obtained from Creston National Fish Hatchery (Kalispell, Montana) and cultured at the Aquatic Research Laboratory, Colorado State University. Embryos were maintained at 4 to 6°C in a Heath incubator until hatching was complete. After hatching, larvae were transferred to fiberglass culture troughs for rearing at a water temperature of 10°C. Fish were fed a commercially prepared diet (BioDiet, Bio-Oregon, Inc., Warrenton, OR).

Table 1. Summary of discharge (m3/sec) and velocity (m/sec) conditions over a horizontal flat plate screen at two sweeping velocities.

Condition	Q_c	Q_d	Q_b	V_s	V_a	Depth (m)
0.6 m/sec treatment	0.19	0.11	0.08	0.6	0.15	0.13
0.6 m/sec control	0.06	0	0.06	0.6	NA	0.13
1.2 m/sec treatment	0.32	0.2	0.12	1.2	0.15	0.13
1.2 m/sec control	0.12	0	0.12	1.2	NA	0.13

NA = not applicable.
Q_c; channel discharge; Q_d; diversion discharge; Q_b; bypass discharge; V_s; sweeping velocity; V_a; approach velocity.

In preparation for testing at the Water Resources Research Laboratory, culture water temperature was increased to 14°C 10 days before the first fish release trials were conducted so that fish were acclimated to testing conditions. Throughout the investigation, water temperature at the Water Resources Research Laboratory ranged from 13.5 to 16.5°C and culture temperatures were manipulated to match test temperatures within ± 1°C.

During thermal acclimation, fish were also exposed to a constant water current by directing the flow of water into the culture trough. This provided a range of velocities within the culture trough and allowed fish to select preferred conditions. By positioning the automatic feeder near the water inlet, fish were forced to encounter relatively high velocities.

On the day of testing, 10 to 25 fish were placed in 4-L resealable bags containing about 1.5 L of water and oxygen-filled head space. Bags were transported to the Water Resources Research Laboratory and held in insulated coolers until selected for a test. Dissolved oxygen concentrations in bags were checked occasionally and were always > 6.0 mg/L.

Three bull trout life stages were investigated including: (1) swim-up larvae approximately the same age and size of young bull trout at the time they emerge from spawning redds in a stream, (2) a later larval stage, and (3) juveniles. Bull trout in each group were 67, 108, and 145 day old (after hatching) and had average total lengths of 28, 37, and 58 mm, respectively (Table 2).

Table 2. Summary of bull trout total lengths (mm) for three life stages studied.

Life Stage	Mean	Standard Error	Minimum	Maximum	*n*
First	27.8	0.204	23.9	32.2	98
Second	36.9	0.351	28.1	46.5	100
Third	58.0	0.409	49.8	69.1	100

Individual Releases

Releases of individual fish were used to estimate the effects of passage on physical condition, passage times, and impingement and entrainment. Twenty-five fish of each life stage were released at both sweeping velocities. Each fish was independently released and captured. Passage times were measured starting with release and ending when fish crossed the downstream edge of the screen. A maximum of 120 s was allowed for fish to exit the screen voluntarily. Fish that remained on the screen for longer than 120 sec were swept into the current and into the capture net by observers. Following capture, each fish was rinsed into a pan, anesthetized (200 mg/L tricaine methanesulfonate), and physical condition was assessed using a binocular microscope at 10X magnification. An *a priori* set of criteria were used to consistently evaluate evidence of physical damage to fish from passage. Measurements collected, and criteria used for each individual were: (1) elapsed time to pass over the screen; (2) survival: yes, no; (3) total length; (4) eyes: normal, abraded, exophthalmic, hemorrhagic, missing; (5) caudal, dorsal, right and left pectoral fins: normal, frayed, trace fin split (≤10%), fin split (.10%), broken fin rays, (one or more rays disrupted into fragments attached by intervening fin tissue), missing; (6) integument: normal, abraded, bruised, cut; and (7) scales: normal, scattered descaling (<20% per side of fish), severe descaling. After assessment, each fish was preserved in 10% formalin.

Because physical damage may arise from handling, transport, release, and capture, a control group of fish was similarly assessed. Control conditions were created by installing a transparent plexiglass sheet over the screen and releasing fish at both sweeping velocities using identical methodology. The plexiglass did not change the appearance of the screen which may

be important for fish orientation but did remove turbulence and approach velocity effects due to the operation of the screen. Control batches allowed the effect of screen passage on survival to be separated from effects caused by other sources.

Batch Releases

Batch releases of fish were used to estimate immediate, 24-, and 96-h survival rates after passage, batch passage times, and potential for impingement and entrainment. Twenty batch releases of 10 fish from each life stage were studied at both sweeping velocities. Batches were released and captured using the same methods described for individuals. Following capture fish were rinsed into a pan where the number of survivors was counted. The live fish were placed into 4-L resealable bags containing about 1.5 L of water and oxygen-filled head space, and transported in insulated coolers to the Aquatic Research Laboratory at Colorado State University. Bags containing fish were transferred to a water bath for 1 hour to allow acclimation to culture conditions (14°C). Batches of fish were then released into separate flow-through aquaria and survival was monitored daily for 96 h. Aquaria were 20 × 40 × 25 cm high, and water depth was about 15 cm. Water temperature was 14°C. Fish were fed once daily during the monitoring period. Cool-white fluorescent lamps were the only source of illumination (530 lx), and a 12:12-h light:dark photoperiod was maintained.

Control batches of fish were also used to assess effects of handling, transport, release, and capture on survival. Control batches were treated similarly to fish released over the screen, except they were released at the downstream end of the screen about 2.4 m from the capture net.

Control fish were not removed from the net until an amount of time equal to the average time required for fish in treatment batches to traverse the screen had elapsed. Control batches allowed the effect of screen passage on survival to be separated from effects caused by other sources.

Video Interpretation

Video recordings of movement of individually release fish were interpreted to quantify several responses including: number of times a fish contacted the screen over the 1.8-m camera observation area; orientation (upstream or downstream) at cameras 1 and 4; and depth in the water column (bottom third, middle third, or top third) at cameras 1 and 4. Fish that were on the surface were difficult to detect during video interpretation, but because fish in the middle and bottom third were easily detected, a depth classification of "top third" was given when a fish was not observed.

Descriptive and Statistical Analysis

In general, descriptive statistics were calculated for the endpoints investigated and summary tables were constructed to facilitate inspection of the data. Because of the number of fins and categories involved in fin assessment, the data were re-classified as normal or non-normal, then the frequency of occurrence of fish with four, three, two, one or no normal fins was calculated.

Survival data were analyzed using the Genmod procedure (options link = logit, dist = binomial, and dscale; SAS Institute 1993). The procedure estimatee mean survival and

associated 95% confidence intervals. In several cases, confidence intervals could not be estimated because no mortality was observed in most or all of the replicates. Lack of variation in treatments precluded useful statistical comparisons. Consequently, data were analyzed by inspection. It should be noted that the responses of the same batches of fish were used to estimate survival at 24 and 96 h. Because the same batches were used, there is a lack of independence between 24- and 96-h estimates (e.g., a replicate with 80% survival at 24 h can only have ≤ 80% survival at 96 h). We advocate that because little is known about effects of horizontal flat plate screens on bull trout, this violation of statistical assumptions is relatively unimportant and that the analysis provides valuable insight about the pattern of mortality that may occur after passage.

Results

Entrainment

No incidences of entrainment of fish through the screen were observed for 37- or 58-mm fish. Reliable estimates of entrainment for 28-mm fish were not obtained because unrecovered fish may have been lost via entrainment, through seams in the screen structure, or escaped the capture net. Data suggested that if entrainment occurred, the rate was low because 99.5% of control fish and 96.0% of treatment fish were recovered at the 1.2 m/s sweeping velocity, and 99.0% of control fish and 98% of treatment fish were recovered at the 0.6 m/s sweeping velocity. Thus, potential entrainment was not greater than 3.5% (maximum difference between recovery rates of control and treatment fish) for any of the conditions studied.

Impingement

No incidences of impingement of fish on the screen were observed for fish in the 28- or 37-mm size groups. Some fish in the 58-mm size group were observed on the screen, but observations suggested that the fish were maintaining desired positions by using downward pressure generated by water approaching the screen (Figure 2). Behaviors that suggested fish were attracted to these areas and were not involuntarily impinged included: (1) demonstration of volitional movement (upstream and downstream) at these locations; (2) demonstration of ability to control body position on the screen; and (3) returning to the locations after being disturbed by an observer. Preliminary observations showed that some fish continued this behavior for at least 10 min.

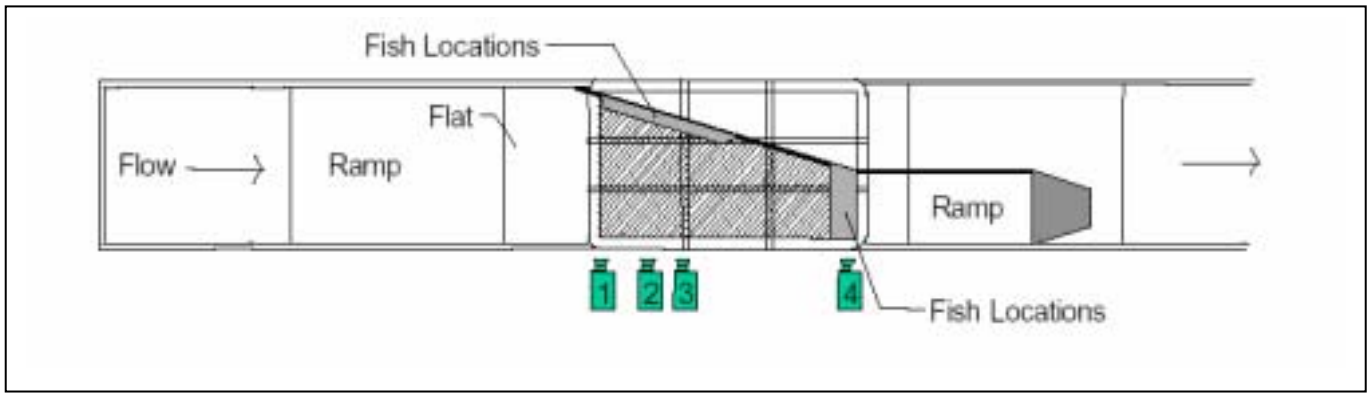

Figure 2. General areas (shaded) on a horizontal flat plate screen occupied by 58-mm bull trout for long periods of time. Downward pressure generated by the approach velocity of water passing through the screen in these areas allowed fish to hold position with relatively little swimming activity.

Passage Times

Average passage times for individual fish ranged from 4 to 17 sec at 1.2 m/sec sweeping velocity and 10 to 61 sec at 0.6 m/sec sweeping velocity (Table 3). Passage times increased with fish size at both sweeping velocities and were generally longer for control fish than for treatment fish.

Average batch passage times ranged from 7 to 45 sec at 1.2 m/sec sweeping velocity and 23 to 120 sec at 0.6 m/sec sweeping velocity (Table 4). Passage times generally increased with fish size at both sweeping velocities. At least one fish in every batch released for the 58-mm, 0.6 m/sec treatment remained over the screen for the maximum time allowed of 120 sec.

Physical Condition After Passage

In general, physical condition of bull trout did not appear to be affected by passage over the screen (Tables 5-10). The effect of passage on condition and coverage of scales was not assessed because the first two life stages did not have scales and very small scales were patchily distributed over the surface of fish in the 58-mm group. Other characteristics were measured as proposed.

Eyes - Only one occurrence of a non-normal (abraded) eye was observed out of 600 fish examined. The single occurrence was for a 58-mm fish (Table 9). Because eye damage was rare, and it was not observed in smaller fish, it is unlikely that the abrasion was caused by screen passage.

Table 3. Summary of elapsed times (sec) for passage of individual bull trout over a horizontal flat plate screen at two sweeping velocities.

Sweeping Velocity = 1.2 m/sec

Treatment	Mean	Standard Error	Minimum	Maximum	*n*
		Life Stage (28 mm)			
Control	10	1.1	5	29	22
Treatment	4	0.2	3	5	22
		Life Stage (37 mm)			
Control	10	0.8	29	46	25
Treatment	5	0.2	4	7.2	20
		Life Stage (58 mm)			
Control	17	2.3	5	54	25
Treatment	10	0.7	5	22	25

Sweeping Velocity = 0.6 m/sec

Treatment	Mean	Standard Error	Minimum	Maximum[a]	*n*
		Life Stage (28 mm)			
Control	13	1.1	5	27	25
Treatment	10	1.0	5	28	23
		Life Stage (37 mm)			
Control	20	1.8	11	54	25
Treatment	12	0.8	7	23	25
		Life Stage (58 mm)			
Control	61	10	9	120	25
Treatment	50	8.0	14	120	25

[a]120 sec was the maximum time allowed.

Table 4. Summary of elapsed times (sec) for passage of batches of 10 bull trout over a horizontal flat plate screen at two sweeping velocities.

Sweeping Velocity = 1.2 m/sec

Life Stage (mm)	Mean	Standard Error	Minimum	Maximum[a]	*n*[b]
28	7	0.2	6	9	20
37	7	0.4	4	12	20
58	45	6.2	20	120	20

Sweeping Velocity = 0.6 m/sec

Life Stage (mm)	Mean	Standard Error	Minimum	Maximum[a]	*n*[b]
28	26	1.4	18	47	20
37	23	2.0	17	56	20
58	120	0	120	120	20

[a]120 sec was the maximum time allowed.
[b]*n* = 20 is equivalent to 20 batches of 10 fish.

Table 5. Summary of condition of 25 28-mm individual bull trout assessed after handling (C) or after passage over a horizontal flat plate screen (T) at a sweeping velocity of 1.2 m/sec.

		Frequency		Percent		Cumulative Percent	
Characteristic	Condition	C	T	C	T	C	T
Eyes	Normal	25	25	100	100	100	100
Finsa	4 of 4 normal	2	6	8	24	8	24
	3 of 4 normal	9	5	36	20	44	44
	2 of 4 normal	8	8	32	32	76	76
	1 of 4 normal	4	6	16	24	92	100
	0 of 4 normal	2		8		100	
Integument	Normal	24	25	96	100	96	100
	Abrasion	1		4		100	
	Bruise						
	Cut						
Total contactsb	0	91	92	91	92	91	92
	1	8	8	8	8	99	100
	2	1		1		100	
	3						
	4						
	5						
Depth, camera 1	Bottom third	14	12	56	48	56	48
	Middle third	0	5	0	20	56	68
	Top third	11	8	44	32	100	100
Depth, camera 4	Bottom third	8	9	32	36	32	36
	Middle third	0	2	0	8	32	44
	Top third	17	14	68	56	100	100
Orientation, camera 1	Upstream	6	8	43	42	43	42
	Downstream	8	11	57	58	100	100
Orientation, camera 4	Upstream	11	7	79	54	79	54
	Downstream	3	6	21	46	100	100

[a]Number of fins assessed as normal; fins were caudal, dorsal, and right and left pectoral.
[b]A total of 100 observations were possible because four cameras were used for all 25 fish released. Collectively, video cameras recorded potential contacts over 1.8 m of the horizontal flat plate screen.

Table 6. Summary of condition of 25 28-mm individual bull trout assessed after handling C) or after passage over a horizontal flat plate screen (T) at a sweeping velocity of 0.6 m/sec.

		Frequency		Percent		Cumulative Percent	
Characteristic	Condition	C	T	C	T	C	T
Eyes	Normal	25	25	100	100	100	100
Fins[a]	4 of 4 normal	3	5	12	20	12	20
	3 of 4 normal	6	8	24	32	36	52
	2 of 4 normal	10	8	40	32	76	84
	1 of 4 normal	5	3	20	12	96	96
	0 of 4 normal	1	1	4	4	100	100
Integument	Normal	25	24	100	96	100	96
	Abrasion		1		4	100	100
	Bruise						
	Cut						
Total contacts[b]	0	81	82	81	82	81	82
	1	11	10	11	10	92	92
	2	8	6	8	6	100	98
	3		2		2		100
	4						
	5						
Depth, camera 1	Bottom third	6	13	24	52	24	52
	Middle third	1	2	4	8	28	60
	Top third	18	10	72	40	100	100
Depth, camera 4	Bottom third	12	14	48	56	48	56
	Middle third	1	1	4	4	52	60
	Top third	12	10	48	40	100	100
Orientation, camera 1	Upstream	7	10	78	59	78	59
	Downstream	2	7	22	41	100	100
Orientation, camera 4	Upstream	11	7	44	47	44	47
	Downstream	14	8	56	53	100	100

[a]Number of fins assessed as normal; fins were caudal, dorsal, and right and left pectoral. [b]A total of 100 observations were possible because four cameras were used for all 25 fish released. Collectively, video cameras recorded potential contacts over 1.8 m of the horizontal flat plate screen.

Table 7. Summary of condition of 25 37-mm individual bull trout assessed after handling (C) or after passage over a horizontal flat plate screen (T) at a sweeping velocity of 1.2 m/sec.

		Frequency		Percent		Cumulative Percent	
Characteristic	Condition	C	T	C	T	C	T
Eyes	Normal	25	25	100	100	100	100
Fins[a]	4 of 4 normal	1	0	4	0	4	0
	3 of 4 normal	2	1	8	4	12	4
	2 of 4 normal	7	2	28	8	40	12
	1 of 4 normal	9	8	36	32	76	44
	0 of 4 normal	6	14	24	56	100	100
Integument	Normal	23	24	92	96	92	96
	Abrasion	2	0	8	0	100	96
	Bruise		1		4		100
	Cut						
Total contacts[b]	0	98	94	98	94	98	94
	1	2	6	2	6	100	100
	2						
	3						
	4						
	5						
Depth, camera 1	Bottom third	13	3	52	3	52	3
	Middle third	0	0	0	0	52	3
	Top third	12	22	48	88	100	100
Depth, camera 4	Bottom third	13	13	52	52	52	52
	Middle third	0	0	0	0	52	52
	Top third	12	12	48	48	100	100
Orientation, camera 1	Upstream	12	3	92	100	92	100
	Downstream	1		8		100	
Orientation, camera 4	Upstream	14	10	67	71	67	71
	Downstream	7	4	33	29	100	100

[a]Number of fins assessed as normal; fins were caudal, dorsal, and right and left pectoral.
[b]A total of 100 observations were possible because four cameras were used for all 25 fish released. Collectively, video cameras recorded potential contacts over 1.8 m of the horizontal flat plate screen.

Table 8. Summary of condition of 25 37-mm individual bull trout assessed after handling (C) or after passage over a horizontal flat plate screen (T) at a sweeping velocity of 0.6 m/sec.

		Frequency		Percent		Cumulative Percent	
Characteristic	Condition	C	T	C	T	C	T
Eyes	Normal	25	25	100	100	100	100
Fins[a]	4 of 4 normal	0	1	0	4	0	4
	3 of 4 normal	1	2	4	8	4	12
	2 of 4 normal	4	6	16	24	20	36
	1 of 4 normal	8	12	32	48	52	84
	0 of 4 normal	12	4	48	16	100	100
Integument	Normal	25	24	100	96	100	96
	Abrasion		1		4	100	100
	Bruise						
	Cut						
Total contacts[b]	0	94	90	94	90	94	90
	1	5	7	5	7	99	97
	2	1	3	1	3	100	100
	3						
	4						
	5						
Depth, camera 1	Bottom third	15	13	60	52	60	52
	Middle third	1	0	4	0	64	52
	Top third	9	12	36	48	100	100
Depth, camera 4	Bottom third	20	21	80	84	80	84
	Middle third	0	0	0	0	80	84
	Top third	5	4	20	16	100	100
Orientation, camera 1	Upstream	15	13	94	100	94	100
	Downstream	1		6		100	
Orientation, camera 4	Upstream	19	22	83	100	83	100
	Downstream	4		17		100	

[a]Number of fins assessed as normal; fins were caudal, dorsal, and right and left pectoral.
[b]A total of 100 observations were possible because four cameras were used for all 25 fish released. Collectively, video cameras recorded potential contacts over 1.8 m of the horizontal flat plate screen.

Table 9. Summary of condition of 25 58-mm individual bull trout assessed after handling (C) or after passage over a horizontal flat plate screen (T) at a sweeping velocity of 1.2 m/sec.

		Frequency		Percent		Cumulative Percent	
Characteristic	Condition	C	T	C	T	C	T
Eyes	Normal	25	24	100	96	100	96
	Abrasion		1		4		100
Fins[a]	4 of 4 normal	0	0	0	0	0	0
	3 of 4 normal	0	2	0	8	0	8
	2 of 4 normal	2	5	8	20	8	28
	1 of 4 normal	8	8	32	32	40	60
	0 of 4 normal	15	10	60	40	100	100
Integument	Normal	24	24	96	96	96	96
	Abrasion	0	0	0	0	96	96
	Bruise	1	0	4	0	100	96
	Cut		1		4		100
Total contacts[b]	0	82	78	82	78	82	78
	1	17	21	17	21	99	99
	2	0	1	0	1	99	100
	3	0		0		99	
	4	0		0		99	
	5	1		1		100	
Depth, camera 1	Bottom third	22	24	88	96	88	96
	Middle third	0	1	0	4	88	100
	Top third	3		12		100	
Depth, camera 4	Bottom third	25	24	100	96	100	96
	Middle third		0	0	0	80	96
	Top third		1	20	4	100	100
Orientation, camera 1	Upstream	20	23	91	92	91	92
	Downstream	2	2	9	8	100	100
Orientation, camera 4	Upstream	25	24	100	100	100	100
	Downstream						

[a]Number of fins assessed as normal; fins were caudal, dorsal, and right and left pectoral.
[b]A total of 100 observations were possible because four cameras were used for all 25 fish released. Collectively, video cameras recorded potential contacts over 1.8 m of the horizontal flat plate screen.

Table 10. Summary of condition of 25 58-mm individual bull trout assessed after handling (C) or after passage over a horizontal flat plate screen (T) at a sweeping velocity of 0.6 m/sec.

		Frequency		Percent		Cumulative Percent	
Characteristic	Condition	C	T	C	T	C	T
Eyes	Normal	25	25	100	100	100	100
	Abrasion						
Fins[a]	4 of 4 normal	0	0	0	0	0	0
	3 of 4 normal	0	2	0	8	0	8
	2 of 4 normal	4	7	16	28	16	36
	1 of 4 normal	5	10	20	40	36	76
	0 of 4 normal	16	6	64	24	100	100
Integument	Normal	20	24	80	96	80	96
	Abrasion	3	1	12	4	92	100
	Bruise	2		8		100	
	Cut						
Total contacts[b]	0	95	82	95	82	95	82
	1	3	11	3	11	98	93
	2	2	6	2	6	100	99
	3		1		1		100
	4						
	5						
Depth, camera 1	Bottom third	25	25	100	100	100	100
	Middle third						
	Top third						
Depth, camera 4	Bottom third	19	21	76	84	76	84
	Middle third	0	2	0	8	76	92
	Top third	6	2	24	8	100	100
Orientation, camera 1	Upstream	24	25	96	100	96	100
	Downstream	1		4		100	
Orientation, camera 4	Upstream	19	21	100	91	100	91
	Downstream		2		9		100

aNumber of fins assessed as normal; fins were caudal, dorsal, and right and left pectoral.
[b]A total of 100 observations were possible because four cameras were used for all 25 fish released. Collectively, video cameras recorded potential contacts over 1.8 m of the horizontal flat plate screen.

Fins - The frequency of fish in control and treatment groups with undamaged fins declined with fish size. The occurrence of fish with damage on all four fins ranged from 0 to 8% for 28-mm fish to 24 to 64% for 58-mm fish. In four cases, occurrence of fish with damage on all four fins was higher for controls than for treatments (Tables 5, 8, 9, 10), in one case the occurrence was equal (Table 6), and in the last case, the occurrence of damage on all fins was higher in treatment fish (Table 7). The types of fin damage most frequently observed were frayed, trace split, and split. Broken fins were observed only on one control and one treatment fish. Both fish had broken pectoral fins and were from the 28-mm size group.

Integument - A total of 9 abrasions were observed: six were on control fish and three were on treatment fish (Tables 5, 6, 7, 8, 10). Also, a total of 4 bruises were observed; three on control fish; one on a treatment fish (Tables 7, 9, 10). Only one occurrence of cut integument was detected (Table 9).

Screen Contacts

Video interpretation showed most fish never contacted the screen. Treatment fish contacted the screen more frequently than control fish. The percentage of one or more contacts was higher for treatment fish in four of the six size-velocity conditions studied (Tables 7, 8, 9, 10). The greatest number of screen contacts observed for a single fish was five. Fish that contacted the screen more than once tended to tumble and swim erratically after the first contact.

Depth in Water Column

Larger fish, especially the 58-mm size group, more frequently inhabited the bottom third of the water column. The percentages for 28-mm fish in the bottom third of the water column ranged from 24 to 56, whereas the percentages for 58-mm fish ranged from 76 to 100. The

percentages of fish in the bottom, middle and top thirds for both cameras and treatments combined were: 44, 6, and 50% for 28-mm fish; 56, 0, and 44% for 37-mm fish; and 92, 2, and 6% for 58-mm fish.

Orientation

The percentage of fish oriented upstream increased with fish size. Forty-two to 79% of 28-mm fish were oriented upstream, compared to 91 to 100% for 58-mm fish. The frequencies of fish oriented upstream for both cameras and treatments combined were 53% for 28-mm fish; 86% for 37-mm fish; and 96% for 58-mm fish.

Survival

An initial assessment of survival was conducted at the time fish were removed from the capture net. The assessments showed that all fish were alive immediately after passage.

The 24-h survival estimates showed that effects of screen passage were small with survival rates ranging from 98.5 to 100% (Table 11). Survival rates were consistently lower for fish that passed over the screen compared to controls, but with a maximum difference of only 1.5%. Lack of variability in the data prevented calculation of 95% confidence intervals in every case. At least one fish died in every 28-mm control or screen treatment (Table 11). Survival was higher for other size classes with no mortalities in five treatments. Very low rates of mortality in some other treatments resulted in estimated 100% (with rounding error) survival rates (denoted by footnote "a"; Table 11). Consequently, values of "100%" in Table 11 should be interpreted with caution because mortality occurred in some treatments.

In general survival rates were lower at 96 h (Table 12) than at 24 h. At 96 h, only two treatments had 100% survival. Survival was lowest for 58 mm fish in the 0.6 m/sec sweeping

velocity treatment. Most mortality for fish in this treatment occurred at 72 and 96 h, and was probably caused by a pathogen. The source of the pathogen was unknown, but water temperatures at the Water Resources Research Laboratory were higher for 58-mm fish (16 to 16.5°C) than for other trials (13.5 to 14°C) because the water cooling system failed. Evidence that some other factor may have influenced survival rates of 58-mm fish, suggested observed 96-h survival rates should be interpreted with caution, or even excluded from analyses intended to infer effects of screen passage. Alternatively, the observed survival rates can be used as worse-case estimates of effects if it is acknowledged that some other factor may have increased mortality. If the 58-mm size is excluded, survival rates were higher for controls in three of four passage conditions; if 58-mm fish are included, survival rates were higher for controls in four of six passage conditions. Lack of variability in the data prevented calculation of 95% confidence intervals in four cases.

Table 11. Summary of 24-h survival for batches of 10 bull trout after passage over a horizontal flat plate screen at two sweeping velocities.

1.2 m/sec Sweeping Velocity

Treatment	Mean % Survival	Lower 95% CI	Upper 95% CI	*n*
		Life Stage (28 mm)		
Control	100[a]	NE	NE	20
Treatment	98.9	NE	NE	20
		Life Stage (37 mm)		
Control	100	NE	NE	20
Treatment	100	NE	NE	19
		Life Stage (58 mm)		
Control	100	NE	NE	20
Treatment	100	NE	NE	19

0.6 m/sec Sweeping Velocity

Treatment	Mean % Survival	Lower 95% CI	Upper 95% CI	*n*
		Life Stage (28 mm)		
Control	100[a]	NE	NE	20
Treatment	98.5	NE	NE	20
		Life Stage (37 mm)		
Control	100[a]	NE	NE	20
Treatment	99.5	NE	NE	20
		Life Stage (58 mm)		
Control	100	NE	NE	20
Treatment	100[a]	NE	NE	20

NE = no estimate.

[a]Some mortality occurred in this treatment group, but estimated survival rates were 100% with rounding error.

Table 12. Summary of 96-h survival for batches of 10 bull trout after passage over a horizontal flat plate screen at two sweeping velocities.

1.2 m/sec Sweeping Velocity

Treatment	Mean % Survival	Lower 95% CI	Upper 95% CI	*n*
		Life Stage (28 mm)		
Control	98.0	95.8	99.2	20
Treatment	94.7	91.5	97.0	20
		Life Stage (37 mm)		
Control	100	NE	NE	20
Treatment	95.3	NE	NE	19[a]
		Life Stage (58 mm)		
Control	98.5	NE	NE	20
Treatment	100	NE	NE	19[a]

0.6 m/sec Sweeping Velocity

Treatment	Mean % Survival	Lower 95% CI	Upper 95% CI	*n*
		Life Stage (28 mm)		
Control	96.4	93.4	98.3	20
Treatment	97.9	95.4	99.3	20
		Life Stage (37 mm)		
Control	98.5	96.7	99.5	20
Treatment	98.0	96.0	99.2	20
		Life Stage (58 mm)		
Control	91.0	84.9	95.3	20
Treatment	81.8	74.1	88.1	20

NE = no estimate.
[a]One replicate lost.

Discussion

Consistent negative effects from passage of bull trout over a horizontal flat plate screen were not observed. Potential entrainment was ≤ 3.5% for 28-mm fish, and was never observed for larger fish. Impingement never occurred. Physical damage to eyes, fins, and integument was either rare (eyes) or less frequent in fish that passed over the screen than in control fish. Fish that passed over the screen did contact the bottom more frequently than control fish, but no immediate mortality occurred from screen passage. Survival at 24 h was consistently lower for fish that passed over the screen compared to controls, but the difference was small (≤ 1.5%). At 96 h after passage, overall survival was reduced, but was not consistently lower for fish that passed over the screen. Thus, the effects of screen passage were at, or near the level of background effects induced by fish culture, handling, transport, and testing.

Water depth and orientation of bull trout changed with fish size and age despite the use of a standardized release methodology. Larger fish were observed near the bottom and oriented upstream more frequently than smaller fish. This tendency to occupy deeper water increased the likelihood that fish contacted the horizontal flat plate screen. It also increased the likelihood that fish discovered attractive hydraulic properties of the screen. We observed several 58-mm fish that appeared to be maintaining position by using the downward pressure generated by the approach velocity of water passing through the screen. This behavior was the main factor responsible for increased passage time for larger fish. Thus, we did observe that certain hydraulic conditions of the horizontal flat plate screen used in this investigation attracted fish and delayed their movement.

Bottom-oriented behavior may have also contributed to the number of times that fish contacted the screen. Fish that contacted the screen more than once tended to tumble and swim erratically after the first contact. Loss of orientation combined with burst swimming to regain

orientation resulted in fish colliding with the screen. Under normal conditions, this behavior would allow a fish to discover microhabitats on the bottom of a stream that offer refuge from water velocity. However, within the confines of a horizontal flat plate screen, the behavior results in multiple screen contacts.

The source of the pathogen presumed to have killed several 58-mm fish in the 0.6 m/sec sweeping velocity treatment was unknown. There was strong evidence that the mortality was caused by a pathogen because fish appeared healthy at 0, 24, and 48 h after passage, but then mortality began to occur at 72 and 96 h. Other evidence of a pathogen was that mortality was clustered within tanks suggesting that infected individuals transferred the disease within an aquarium. Two characteristics were different during 58-mm trials compared to previous trials: (1) the water temperature was 2 to 2.5°C warmer; and (2) passage times were longer which would have increased exposure to resident pathogens. Regardless of the cause(s), the presence of additional sources of mortality should be acknowledged when interpreting results for 58-mm fish.

References

Frizell, K., and B. Mefford. 2001. Hydraulic Performance of a Horizontal Flat Plate Screen. Final report. U.S. Bureau of Reclamation, Water Resources Research Laboratory, Denver, Colorado.

Lee, D.S, C.R. Gilbert, C.H. Hocutt, R.E. Jenkins, D.E. McAllister, and J.R. Stauffer, Jr. 1980. Atlas of North American freshwater fishes. North Carolina State Museum, Raleigh, North Carolina.

SAS Institute. 1993. SAS Technical Report P-243, SAS/STAT Software: GENMOD procedure, release 6.09. Cary, North Carolina.

Physcial Model and Computational Fluid Dynamics Summary

Farmers Conservation Alliance (FCA) coordinated two studies emulating the Derby Dam screen design for verification and analysis of hydraulic operating conditions when a single Farmers Screen is scaled to a screened flow rate of 132 cfs. The two studies included a real-world prototype-scale physical model and a computational fluid dynamics (CFD) model. A real-world physical model was constructed at Farmers Irrigation District's (FID) existing Davenport screen by retrofitting the existing screen utilizing wedge-wire screen material and the proposed taper ratio of 14 to 1, which created the Davenport physical model. In concert with this real-world physical model, CFD modeling was performed on the Davenport screen as a validation exercise and then extended to the Derby screen to determine the hydraulic flow conditions through the proposed screen design. While each of these studies is useful on its own, there is greater benefit from corroborating and comparing the two. Reports were produced for each respective study. This document summarizes each of the studies and details the benefits of the two studies collectively.

SUMMARY OF CFD AND PHYSICAL MODEL BENEFITS

- Flow surveys were completed on the Davenport physical model to gather data pertaining to velocity vectors in the water column over the screen, flow through the screen, and water depth. These data were used to empirically calibrate the Davenport CFD model.
- Calibration of the Davenport CFD model using real-world conditions provided a baseline for modeling inputs used in the creation of the Derby Dam CFD model. The Davenport CFD model served as a basis for comparison when generating and running different scenarios using the Derby Dam CFD model.
- Measurements and observations of the retrofitted Davenport screen were requested throughout the modeling process for calibration purposes. Data were collected and provided within 2 to 3 days, allowing for rapid modeling corrections and changes, saving valuable time, and creating a more adaptive modeling environment.
- Visual observations of the retrofitted Davenport physical model were compared to CFD results to aid in modeling considerations. Modeling considerations ranged from changes in geometry to changes in modeling techniques (e.g., mesh resolution in specific locations, roughness coefficients, boundary conditions, etc.).
- Results and modeling assumptions from the empirically corroborated Davenport CFD model were utilized to create the Derby Dam CFD model. The corroborated CFD model allowed for a more focused and effective Derby Dam CFD model.
- The two models in tandem represent a so-called hybrid model, which is state-of-the-art in hydraulic modeling and lends confidence to the overall design. Specific benefits include:
    - better understanding of the flow split between screened canal water and bypass water;
    - added assurance that target canal flows will be achieved at the forthcoming Derby Dam Facility; and
    - added assurance that the fish passage design criteria (e.g., minimum flow depth; minimum sweeping velocity; maximum approach velocity) will be achieved over the range of flows expected at the Derby Dam Facility.

SUMMARY OF FINDINGS

- Non-Backwatered Conditions (Typical Operation) – Screened water is freely falling over the weir wall.
    - Sweeping Velocity – Minimum sweeping velocity is predicted to be 5.8 ft/s, exceeding the design requirements of a minimum of 2.5 ft/s.
    - Approach Velocity – Ranges from 0.10 ft/s to 0.22 ft/s, which is below the maximum design requirements of 0.25 ft/s.
    - The water depth over the screen surface under non-backwater conditions is set by the weir wall height and will be above the minimum design requirement of 1.0 feet.
    - Irrigation flow – At 150 cfs inlet flow conditions, approximately 126 cfs (84 percent) will be screened for irrigation and 24 cfs (16 percent) will go to bypass flows.
        - From observation of the Davenport screen and other large screens, FCA believes that the bypass of 24 cfs predicted by the CFD model is an overestimate. Based on previous screen installations, the bypass flow is not linearly related to incoming flow, but rather is related to the cross-sectional area of the bypass outlet combined with the sweeping velocity and water depth at the outlet. Over-prediction by the CFD model can be attributed to a number of factors, but ultimately can be traced back to finite computing power, which limits the model design.
- Backwatered Conditions – Backwatered flow conditions occur when the water surface elevation in the attenuation bay is greater than the elevation of the weir wall.
    - Sweeping Velocity – Minimum sweeping velocity is predicted to be 4.5 to 5.0 ft/s, exceeding the design requirements of a minimum of 2.5 ft/s.
    - Approach Velocity – Ranges from 0.10 ft/s to 0.17 ft/s, which is below the maximum design requirements of 0.25 ft/s.
    - Under extreme backwatered conditions, the water depth over the screen surface is expected to be 2.2 feet, which is well above the minimum of 1.0 feet.
    - Irrigation flow – At 150 cfs inlet flow conditions, approximately 120 cfs (80 percent) will be screened for irrigation and 30 cfs (20 percent) will go to bypass flows.
        - From observation of the Davenport screen and other large screens, FCA believes that the bypass of 30 cfs predicted by the CFD model is an overestimate. Based on previous screen installations, the bypass flow is not linearly related to incoming flow, but rather is related to the cross-sectional area of the bypass outlet combined with the sweeping velocity and water depth at the outlet. Over-prediction by the CFD model can be attributed to a number of factors, but ultimately can be traced back to finite computing power, which limits model design.

PHYSICAL MODEL

FCA designed and coordinated the construction of a physical model intended to simulate the hydraulic operating conditions of the Derby Dam screens. FID's Davenport screen was selected to be constructed and used as the physical model. Davenport was chosen because it housed an existing Farmers Screen that was used for early research and development of the technology, therefore, the majority of the infrastructure already existed, and its close proximity to FCA's main office allowed for ease of testing and observation. In addition, FID was a willing and interested partner who allowed repeated flow adjustments in order to gather the necessary data, along with bringing 16 years' worth of operational data, of a horizontal screen at this site, for use in operational comparison. The Davenport physical model is geometrically similar to the screens designed at the Derby Dam, with a design taper ratio of 14 to 1. The retrofitted Davenport physical model screen is 105 feet in length. This is 20 feet shorter than the four large screens at the Derby Dam, and 15 feet longer than the small screen at the Derby Dam. Figure 1 shows the completed retrofit of the

Davenport screen. Construction was completed in April 2019, with subsequent flow and observational studies performed throughout the summer of 2019.

Figure 1. Finished retrofitted Davenport screen with a 14 to 1 taper ratio, emulating the geometry of the screen at the Derby Dam.

The close proximity of the Davenport screen to FCA allowed for frequent observation of the screen's operation by both FCA and FID staff over the entire 2019 irrigation season. The 2019 irrigation season included a wide range of flows, temperatures, and water quality. Over the 2019 season, the screen was subjected to high sediment loading, high organic debris loading, frazzle ice, and anchor ice. The screen remained functional throughout the range of design flows and conditions, and required minimal maintenance.

Within the 2019 irrigation season, the screen did experience one complete fouling event. The fouling event occurred in the fall, when, as water levels rose, high amounts of leaf litter from the banks were concentrated into the river, carrying the organic material through the Davenport diversion structure. Leaf material overwhelmed the screen, reducing and eliminating the ability for water to go through the screen. The screen is designed in these scenarios to spill water into the attenuation bay so that water will continue to be diverted, while sending an emergency alarm to the district. During the fouling event, an increased load was imparted on the taper wall by the organic material and water, causing the taper wall to bow out slightly, up to 1.5 inches. Debris filled the gap between the screen and taper wall restricting the taper wall from returning to its normal position after the issue was resolved. FCA supplied this information to the structural engineer for the Derby Dam project. Modifications were made to the taper wall stiffness and the attachment method to eliminate the possibility of this occurring at the Derby Dam.

In addition to observational studies, flow measurement studies were conducted using a Flow Tracker 2 with a 3D head to measure flow velocities in the x, y, and z directions. This provided data for the water depth over the screen, and was used to calculate the total flow per 10-foot section. Velocities measured in the x-direction indicated the velocity of water parallel to the screen surface, the y-direction indicated lateral flow, and the z-direction indicated the velocity of water in the direction of the screen. Flow velocities and water depth were vital in calibrating the Davenport CFD model. Velocities in the z-direction varied significantly in the upward and downward direction, confirming assumptions of the chaotic nature over the screen. The chaos or turbulence helps to explain the waveforms that occur and likely aid in the passive cleaning of the

screen, keeping debris and fish in the water column. Figure 2 identifies the flow measurement locations along the length of the screen and the z-velocities at each measurement.

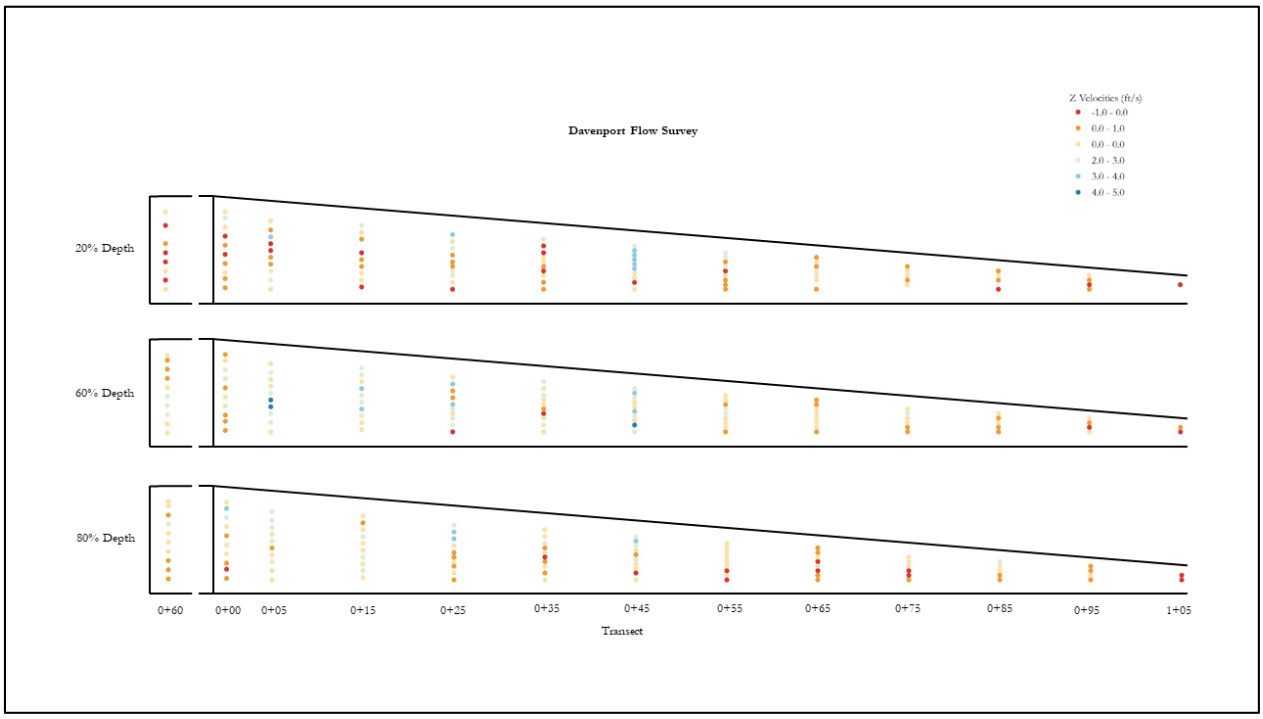

Figure 2. Flow measurements along the length of the Davenport physical model identifying the z-velocity component. The percent depth is indicative of the depth of the measurement relative to the water surface elevation.

The Flow Tracker 2 calculated the total discharge, or flow, using velocity measurements taken along each transect. The difference between each transect measurement indicates the quantity of water that passed through the screen. Data from multiple flow surveys indicated that higher rates of screened water existed roughly one-third to one-half of the way down the screen in the longitudinal (x-) direction. This is a function of the wider entrance with the 14 to 1 taper ratio compared to the original design of 20 to 1. Higher approach velocities on the 20 to 1 taper ratio were seen at the beginning of the screen. The fact that the Davenport screen is experiencing higher approach velocities near the middle is extremely promising, creating a more uniform approach velocity across the entire screen structure and maintaining a more consistent sweeping velocity from the leading edge to the tailing edge.

CFD MODEL

FCA commissioned Dr. Jo Scott with Gilbert Gilkes and Gordon Ltd. (Gilkes) to develop and complete a CFD model emulating one of the four large screen designs of the Derby Dam screen. A CFD model predicts the fluid flow characteristics in and around a fixed structure by solving the Reynolds-Averaged Navier-Stokes (RANS) equations, which govern fluid flow. In the case of Derby Dam, the fluid is water and the structure is the fish screen, inlet flume, and attenuation bay (see Figure 3). The larger screens at the Derby Dam will be 125 feet in length. The CFD model was designed to simulate the fluid flow through the screen structure at high-flow (backwatered), typical-flow (non-backwatered), and low-flow (non-backwatered) operating conditions to predict the following:

- Estimated screened flow vs bypass flow

- Water velocities and flow patterns through the screen (approach velocity) and over the screen (sweeping velocity)
- Varying water depths along the length of the screen

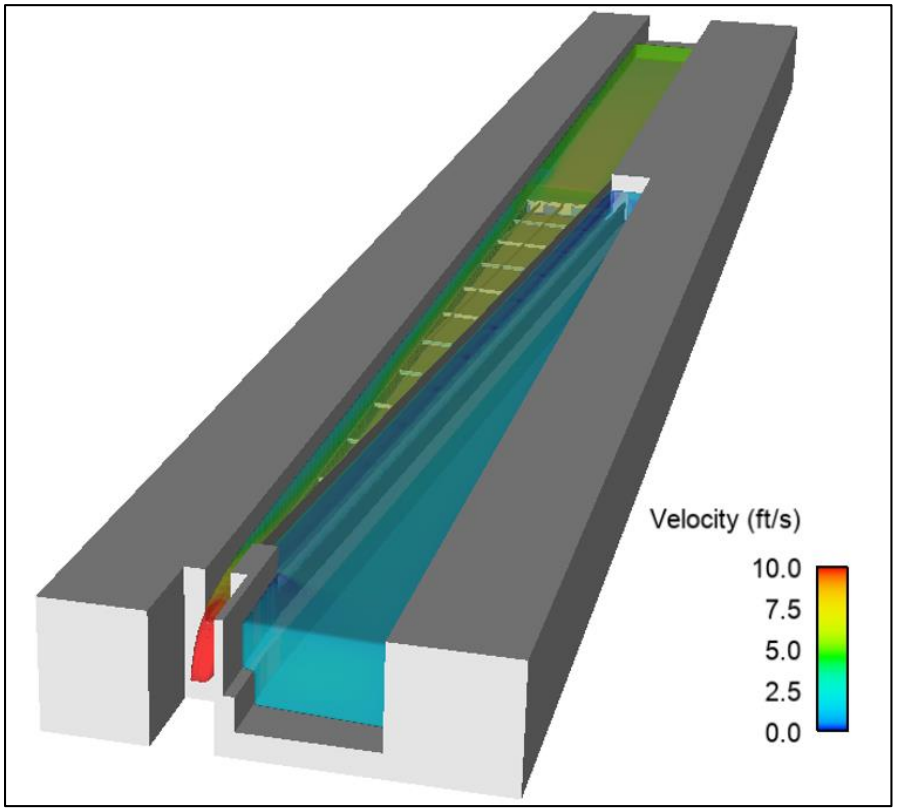

Figure 3. Flow-3D model of the Derby Dam screen structure.

Dr. Jo Scott selected Flow-3D to model the Derby Dam screen. The Flow-3D software is specifically designed to solve transient-free surface flows of incompressible fluids under turbulent conditions. The bulk of the work completed by Gilkes included the creation and calibration of a baseline model determining input parameters for the Flow-3D model. Davenport was chosen as the screen to model as a baseline, creating a virtual replica of the Davenport physical model. FCA gathered flow data under a number of operating conditions to provide a comparison to the outputs of the Flow-3D simulated model. Outputs from the CFD model were corroborated with the measured-flow studies completed by FCA. Figure 4 shows a comparison between the outputs from the Davenport CFD model and the measured data. Multiple weeks of iterations of the CFD model were required to obtain an accurate baseline model and discern the appropriate modeling assumptions. More information on the calibration process can be found in the CFD study.

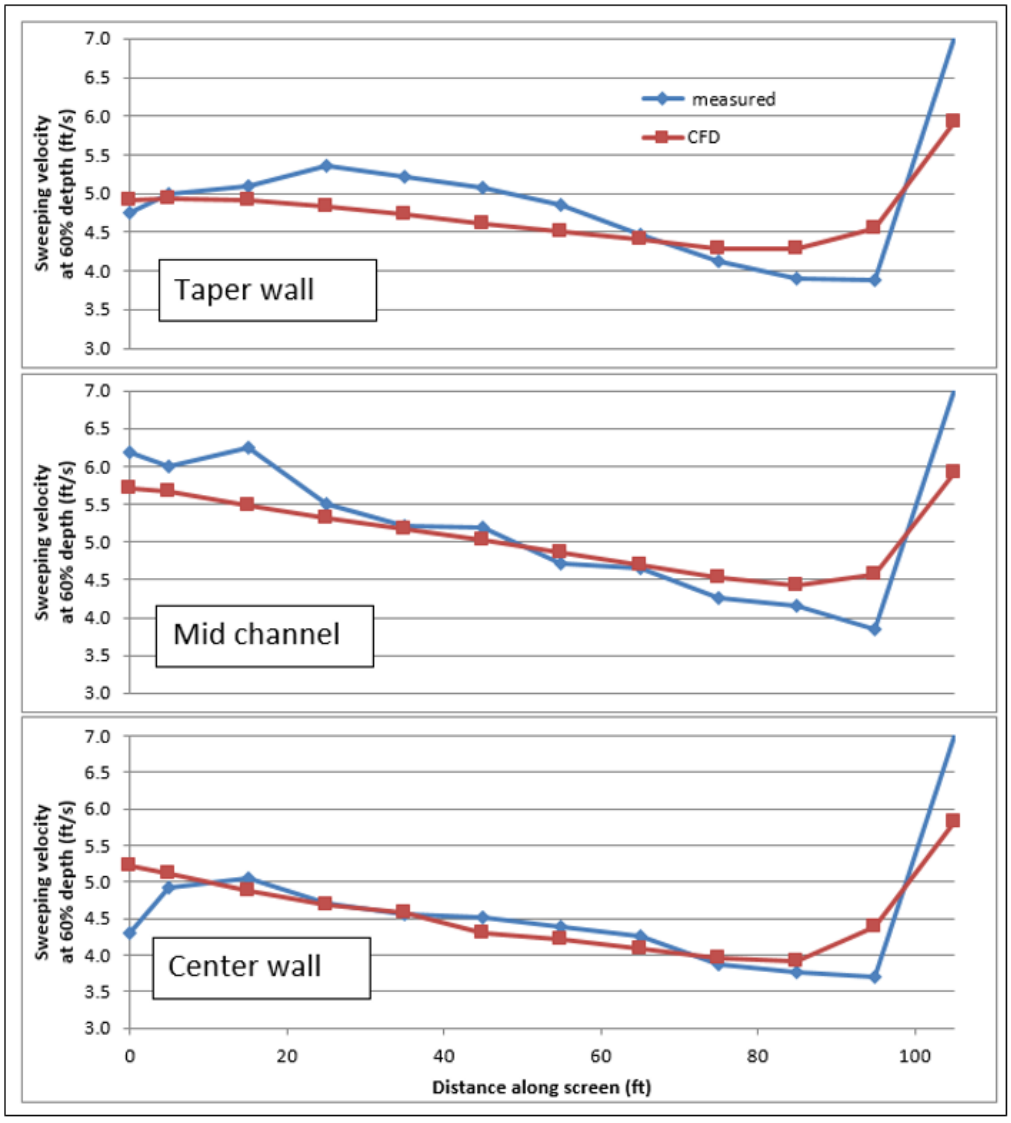

Figure 4. Comparison between the measured sweeping velocity at the Davenport screen and the calculated sweeping velocity predicted by the CFD model.

Following completion and calibration of the baseline model, a CFD model was created of one of the large screens at Derby Dam using the same methodology employed for the baseline model. Seven runs were executed for the Derby Dam model simulating different operating conditions and changes to the design geometry. Operating conditions that were analyzed consisted of high flows during backwatered scenarios, typical operations during non-backwatered conditions, and minimum flow conditions. Modifications to the under-screen geometry were tested to investigate the effects on flow patterns and velocities. Ultimately, the results of the CFD model indicated no change to the proposed design and provided confidence that the design would operate within the hydraulic design parameters. Figure 5 and Figure 6 show the predicted sweeping velocity for separate runs and a comparison of bypass flow to screened irrigation flow as a function of inlet flow, respectively.

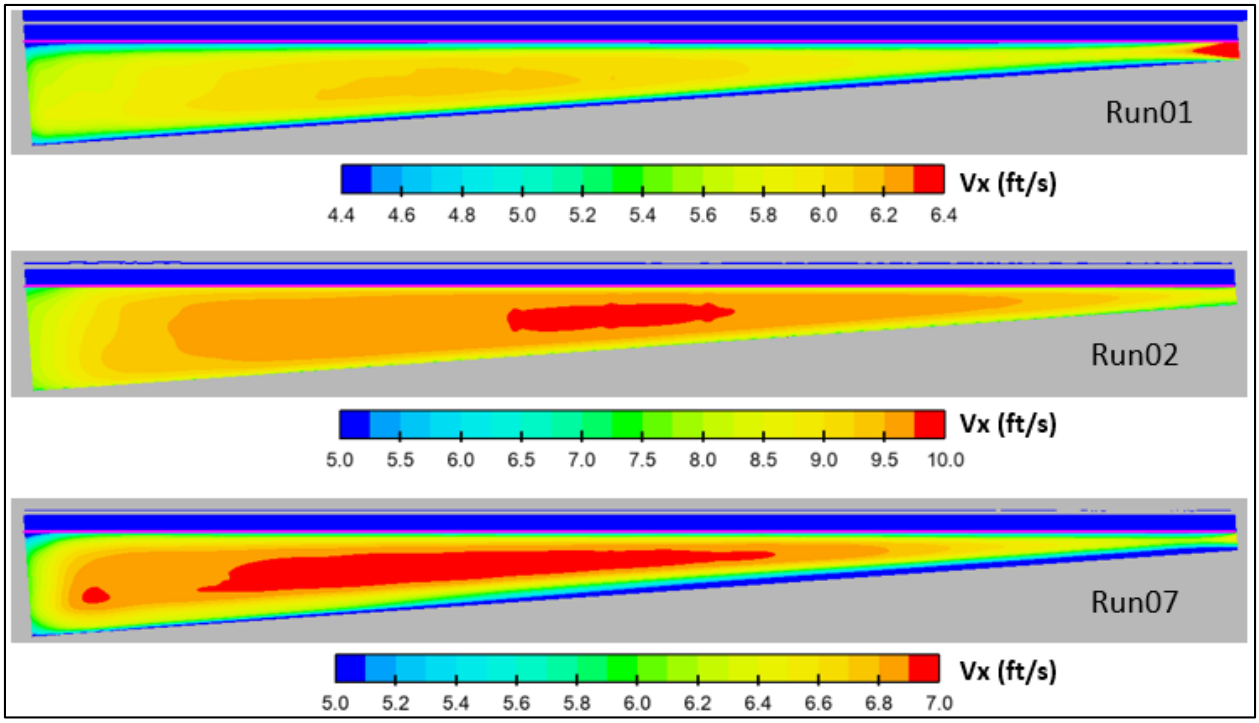

Figure 5. **CFD-predicted sweeping velocities for the large screen at the Derby Dam under various operating conditions.**

Run01 indicated an inlet-flume flow of 150 cfs under full backwatered conditions. Run02 indicated an inlet-flume flow of 150 cfs under non-backwatered conditions. Run07 indicated an inlet-flume flow of 78 cfs under non-backwatered conditions simulating minimum flow conditions.

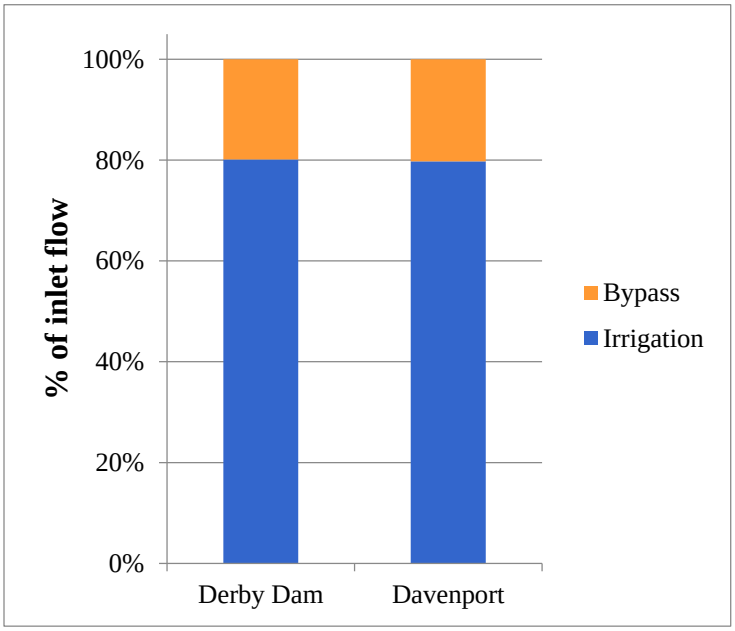

Figure 6. CFD-simulated comparison between bypass flow and screened irrigation flow as a function of percent inlet flow for Run01.

The CFD model generated useful graphics of predicted flow patterns through the screen structure. Observationally, it is difficult to deduce the interactions between the water and the structural components. FCA has hypothesized about the passive cleaning mechanism of the screen and the vibrational frequency that is audible to the human ear. These graphics assist in corroborating the hypotheses and give further confidence to the Derby Dam screen design. Figure 7 and Figure 8 show the interaction of water flowing across and through the wedge-wire screen and the flow patterns through a cut-section of the Derby Dam screen, respectively.

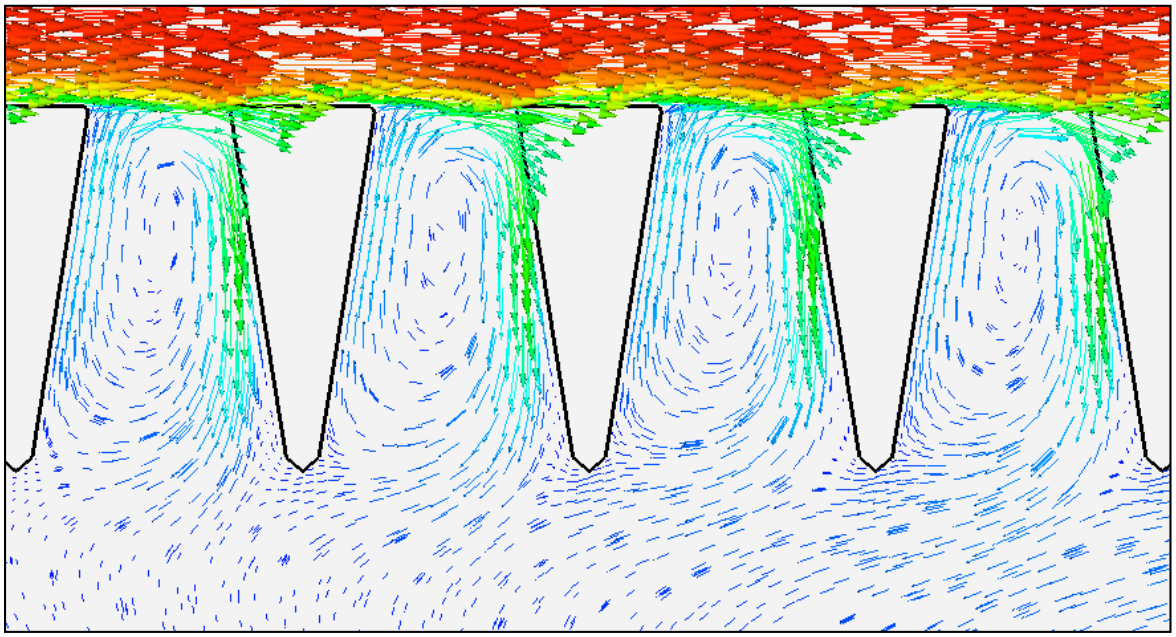

Figure 7. CFD-simulated flow pattern of water through the wedge-wire screen. Each opening is approximately 0.07 inch. Colors indicate the magnitude of the velocity ranging from red (high velocity) to blue (low velocity).

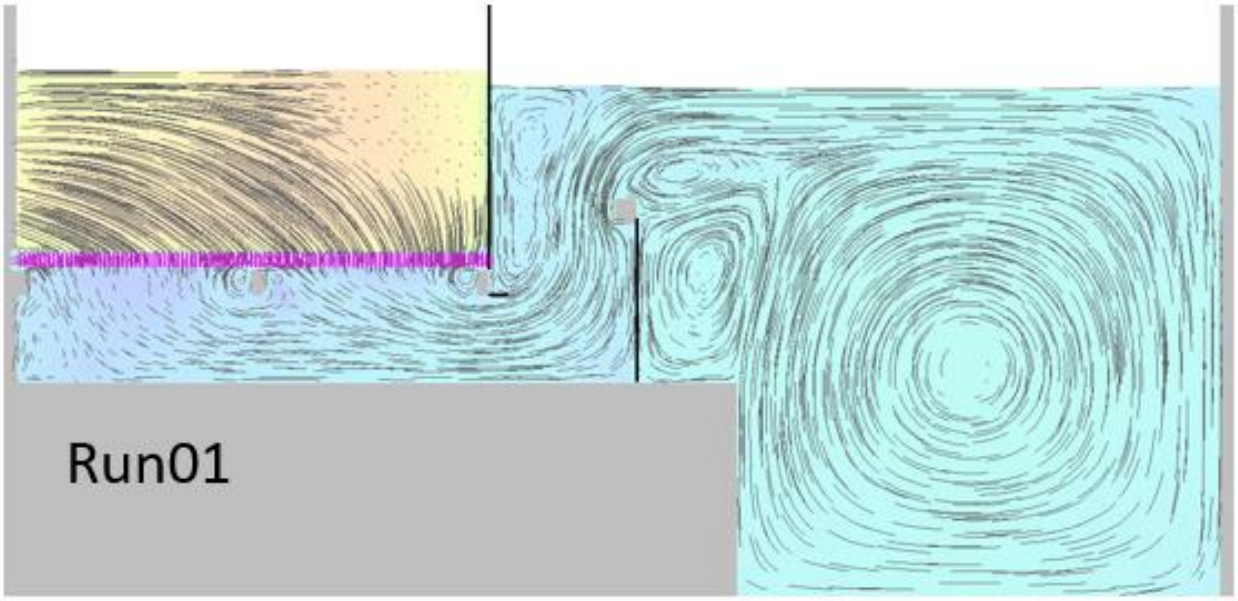

Figure 8. CFD-simulated flow pattern of water through a cut-section of the screen structure.

Theoretical studies aim to solve complex numerical algorithms, and thus inherently include assumptions and limitations. Below is a list of the limitations that the design team found to have a potential impact on the CFD outputs.

- Due to limitations of computing power, the screen material was modeled as a porous material with a porosity factor rather than the actual wedge-wire material. Computing power also limited the mesh resolution that was applied to the physical structure.
- Due to limitations of computing power and run times, assumptions were made regarding the inlet conditions and water quality.
- The CFD model was unable to predict vibrations of the screen material and assumed the screen was a fixed structure. An oscillating frequency was applied to the screen; however, it did not have any impact on CFD-modeled performance.
- Debris and organic material transferred over the screen and out the bypass were not included in the model.
- Flow within the Farmers Screen is turbulent. Attempting to simulate all turbulent conditions is limited by computing power and processing time, and thus an empirically derived formula, RNG k-epsilon, was selected to simulate the turbulent conditions.
- The data obtained from the Davenport physical model, and used to calibrate the CFD model, likely have a degree of uncertainty. Human and equipment error can contribute to measurement uncertainty.

CONCLUSIONS

The physical model and CFD studies created showed that the Derby Dam screens are likely to perform similarly to the Davenport screen under all operating conditions. This provides confidence in the idea that, if the Davenport screen operates successfully under operating conditions ranging from fully backwatered to low flow conditions, then the Derby Dam screens will likewise operate successfully. While the CFD model did not accurately predict all aspects of screen performance, the model did correlate well in most key areas that are predictive of screen performance. In the case of bypass flows, the presumed over-prediction by the model is not a cause for concern as higher bypass flows would not cause screen performance to decrease. If the model predictions regarding bypass flow were correct, decreasing bypass flows could be accomplished under non-backwatered conditions through weir-height adjustments. Typically, bypass flows would only be a concern during lower river flow conditions and not during the times when the screen would be running in backwatered conditions (i.e., during much higher river flow conditions). The combination of a physical model with a CFD model proved to be an excellent approach, allowing real-world data to inform the development and calibration of the CFD model. These studies provided the design team with the confidence that, when scaled, the Derby Dam screen will function under all operating conditions expected at Derby Dam.

Report: RDH048-CFD14 (Rev 2)

Computational Fluid Dynamics Studies of the Derby Dam

Jo Scott PhD, CEng

Gilbert Gilkes & Gordon Ltd

16th December 2019

Contents

List of Figures 3
List of Tables 5
Executive Summary 6
1. Introduction 17
1.1 Background 17
1.2 Project Objectives 19
1.3 Project Exclusions 20
1.4 Project Structure 20
2. CFD Model Development 22
2.1 CFD for Fish Screen Modeling 22
2.2 Model of the Wedge-Wire Screen Material 30
2.3 Correlation of the CFD Model to Test Data From the Davenport Physical Model 39
2.4 CFD Assumptions and Accuracy 66
2.5 Conclusions 69
3. CFD Simulations of the Derby Dam 71
3.1 Introduction 71
3.2 CFD Model 71
3.3 Run List 77
3.4 Results and Discussion of the Primary CFD Simulations of the Derby Dam 78
3.5 Results and Discussion of the Ancillary CFD Simulations of the Derby Dam 92
3.6 Overall Conclusions of the Derby Dam CFD Simulations 102
Appendix A – Flow3D Settings for CFD Simulations of Davenport and Derby Dam 104
Appendix B – Results of CFD Simulations of the Davenport Screen 106

List of Figures

Figure 1 – Overview of the CFD model of the Davenport screen 7
Figure 2 - Vectors colored by velocity on a vertical slice through the wedge-wire model....9
Figure 3 – Predicted sweeping velocity and water depth for backwatered weir operation 10
Figure 4 – Predicted sweeping velocity and water depth for non-backwatered operation....11
Figure 5 – Predicted flow balance; backwatered (left), non-backwatered (right)....11
Figure 6 – Overview of the CFD model of the Derby Dam in backwatered operation (Run01) 13
Figure 7 – Vertical slice mid-screen showing streamlines in the plane of the slice....14
Figure 8 – Contours of sweeping velocity at 5.9 inches above the screen....14
Figure 9 – Predicted water depth along the screen 14
Figure 10 – Schematic of the Farmers Screen 22
Figure 11 - Typical CFD model of the Farmers Screen 25
Figure 12 - Water surface colored by velocity in a typical simulation of the Farmers Screen 28
Figure 13 - Dimensions of the wedge-wire screen 30
Figure 14 - Photo looking down on wedge-wire screen with millimeter rule for scale....31
Figure 15 - Geometry of CFD model of wedge-wire screen 32
Figure 16 - Slice through the CFD mesh of the wedge-wire screen....32
Figure 17 - Extension of screen (unlimited), as seen by the flow in the CFD model 33
Figure 18 - CFD model inputs; through-flow model (left), cross-flow model (right) 33
Figure 19 - Vectors colored by velocity on a slice through the “through-flow” model....35
Figure 20 - Vectors colored by velocity on a slice through the “cross-flow” model....35
Figure 21 - Prediction of pressure drop versus flow rate for the CFD models of the wedge wire 36
Figure 22 - Porous region (blue) within the CFD mesh of the Farmers Screen 37
Figure 23 – The re-built Davenport screen prior to operation 39
Figure 24 – Schematic of Davenport screen showing location of measurement points 40
Figure 25 – Location of lines for comparison of sweeping velocity to CFD predictions 40
Figure 26 – Location of points at each transect for comparison of sweeping velocity to CFD predictions....41
Figure 27 – CFD model geometry 42
Figure 28 – Simplification of geometry within the CFD model 43
Figure 29 – Schematic of the Farmers Screen illustrating flow measurements for CFD correlation....44
Figure 30 – Results of initial CFD simulation of the Davenport screen at OP1....45
Figure 31 – Mesh block structure for CFD model of the Davenport screen 47
Figure 32 – Vertical slice through CFD mesh of the Davenport screen in operating conditions OP1; coarse (top), fine (bottom) 48
Figure 33 – Horizontal slice through CFD mesh of the Davenport screen in operating condition OP1; coarse (left), fine (right)....48
Figure 34 – Mesh block structure for CFD model of the Davenport screen in operating condition OP4....49
Figure 35 – Vertical slice through CFD mesh of Davenport screen in operating condition OP4; coarse (top), fine (bottom) 49
Figure 36 – Effect of choice of turbulence model on flow balance at OP1 50
Figure 37 – Effect of turbulence model on sweeping velocity and water depth at OP1....51
Figure 38 – Pressure drop versus velocity curves for the different screen resistances tested 52
Figure 39 – Predicted flow balance for different values of screen resistance at OP1....53
Figure 40 – Effect of screen resistance on sweeping velocity and water depth at OP1....54
Figure 41 – Effect of wall roughness on flow balance at OP1 55
Figure 42 – Effect of wall roughness on sweeping velocity and water depth at OP1....56

Figure 43 – Overview of CFD model of the Davenport screen at OP1 58
Figure 44 – Slice through the Davenport screen at OP1, showing streamlines in the plane of the slice 58
Figure 45 – Predicted sweeping velocity and water depth at OP1 60
Figure 46 - Predicted water depth along the screen at OP1 61
Figure 47 – Predicted flow balance at OP1 61
Figure 48 – Overview of CFD model of the Davenport screen at OP4 62
Figure 49 – Slice through the Davenport screen at OP4 showing streamlines in the plane of the slice 63
Figure 50 – Predicted sweeping velocity and water depth at OP4 64
Figure 51 – Predicted water depth along the screen at OP4 65
Figure 52 – Predicted flow balance at OP4 65
Figure 53 – CFD model geometry of the Derby Dam 71
Figure 54 – Mesh block structure for CFD models of the Derby Dam; 72
Figure 55 – Slice A-A through fine mesh of the Derby Dam for backwatered simulations 73
Figure 56 – Slice A-A through fine mesh of the Derby Dam for non-backwatered simulations 73
Figure 57 – Slice B-B through fine mesh of the Derby Dam for backwatered simulations 74
Figure 58 – Overview of the Derby Dam CFD model showing the main boundary conditions 75
Figure 59 – Design variations to the Derby Dam simulated in CFD 78
Figure 60 – Predicted flow balance for primary CFD simulations of the Derby Dam 79
Figure 61 – Location of streamline slices 79
Figure 62 – Vertical slice through primary Derby Dam simulations showing streamlines 80
Figure 63 – Contours of y-velocity on a horizontal slice 0.2 inch above the floor of the underbay 81
Figure 64 – Contours of downwards vertical velocity on a slice through the porous screen 81
Figure 65 – Contours of sweeping velocity at 5.9 inches above the screen (i.e., approximately 80 percent depth for Run01) 82
Figure 66 – Contours of sweeping velocity at 11.8 inches above the screen (i.e., approximately 60 percent depth for Run01) 82
Figure 67 – Predicted water depth along the screen 83
Figure 68 – Predicted flow balance as a percent of inlet flow 84
Figure 69 – Predicted water depth along the screen 84
Figure 70 – Predicted sweeping velocity 4 inches above the surface of the screen 85
Figure 71 – Predicted flow balance as a percent of inlet flow 86
Figure 72 – Predicted water depth along the screen 86
Figure 73 – Predicted sweeping velocity 4 inches above the surface of the screen 87
Figure 74 – Predicted flow balance for ancillary CFD simulations of the Derby Dam 93
Figure 75 – Vertical slice through ancillary Derby Dam simulations showing streamlines 95
Figure 76 – Contours of y-velocity on a horizontal slice 0.2 inches above the floor of the underbay 96
Figure 77 – Contours of downwards vertical velocity on a slice through the porous screen 97
Figure 78 – Contours of sweeping velocity at 5.9 inches above the screen (i.e., approximately 80 percent depth) 98
Figure 79 – Contours of sweeping velocity at 11.8 inches above the screen (i.e., approximately 60 percent depth) 99
Figure 80 – Contours of sweeping velocity at 23.6 inches above the screen (i.e., approximately 20 percent depth) 100
Figure 81 – Predicted water depth along the screen 101
Figure 82 – Location of measurement lines for sweeping velocity 106
Figure 83 – Predicted flow balance 107
Figure 84 – In-plane streamlines on a vertical slice mid-distance along the screen 107
Figure 85 – Predicted water depth along the screen 107
Figure 86 – Predicted sweeping velocity near the center wall 108

Figure 87 – Predicted sweeping velocity mid-channel 109
Figure 88 – Predicted sweeping velocity near the taper wall.....110
Figure 89 – Predicted flow balance 111
Figure 90 – In-plane streamlines on a vertical slice mid-distance along the screen 111
Figure 91 – Predicted water depth along the screen 111
Figure 92 – Predicted sweeping velocity near the center wall.....112
Figure 93 – Predicted sweeping velocity mid-channel 113
Figure 94 – Predicted sweeping velocity near the taper wall.....114

List of Tables

Table 1 – Hydraulic criteria for the standard size fish screens at the Derby Dam.....6
Table 2 – Hydraulic criteria for the standard size fish screens at the Derby Dam taken from McMillen Jacobs 20
Table 3 – Operating conditions at Davenport screen.....41
Table 4 – Mesh size and run time for typical CFD simulations of the Derby Dam.....77
Table 5 – List of CFD simulations of the Derby Dam.....77
Table 6 – Predicted flow balance for primary CFD simulations of the Derby Dam 78
Table 7 – Predicted flow balance for ancillary CFD simulations of the Derby Dam.....93
Table 8 – Operating conditions simulated for the Davenport screen 106

Executive Summary

Background

This document presents the results of computational fluid dynamics (CFD) studies of the Farmers Screens being installed by Farmers Conservation Alliance (FCA) and the U.S. Bureau of Reclamation at the Derby Dam near Sparks, Nevada. The CFD studies complement physical model tests from an existing FCA screen, which was retrofitted to be a near-replica scaled model of the Derby Dam screens.

The physical model provides real-world data against which to correlate the CFD model. The CFD model provides confirmation that the physical model data are a good indicator of the real-world flows to be expected at the Derby Dam. Utilizing the CFD model and the physical model in combination affords greater benefit than either in isolation, providing a powerful tool for corroborating the Derby Dam Fish Screen design.

Project Objectives

The general objectives of the project were to:

- Develop a CFD model of the physical model.
- Calibrate the CFD model of the physical model based on field data.
- Extend the calibrated CFD model to the Derby Dam screens.

The National Marine Fisheries Service provides specific hydraulic requirements for screen performance for anadromous fish species in the Pacific Northwest, against which the CFD model predictions can be judged. Lahontan Cutthroat Trout are similar in size and swimming capabilities to those anadromous species, therefore the same criteria were used for the design of the Derby Dam Fish Screen. These are summarized in *Table 1* below.

Table 1 – Hydraulic criteria for the fish screens at the Derby Dam

Criteria	Value
Minimum water depth over screen	1 ft
Bypass flow amount per screen	approximately 15% of total flow for diversions < 100 cfs approximately 10% of total flow for diversions > 100 cfs
Screen sweeping velocity	> 2.5 ft/s

Development and Calibration of the CFD Model

Davenport Physical Model

An existing FCA screen, known as the Davenport screen, on the Hood River, Oregon was retrofitted to be a near-replica scaled model of the Derby Dam screens. The retrofitted Davenport screen utilizes the proposed 14:1 taper ratio and has an overall length of 105 feet. This means that the Davenport screen is 20 feet shy of the large screens at the Derby Dam and 15 feet longer than screen 5 at the Derby Dam. In its role as a test facility, the retrofitted Davenport screen is commonly referred to as the Davenport physical model within this report.

FCA engineers gathered data from the Davenport physical model under a number of operating conditions. The data included measurements of velocity and water depth across the length and breadth of the screen. The flow rate over the screen was estimated from these measurements.

Davenport CFD Model

A visual overview of the CFD model of the Davenport screen is shown in *Figure 1* below, followed by a discussion of the key inputs.

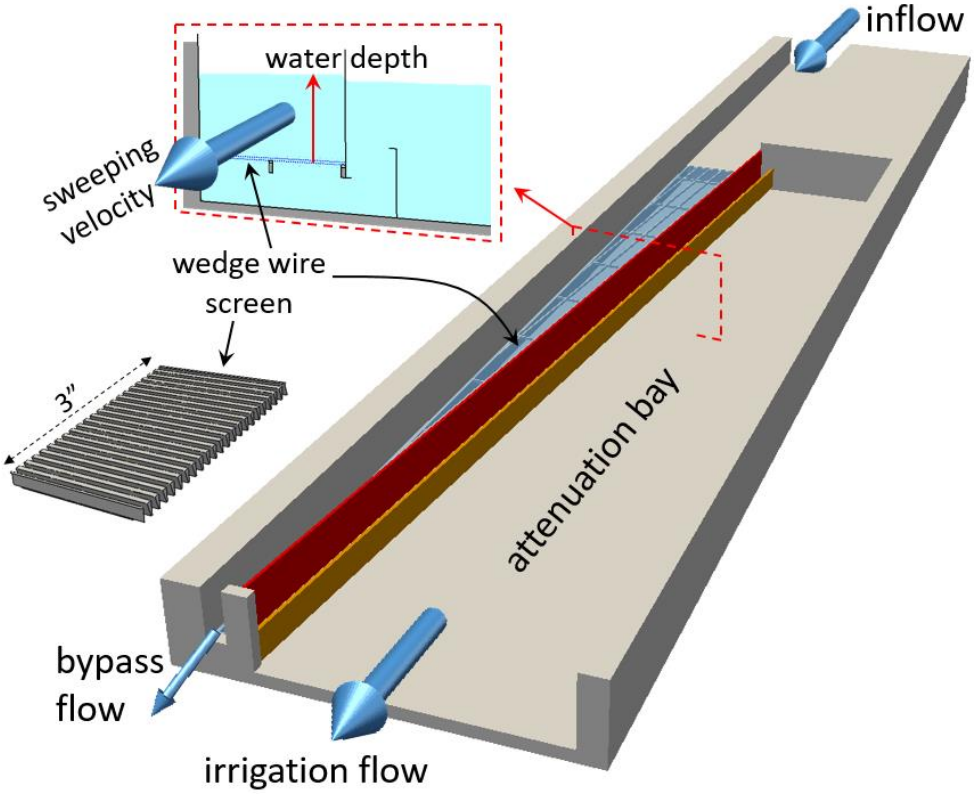

Figure 1 – Overview of the CFD model of the Davenport screen

Geometry

The geometry of the CFD model of the Davenport screen is shown in *Figure 1*. The CFD model extends from the inlet flume upstream of the wedge-wire screen, to the exit from the attenuation bay, and to the point at which water falls off the end of the screen into the bypass channel.

In order to reduce the mesh size and subsequent simulation time, the small features close to or below the level of resolution of the CFD mesh were omitted, e.g., the legs beneath the screen that support the frame and the legs beneath the taper wall.

Mesh

Any CFD mesh is always a trade-off between simulation time and accuracy, i.e., the more cells included in the mesh, the greater the accuracy of the CFD model, and the greater the simulation time. The Farmers Screen presents a particular challenge because of the length scales involved; the screen itself is on the order of 100 feet long while the wedge wires comprising the screen are just 0.07-inch thick. In order to keep the simulation time manageable, the smallest cells in the CFD mesh of the Davenport screen are approximately 1-inch across with a total of approximately 3 million cells.

Wedge-Wire Screen

Given the minimum cell size, the wedge wires cannot be modeled explicitly. Instead, the wedge-wire screen is approximated as a porous region without the geometric detail of the wires, but with the same resistance to through-flow.

To determine the resistance of the wedge wires, a separate small-scale CFD model was built in which a representative portion of the wires was modeled explicitly. By varying the flow rate through the wires, this small-scale model was used to create a pressure drop versus a flow rate curve, which could then be applied to the porous region in the model of the full Farmers Screen.

The CFD model of the wedge wires also gave insight into the flow patterns around the wires as shown in *Figure 2*. The strong sweeping flow over the top of the wires drives a recirculation between each wire. These tiny recirculations have the effect of lubricating the flow of water across the top of the screen. The horizontal velocity at the top of each slot reduces the boundary layer in the water above the screen and likely is the cause of agitating any debris that becomes lodged on the screen. It is theorized that this process is a fundamental aspect of the self-cleaning nature of the Farmers Screen.

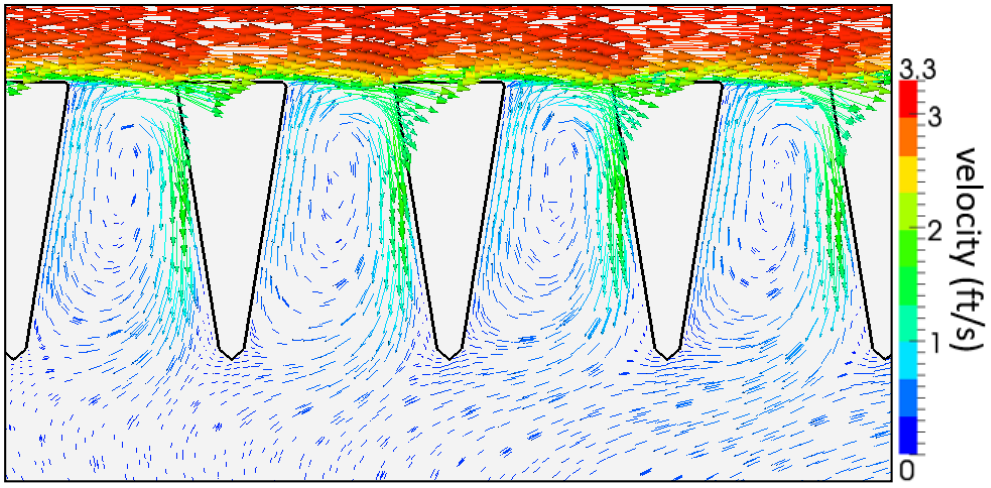

Figure 2 - Vectors colored by velocity on a vertical slice through the wedge-wire model

Boundary Conditions

At the upstream and downstream extents of the CFD model, the boundary conditions must be fixed prior to initiating the model. The boundary conditions for this model were flow rate, water depth, and/or water pressure. These boundary conditions impose artificial constraints on the flow, and care must be taken to ensure that any inaccuracies have minimal effects on the region of interest. The boundary conditions in the CFD model of the Farmers Screen are located at the start of the inlet flume, the irrigation flow exit, and the bypass flow exit (see *Figure 1*).

Calibration of the CFD Model Against Davenport Physical Model Data

The CFD model development took the form of extensive tests of different options for the CFD model inputs described above, as well as other factors such as the turbulence approach and wall roughness. Through this development work, a definitive CFD approach for modeling the Farmers Screen was generated, which provided the closest correlation to the measured data from the Davenport physical model. A detailed description of the model development process is given in *Section 2*.

The resulting CFD model contains assumptions and limitations that yield certain strengths and weaknesses, which must be taken into consideration when interpreting the results. These are discussed in *Section 2.4*.

Comparison of the CFD Model to Davenport Physical Model Data

The CFD model was compared to data from the Davenport physical model at two operating conditions: 1) with the weir wall backwatered and 2) with the weir wall non-backwatered. Selected results are shown below, followed by comments on the comparison to the measured data. Full details of both simulations are given in *Section 2.3.4*.

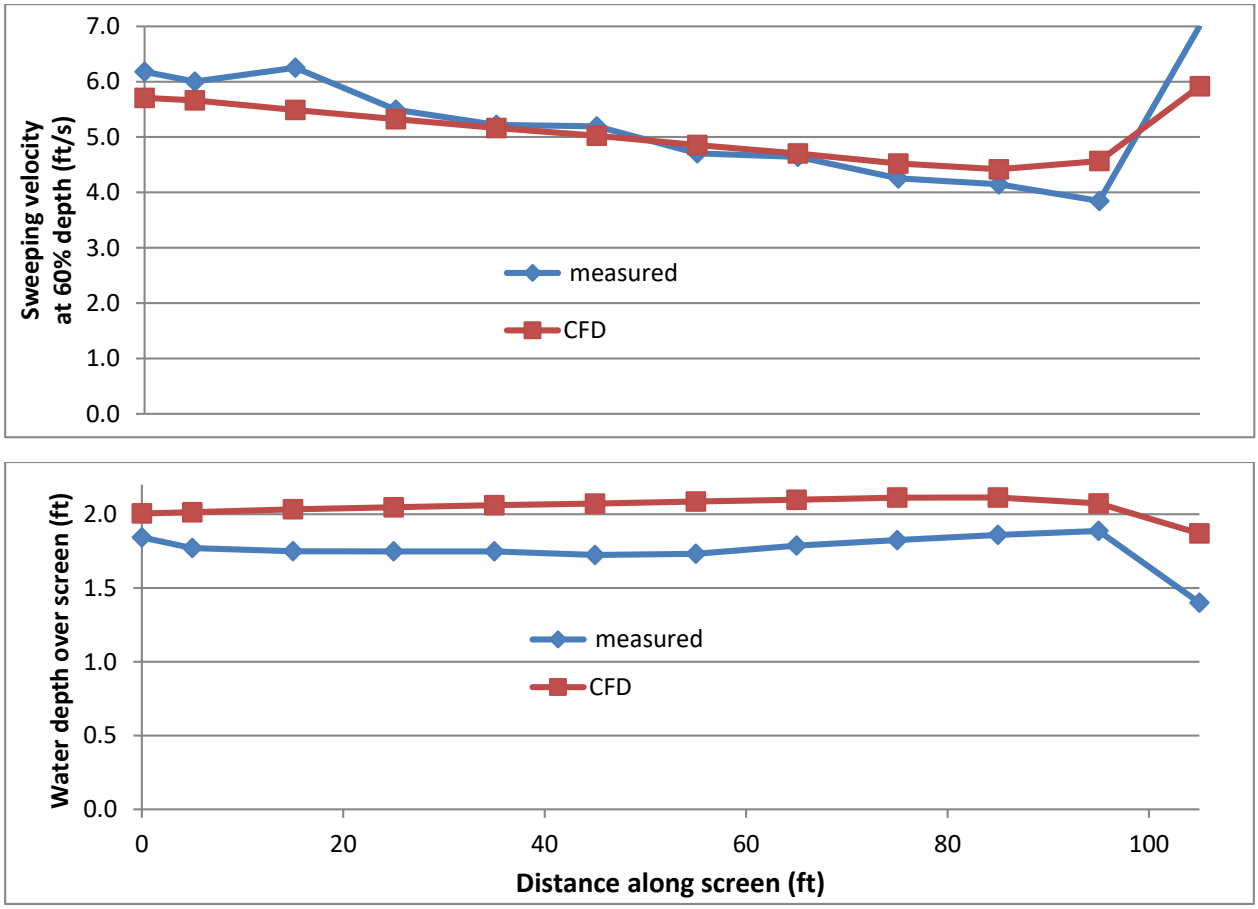

Figure 3 – Predicted sweeping velocity (top) and water depth (bottom) for backwatered weir operation

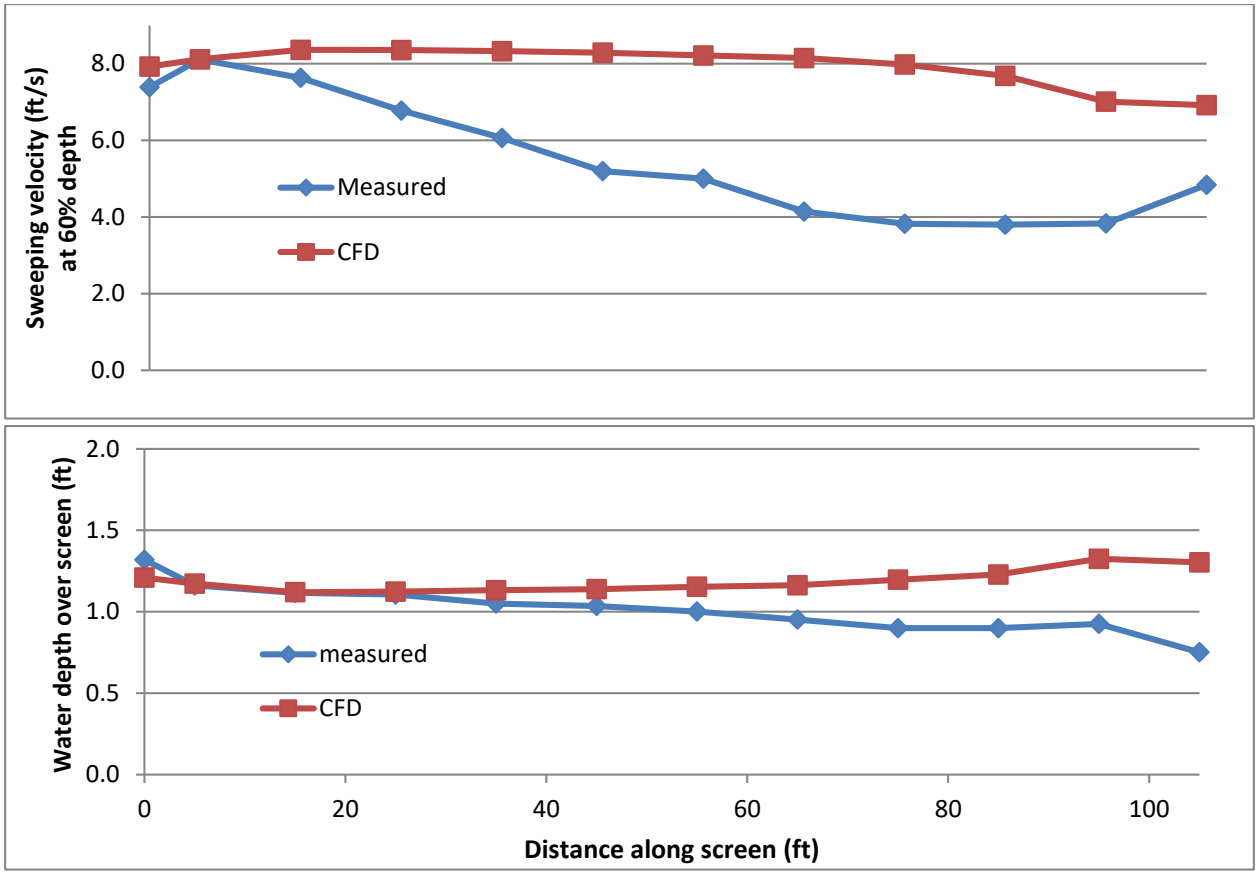

Figure 4 – Predicted sweeping velocity (top) and water depth (bottom) for non-backwatered operation

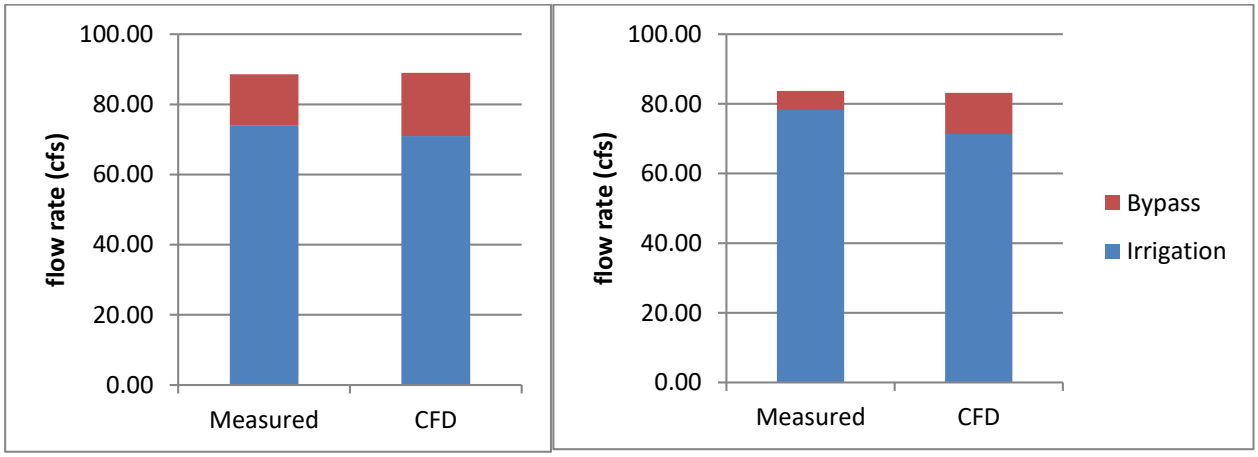

Figure 5 – Predicted flow balance; backwatered (left), non-backwatered (right)

Comments on the Comparison Between CFD and Physical Data

Sweeping Velocity

In the backwatered condition, the CFD model gives a generally good prediction of the sweeping velocity across the screen following both the shape and the magnitude of the measured data (see *Figure 3*).

In the non-backwatered condition, the CFD model shows markedly less deceleration along the screen than was measured. This results in a significant over-prediction of the magnitude of the sweeping velocity towards the end of the screen (see *Figure 4*).

Water Depth

In the backwatered condition, the CFD model over-predicts the water depth over the screen by up to 20 percent. The predicted profile shows a gradually increasing water depth from the beginning to the end of the screen, which is broadly in line with the measured data (see *Figure 3*).

In the non-backwatered condition, the CFD model gives a good prediction of the water depth at the start of the screen, but over-predicts the water depth towards the end of the screen by 30 to 40 percent compared to measured values (see *Figure 4*).

Flow Balance

Despite numerous tests of different treatments for the wedge-wire screen, all CFD models consistently under-predict the amount of irrigation flow compared to the measured data. The effect is more marked in the non-backwatered condition (see *Figure 5*). The CFD model is therefore likely to under-predict the irrigation flow and over-predict bypass flow when applied to the Derby Dam.

Overall

The key benefit of the CFD model of the Davenport screen is that, in combination with the Davenport physical model data, it provides a good indicator of the real-world flows to be expected at the Derby Dam. By applying the same definitive CFD approach to the Derby Dam as to the Davenport screen, the differences between CFD predictions and real-world conditions will be very similar in both cases. Hence, if the CFD model under-predicts the irrigation flow by 5 percent at the Davenport screen, it can be expected to under-predict the irrigation flow by approximately 5 percent at the Derby Dam, when subject to similar flow conditions.

CFD Simulations of the Derby Dam

The definitive CFD model that was developed in correlation with data from the Davenport physical model was then applied to the simulation of one of the four larger screens at the Derby Dam. Three primary CFD simulations of the Derby Dam were performed:

- Run01 - Backwatered weir, maximum irrigation flow
- Run02 - Non-backwatered weir, maximum irrigation flow
- Run07 - Non-backwatered weir, minimum irrigation flow

Selected Results of the Derby Dam CFD Simulations

Selected results from Run01 and Run02 are shown below. Full details of all models are given in *Section 3*.

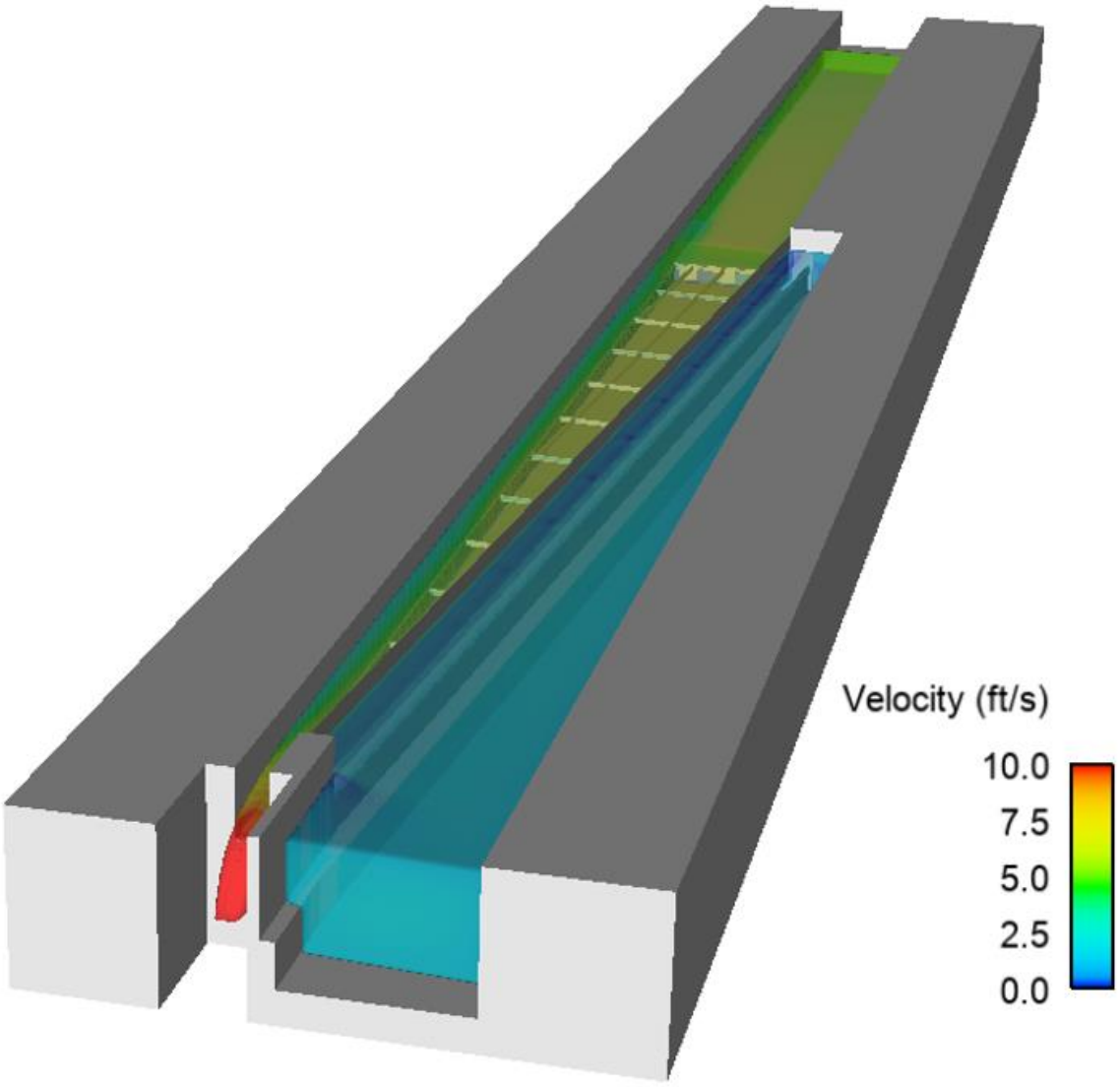

Figure 6 – Overview of the CFD model of the Derby Dam in backwatered operation (Run01)

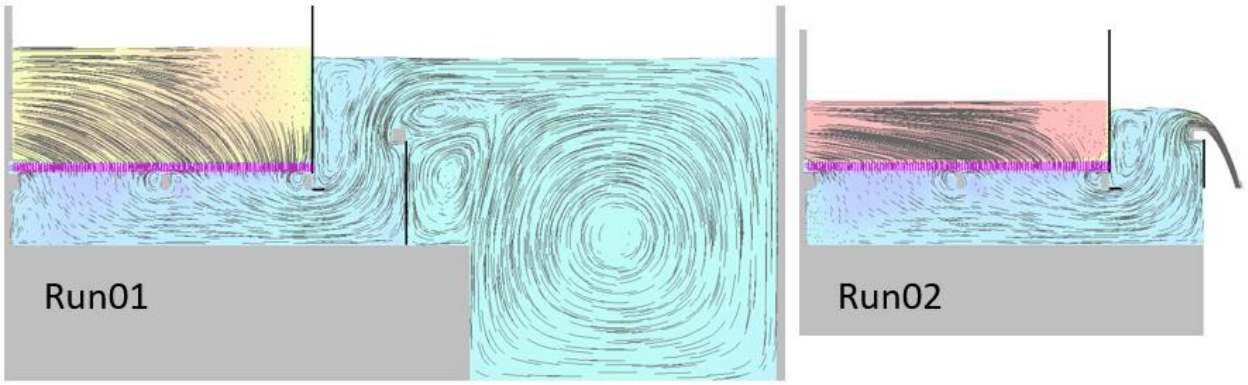

Figure 7 – Vertical slice mid-screen showing streamlines in the plane of the slice

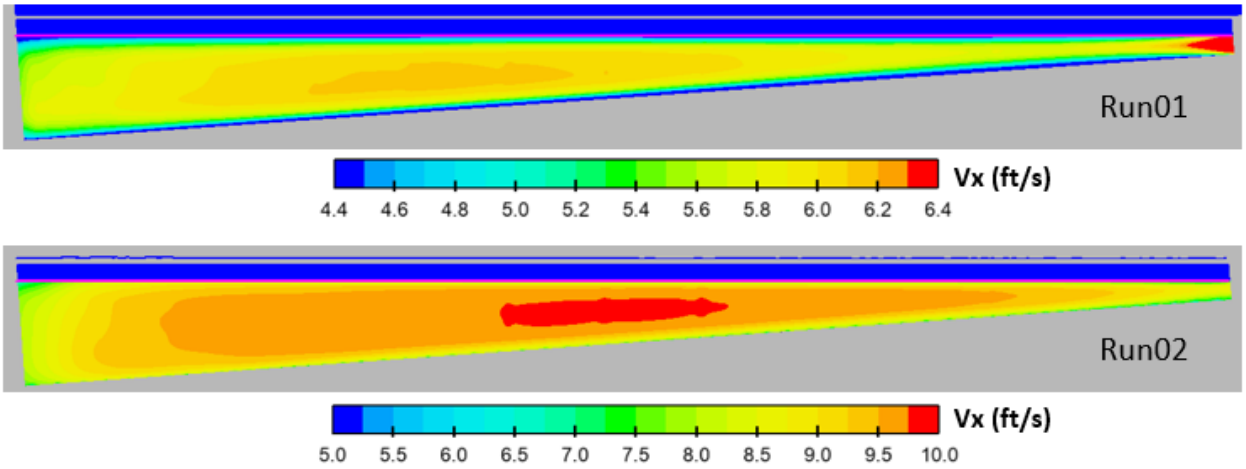

Figure 8 – Contours of sweeping velocity at 5.9 inches above the screen

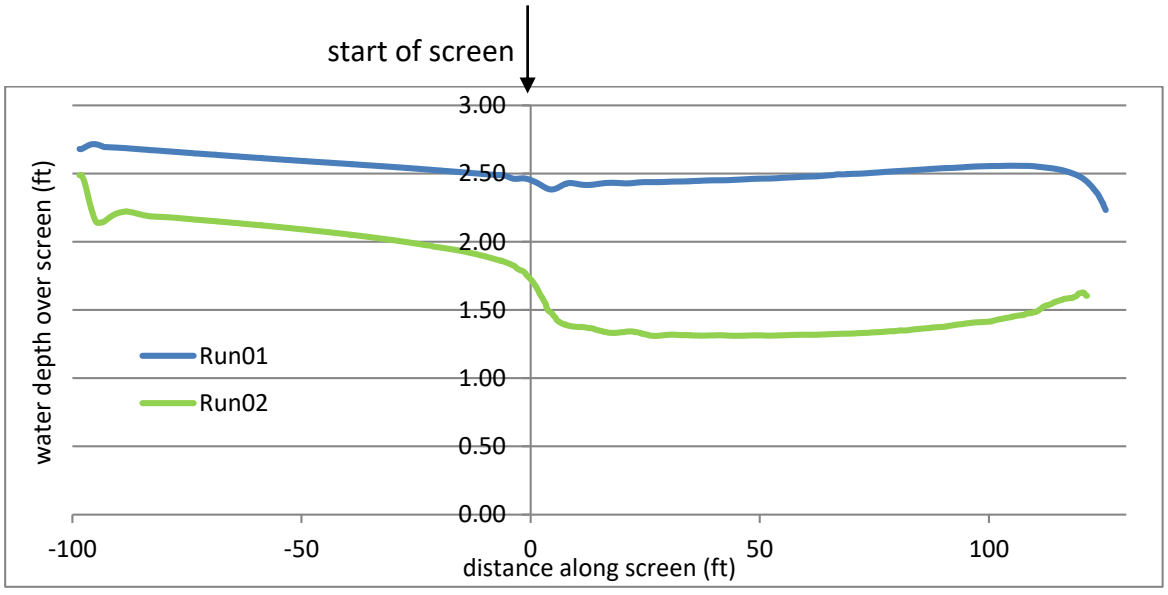

Figure 9 – Predicted water depth along the screen

Key Conclusions from the Derby Dam CFD Simulations

Based on the full set of results in *Section 3*, the following overall conclusions were drawn from the CFD studies of the Farmers Screens at the Derby Dam:

Backwatered Weir, Maximum Flow

With respect to the hydraulic design criteria in *Table 1*:

Sweeping Velocity – The minimum sweeping velocity at the surface of the screen is expected to be 4.5-5.0 ft/s. This is well above the minimum required sweeping velocity of 2.5 ft/s specified in *Table 1.*

Minimum Water Depth – The minimum real-world water level at the Derby Dam fish screens is expected to be approximately 2.2 feet. This is well above the minimum required water depth of 1 foot specified in *Table 1.*

Irrigation Flow – A best estimate is that, given 150 cfs inlet flow at the Derby Dam, approximately 84 percent (i.e., 126 cfs) will go to irrigation and approximately 16 percent (i.e., 24 cfs) will go to bypass.

Weir Not Backwatered

With respect to the hydraulic design criteria in *Table 1*:

Sweeping Velocity – At a maximum flow rate, it is certain that the criterion for sweeping velocity (i.e., >2.5 ft/s) will be met. At a minimum flow rate (65 cfs to irrigation), the sweeping velocities will be approximately 70 percent of those at the maximum flow rate and are also likely to be above the 2.5 ft/s criterion.

Minimum Water Depth – The water depth over the screen will be lowest at minimum flow conditions. The height of the weir wall can be tuned to ensure that this meets the minimum required water depth of 1 foot specified in *Table 1*. At maximum flow non-backwatered conditions, the water depth is predicted to be approximately 0.2 foot higher throughout.

Irrigation Flow – The CFD model predicts 84 percent of flow to irrigation under non-backwatered conditions. However, in similar flow conditions for the Davenport screen, the CFD model predicted 86 percent flow to irrigation when the actual measured value was 93 percent of the total. It is therefore very likely that the CFD model of the Derby Dam is significantly under-predicting the irrigation flow rate at these conditions.

All Operating Conditions

In general, the CFD studies showed that the Derby Dam screens are likely to perform in a very similar manner to the Davenport screen at all operating conditions. The power of this conclusion is that if the Davenport physical model operates successfully, then this gives confidence that the

screens at the Derby Dam will likewise operate successfully. It also reinforces the benefit of the combined approach of using the Davenport physical model and CFD studies to validate the screen performance at the Derby Dam.

1. Introduction

This document presents the results of computational fluid dynamics (CFD) studies conducted by Gilbert Gilkes and Gordon (Gilkes) Ltd for Farmers Conservation Alliance (FCA). The CFD studies form part of a larger program of validation studies undertaken by FCA in order to minimize project risk and optimize the performance of the Farmers Screens being installed by FCA and the U.S. Bureau of Reclamation at the Derby Dam in Sparks, Nevada. These validation studies comprise:

Physical Model Tests - using an existing FCA screen, which was retrofitted to be a near-replica scaled model of the Derby Dam screens.

CFD Studies - to compare to the physical model tests, and used to predict the performance of the screens at the Derby Dam.

The physical model provides real-world data against which to correlate the CFD model. The CFD model provides confirmation that the physical model data are a good indicator of the real-world flows to be expected at the Derby Dam. Utilizing the CFD model and the physical model in combination affords greater benefit than either in isolation, providing a powerful tool for corroborating the Derby Dam Fish Screen design.

1.1 Background

1.1.1 Fish Screens

A fish screen is designed to prevent fish from swimming or being drawn into a diversion from a waterway where water is withdrawn for human use. They are designed to supply debris-free water to the intended use without harming aquatic life. Fish screens typically include some form of barrier that physically prevents the fish from being entrained and enables fish to remain in the natural waterway.

1.1.2 The FCA Screen

FCA designs and manufactures its own fish screen system (the Farmers Screen) for irrigation and hydropower applications. The Farmers Screen is a horizontal, passive fish screen that uses hydraulics to manage debris and protect fish from irrigation and hydroelectric water intakes.

FCA has successfully installed the Farmers Screen at many sites in the northwestern United States. The dimensions and configuration of each Farmers Screen are tailored to the local flow conditions.

FCA was recently awarded a contract by the United States Bureau of Reclamation for a multi-screen installation at the Derby Dam on the Truckee River in Nevada. With a maximum screened flow of 600 cfs in total, the Derby Dam installation will be the largest FCA project to date.

1.1.3 The Davenport Physical Model

An existing FCA screen, known as the Davenport screen, a 90 cfs diversion on the Hood River, Oregon was retrofitted to be a near-replica scaled model of the Derby Dam screens. The retrofitted Davenport screen utilizes the proposed 14:1 taper ratio and has an overall length of 105 feet. This means that the Davenport screen is 20 feet shy of the large screens at the Derby Dam and 15 feet longer than screen 5 at the Derby Dam. In its role as a test facility, the retrofitted Davenport screen is commonly referred to as the Davenport physical model within this report.

FCA engineers gathered data from the Davenport physical model under a number of operating conditions to provide calibration data for the CFD studies. The data included measurements of velocity and water depth across the length and breadth of the screen. The flow rate over the screen was estimated from these measurements.

1.1.4 Gilkes

Gilkes is a UK hydropower company with expertise in fluid flow consultancy and specific experience with the Farmers Screen. Gilkes has previously performed CFD studies for FCA aimed at understanding the flow within the Farmers Screen and the factors affecting performance.

1.1.5 Overview of CFD

CFD is the simulation of fluid flow using computer models. CFD can be applied to any fluid (liquid or gas) in any application from scales of millimeters to kilometers. At its heart, CFD solves the Navier-Stokes equations that govern fluid motion, and, therefore, in theory, it has the capability to accurately predict all aspects of flow. However, the accuracy and applicability of CFD is often limited by the available computer power. With increases in computer power, CFD is increasingly used across a wide range of industries.

1.1.6 CFD in Application to the Farmers Screen

The key benefits of CFD modeling the Farmers Screen are:

- The ability to predict performance of a full-scale screen ahead of the build
- The ability to measure flow parameters at all points within the system, not just discrete locations
- Once a baseline CFD model is built, it is relatively simple to test the effect of changes to the geometry and/or flow
- The ability to test the most efficient operating conditions to optimize performance when multiple screens are required

Specific screen parameters that can be predicted by a CFD model include:

- Sweeping velocity over the screen –the ability of the screen to stay clear of debris and reduce any interaction between fish and the screen surface
- Through-screen velocity – the downward velocity of water passing through the screen
- Water depth – a minimum water depth required for safe passage of fish
- Screened flow as a percentage of total flow
- Flow streamlines through the screen material and structure

Criteria for these parameters are given in the project objectives below.

1.2 Project Objectives

1.2.1 Overall Project Objectives

The general project objectives of the CFD studies are to:

- Develop a CFD model of the Davenport screen
- Calibrate the CFD model of Davenport screen based on field data

  Data and observations from the Davenport physical model as well as data and observations from nearly 50 operating Farmers Screens will be used to compare to the CFD model outputs to optimize the CFD approach.
- Extend the calibrated CFD model to the Derby Dam screens

  The CFD studies will predict how the screens perform in different flow conditions and subject to different layouts and design. The CFD model will thereby aid in verifying the screen geometry, determining the optimum operating ranges, and defining operational sequencing for the Derby Dam project.

1.2.2 Screen Hydraulic Criteria

In addition to the broad project objectives above, there are specific hydraulic requirements for screen performance against which the CFD model predictions can be judged. These are detailed in *Table 2* below. The requirements are taken from a wider set of design criteria for the Derby Dam installation compiled by McMillen Jacobs [1]. In turn, the hydraulic criteria [1] are largely taken from a general set of design criteria and guidelines for the design of fish passage facilities published by the National Marine Fisheries Service Northwest Region [2].

[1] Technical Memorandum No.001 “Design Criteria Rev1” McMillen Jacobs Associates
[2] “Anadromous Salmonid Passage Facility Design” National Marine Fisheries Service Northwest Region, 2011

Table 2 – Hydraulic criteria for the standard size fish screens at the Derby Dam taken from McMillen Jacobs

Criteria	Value	Comments
Minimum water depth over screen	1 ft	Per [2] 11.6.1.7.7
Bypass flow amount per screen	15% of total flow for diversions < 100 cfs 10% of total flow for diversions > 100 cfs	Per [2] 11.6.1.7.8
Screen sweeping velocity	> 2.5 ft/s	Per [2] 11.6.1.7.12, sweeping velocity must be maintained or gradually increase for the entire length of screen
Screen approach velocity	< 0.25 ft/s	Per [2] 11.6.1.7.11, screen approach velocity is calculated by dividing the maximum flow rate by the effective screen area and must be uniform over the entire screen surface area

1.3 Project Exclusions

There are certain aspects of the screen operation that were specifically excluded from the scope of the CFD study prior to commencing the project. These are:

Debris – The CFD model does not simulate debris within the water. Hence, any deposition of debris or sediment on the screen or under the screen will not be modeled. Unless the debris load is exceptionally high, or the screen has become clogged, this is unlikely to affect the accuracy of the CFD predictions. The ability of the screen to self-clean will be inferred from the sweeping velocity and through-screen velocity.

Screen Vibration – It is known that the wedge-wire screen material vibrates when the Farmers Screen is in operation. This vibration and its effect on the water flow is not included in the CFD simulations.

A more detailed discussion of the limitations and challenges of applying CFD to the Farmers Screen is given in *Section 2.1*.

1.4 Project Structure

The CFD studies were split into two stages:

1 Baseline Development

The development and calibration of a baseline CFD model were measured against data from the Davenport physical model. This covered the bulk of the work effort.

The development of the Davenport CFD model is presented in *Section 2*.

2 Derby Dam Fish Screen Analysis

The second stage focused primarily on predicting the performance of the large screens at the Derby Dam using the baseline CFD methods developed in Stage 1.

The CFD predictions for the Derby Dam are presented in *Section 3*.

2. CFD Model Development

This section presents the work undertaken to develop the CFD model to the point at which it could be applied to the Derby Dam. Included in this section are a description of how CFD is applied to the Farmers Screen along with a discussion of the limitations and accuracy of the CFD model.

2.1 CFD for Fish Screen Modeling

2.1.1 Overview of the Farmers Screen

The schematic in *Figure 10* below illustrates the flow of water through a typical Farmers Screen with the key components labeled:

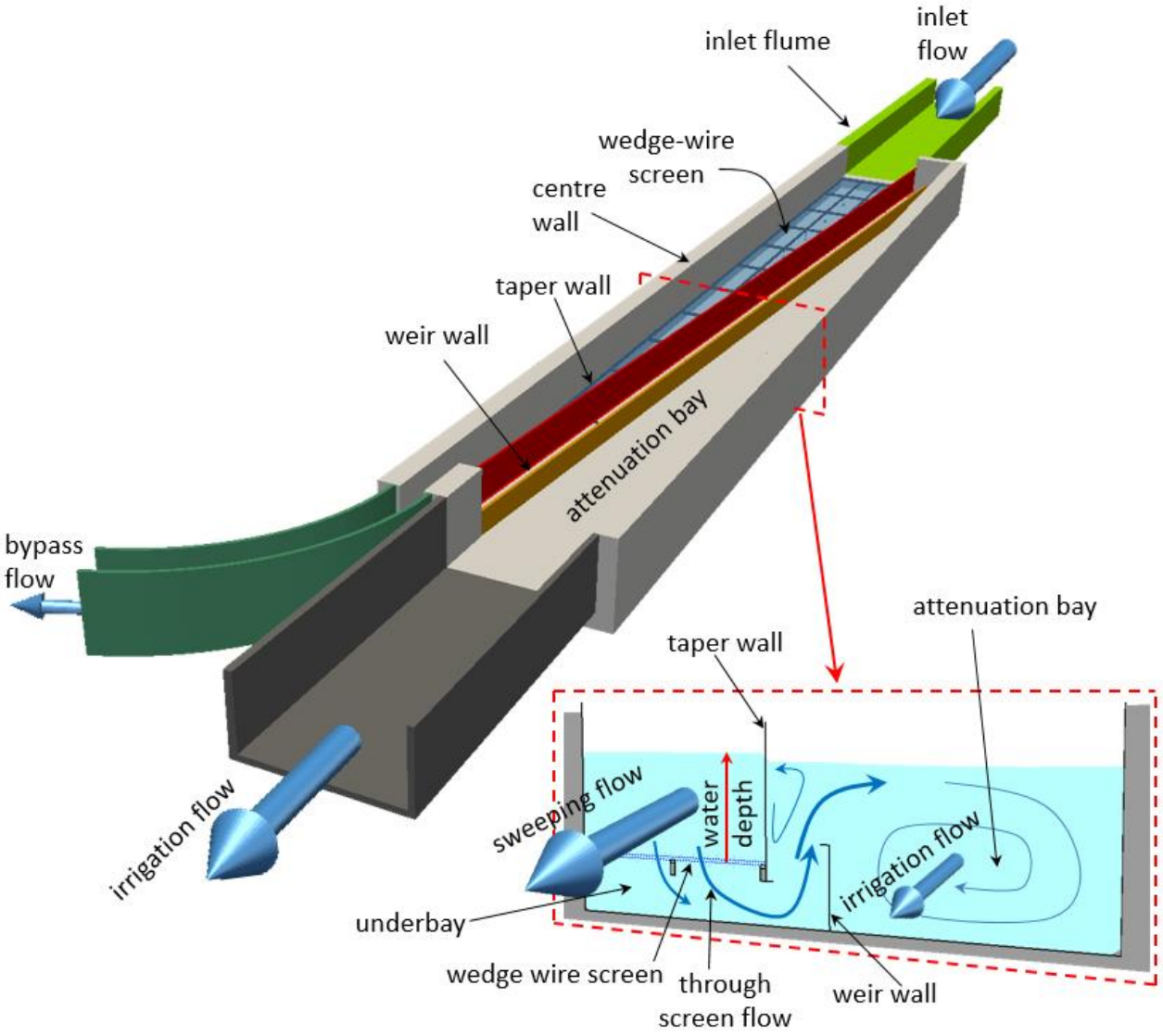

Figure 10 – Schematic of the Farmers Screen

With reference to *Figure 10*:

- Water enters the inlet flume at a controlled flow rate.
- At the end of the inlet flume (screen entrance), the water begins to pass over a porous wedge-wire screen.
- As water passes through the wedge-wire screen, the amount of water above the screen will diminish. The angle of the taper wall in conjunction with the height of the weir wall maintains the velocity and depth of water over the screen.
- Maintaining sufficient speed of water over the screen (sweeping velocity), as well as controlling the flow through the screen, are critical for keeping debris from accumulating on top of the screen and keeping fish moving toward the bypass.
- Water that has passed through the screen flows underneath the screen surface, then up and over the weir wall.
- The depth of water over the screen is controlled by the height of the weir wall, the flow over the weir wall, and the depth of water downstream of the weir wall.
- A minimum one foot of water depth over the screen must be maintained for safe fish passage (see *Table 2*).
- Screened water passes over the weir wall into the attenuation bay and is diverted for beneficial use.
- The remaining flow above the screen passes off the end of the screen (bypass flow) and returns via a channel or pipe to the river, bypassing fish and debris.

2.1.2 Nomenclature

For the purposes of this report, the following naming conventions will be used:

Bypass flow – the flow that does not pass through the wedge-wire screen and returns to the river

Center wall – the concrete wall at the side of the wedge-wire screen furthest from the weir wall

Inlet flow – the flow entering the inlet flume; Inlet flow = Irrigation flow + Bypass Flow

Irrigation flow – the flow passing through the screen material and over the weir wall

Simulated time – the period of time represented by the CFD simulation, e.g., water travelling at 1 ft/s will travel 1 foot in 1 second of simulated time

Simulation time – the length of time taken by the CFD computation, e.g., a CFD model may take 5 hours of simulation time to calculate the flow for 1 minute of simulated time

Sweeping flow, Sweeping velocity – the horizontal component of flow and velocity over the top of the wedge-wire screen in the bypass flow direction

Taper wall – the angled wall at the side of the wedge-wire screen closest to the weir wall, which works together with the weir wall to maintain proper depth and sweeping velocity over the screen

The Farmers Screen – the entire intake system as shown in *Figure 10*

Underscreen bay, Underbay – the region beneath the wedge-wire screen

Water depth – the depth of water above the top surface of the wedge-wire screen

Wedge-wire screen material – the wedge-wire screen described in detail in *Section 2.2*

Weir wall – the vertical wall separating the attenuation bay from the underbay

Note: The term **"Screen"** will be used interchangeably for the Farmers Screen as a whole and the wedge-wire screen. To which it refers, should be apparent from the context.

2.1.3 How CFD is Applied to the Farmers Screen

This section gives an overview of the key elements of a CFD model and how these are applied to the Farmers Screen. This will provide the basis for a more detailed discussion of model development in subsequent sections.

CFD Model Inputs

The inputs to any CFD model comprise: the geometry of the structure being modeled, the mesh, the boundary conditions, the fluid properties, the turbulence model, and other CFD model parameters. Subject to these inputs, the flow can be simulated as accurately as the available computing resources allow. A brief discussion of each of these inputs is given below in reference to a typical CFD model of the Farmers Screen shown in *Figure 11*.

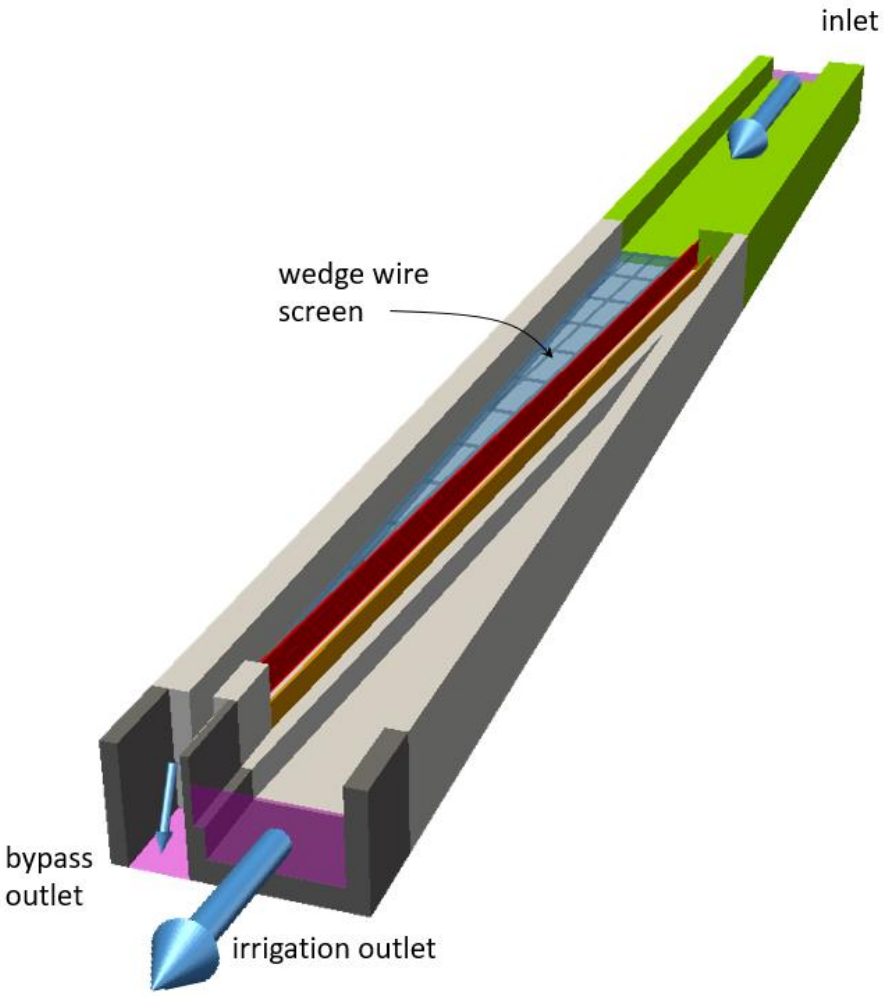

Figure 11 - Typical CFD model of the Farmers Screen

Geometry

Computer-aided-design (CAD) models of the solid bodies with which the fluid interacts are used to define a fluid region. The fluid region contains the area of interest, but also extends upstream and downstream to include regions that will affect the flow in the area of interest. In the case of the Farmers Screen model, the area of interest refers to the wedge-wire screen, bypass flow over the top of the screen, water movement under the screen and over the weir wall, and effects of the taper wall on fluid dynamics. Although the inlet flume was not considered part of the area of interest, it was included in the model upstream of the wedge-wire screen to predict inlet flow conditions.

Mesh

The fluid region is broken down into a mesh containing millions of cells. The size of the cells determines the level of detail that can be captured within the CFD simulation. The number of cells, level of detail, computational time required, and model output accuracy are directly

proportional to one another. Therefore, the more cells included in the mesh, the greater the accuracy of the CFD model, and the greater the simulation time.

The mesh resolution can be varied within the model to resolve areas of greatest flow variability in more detail while increasing the cell size in less critical areas. However, geometric detail smaller than the cells cannot be modeled explicitly and is typically ignored.

In order to keep the simulation time manageable, the smallest cells in the CFD mesh of the Farmers Screen are typically on the order of 1 inch. The wedge-wire thickness (0.07 inch) and wire spacing (0.069 inch) are much smaller than the minimum cell size but are critical to the flow. The wedge wire is therefore modeled indirectly (see *Section 2.2*).

Flow Boundary Conditions

Flow boundary conditions are used at the extents of the CFD model domain, e.g., where the water enters and exits the model, at the air-water interface, and at solid boundaries. At these boundaries, a best estimate of one or more of the flow variables (e.g., velocity, flow rate, pressure, water depth) must be specified. The choice of the location of the boundaries is a trade-off between having an overly large model and applying estimated flow conditions too close to the area of interest. A flow boundary too close to the area of interest could adversely impact the model predictions. Conversely, boundary conditions too far away from the area of interest increase the complexity and simulation time of the model.

The CFD model of the Farmers Screen has three flow boundaries at the extents of the model as shown in *Figure 11*:

- Inlet
- Irrigation outlet
- Bypass outlet

Fluid Properties

The fluid properties determine how the fluid behaves. In the case of the Farmers Screen, the water density and viscosity are set for water at 20°C (68°F). Any variation due to temperature will have negligible effect on the simulations.

Turbulence Model

The velocity and the length scales of flow within the Farmers Screen dictate that the flow will be predominantly turbulent. Turbulence is characterized by chaotic fluctuations at a wide range of length scales. Direct analysis of turbulent flow in CFD is not practical for real life problems. Instead, CFD simulations introduce additional empirical equations or “turbulence models” that describe the effect of turbulence on the bulk flow. Most CFD software will contain a variety of turbulence models that can be employed. The best choice of turbulence model will vary depending on the characteristics of the flow being modeled.

Other CFD Model Parameters

The CFD model contains other parameters internal to the software that affect how the equations are solved. The choice of these parameters is usually a trade-off between the stability of the model, the level of accuracy of the model, and the simulation time.

CFD Simulation

The starting point for the CFD simulation is defining an initial condition. For the Farmers Screen, this is a fixed elevation of stationary water throughout the model. From this initial condition, the CFD model simulates how the flow moves with time subject to the specified inputs. The solution progresses at discrete small timesteps until a steady-state condition is reached that represents the flow at those boundary conditions. In the case of the Farmers Screen, this takes approximately 100 seconds of simulated time.

CFD Outputs

The output from the CFD model is a prediction of all flow variables at each cell in the mesh at the final steady flow condition. In the case of the Farmers Screen model, the flow variables are:

- Water velocity (speed and direction)
- Pressure
- Water surface elevation (relative to the screen)

These can be interpreted graphically or visualized as images of contours, surfaces, and streamlines. A typical flow image from the CFD simulation of a Farmers Screen is shown in *Figure 12* below.

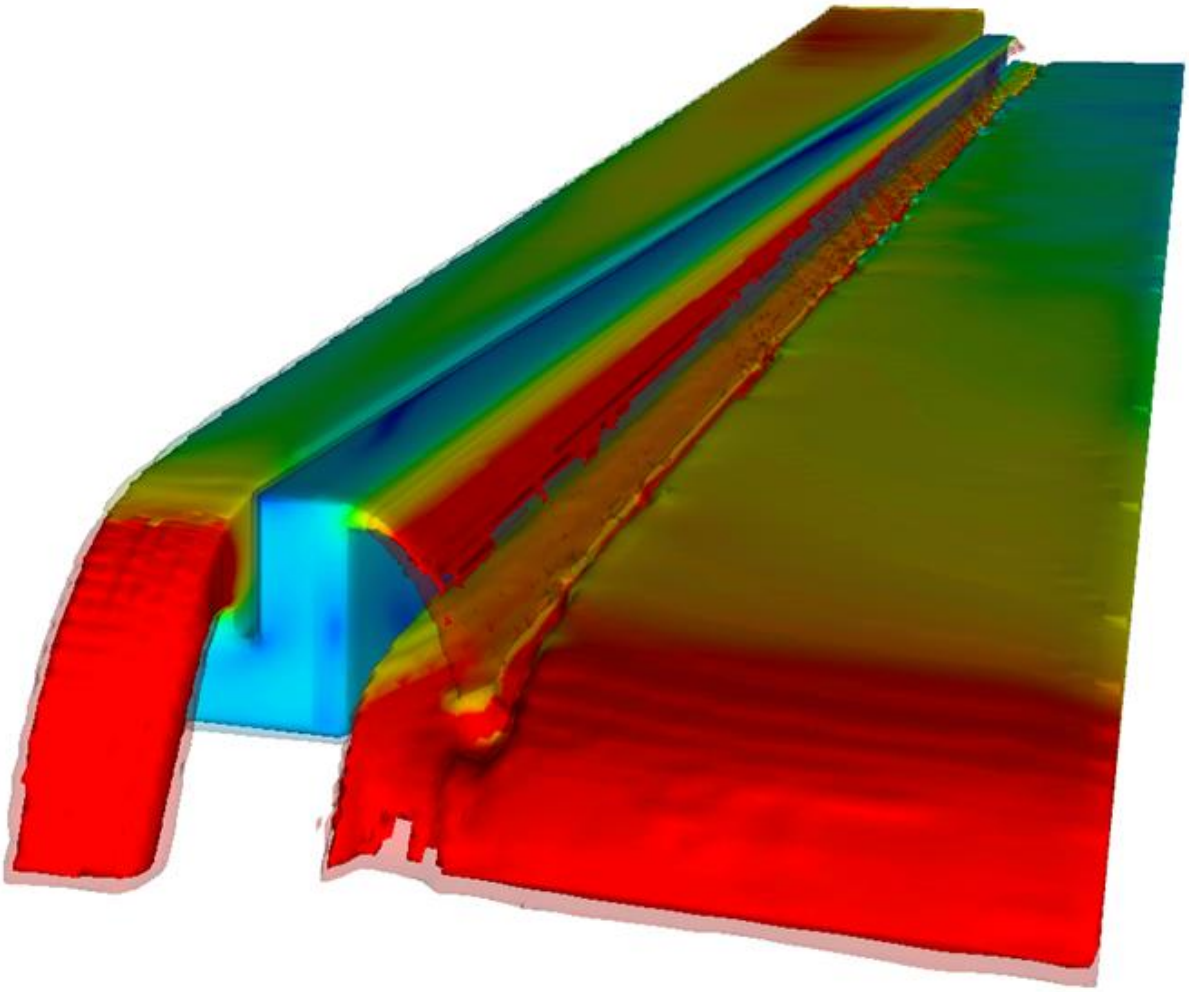

Figure 12 - Water surface colored by velocity in a typical simulation of the Farmers Screen

Challenges of Modeling the Farmers Screen

The Farmers Screen presents some particular challenges for CFD modeling, specifically:

Wide range of length scales

- Scales range from the order of 0.1 inch (slots between the wedge wires) to the order of 100 feet (the overall length of the screen). This places requirements on the mesh size and consequent simulation time that would be prohibitive without an approximation of the wedge-wire screen hydraulics.

Wide range of time scales

- The timestep at which the CFD model progresses is constrained by the requirement that fluid cannot traverse more than one cell in one timestep. This places a further penalty on the simulation time required for more detailed meshes. Typically, a CFD timestep on the order of 0.001 second is the minimum that can be used, given that on the order of 100 seconds simulated time is required for steady flow conditions to be reached.

2.1.4 Choice of CFD Software

Different CFD codes all solve the same Navier-Stokes equations. However, each CFD software will tend to be more or less tailored to certain types of application.

Gilkes has previously attempted analysis of earlier versions of the Farmers Screen using the market leading CFD software, ANSYS Fluent. This is a general-purpose software suitable for simulation of any fluid flow problem.

By contrast, Flow-3D, from Flow Science, is a CFD code developed specifically for solving transient free-surface problems such as dam-breaks and spillways. For these types of modeling applications, Flow-3D has algorithms that aim to achieve greater accuracy for the same level of computational effort as ANSYS Fluent.

An early part of the CFD work on this project was to evaluate the benefits of Flow3D simulation of the Farmers Screen. The evaluation comprised:

- a review of existing studies, in particular the application of Flow3D to a vertical fish screen by Isfahani [3]
- application-specific training from Flow Science consultants XC Engineering
- tests of simple Flow3D models to test different elements of the intended approach to simulating the Farmers Screen

The conclusion of the evaluation process was that Flow3D offered a better compromise between accuracy and computational requirements than ANSYS Fluent for modeling the Farmers Screen. Therefore, it was decided to continue the project using the Flow3D software.

2.1.5 Requirements for Model Development

Once the choice of CFD software was finalized, the next stage of the project was to develop a CFD model that would give accurate predictions of the flow through the proposed screen design for the Derby Dam.

In theory, the flow at the Derby Dam could be predicted by simply creating a mesh of the geometry, applying the desired flow rate, and running the software. In practice, the accuracy of such a CFD model would be unknown and would likely be poor. This is because numerous choices must be made by the user when creating a CFD model of the Farmers Screen in order to keep the problem within a manageable size and timescale (e.g., mesh resolution, CFD settings, and geometry simplifications).

Instead, the best practice for CFD simulation of the Derby Dam horizontal screen was determined by validation and calibration against real-world data from the Davenport physical model. This

[3] “CFD modeling of fish exclusion screens” Isfahani, A., presented at Fish Passage 2018

development phase formed the bulk of Gilkes' work on the project, and is described in more detail in *Section 2.3*.

A secondary development study was performed to determine the best approach to simulating the wedge-wire screen. This is described in *Section 2.2*.

2.2 Model of the Wedge-Wire Screen Material

2.2.1 Introduction

The surface material of the Farmers Screen is made of wedge wires aligned transverse to the flow of water over the screen and welded to a framework of supports at 3-inch-by-6-inch spacing (see *Figure 13* below and *Figure 14* over).

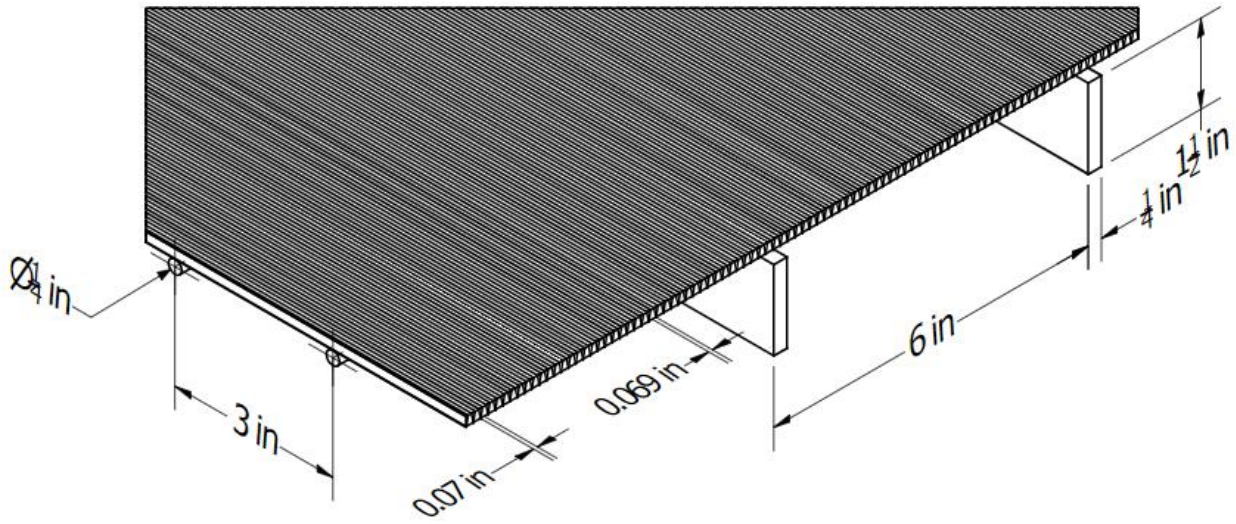

Figure 13 - Dimensions of the wedge-wire screen

The wires are 0.070-inch wide with a spacing of 0.069 inch between the wires, resulting in an open area of approximately 50 percent.

To simulate the flow of water around and between the wires in CFD, a simulated cell size, in Flow3D, on the order of 0.02 inch would be required. The larger screens at the Derby Dam each have a wedge-wire area of approximately 800 square feet. This would require a CFD mesh of over 1 billion cells to model the entire wedge-wire screen surface. Due to the computational power required, for the foreseeable future, this is well beyond the scope of any CFD model.

Therefore, the screen material must be approximated within the CFD model of the full installation. The standard approach to approximating sub-grid scale barriers in CFD, and the approach taken by Isfahani [4], is to define the screen material as a porous zone with the same

[4] "CFD modeling of fish exclusion screens" Isfahani, A., presented at Fish Passage 2018

large-scale flow properties as the actual screen. The porous zone has no internal geometric detail, and hence can be meshed with much larger cells.

While there will be some localized flow patterns created due to the wedge shape of the wires, the key global property of the screen is to provide a resistance to flow. Flow resistance characteristics for screens can usually be calculated from empirical formulae (see for example "Internal Flow Systems" by Miller [5]). However, these formulae assume the flow approaching the screen is normal to the screen. In the case of the Farmers Screen, water typically moves over the screen at approximately 20 times the speed at which it moves through the screen (see *Figure 14* below). This creates very different flow patterns and flow resistance characteristics.

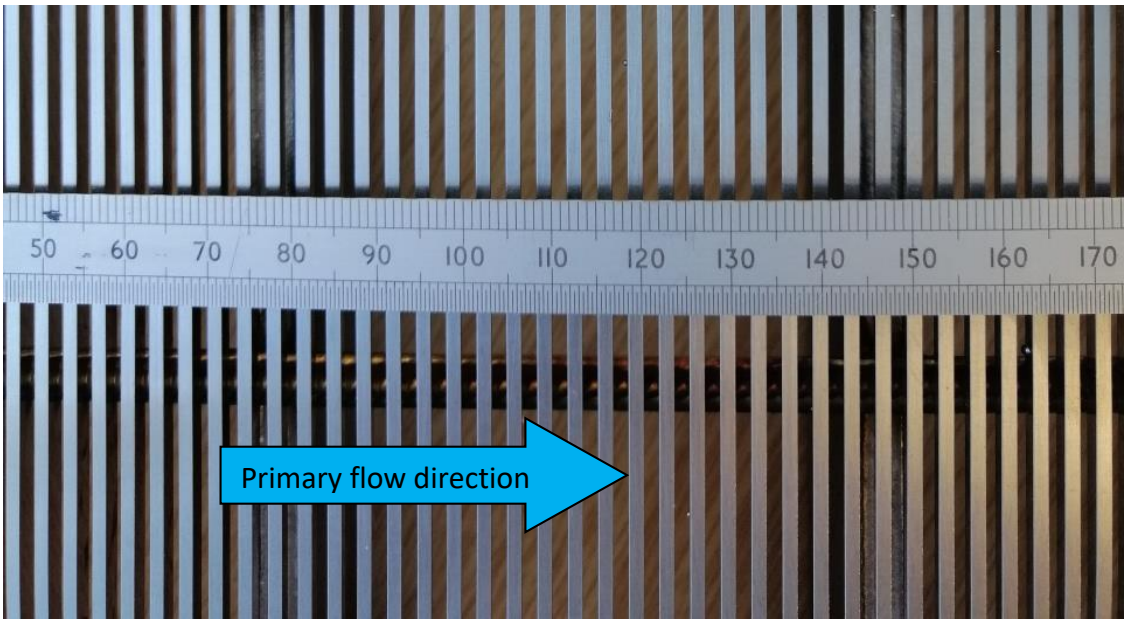

Figure 14 - Photo looking down on wedge-wire screen with millimeter rule for scale

To determine an appropriate flow resistance for this "cross-flow" operation, the current study used a small-scale CFD model of a representative 2-inch-by-3-inch portion of the screen. At this scale, the full detail of the flow in and around the wires could be captured within a manageable number of cells.

The details of the small-scale CFD model of the wedge-wire screen and the predicted flow properties are presented below.

[5] "Internal Flow Systems" Miller 2nd Edition 1990

2.2.2 Detailed CFD Model of the Wedge-Wire Screen

Model Geometry

The CFD model geometry is shown in *Figure 15*. The model comprises a single 2-inch-by-3-inch section of the wedge-wire screen. The model extends above and below the screen as shown.

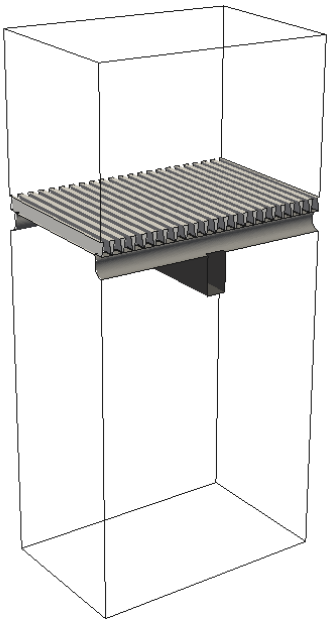

Figure 15 - Geometry of CFD model of wedge-wire screen

Mesh

This small portion of the screen was meshed with 4.1 million cells with increased resolution around the wedge wires. A slice through the mesh around the wires is shown in *Figure 16*.

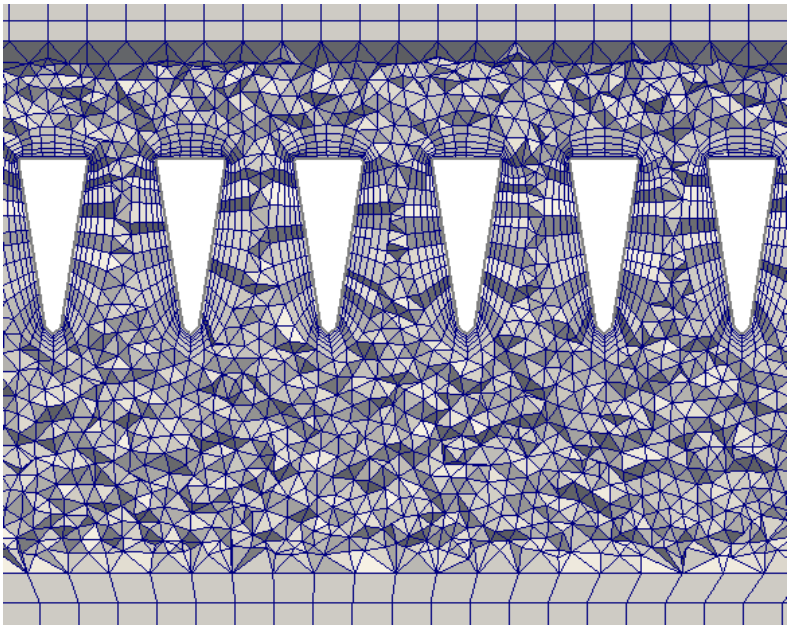

Figure 16 - Slice through the CFD mesh of the wedge-wire screen

Boundary Conditions

The repeating nature of the screen's geometry is captured by the use of symmetry and periodic boundaries in the CFD model, such that the flow sees an unlimited area of screen stretching in the longitudinal and transverse directions as shown in *Figure 17.*

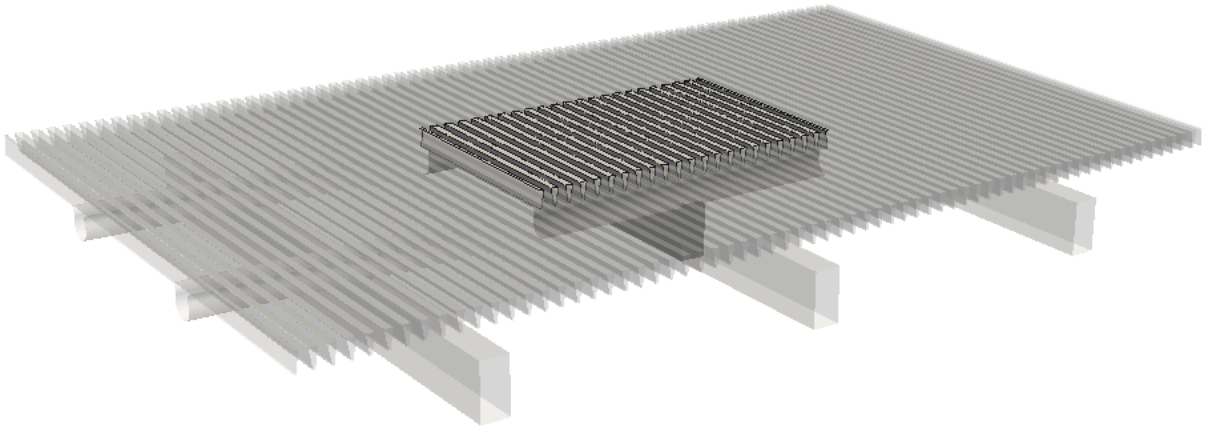

Figure 17 - Extension of screen (unlimited), as seen by the flow in the CFD model

Two sets of simulations were performed to compare the performance of the screen in a conventional "through-flow" condition and in the "cross-flow" condition that will be present in the Farmers Screen (see *Figure 18*).

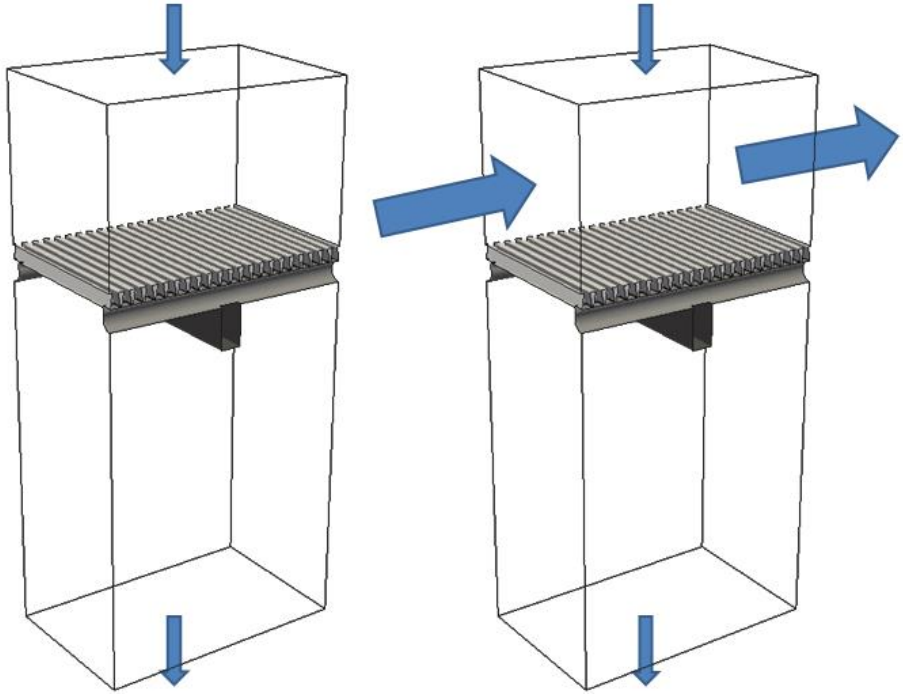

Figure 18 - CFD model inputs; through-flow model (left), cross-flow model (right)

In both models, water is drawn through the screen by applying a fixed uniform velocity into the top face of the model above the screen and out of the bottom face of the model below the screen (see *Figure 18*).

In the "cross-flow" model, a sweeping velocity across the top of the screen of approximately 3.5 ft/s is also included by fixing the mass flow of water over the screen.

In all simulations, the pressure is measured a short distance above and below the wedge wire to give the pressure drop across the screen.

By varying the vertical velocity through the screen, the CFD model can be used to establish a relationship between the flow rate through the screen and the pressure drop across it.

Other CFD Inputs

It is assumed that the whole extent of the CFD model is submerged beneath the water surface. This means that only the water flow needs to be simulated (single-phase flow), and avoids the additional complexity of modelling the air-water interface (multi-phase flow).

While the flow above the screen will be turbulent, the small spacing and relatively low through-screen velocities mean that laminar flow may exist in the slots between the wedge wires. In a CFD model, the flow must be specified prior to simulation as either laminar or turbulent. In order to determine the best approach, separate CFD simulations were performed assuming turbulent flow and laminar flow. These showed little difference in the flow resistance, therefore the laminar flow model was not pursued. The results presented below are for turbulent flow simulations using the realizable k-epsilon turbulence model.

Simulations of the 2-inch-by-3-inch wedge-wire screen section were performed using ANSYS Fluent v19.0, as it is well-suited for this type of small-scale single-phase flow.

Assumptions

As noted in *Section 1*, the CFD simulations do not take into account any screen vibration or the effect of any sediment present in the water. Further discussion of the effect of these assumptions is given in *Section 2.4*.

Results

Flow Visualization

The predicted flow patterns between the wedge wires for the "through flow" and "cross flow" CFD models are compared in *Figure 19* and *Figure 20* below.

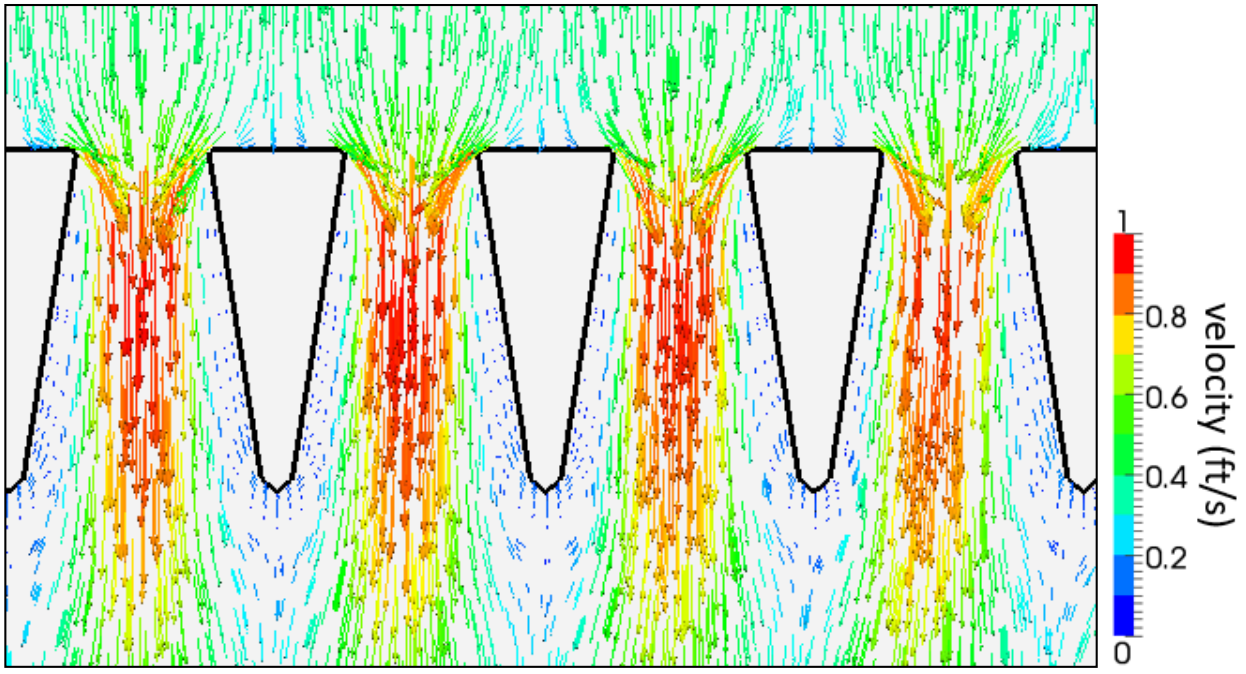

Figure 19 - Vectors colored by velocity on a slice through the “through-flow” model

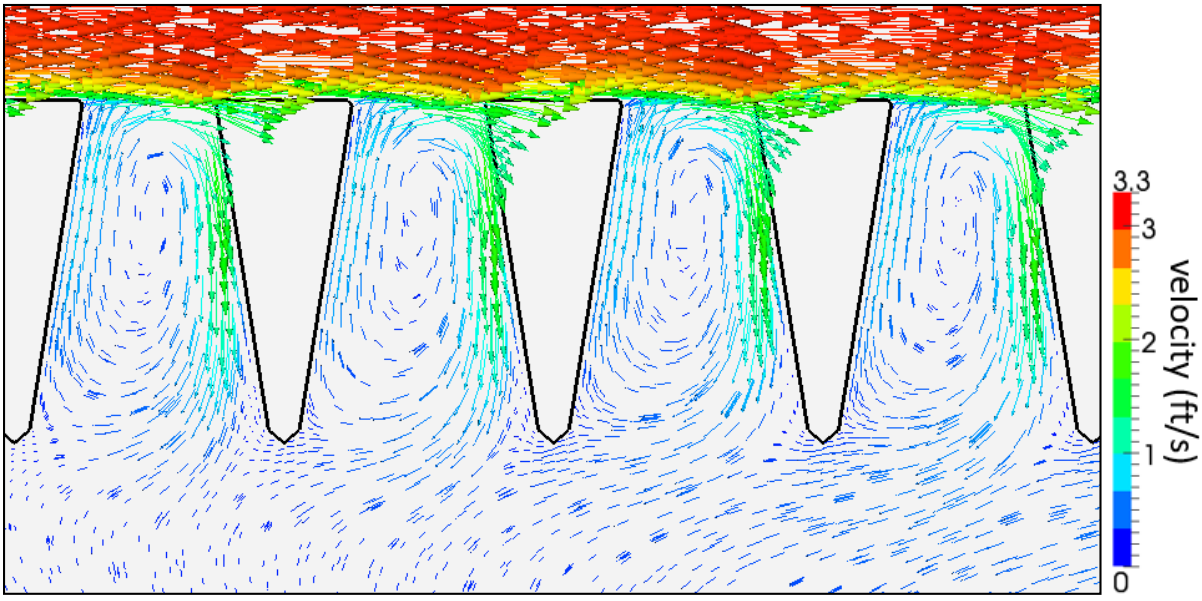

Figure 20 - Vectors colored by velocity on a slice through the “cross-flow” model

As expected, there is a large difference in how the water interacts with the wires between the two simulations. In the “through-flow” model, a fast downward stream of water is seen between the wires. However, in the “cross-flow” model, the strong sweeping flow over the top of the wires drives a recirculation between each wire. This dramatically reduces the space for downwards flow and will tend to increase the flow resistance.

These tiny recirculations between each wedge wire have the effect of lubricating the flow of water across the top of the screen. The horizontal flow velocity at the top of each slot reduces the boundary layer in the water above the screen and will likely agitate any debris that becomes

lodged on the screen. It is theorized that this process is a fundamental aspect of the self-cleaning nature of the Farmers Screen.

Pressure Drop

Figure 21 shows the predicted relationship between pressure drop and flow rate from the CFD models of the two flow conditions.

The pressure drop across the screen is much higher in the "cross-flow" case. Nevertheless, the pressure drop is still relatively small; 250 Pa being equivalent to 1 inch of head loss.

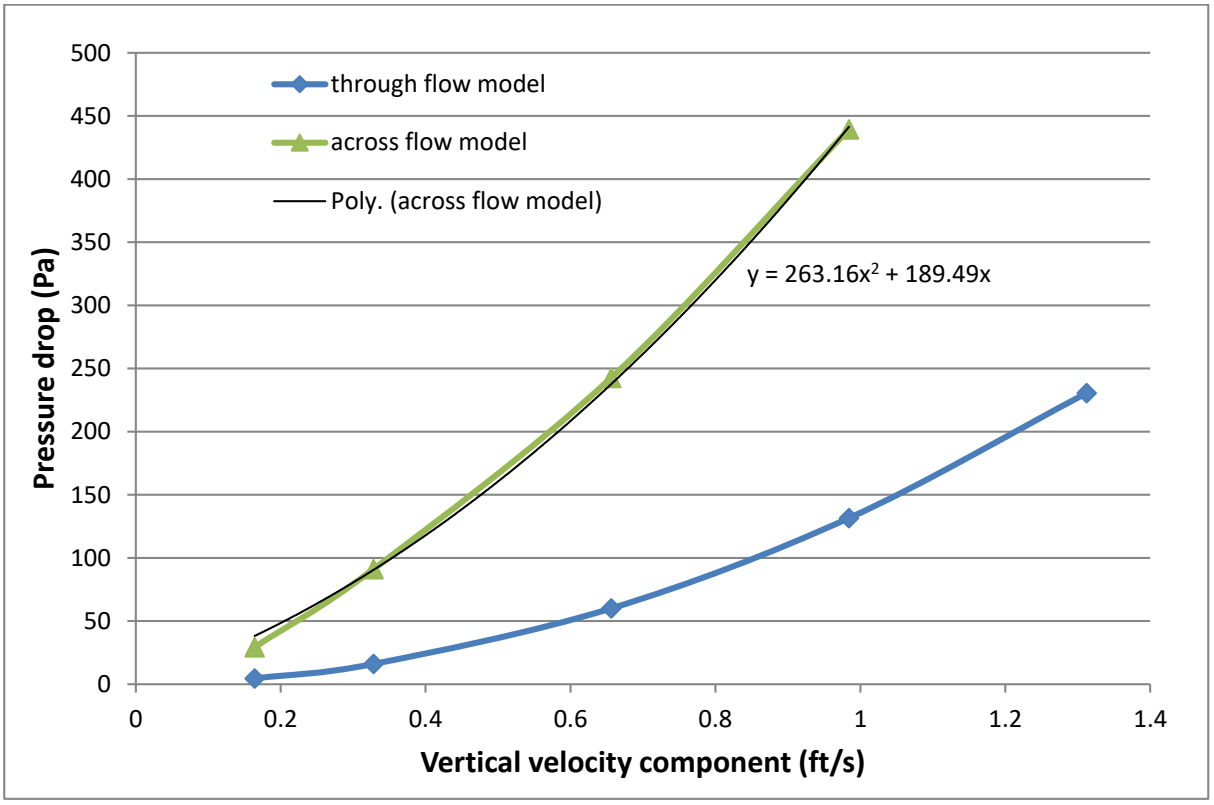

Figure 21 - Prediction of pressure drop versus flow rate for the CFD models of the wedge wire

2.2.3 Approximation of the Screen Material Within the Full CFD Model of the Farmers Screen

As discussed above, the CFD models developed for this study of the entire Farmers Screen require an approximation of the wedge-wire screen. This is modeled as a porous region with the same flow resistance. A porous region is achieved in Flow 3D by applying a "Drag Model" to the screen region that specifies the relationship between pressure drop and flow rate.

Drag Model

Flow3D software contains two main drag models for saturated porous media:

Darcian drag model, in which $\Delta P = a\mu V$

Forchheimer drag model, in which $\Delta P = a\mu V + b\rho V^2$

where ΔP (Pa/m) is the pressure drop per unit thickness across the screen

V (m/s) is the superficial velocity through the screen

μ (kg/m-s) is the fluid viscosity

ρ (kg/m^3) is the fluid density

and "a" and "b" are coefficients with units (1/m^2) and (1/m) respectively

Given the shape of the predicted pressure drop versus flow rate curve shown in *Figure 21*, the Forchheimer model was chosen with coefficients a and b calculated from the quadratic trendline equation.

Mesh Resolution

Tests were performed on simplified models in Flow3D to evaluate the effect of the mesh resolution of the porous screen region. As with other settings, the choice is a tradeoff between accuracy and run time. The chosen method was to use a porous region, approximately 4/5-inch thick, extending across parts of three cells, as shown in *Figure 22*. At this resolution, the porous region is still much deeper than the wedge wires, which are 3/16-inch deep. To compensate for this, the pressure drop per inch is adjusted to give the required overall resistance.

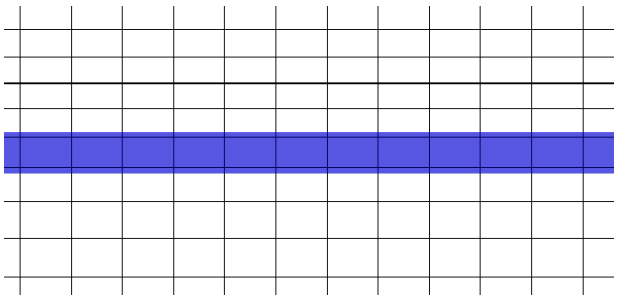

Figure 22 - Porous region (blue) within the CFD mesh of the Farmers Screen

Directional Porosity

The orientation of the wedge wires is such that the flow resistance will be different in the three orthogonal directions. While the screen is 50 percent open when viewed from above, it could be considered to be significantly less open in the direction of flow along the screen. This is because of the recirculations between the wires causing resistance to flow as shown in *Figure 20*. Further tests were performed on a simplified Flow3D model to determine appropriate porosities in the x, y, and z directions.

Exact details of the Flow3D model settings can be found in *Appendix A*.

2.3 Correlation of the CFD Model to Test Data from the Davenport Physical Model

This section describes the work done to define the CFD best practices for simulating the Farmers Screen prior to applying the CFD model to the Derby Dam. Best practices were determined by developing and calibrating the CFD model against the test measurements taken from the Davenport physical model. This section formed the bulk of Gilkes' work on the project.

The Davenport screen on the Hood River, Oregon was one of the first installations of the Farmers Screen. As part of the Derby Dam project, the Davenport screen was retrofitted as a near-replica scaled model of the proposed Derby Dam design. At 105 feet in length, the retrofitted Davenport screen is 20 feet shy of the large screens at the Derby Dam and 15 feet longer than screen 5 at the Derby Dam. A photo of the retrofitited Davenport screen is shown in *Figure 23* below.

As well as testing the overall screen performance, the Davenport screen was used to collect measurements of flow velocity and water depth to calibrate and compare to the CFD model. By varying the inlet flow rate and downstream conditions, a variety of conditions including high flow, low flow, backwatered, and free flow over the weir could be tested and logged at Davenport.

Figure 23 – The re-built Davenport screen prior to operation

2.3.1 Davenport Physical Model Data

FCA engineers gathered flow data from Davenport physical model under a number of operating conditions. Flow data included velocity measurements in the three component directions and water depth measurements at 12 transects along the length of the screen. One transect was taken at the inlet flume as a control. At each transect, measurements were taken at up to 10 locations across the width of the screen as shown in *Figure 24.*

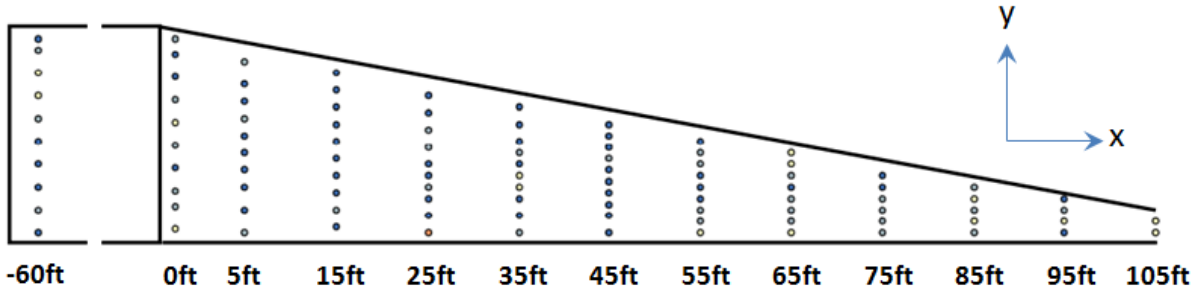

Figure 24 – Schematic of Davenport screen showing location of measurement points

At each of the (x,y) locations shown in *Figure 24*, velocity measurements were taken at three heights in the water column based on the local water depth over the screen: 20 percent depth, 60 percent depth, and 80 percent depth. The flow rate over the screen was estimated at each transect using a weighted average of the measurements at each depth that accounts for the vertical velocity profile.

For comparison to CFD predictions, the sweeping velocities at the data points shown in *Figure 24* above were interpolated onto three lines: 9 inches from the taper wall, 9 inches from the center wall, and mid-channel as shown in *Figure 25* below.

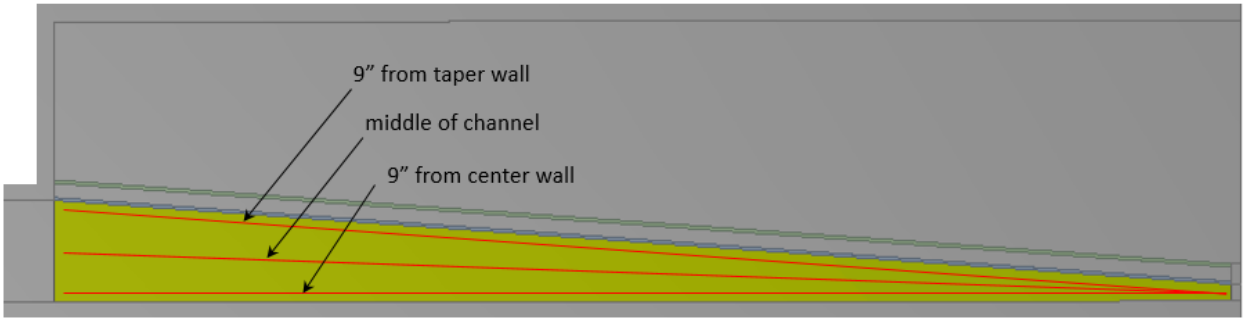

Figure 25 – Location of lines for comparison of sweeping velocity to CFD predictions

The three lines were replicated at each of the three water depths (20-percent, 60-percent, and 80-percent depth), giving a set of comparison points at each transect, as shown in *Figure 26* below.

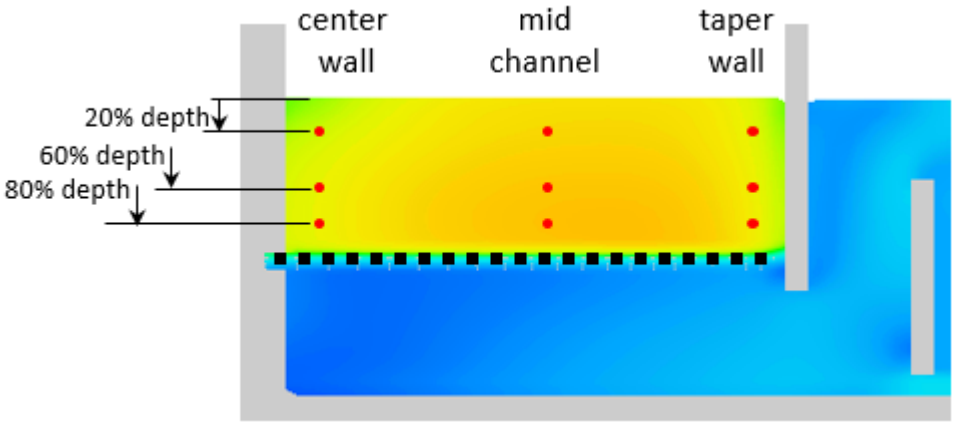

Figure 26 – Location of points at each transect for comparison of sweeping velocity to CFD predictions

Measured data were gathered at four operating conditions, as detailed in *Table* 3 below. In operating conditions 1 and 2 (OP1, OP2), there was a gap under the weir wall, creating a high velocity area to clear sediment and silt from under the screen. This gap is necessary at Davenport, since the water frequently carries a very high glacial sediment load.

Table 3 – Operating conditions at Davenport screen

Operating point	Inlet flow rate	Weir flow	Weir height	FCA data
OP1	88.6 cfs	backwatered	11.25” above screen 3” gap under weir	Survey Summary_20190618.xls XYZ_Velocities_20190618.xls
OP2	93.2 cfs	semi-backwatered	11.25” above screen 3” gap under weir	DV3_Flow Survey_20190625.xls
OP3	83.6 cfs	backwatered	8.25” above screen no gap	DV5_Backwatering_20190718.xls
OP4	83.7 cfs	no backwatering	8.25” above screen no gap	DV4_No Backwatering_20190717.xls

Operating conditions OP3 and OP4 are more closely representative of the installation at the Derby Dam, where the lower sediment load does not necessitate a gap under the weir wall. The operating condition OP3 represents a situation in which there is sufficient flow in the canal, and hence sufficient water depth in the attenuation bay, so that the weir wall is fully submerged or backwatered. Operating condition OP4 represents the non-backwatered situation in which the water level in the attenuation bay is far enough below the top of the weir wall not to influence the flow upstream.

2.3.2 Davenport CFD Model Geometry

A CFD model of the Davenport screen was created based on drawings supplied by FCA. The CFD model extends from the inlet flume, 54 feet upstream of the porous screen, to the exit, to the attenuation bay, and to the point at which water falls off the end of the screen into the bypass channel as shown in *Figure 27* below.

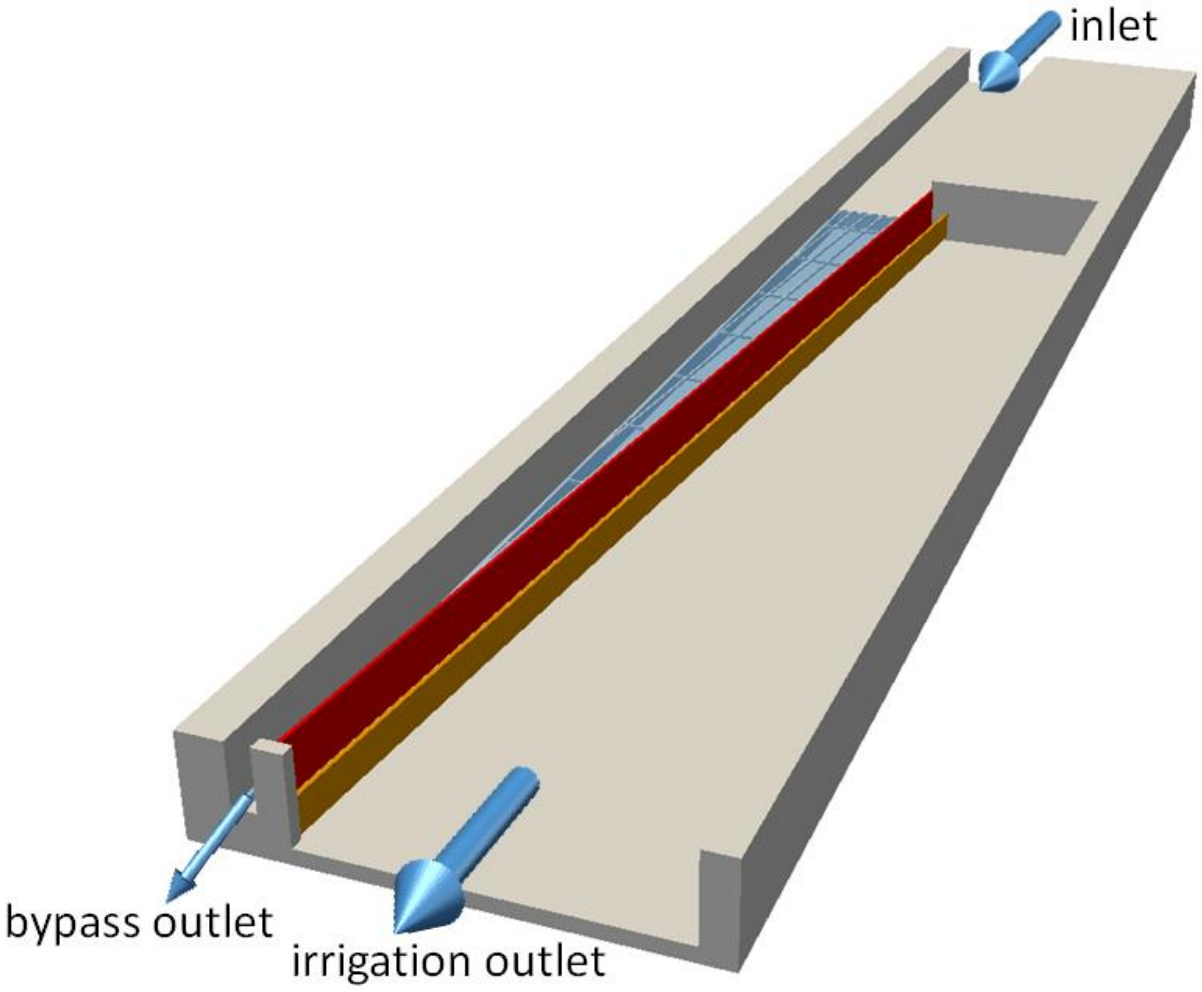

Figure 27 – CFD model geometry

In order to reduce the mesh size and consequent simulation time, the CFD model contains a number of simplifications to the geometry. In particular:

- Small features close to or below the level of resolution of the CFD mesh were omitted, e.g., the legs beneath the screen support frame and the legs beneath the taper wall (see *Figure 28*).
- The taper wall was turned from a thin-wall structure to a solid wall of equivalent thickness (see *Figure 28*).
- As discussed in *Section 2.2*, the wedge-wire screen was approximated as a porous region without geometric detail but with a specified flow resistance.

- The frame that supports the wedge-wire screen was re-oriented to be parallel to the taper wall rather than parallel to the center wall (see *Figure 28*). This was done because the mesh lines run parallel to the taper wall and the frame could be resolved better in this orientation.
- The attenuation bay was blocked upstream of the start of the screen to reduce the mesh size.

Other than the approximation of the wedge-wire screen, these simplifications are expected to have negligible effect on the predicted flow measurements in the region of interest within the CFD model.

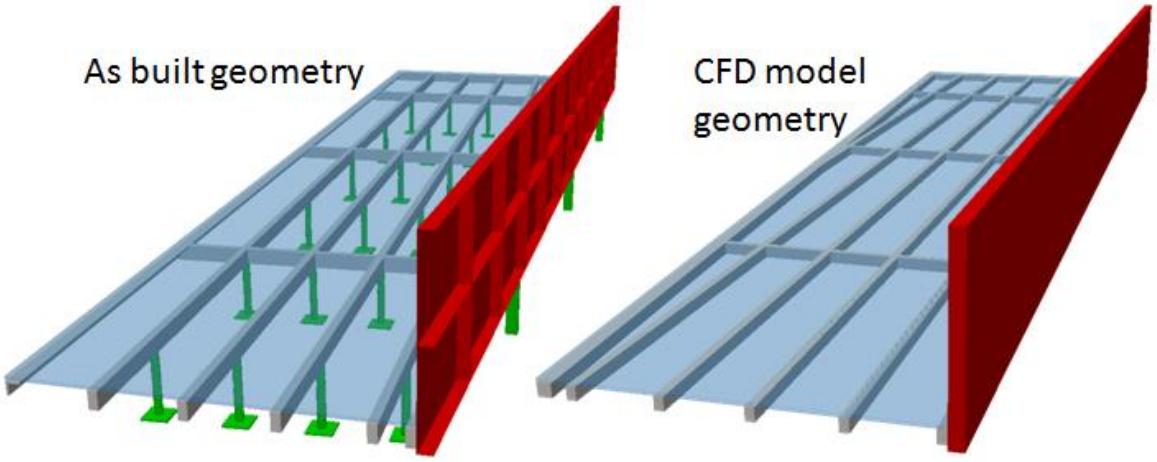

Figure 28 – Simplification of geometry within the CFD model

2.3.3 Evaluation of CFD Settings

The performance of each CFD simulation was judged by how well it correlated to test data for three key measures as shown in *Figure 29* below:

Sweeping velocity – the speed of flow of water over the screen in the bypass direction

Water depth – the depth of water above the screen

Flow balance – the proportion of the inflow into the screen that goes to irrigation versus the proportion that returns as bypass flow

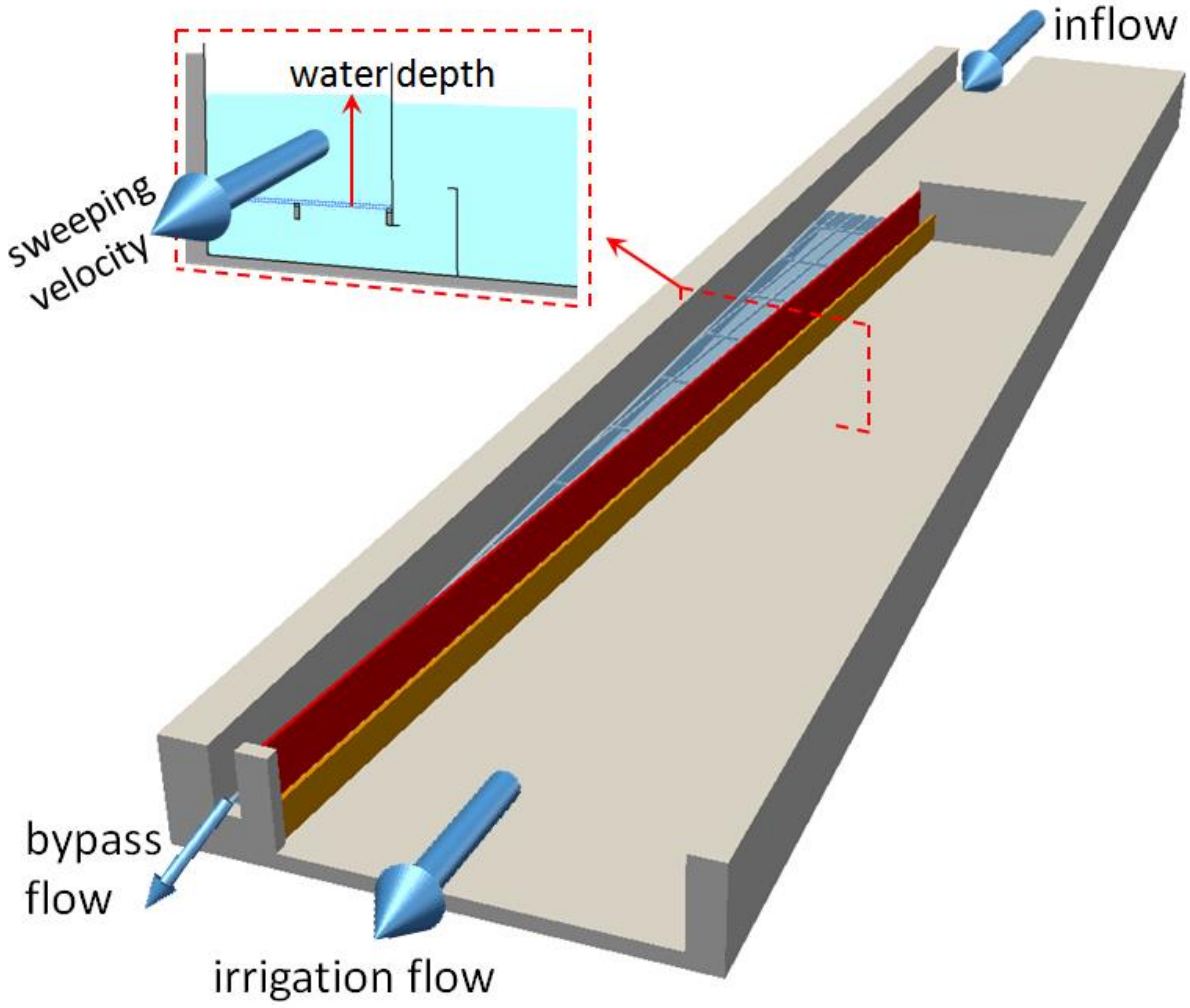

Figure 29 – Schematic of the Farmers Screen illustrating flow measurements for CFD correlation

Initial Model

An initial CFD model of Davenport was run at operating condition OP1. The predicted values of sweeping velocity and water depth over the screen are compared to the measured data in *Figure 30* below. In this initial model, the percent of irrigation flow was fixed to match the measured value rather than predicted by the CFD model.

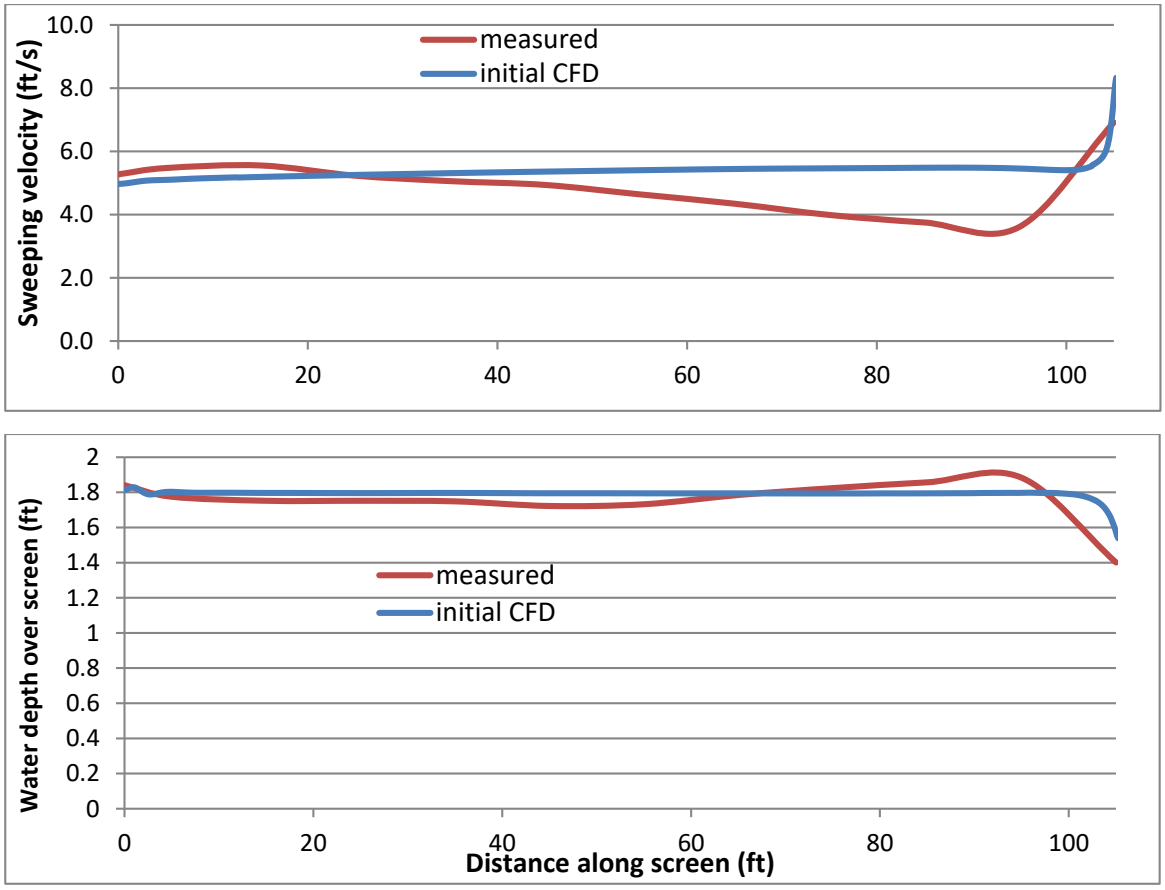

Figure 30 – Predicted sweeping velocity (top) and water depth (bottom) from the initial CFD simulation of the Davenport screen at OP1

The CFD model does not give a good approximation to the measured flow over the screen. Areas of discrepancy between real-world data and CFD results are:

- The measured data shows a gradual deceleration in the sweeping velocity over the length of the screen. In contrast, the CFD model shows a small increase in velocity from the beginning to end of the screen.
- The measured data shows a drop in the water surface "draw down" in the first few feet of the screen with a gradual increase in water depth towards the end of the screen. The CFD model predicts a completely flat water surface.

Following this initial simulation, Gilkes undertook an extensive series of tests of CFD model inputs and methods to improve the correlation to measured data and define best practices for CFD modeling of the Farmers Screen. Numerous settings and inputs were investigated. These are summarized briefly below with the chosen methods underlined. The choice of the key model settings is discussed in detail in the following sections:

Wedge-wire screen:

- Porous region versus porous baffle

- Effect of number of cells across porous region
- Higher flow resistance through screen versus lower flow resistance through screen
- Effect of screen porosity in X direction
- Sinusoidal oscillation of screen
- Variation of screen resistance with distance along the screen

Mesh:

- Running on coarse model then swapping to finer mesh
- Single mesh block versus adjacent blocks versus nested blocks versus conforming blocks
- Increased resolution of the center wall using a nested block
- Reducing aspect ratio to improve mesh quality
- Use of separate mesh blocks at the inlet and outlets to reduce simulation time
- Increased resolution of the weir wall for non-backwatered operating conditions

Numerical methods:

- Immersed boundary method
- 2nd order for momentum advection
- Implicit advection to reduce simulation time
- Steady-state accelerator
- Tiny amount of compressibility to facilitate convergence

Turbulence model:

- RNG k-epsilon model
- k-omega model
- LES model
- Running inviscid initially to reduce simulation time

Geometry:

- Inclusion of screen support frame
- Suitable surface roughness on walls depending on material
- Use of cut-out in weir wall to promote flow separation in non-backwatered condition

Boundary conditions:

Inlet

- Channel length increased
- Tuning free surface elevation to match measured water depth at start of screen

Irrigation outlet

- Pressure condition with specified water depth versus volume flow rate condition

Initial conditions:

- Improved specification of initial flow depths and velocities to reduce simulation time

Mesh

The Flow3D software requires a fully structured hexahedral mesh aligned to the coordinate axes made out of one or more adjacent or overlapping blocks. These requirements are critical to the

accuracy of the software, but place additional constraints on the mesh compared to other CFD software.

Any CFD mesh is always a trade-off between simulation time and accuracy. Ideally, a mesh sensitivity study would be performed in which the mesh resolution is gradually increased until the CFD results show no change. In the case of the Farmers Screen, the range of length scales involved means that mesh sensitivity will not be reached before the mesh becomes unmanageably large. Therefore, it must be accepted that the mesh will affect the results and a compromise must be made based on testing and experience, which maximizes accuracy with the available resources.

Many strategies for meshing the Farmers Screen were evaluated, with the aim of finding the best resolution that could be achieved within an acceptable solution time. The different mesh strategies covered variations in:

- mesh blocking (using one or more overlapping or adjacent blocks)
- mesh resolution (globally or locally changing the size of the cells in the CFD mesh)
- mesh quality (modifying the mesh to reduce the maximum aspect ratio of the cells)

The final chosen method was to employ two levels of mesh for each simulation:

- a coarse mesh to get most of the way to the solution (e.g., 200 seconds simulated time)
- a fine mesh to run on from the coarse mesh model (e.g., 20 seconds simulated time) to improve the accuracy of the solution

A single mesh block was used to cover the screen with adjacent blocks used for the inlet, the attenuation bay, and the bypass flow outlet (see *Figure 31*).

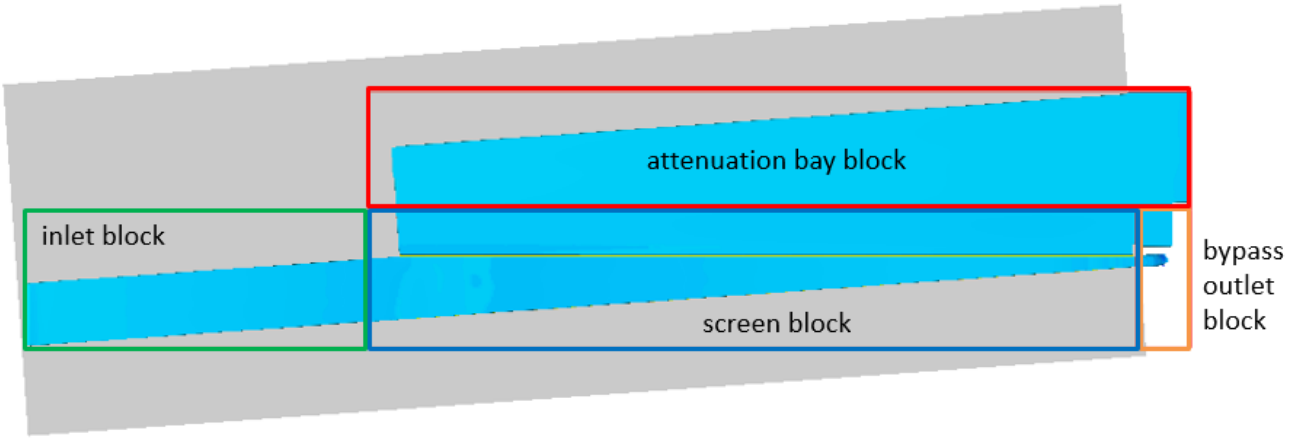

Figure 31 – Mesh block structure for CFD model of the Davenport screen

Figure 32 and *Figure 33* show slices through the mesh for the coarse and fine models of the Davenport screen in operating condition OP1. The number of fluid cells in each mesh is:

- 1.25 million (coarse model)
- 3.01 million (fine mesh model)

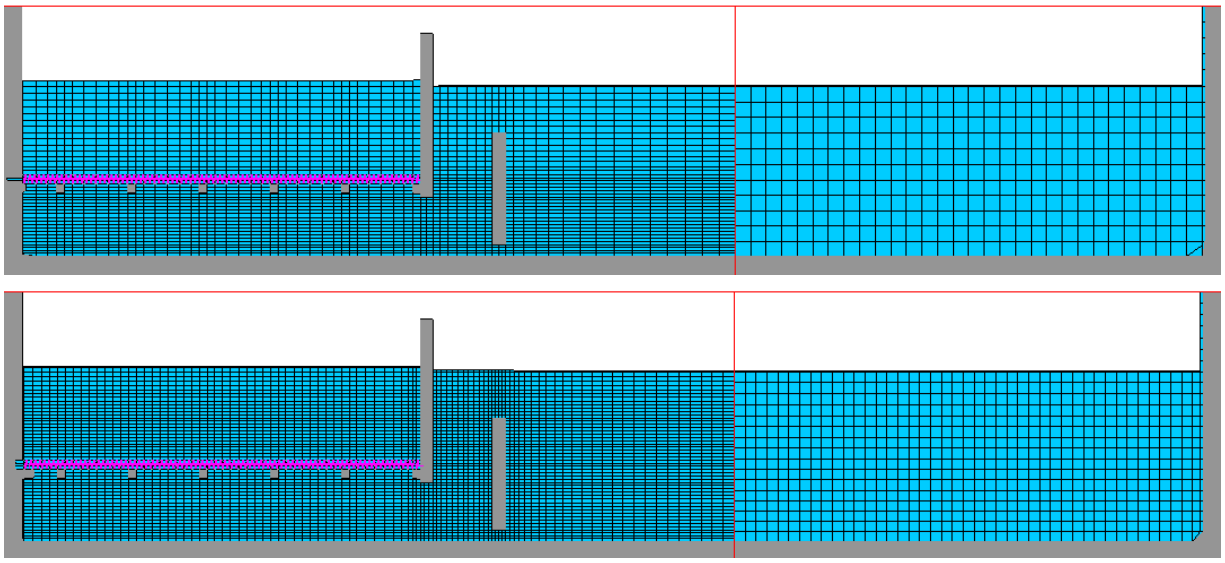

Figure 32 – Vertical slice through CFD mesh of the Davenport screen in operating conditions OP1; coarse (top), fine (bottom)

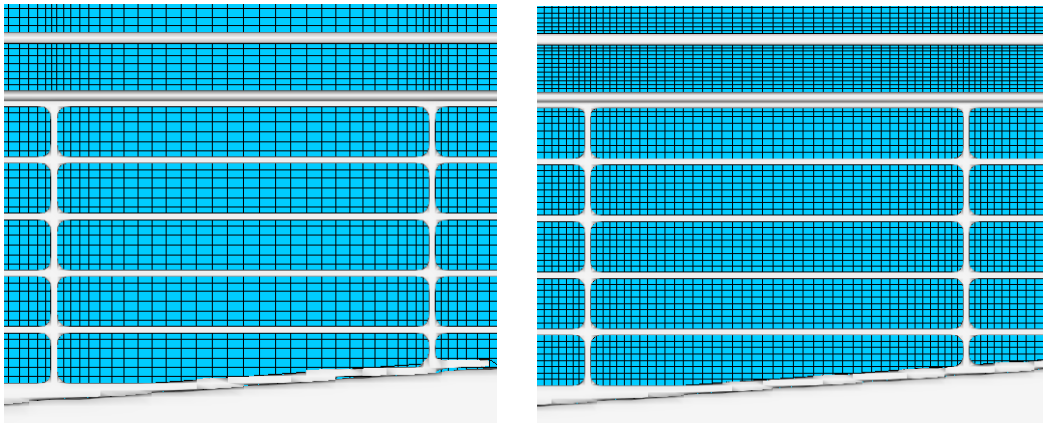

Figure 33 – Horizontal slice through CFD mesh of the Davenport screen in operating condition OP1; coarse (left), fine (right)

When the weir wall is not backwatered and there is no gap under the weir wall (operating condition OP4), the flow in the attenuation bay has no effect on the flow over the screen because the weir is acting as the hydraulic control for the attenuation bay. Hence, the model can be truncated just downstream of the weir wall. In this case, an additional mesh block was used to give greater resolution of the weir wall as shown in *Figure 34* and *Figure 35.*

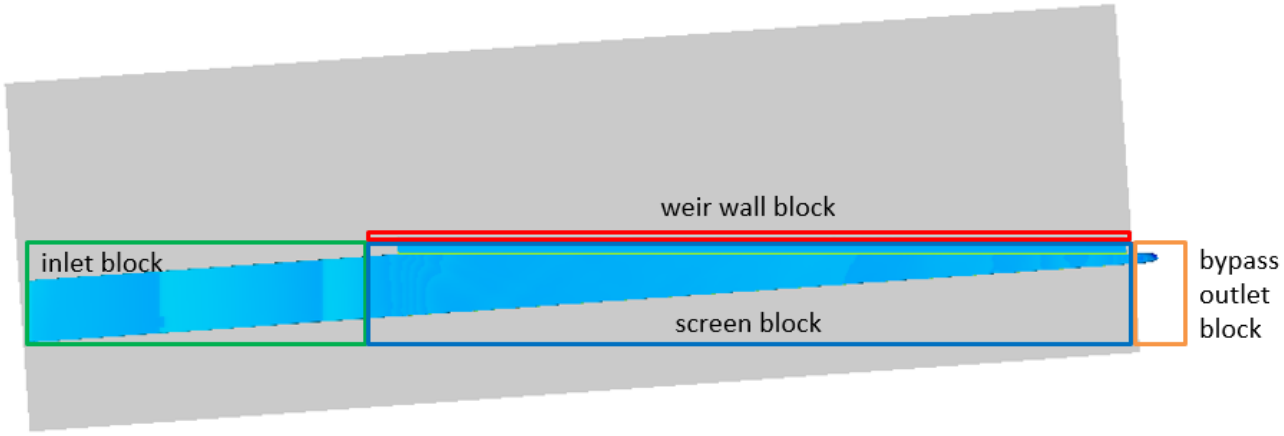

Figure 34 – Mesh block structure for CFD model of the Davenport screen in operating condition OP4

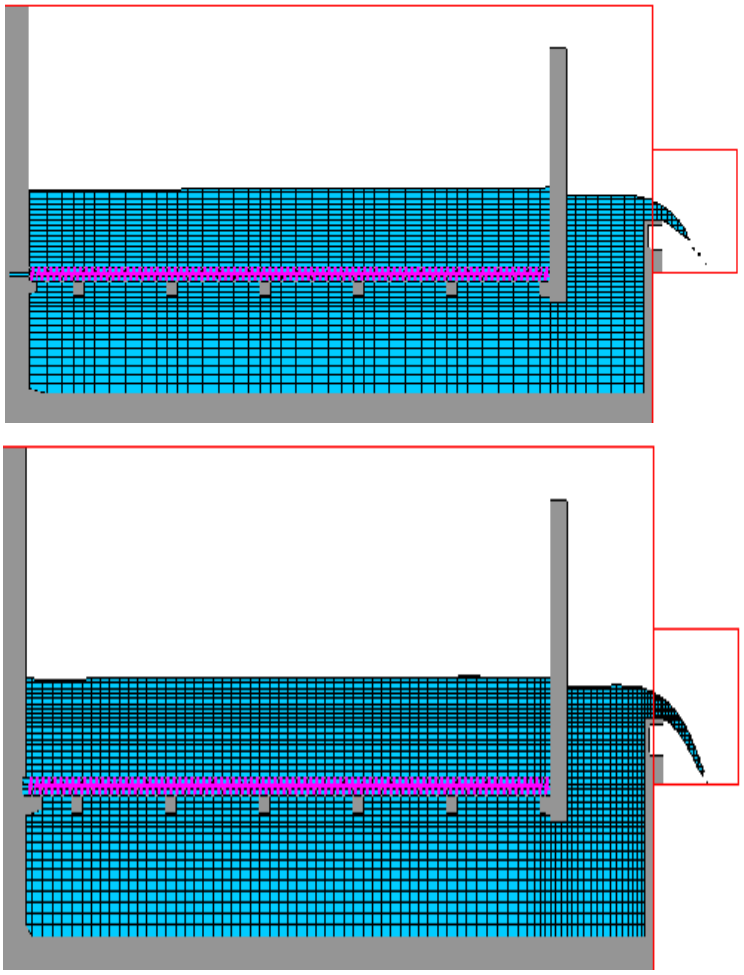

Figure 35 – Vertical slice through CFD mesh of Davenport screen in operating condition OP4; coarse (top), fine (bottom)

Turbulence Model

The flow within the Farmers Screen will be turbulent. Turbulence is characterized by the existence of chaotic eddies over a large range of length and time scales. In theory, a CFD software could provide a full description of these turbulent eddies. In practice, computer memory and processing time limitations mean that this is not possible for real-world applications. Therefore, it is necessary to use an empirical turbulence closure model that describes the effects of turbulence on the mean flow characteristics. Two main turbulence closure models are available within Flow3D: the renormalized group (RNG) k-epsilon model and the k-omega model. Either would be appropriate in application to the Farmers Screen.

In order to determine the best choice, simulations of the Davenport screen at operating condition OP1 were performed using each turbulence model. The results are shown alongside the measured data in *Figure 36* and *Figure 37* below. There is some difference in the sweeping velocity near the taper wall, but overall there is little difference between how well the two models correlate to the measured data. The RNG k-epsilon model was therefore deemed an acceptable choice to use as standard.

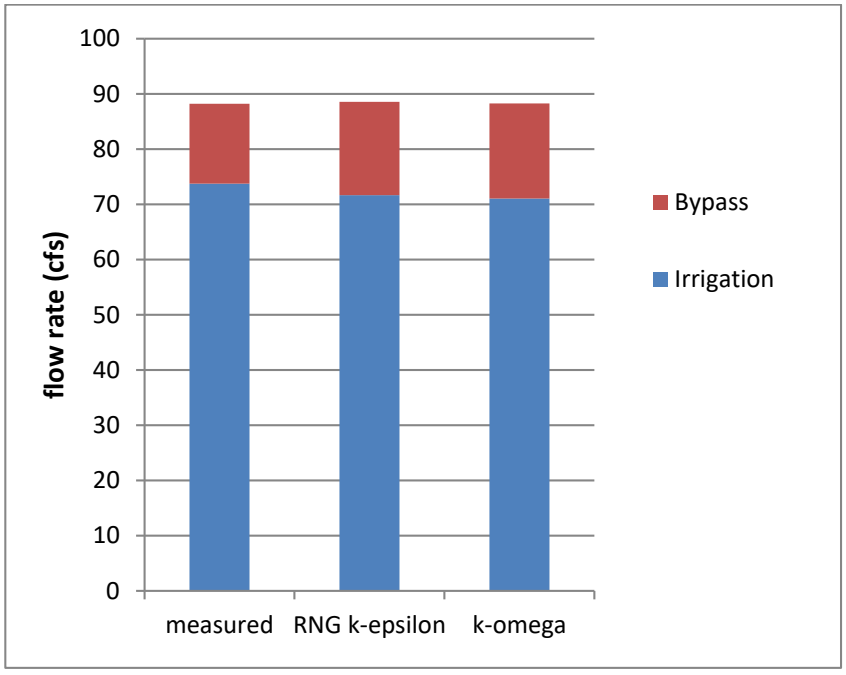

Figure 36 – Effect of choice of turbulence model on flow balance at OP1

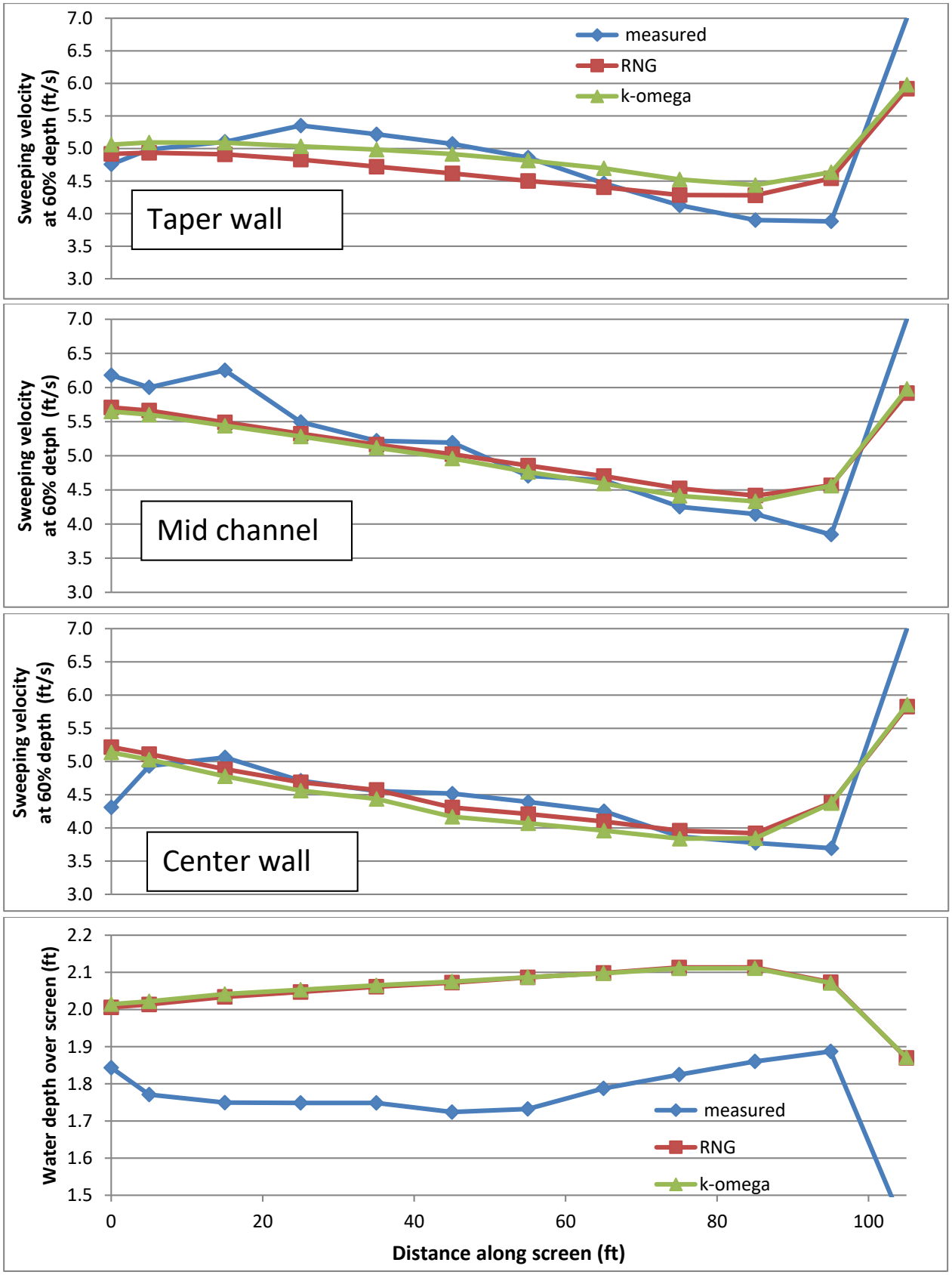

Figure 37 – Effect of turbulence model on sweeping velocity and water depth at OP1

Porous Screen Resistance

The flow resistance settings for the porous region that approximates the wedge-wire screen in the CFD model are derived from the coefficients *a* and *b* in the equation:

$$\Delta P = a\mathrm{V} + b\mathrm{V}^2$$

where ΔP = pressure drop across the screen

V = vertical velocity through the screen

Initial values for *a* and *b* were calculated directly from the detailed CFD sub-model of a portion of the wedge-wire screen (see *Section 2.2*). However, given the poor correlation of the initial CFD model to the measured flow data, tests were performed on both higher and lower levels of screen resistance to see how this influenced the predicted flow. It was found that increasing the flow resistance through the screen caused a deceleration in the sweeping velocity over the screen, which is seen in all measured data. Simulations of the Davenport screen were therefore performed with increasing values for the screen resistance to find the best correlation. The predicted flow measurements for a low resistance (as derived from the detailed wedge-wire model in *Section 2.2*), a medium screen resistance, and a high screen resistance are shown in *Figure 39* and *Figure 40*. The relationship between pressure drop and velocity for each level of resistance are compared in *Figure 38* below.

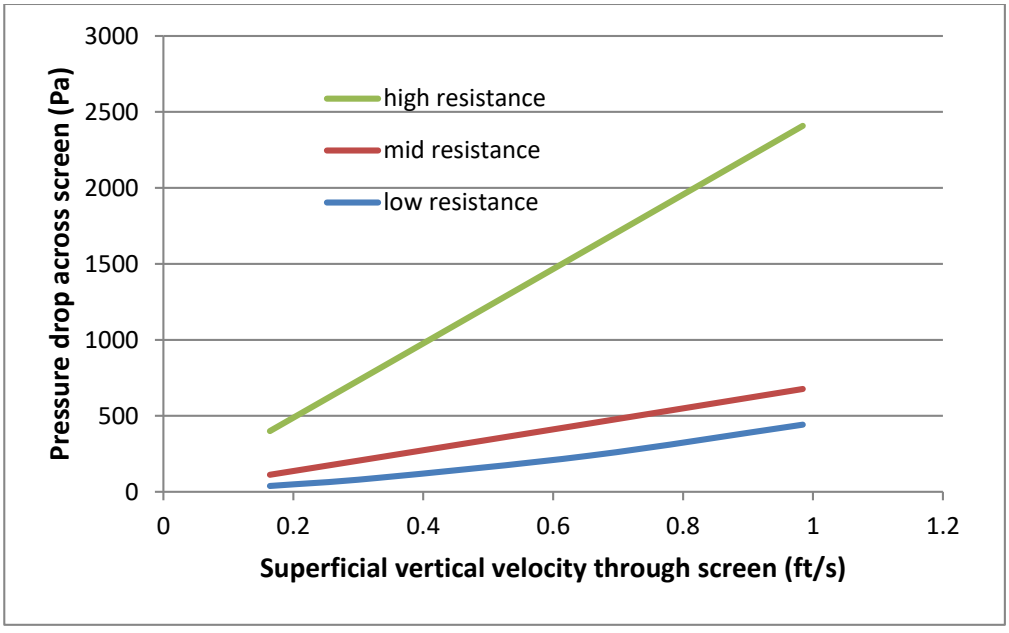

Figure 38 – Pressure drop versus velocity curves for the different screen resistances tested

It can be seen that at the high resistance the sweeping velocity exhibits a similar level of deceleration over the screen to that which is observed in the measured data. The high screen resistance was therefore used as the standard value for future CFD simulations. A case could be made for this increase in resistance, based on the effect of screen vibration and consequent short

scale fluctuations in flow that were not captured in the detailed wedge-wire model. However, this change was primarily made because it improves the correlation to measured data.

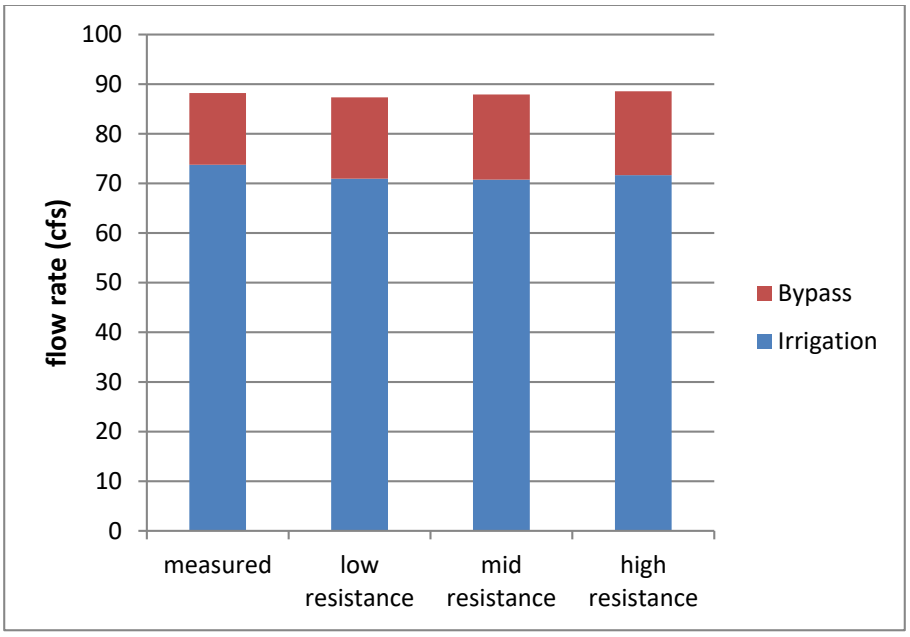

Figure 39 – Predicted flow balance for different values of screen resistance at OP1

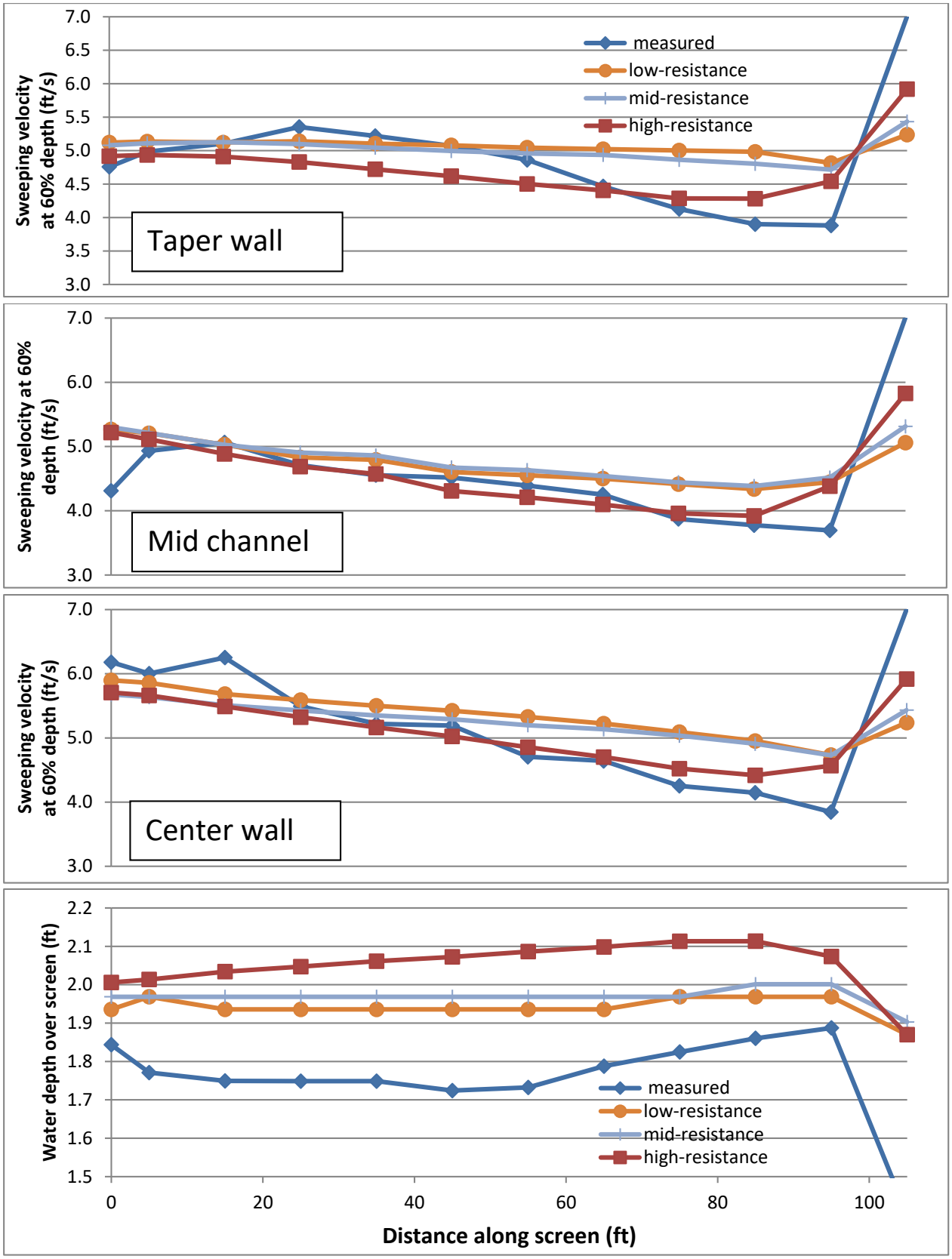

Figure 40 – Effect of screen resistance on sweeping velocity and water depth at OP1

Wall Surface Roughness

All surfaces in the CFD model are treated by default as no-slip walls without roughness. The no-slip condition enforces zero velocity at the wall, while the zero roughness condition is acceptable for relatively smooth surfaces. However, the concrete channel walls in particular are likely to have roughness, which will increase frictional losses. This roughness can be incorporated in the CFD model by applying a suitable value for the "roughness height" to relevant surfaces. The roughness height is the diameter of sand-grains that would give the same frictional effect if the surface was covered in them.

After some testing the following values were chosen:

Framework, weir wall: roughness height = 0.5 mm

Channel walls, stop logs: roughness height = 2.0 mm

Figure 41 and *Figure 42* compare the predicted flow measurements for a model with zero roughness to one with roughness applied as above. The results show no obvious improvement in the correlation of the CFD model to measured data when roughness is included. Nevertheless, the above roughness settings were adopted as standards in the baseline CFD model since they are appropriate to the on-site conditions.

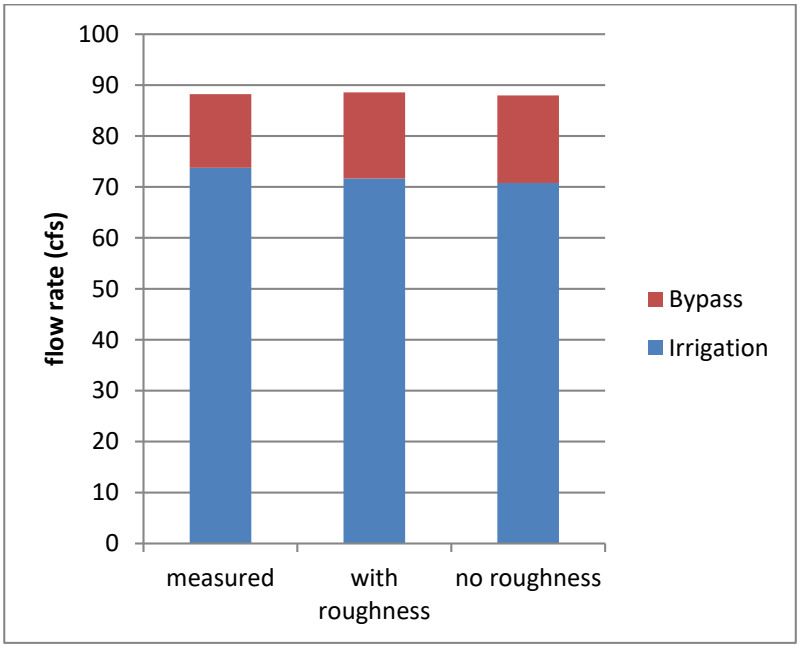

Figure 41 – Effect of wall roughness on flow balance at OP1

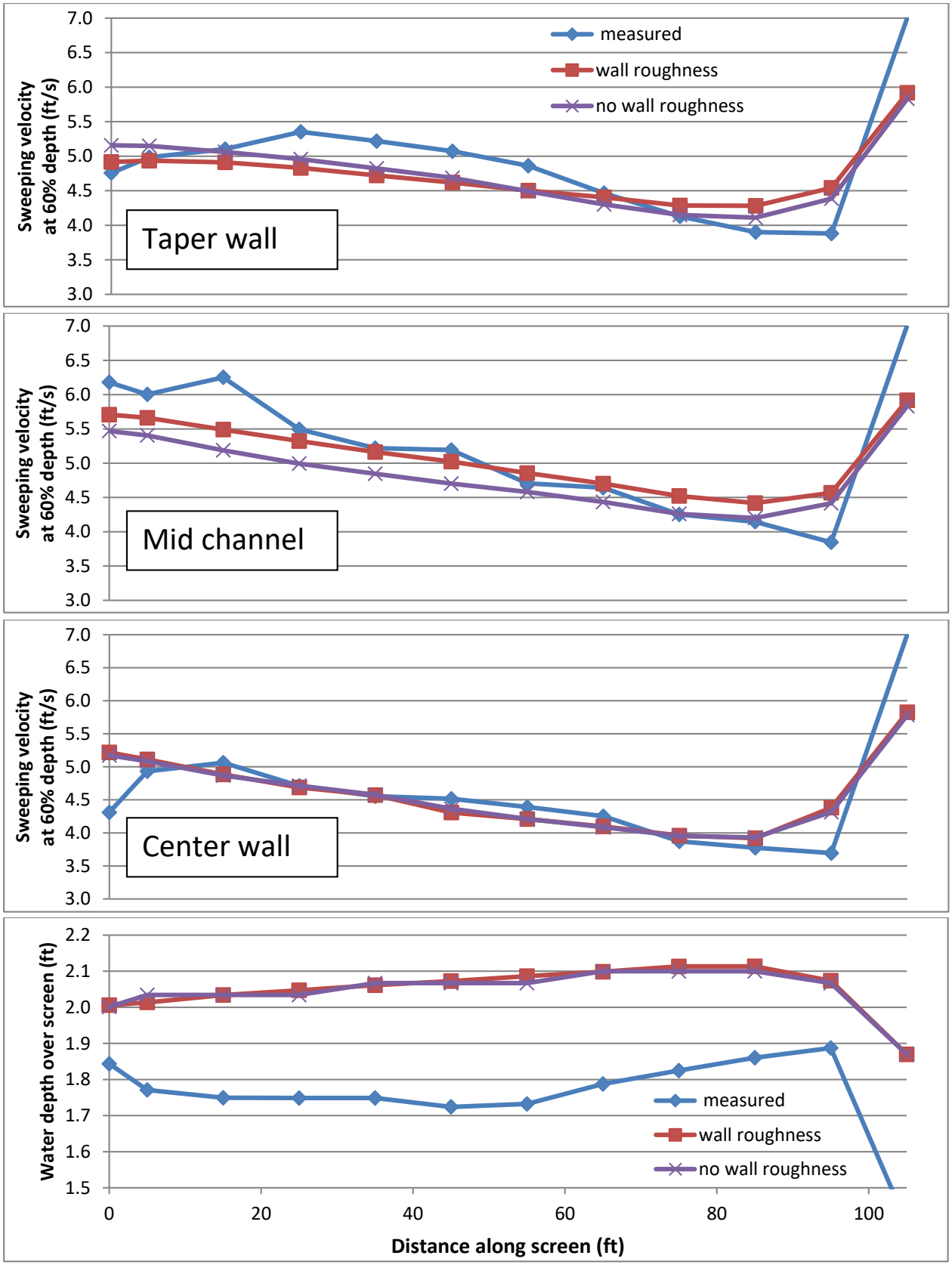

Figure 42 – Effect of wall roughness on sweeping velocity and water depth at OP1

Oscillation of Screen

Although it is not feasible to model the full fluid-structure interaction that drives the vibration of the wedge-wire screen, there is a basic capability within Flow3D to apply a sinusoidal motion to any region.

Tests were performed in which a vertical oscillation was applied to the porous region representing the wedge-wire screen. The frequency of oscillation was set to 300 Hz based on previous frequency measurements by FCA, while a peak-to-peak amplitude on the order of 0.1 mm was applied.

The results showed a slight increase in the flow resistance through the screen, which improved the correlation to the measured data; however, this setting was later discarded for being too crude and unreliable.

2.3.4 Results and Comments

Through the development work described above, a definitive CFD approach for modeling the Farmers Screen was determined, which provided the closest correlation to the measured data from the Davenport physical model. The Flow3D settings for the definitive CFD model are given in *Appendix A*.

Figures highlighting the results of the definitive CFD simulations of the Davenport screen at operating conditions OP1 and OP4 are presented below. Comments on the results are given below each figure. A more general discussion of the confirmations, limitations, assumptions, and accuracy of the CFD model is given in *Section 2.4*. A full set of figures for OP1 and OP4, comparing the flow at all locations, are given in *Appendix B*.

Operating Condition OP1

Operating condition OP1 is typical of how the Davenport screen operates under high flow rates. The weir wall is fully backwatered and the level of water in the attenuation bay is very similar to the water surface over the screen. Note: In the Davenport screen, this operating point also includes a 3-inch gap under the weir wall, which will not be present at the Derby Dam.

Figure 43 and *Figure 44* below show flow visualization from the CFD model, while *Figure 45* and *Figure 46* show selected comparisons of the CFD results to measured data. Comments on the results are given below each figure.

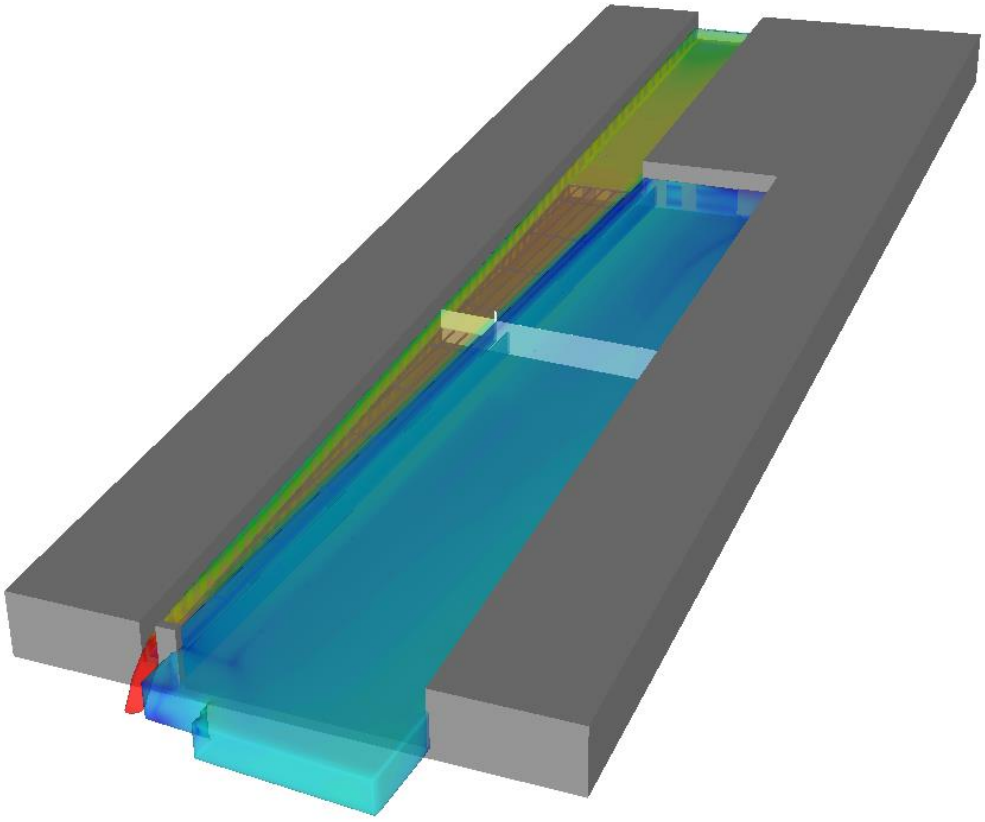

Figure 43 – Overview of CFD model of the Davenport screen at OP1

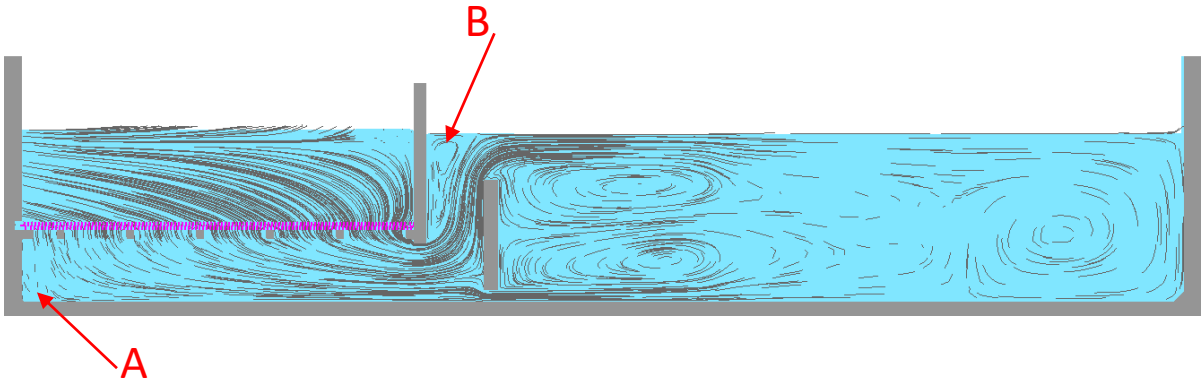

Figure 44 – Slice through the Davenport screen at OP1, showing streamlines in the plane of the slice

Streamline plot - *Figure 44*

- Above the screen, the streamlines show a clear movement of water towards the taper wall. While this appears dramatic, nowhere is the velocity towards the taper wall above the screen ~~above~~ greater than 0.3 ft/s.

- Beneath the screen, the streamline plot shows a small area of recirculation up against the center wall, marked A. Any sediment in this region may not be transported towards the weir wall.
- There is a strong upwelling of water between the taper wall and the weir wall. This is strongest against the weir wall, and leaves a small recirculation against the downstream side of the taper wall, marked B.
- The double recirculation seen in the attenuation bay against the weir wall is driven by the presence of the gap beneath the weir wall. The lower recirculation would not be present without this gap.

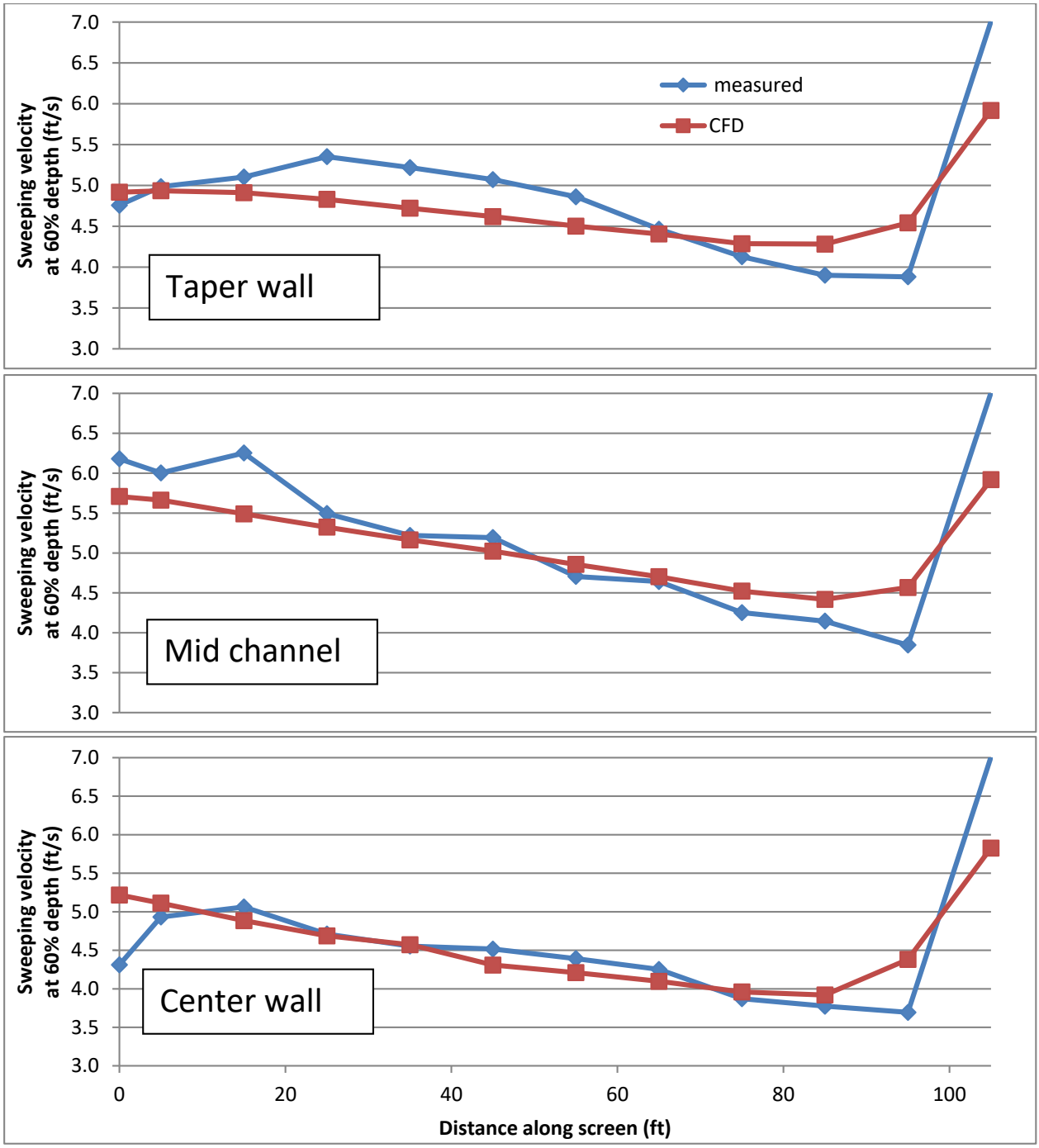

Figure 45 – Predicted sweeping velocity and water depth at OP1

Sweeping velocity – *Figure 45*

- The CFD model gives a generally good prediction of the sweeping velocity across the screen. The decrease in velocity from the start to the end of the screen is well replicated.
- The only notable discrepancy at this operating condition is that the CFD model over-predicts the minimum sweeping velocity by approximately 0.5 ft/s compared to the minimum observed value.

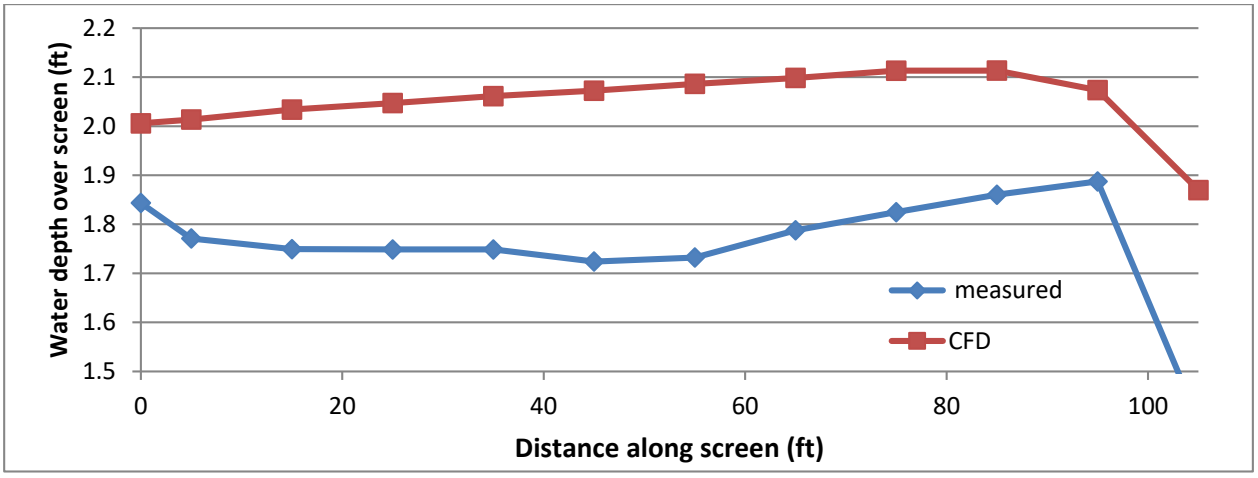

Figure 46 - Predicted water depth along the screen at OP1

Water depth - *Figure 46*

- The CFD model over-predicts the water depth along the length of the screen with a maximum disparity mid-screen of approximately 20 percent higher than measured values.
- The CFD model predicts a gradually increasing water depth from the beginning to the end of the screen. This is broadly in line with the measured data, but fails to capture the initial draw down in the water surface that is seen in the field.

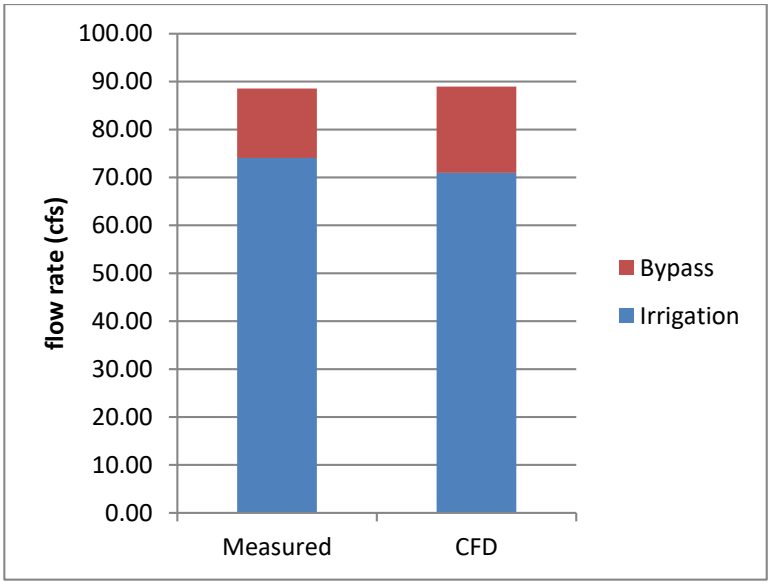

Figure 47 – Predicted flow balance at OP1

Flow balance - *Figure 47*

- The CFD model under-predicts the amount of flow that passes through the wedge-wire screen to irrigation. This is consistent with the over-prediction of the water depth and the relatively accurate prediction of the sweeping velocity.

- Under-prediction of the irrigation flow was found to be a common feature of the CFD models of the Farmers Screen, despite investigations into the effect of different screen properties. The CFD model is therefore likely to under-predict the irrigation flow when applied to the Derby Dam.

Operating Condition OP4

In operating condition OP4, there is no gap under the weir wall, the weir wall is not backwatered, and water drops over the weir providing a disconnect from the attenuation bay. In this scenario, the water depth over the screen is controlled by the height of the weir wall rather than the water level in the attenuation bay. Hence, as discussed earlier, the CFD model can be truncated just below the weir wall.

Figure 48 and *Figure 49* below show flow visualization from the CFD model, while *Figure 50*, *Figure 51*, and *Figure 52* show selected comparisons of the CFD results to the measured data. Comments on the results are given below each figure.

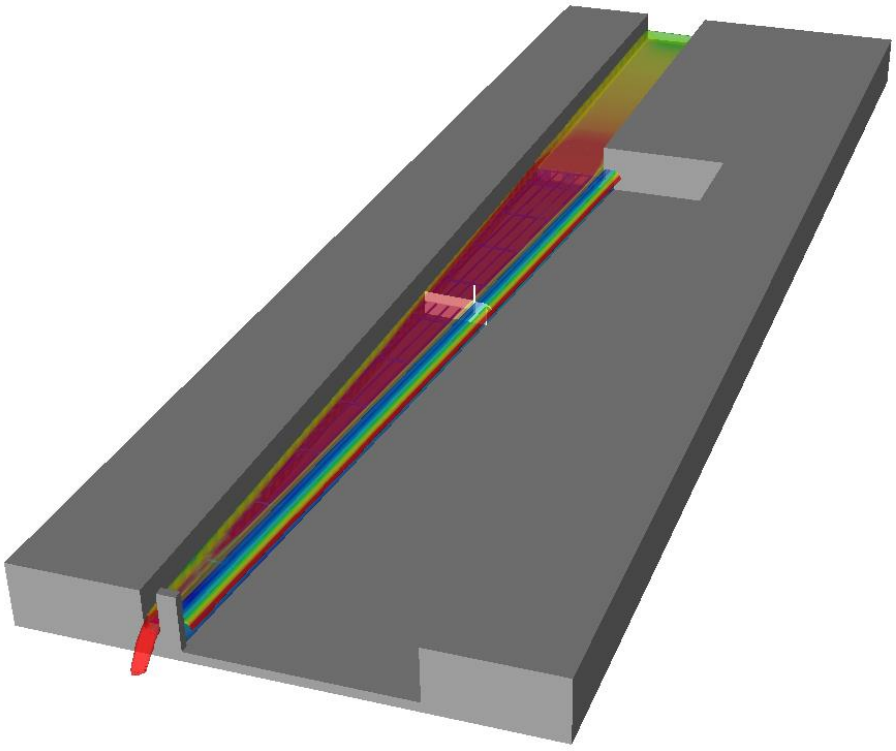

Figure 48 – Overview of CFD model of the Davenport screen at OP4

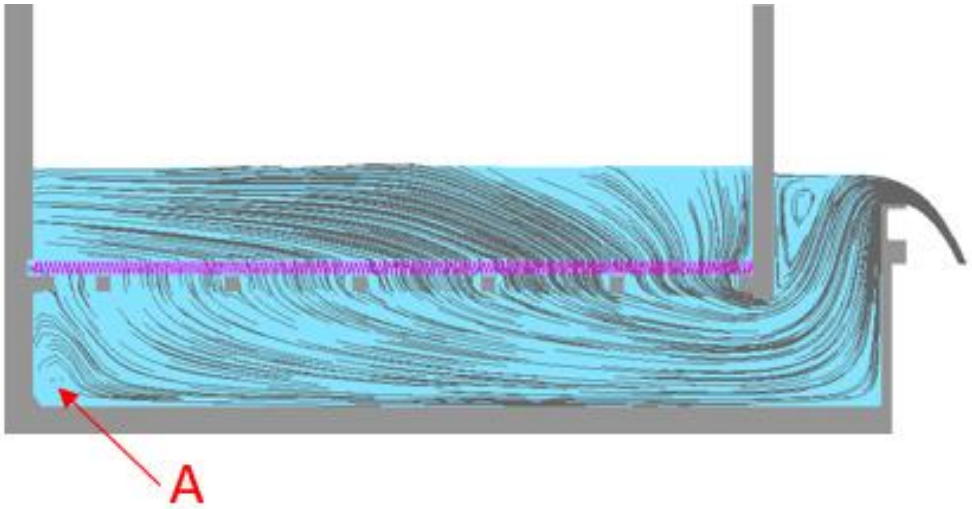

Figure 49 – Slice through the Davenport screen at OP4 showing streamlines in the plane of the slice

Streamline plot - *Figure 49*

- The streamline plot shows that, as in the high-flow condition (OP1), there is a small recirculation beneath the screen up against the center wall, marked A.

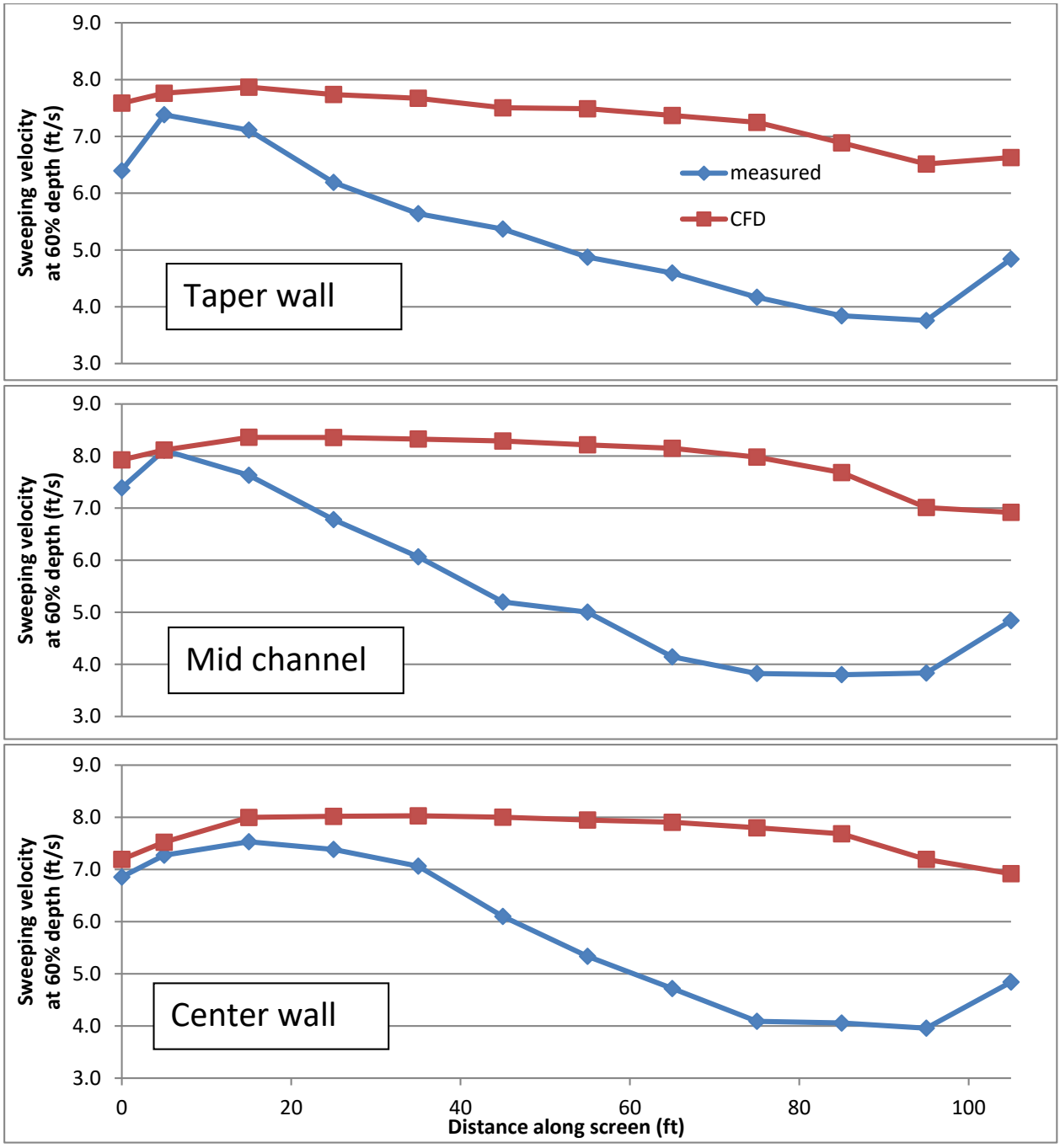

Figure 50 – Predicted sweeping velocity and water depth at OP4

Sweeping velocity – Figure 50

- The measured velocities at the end of the screen are approximately 50 percent of the velocity at the start of the screen. The CFD model predicts a small deceleration along the length of the screen, but it is much less marked than in the field.

- The main consequence of this is that the minimum measured velocities are up to 3 ft/s (45 percent) lower than those predicted by CFD. This should clearly prompt caution when interpreting the CFD predictions of the Derby Dam in non-backwatered conditions.

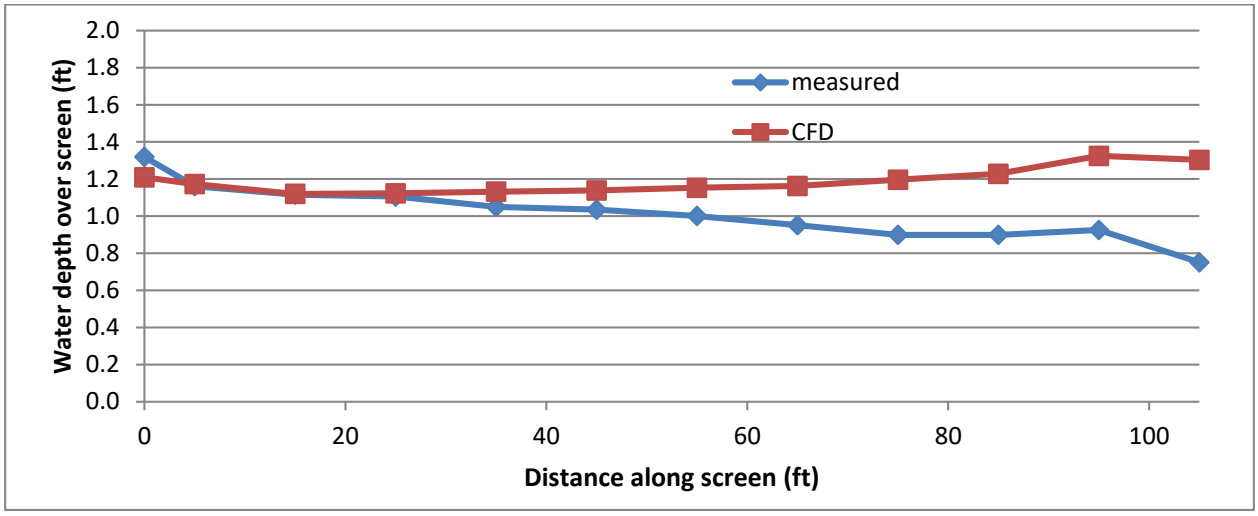

Figure 51 – Predicted water depth along the screen at OP4

Water depth – *Figure 51*

- The CFD model gives a good prediction of the water depth at the start of the screen.
- The CFD model predicts a gradually increasing water depth along the screen. This is in contrast to the gradually decreasing water depth that was measured. This results in an over-prediction of the water depth towards the end of the screen of 30 to 40 percent above the measured values.

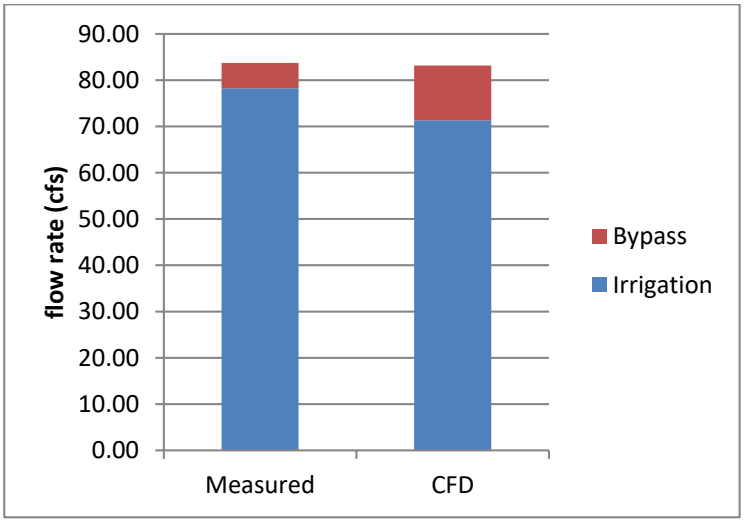

Figure 52 – Predicted flow balance at OP4

Flow balance – *Figure 52*

- The CFD model over-predicts the bypass flow. This is consistent with the over-prediction of the water depth and over-prediction of the sweeping velocity. The discrepancy between the measured and predicted flow balance is more pronounced than in the backwatered condition (OP1).

2.4 CFD Assumptions and Accuracy

2.4.1 Introduction

The CFD simulations of flow through the Davenport screen (*Section 2.3*, *Appendix B*) show some areas of good correlation with measured data and some areas of poor correlation. This section discusses the likely sources of discrepancy between the CFD predictions and the measured data, and highlights the overall strengths and weaknesses of the CFD model.

As discussed in *Section 2.1*, CFD solves the governing equations of fluid motion, and therefore, in theory, a CFD simulation of a given application should give an exact representation of the flow. However, in reality, limitations of computing hardware and simulation time force simplifications to the CFD process. These take the form of simplifications to the geometry modeled, to the physics included, and to the resolution of the simulation. Where possible, simplifications are made that will have minimal effect on the flow measures that will be reported. However, assumptions are sometimes unavoidable, which may affect the CFD predictions. In light of this, it is important to be aware of the limitations to the accuracy, which are imposed by the assumptions within the CFD model of the Farmers Screen, and to interpret the results in the light of known strengths and weaknesses. A discussion of the assumptions and accuracy of the CFD model of the Farmers Screen is given below.

Sources of Discrepancy Between the CFD Model and the Measured Data from the Davenport Screen

To understand the sources of discrepancy between the CFD predictions and measured data, it is necessary to review all simplifications and assumptions within the CFD model as well as the measured data.

It is estimated that the likely sources of discrepancy between the CFD model and the measured data, in decreasing level of importance, are:

1. Wedge-wire screen
2. Mesh resolution
3. Turbulence model
4. Screen vibration

5. Uncertainty in upstream and downstream conditions
6. Measurement uncertainty
7. Geometric differences between the model and the prototype

More detailed discussion of the aforementioned assumptions is given below.

Wedge-Wire Screen

The wedge-wire screen is approximated in the CFD model as a porous region with a specified flow resistance. Extensive studies were performed to derive appropriate values for the flow resistance of this porous region (see *Section 2.2*).

In the case of the Farmers Screen, the cross-flow nature of the water approaching the wedge wire, the proximity of the water surface, and the screen vibration means that the porous region may not provide a complete understanding of the interaction between the screen and the water.

Particular areas not fully captured by modelling the screen as a porous media are:

Directional porosity - The orientation of the wedge wires means that the resistance of the screen will vary in the three component directions. Similarly, the resistance will be different for flow upwards through the screen compared to flow downwards. The CFD software allows for different values of porosity in the three coordinate directions, but the full complexity cannot be captured.

Boundary layer - The porous region approach does not simulate the recirculations in between the wedge wires seen in *Figure 20*. While these motions are very small scale, they have the effect of suppressing the boundary layer on top of the screen (as discussed in *Section 2.2*), and hence, may have a large-scale impact on the flow above the screen.

Screen vibration – This is discussed separately below.

Screen resistance – The values of resistance used for the porous region in the definitive CFD model are greatly increased from the ones calculated in *Section 2.2*. The increased resistance was implemented because it gives improved correlation to the Davenport test data and could potentially be justified based on the omission of the other flow effects noted above.

The overall effect of these simplifications reduces the accuracy of how the CFD model predicts flow interaction with the wedge-wire screen. The primary measures this will affect are the flow balance and the sweeping velocity near the surface of the screen.

Mesh Resolution

The mesh resolution varies throughout the model. In the key areas of the wedge-wire screen and the weir wall, there is a minimum cell size of approximately 0.1 inch. Away from the key areas, the cell size increases up to a maximum of 8 inches. Geometric detail smaller than the mesh, and flow features smaller than the mesh, are not captured. Key areas where the mesh resolution will affect accuracy are:

Boundary layers - The relatively coarse mesh resolution near the walls means that boundary layers will be poorly represented. Screens 1-4 at the Derby Dam are 125 feet long. Over this distance, any discrepancy in the representation of the boundary layer will have time to grow. This effect will be magnified in non-backwatered conditions when the sweeping velocity is higher, since frictional losses are approximately proportional to the velocity squared.

Water surface - The representation of the water surface will not be detailed enough to capture the surface water waves that are typically observed during operation of the Farmers Screen.

Turbulence Modeling Approach

The turbulence model approximates flow fluctuations smaller than the mesh size. The two turbulence models tested (RNG k-epsilon and k-omega) showed very similar results, but both will be compromised by the poor resolution of the boundary layer where turbulence is greatest.

Both models that were tested also assume isotropic turbulence, i.e., the same strength in all directions. However, there is a strong argument that the turbulence in the direction along the screen should be different from that across the screen or in the vertical component.

Screen Vibration

The Farmers Screen wedge-wire screen is known to vibrate when in operation. This can be heard as a distinctive hum, felt when touching the wedge-wire screen surface, and seen in the continual agitation of any leaves or sediment on the surface of the screen. The driver behind the screen vibration is not conclusively known, however, the small amplitude, high frequency vibrations will impart a force on the water flow around and through the wedge-wire screen.

It was accepted at the outset of this project that vibration of the wedge-wire screen would not be captured in the CFD simulations. While the CFD software has the capability to couple fluid-flow simulation with structural analysis to simulate fluid-solid interactions, the reality is that such a simulation would add several layers of complexity and associated run-time. Modeling the true geometry of the wedge wire in a full Farmers Screen installation is already beyond CFD computational capability without this added complexity.

It is hoped that ignoring this vibration will only affect the flow in the immediate neighborhood of the wedge-wire screen. However, it is possible that the vibration causes differences in the larger-scale flow patterns affecting flow resistance through the screen.

Upstream and Downstream Boundary Conditions

Inlet Flume Entrance

The upstream boundary of the CFD model of the Farmers Screen is located at the entrance to the inlet flume (see *Figure 11*). The water depth and velocity are fixed at this boundary. However, as the water travels down the inlet flume it settles to a natural profile that is solely a function of

the specified flow rate. Simplification of the flow at the upstream boundary therefore has minimal effect on the results.

Attenuation Bay Exit

In operating condition OP1, when the weir wall is backwatered, the water depth must be specified at the exit to the attenuation bay. The chosen depth affects the flow rate of water under and over the weir wall, the flow rate through the wedge-wire screen, and the water depth over the wedge-wire screen. Although a good estimate for the water depth can be made (either from physical measurements at the Davenport screen, or the canal water level at the Derby Dam), the chosen value will clearly have a knock-on effect on the flow throughout the model.

In operating condition OP4, when the weir wall is not backwatered, the flow in the attenuation bay has no effect on the flow through the wedge-wire screen or over the weir wall. Hence, the attenuation bay boundary condition has no wider impact.

Bypass Channel Exit

Likewise, the boundary condition at the bypass channel exit is disconnected from the rest of the model and will have no wider impact.

Measurement Uncertainty

Some discrepancy will arise from uncertainty in the measurements taken from the physical model at the Davenport screen. Likely sources of measurement uncertainty are:

- Transient fluctuations in the water flow over the wedge-wire screen, which makes it difficult to measure the water depth and velocity.
- Calculation of the measured-flow rate over the screen based on a weighted average of the measured velocities. The weightings must assume a typical velocity profile, which may not be wholly appropriate for the screen flow.
- Equipment uncertainty. There is inherently error associated with any measuring device. This uncertainty/error may compound on the aforementioned.

Geometric Differences

Aside from the wedge-wire screen, the CFD model contains a known number of simplifications to the Davenport screen geometry, as discussed in *Section 2.3.2*. These are expected to have negligible effects on the predicted flow measurements.

2.5 Conclusions

A CFD model for the Farmers Screen has been developed. Physical tests from the Davenport screen provided real-world data against which the CFD model was calibrated. Thorough testing of the model inputs, comparison to the physical data, and analysis of the model assumptions

leads to the following conclusions about the strengths and weaknesses of the CFD model of the Farmers Screen:

Strengths

- The key benefit of the CFD model is that in combination with the real-world data from the Davenport screen, it provides a good indicator of the real-world flows to be expected at the Derby Dam. By applying the same definitive CFD approach to the Derby Dam as to the Davenport screen, the differences between CFD predictions and real-world conditions will be very similar in both cases. Hence, if the CFD model under-predicts the irrigation flow by 5 percent at the Davenport screen, it can be expected to under-predict the irrigation flow by approximately 5 percent at the Derby Dam, when subject to similar flow conditions.
- The CFD model gives a good prediction of the magnitude and profile of the sweeping velocity across the screen when the weir wall is backwatered at higher flow rates.
- The CFD model reveals the flow patterns throughout the Farmers Screen that would not otherwise be visible (see for example *Figure 44* and *Figure 49*). This highlights areas of recirculation and aids in understanding the functioning of the screen.
- The detailed CFD model of the wedge-wire screen gave great insight into the small-scale flow between individual wedge wires. This helped to illuminate the likely mechanism behind the self-cleaning nature of the Farmers Screen.

Weaknesses

- The CFD model under-predicts the percentage of flow to irrigation. This is likely to be a consequence of the simplifications to the screen material, limited mesh resolution, and inability to model screen vibration.
- In backwatered conditions, the CFD model does not exhibit the draw down at the start of the screen that is seen in the measured data. This results in an over-prediction of water depth along the length of the screen.
- In non-backwatered conditions, the CFD model is a poor predictor of the sweeping velocity over the screen. This is likely because the CFD model simplifies the representation of the boundary layer above the wedge-wire screen, and this simplification is more significant in non-backwatered conditions when the sweeping velocity is higher.

Keeping in mind the strengths and weaknesses highlighted above, the CFD model can now be applied to predict performance at the Derby Dam.

3. CFD Simulations of the Derby Dam

3.1 Introduction

Following the development work described in *Section 2*, the chosen CFD model settings and methodology were applied to simulations of the Derby Dam. The installation at the Derby Dam will comprise five individual Farmers Screens: four larger screens with a maximum screen flow of 132 cfs each and one smaller screen with a maximum screen flow of 72 cfs. The CFD simulations focused solely on one of the larger screens.

3.2 CFD Model

3.2.1. CFD Model Geometry

A CFD model of the Derby Dam geometry was built based on the drawings supplied by FCA; *"Farmers Conservation Alliance USBR Derby Dam Horizontal Fish Screen, Storey County, Nevada - Volume 2 Construction Drawings August 09, 2019".*

An overview of the CFD model geometry is shown in *Figure 53*. The main difference from the Davenport model is that the Derby screens have a step-down in the floor of the attenuation bay, 16 inches from the weir wall.

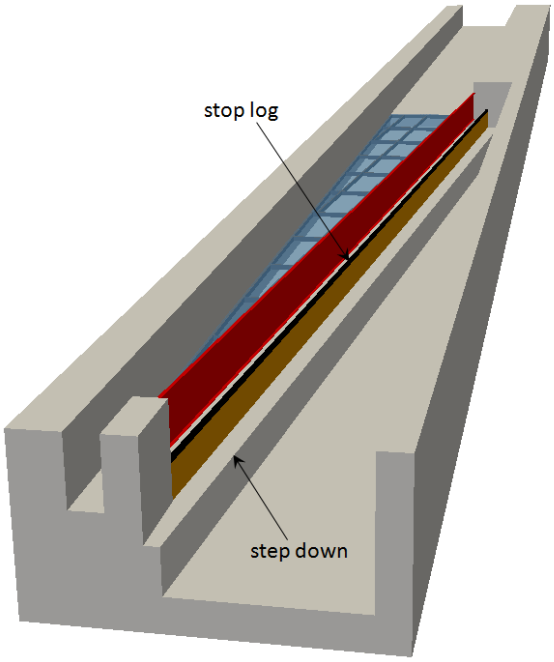

Figure 53 – CFD model geometry of the Derby Dam

The top of the permanent weir-wall structure is 6.25 inches above the top of the wedge-wire screen. The weir-wall height was increased to 9.25 inches above the screen by the addition of a 3-inch stop log. This was done to allow the weir to pass the expected minimum flow rate of 65 cfs, given a water depth of 13 inches over the screen.

As with the Davenport CFD model, a number of simplifications were made to the Derby Dam geometry to remove unnecessary detail and simplify the meshing process. Specifically:

- Small features were omitted where these were below the level of resolution of the CFD mesh and/or where they would have minimal effect on the flow, e.g., the legs beneath the screen support frame and the legs beneath the taper wall.
- As discussed in *Section 2.2*, the wedge-wire screen was approximated as a porous region without geometric detail but with a specified flow resistance.
- The frame that supports the wedge-wire screen was re-oriented to be parallel to the taper wall rather than parallel to the center wall. This was done because the mesh lines run parallel to the taper wall and the frame could be resolved better in this orientation.

Other than the approximation of the wedge-wire screen, these simplifications are expected to have negligible effect on the predicted flow measurements of interest within the CFD model.

3.2.2 CFD Mesh

The mesh block strategy used for the CFD models of the Derby Dam is shown below in *Figure 54*. In the backwatered condition, a single mesh block covers the screen and attenuation bay with adjacent blocks used for the inlet, the attenuation bay outlet, and the bypass flow outlet. In the non-backwatered condition, the attenuation bay is not modeled and an additional mesh block is used to capture the flow over the weir wall.

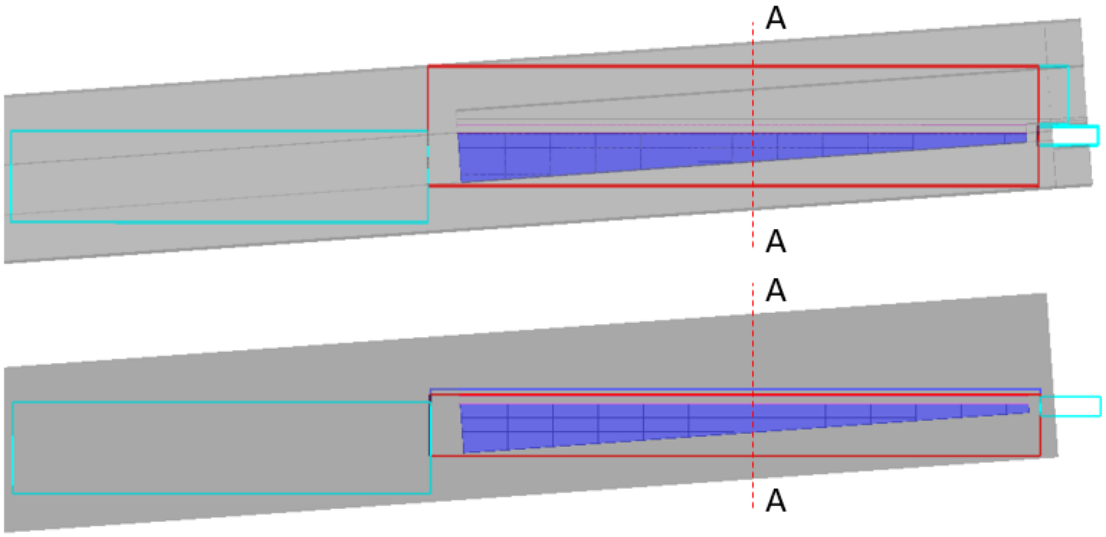

Figure 54 – Mesh block structure for CFD models of the Derby Dam; backwatered conditions (top), non-backwatered conditions (bottom)

Similar to the Davenport model, two levels of mesh were used in each simulation; a coarse mesh to get most of the way to the solution, and a fine mesh to run on from the coarse mesh model to improve the accuracy. *Figure 55* and *Figure 56* show vertical slices through the fine mesh model of the Derby Dam in backwatered and non-backwatered conditions. *Figure 57* shows a horizontal slice through the mesh of the Derby Dam for backwatered simulations.

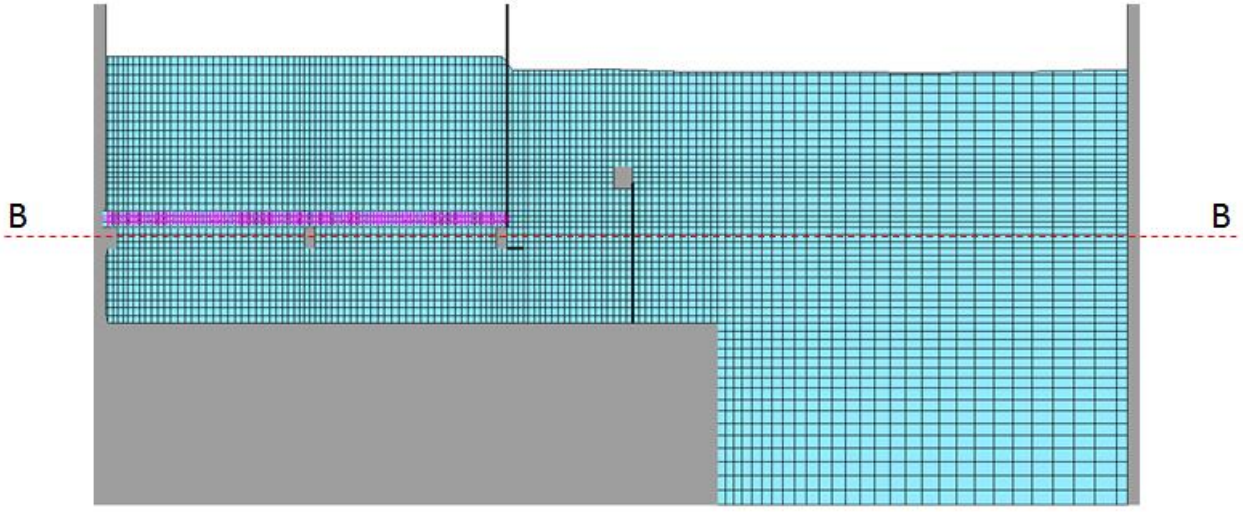

Figure 55 – Slice A-A through fine mesh of the Derby Dam for backwatered simulations

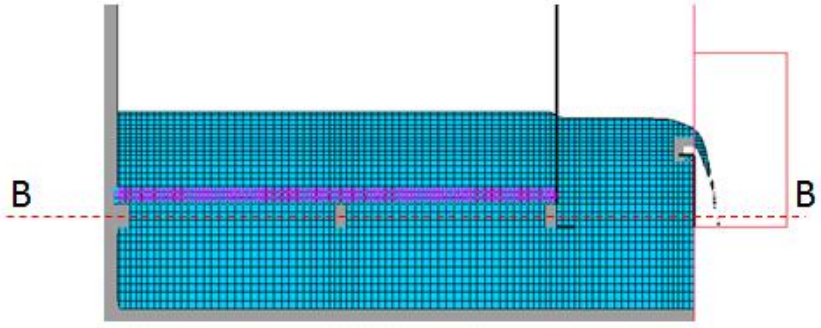

Figure 56 – Slice A-A through fine mesh of the Derby Dam for non-backwatered simulations

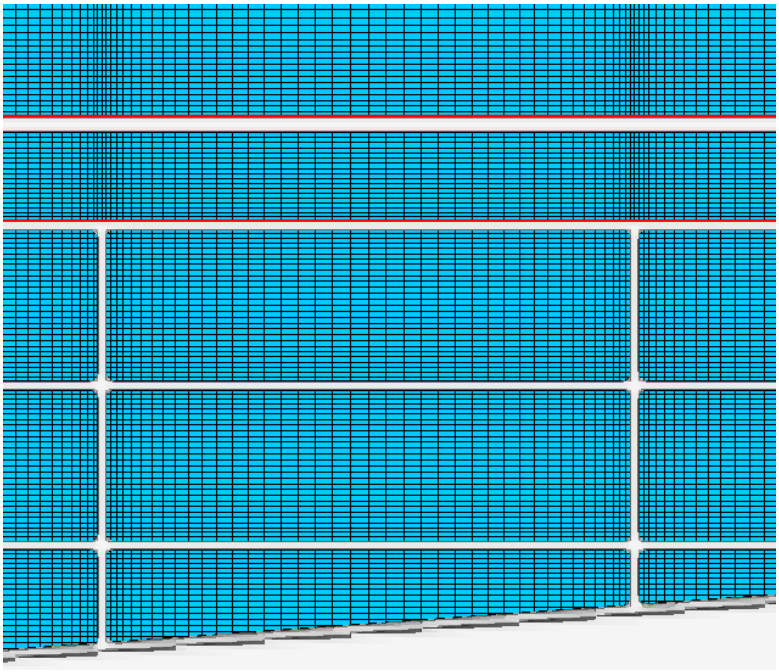

Figure 57 – Slice B-B through fine mesh of the Derby Dam for backwatered simulations

3.2.3 CFD Boundary Conditions

The CFD settings that were developed in correlation to the test data from the Davenport physical model were applied directly to the CFD models of the Derby Dam. A definitive list of Flow3D settings used in all simulations of the Derby Dam is given in *Appendix A*. The main boundary conditions are shown in *Figure 58* below and described beneath.

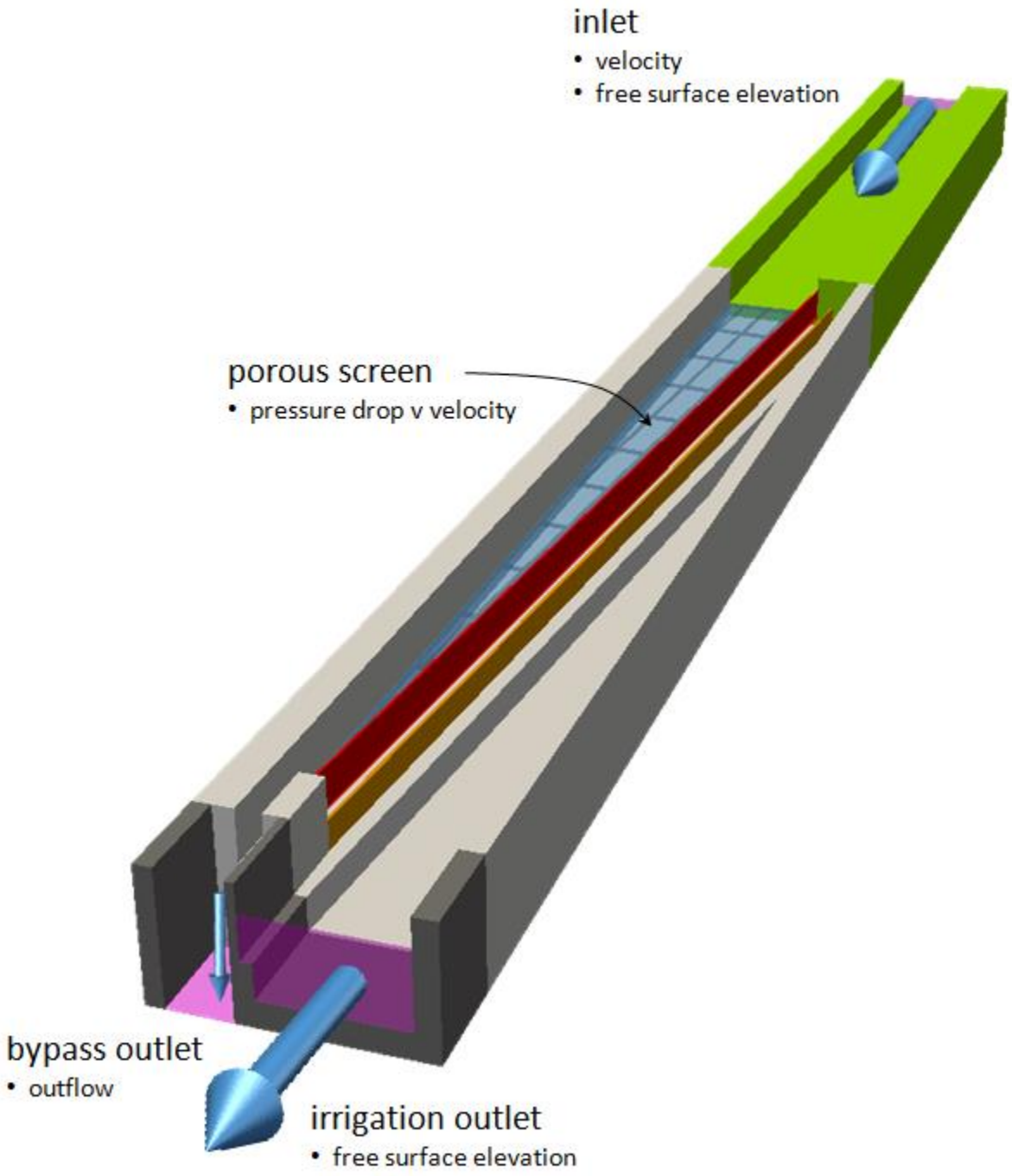

Figure 58 – Overview of the Derby Dam CFD model showing the main boundary conditions

Inlet

Specified Values

- Velocity (based on the required flow rate and free surface elevation)
- Free surface elevation (based on a calculation of the water elevation at the start of the inlet flume at the required flow rate)

Note: As water travels down the inlet flume, it settles to a depth that is a function of the flow rate and screen conditions, and is largely independent of the free surface elevation specified at the inlet.

Irrigation Outlet

Specified Values

- Free surface elevation – based on a calculation of the water level in the canal

Predicted Values

- Flow rate

Bypass Outlet

Specified Values

- None

Predicted Values

- Flow rate

Porous Screen

Specified Values

- Pressure drop versus vertical velocity (see *Section 2.2*)

Predicted Values

- Flow rate
- Velocities

3.2.4 CFD Solution Methodology

The starting point for the CFD simulations is an initial condition with a fixed elevation of stationary water throughout the model. From this initial condition, the CFD simulation progresses over a period of simulated time until a steady settled condition is achieved, which represents the flow in the Derby Dam screen subject to the specified boundary conditions.

The time to settle to the final steady flow condition is dependent on the initial condition, but is typically approximately 100 seconds in the Derby Dam simulations.

The solution methodology was therefore to simulate 150 seconds on the coarse mesh model to achieve a coarse prediction of the steady flow condition, then transfer the predicted flow field to the fine mesh model and continue for another 20-second simulated time. This provides a balance between accuracy and computation time.

Table 4 shows typical values for the mesh size, simulated time, and simulation time for both backwatered and non-backwatered simulations.

Table 4 – Mesh size and run time for typical CFD simulations of the Derby Dam

	Coarse mesh model			Fine mesh model		
	Fluid cells	Simulated time	Simulation time	Fluid cells	Simulated time	Simulation time
Backwatered simulation	1.65 million	150 s	5 hrs	3.64 million	20 s	2.5 hrs
Non-backwatered simulation	0.92 million	150 s	7 hrs	3.21 million	20 s	6 hrs

The timestep with which the Flow3D software progresses is typically on the order of 0.001 second, but varies depending on the flow at any instant, hence, the actual simulation time is somewhat variable.

All simulations were performed using Flow3D version 12.0 on a 16-core (32 thread) workstation with Intel E5-2687Wv2 processors.

3.3 Run List

Seven simulations of the Derby Dam were performed, as detailed below in *Table 5* and *Figure 59*. The three "Primary CFD simulations" cover operation of the baseline design for the Derby Dam screens in key flow conditions. The "Ancillary CFD simulations" were experimental tests of variations to the underbay geometry to assess their effect on the bypass flow.

Table 5 – List of CFD simulations of the Derby Dam

		entrance to inlet flume		irrigation outlet
Primary CFD simulations		flow rate (cfs)	water depth above top of screen (ft)	water depth above top of screen (ft)
Run01	maximum flow, backwatered	150	2.66	2.20
Run02	as Run01 but non-backwatered	150	2.66	n/a
Run07	as Run01, minimum flow, non-backwatered	78	1.64	n/a
Ancillary CFD simulations				
Run03	as Run01 with floor lowered by 8"	150	2.66	2.20
Run04	as Run01 with 10" wedge against center wall	150	2.66	2.20
Run05	as Run03 with 14" wedge against center wall	150	2.66	2.20
Run06	as Run01 with weir wall moved 10"	150	2.66	2.20

Run01	Run03
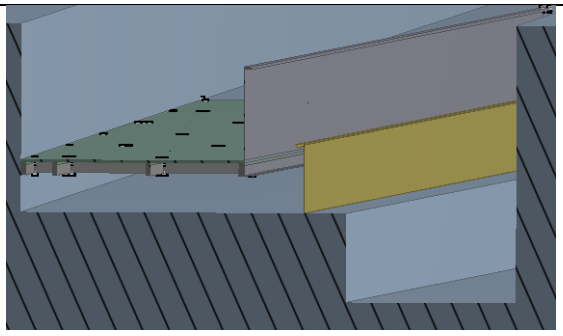	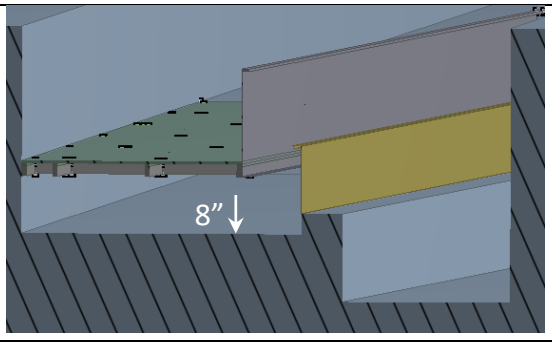

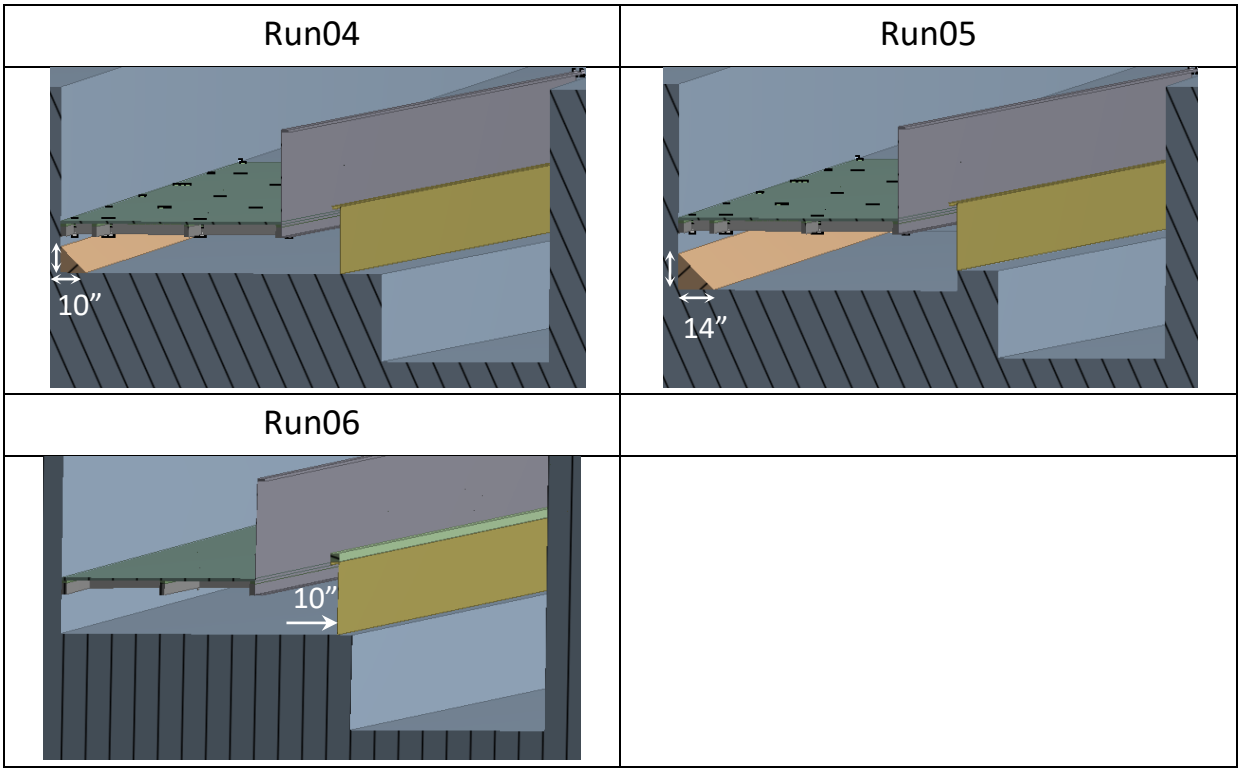

Figure 59 – Design variations to the Derby Dam simulated in CFD

Results and discussion of the primary simulations are given in *Section 3.4*. Results and discussion of the ancillary simulations follow in *Section 3.5*.

3.4 Results and Discussion of the Primary CFD Simulations of the Derby Dam

Results from the three primary CFD simulations of the Derby Dam, in the form of predicted flow measures and flow visualization, are presented in *Section 3.4.1* below. These results are then compared to the results from CFD simulations of the Davenport physical model at similar operating conditions in *Section 3.4.2*. Comments on all results are given in *Section 3.4.3*.

3.4.1 Results of Primary CFD Simulations

Table 6 – Predicted flow balance for primary CFD simulations of the Derby Dam

	Flow rate (cfs)		
	Intake	Irrigation	Bypass
Run01	150	120	30
Run02	150	126	24
Run07	78	66	13

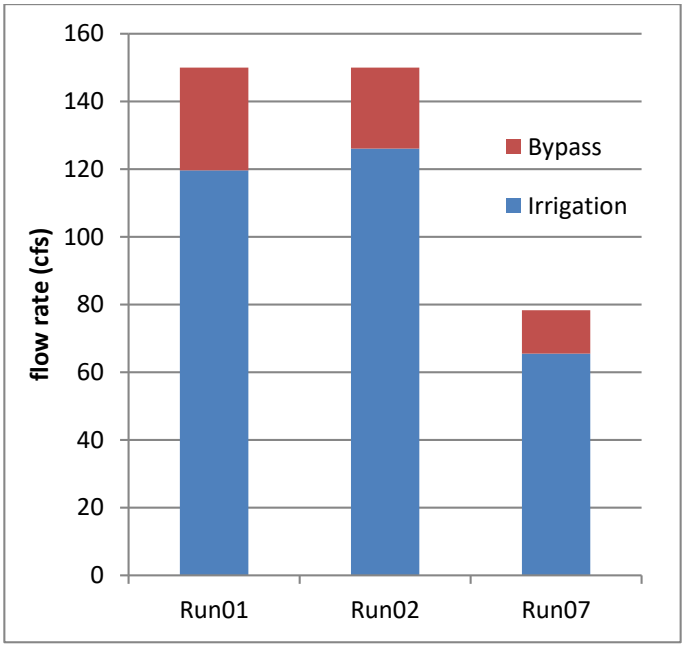

Figure 60 – Predicted flow balance for primary CFD simulations of the Derby Dam

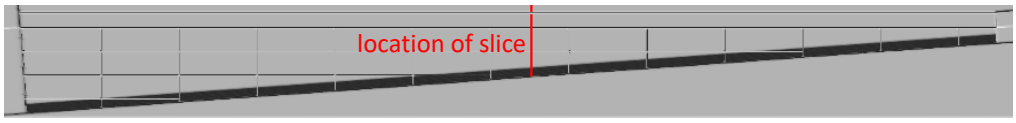

Figure 61 – Location of streamline slices

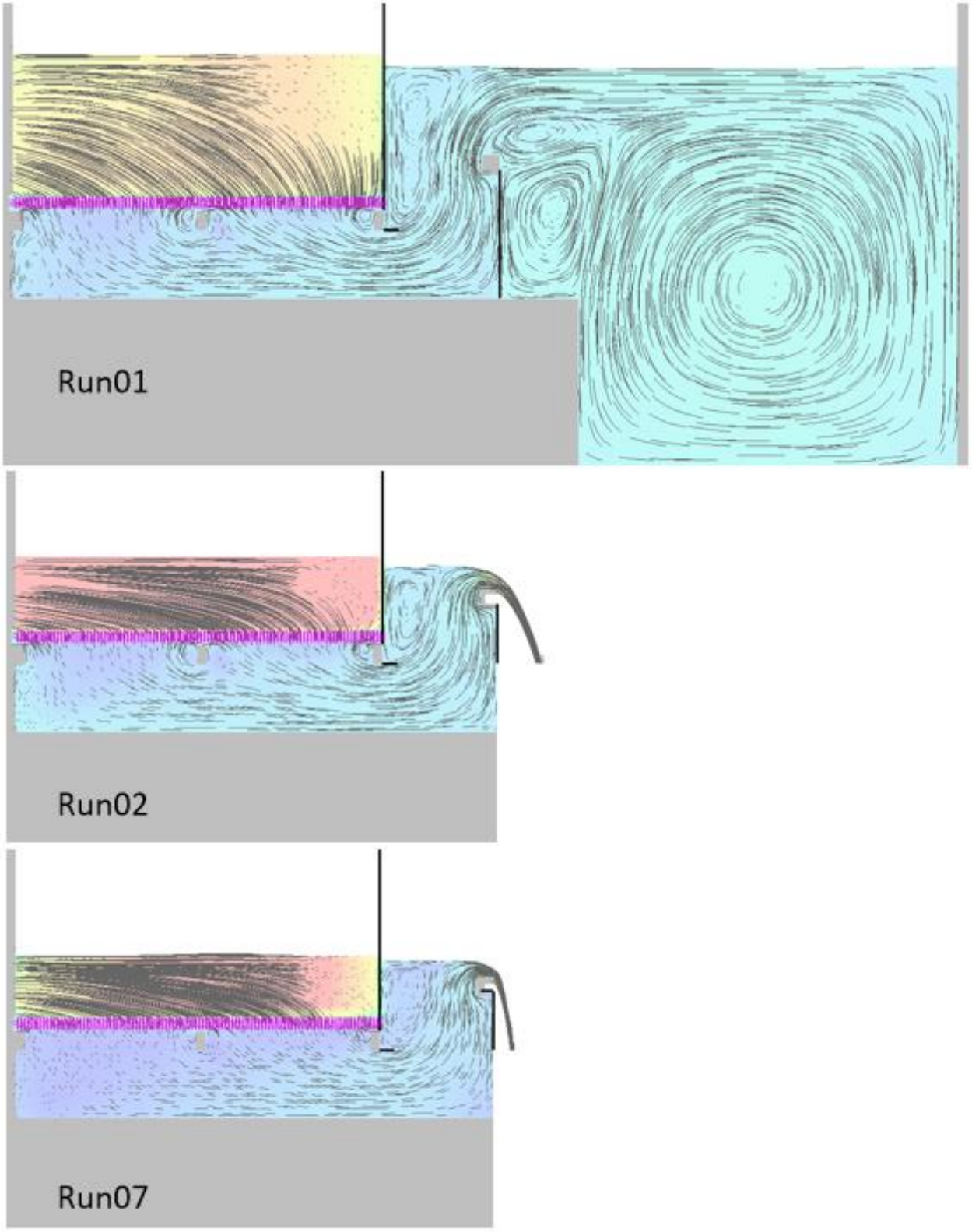

Figure 62 – Vertical slice through primary Derby Dam simulations showing streamlines in the plane of the slice (slice location as Figure 61)

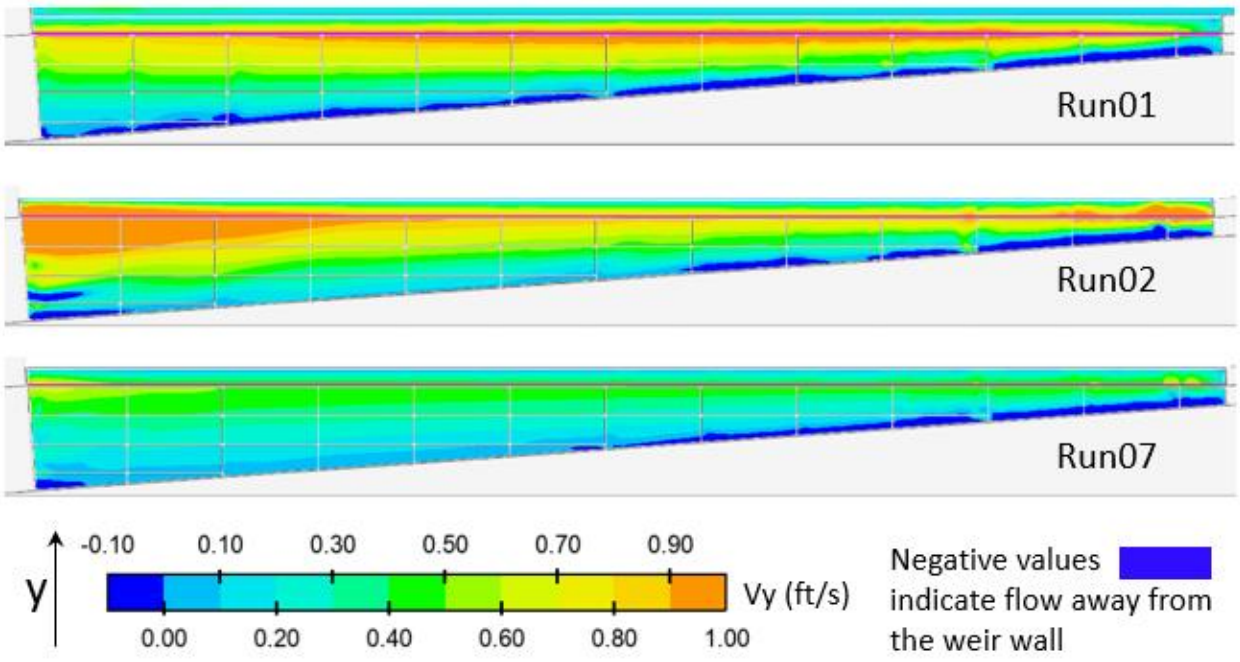

Figure 63 – Contours of y-velocity on a horizontal slice 0.2 inch above the floor of the underbay

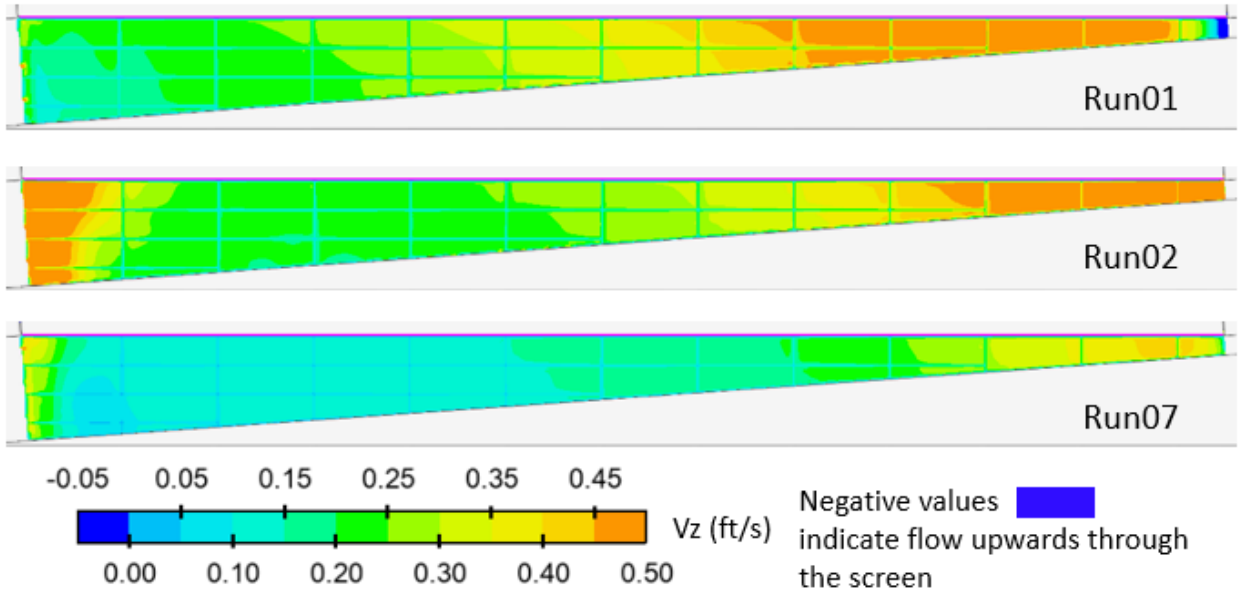

Figure 64 – Contours of downwards vertical velocity on a slice through the porous screen

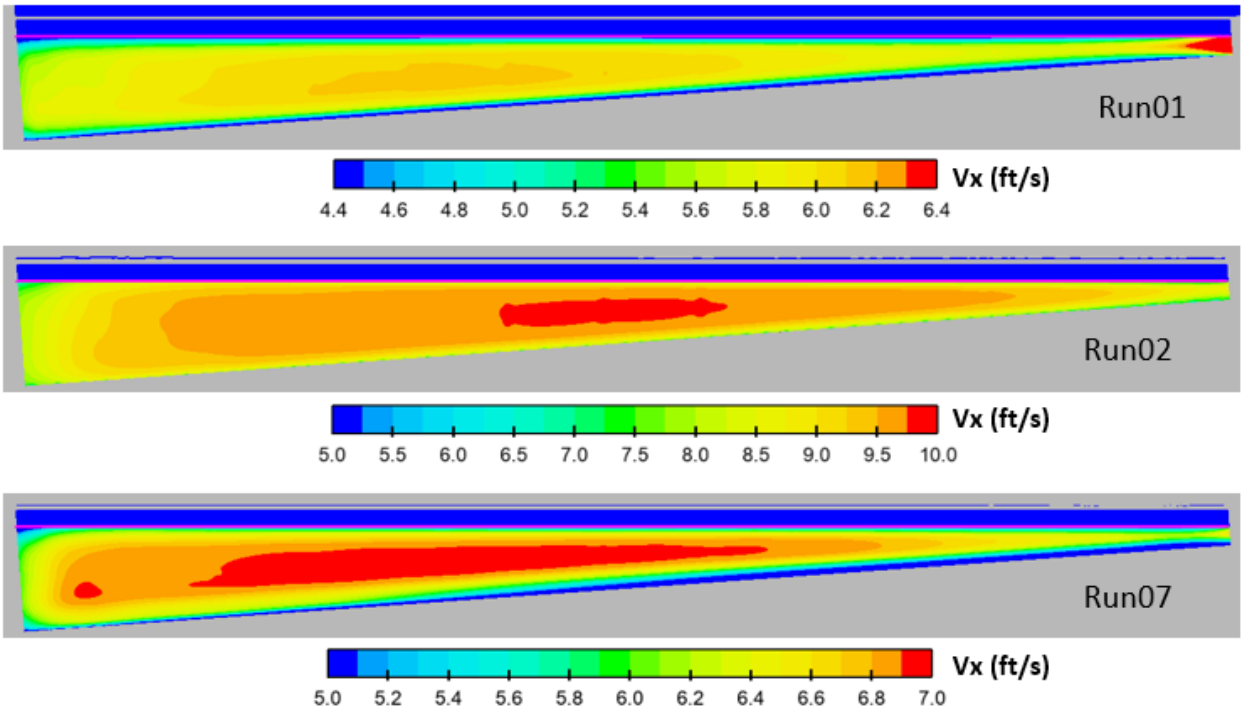

Figure 65 – Contours of sweeping velocity at 5.9 inches above the screen (i.e., approximately 80 percent depth for Run01)

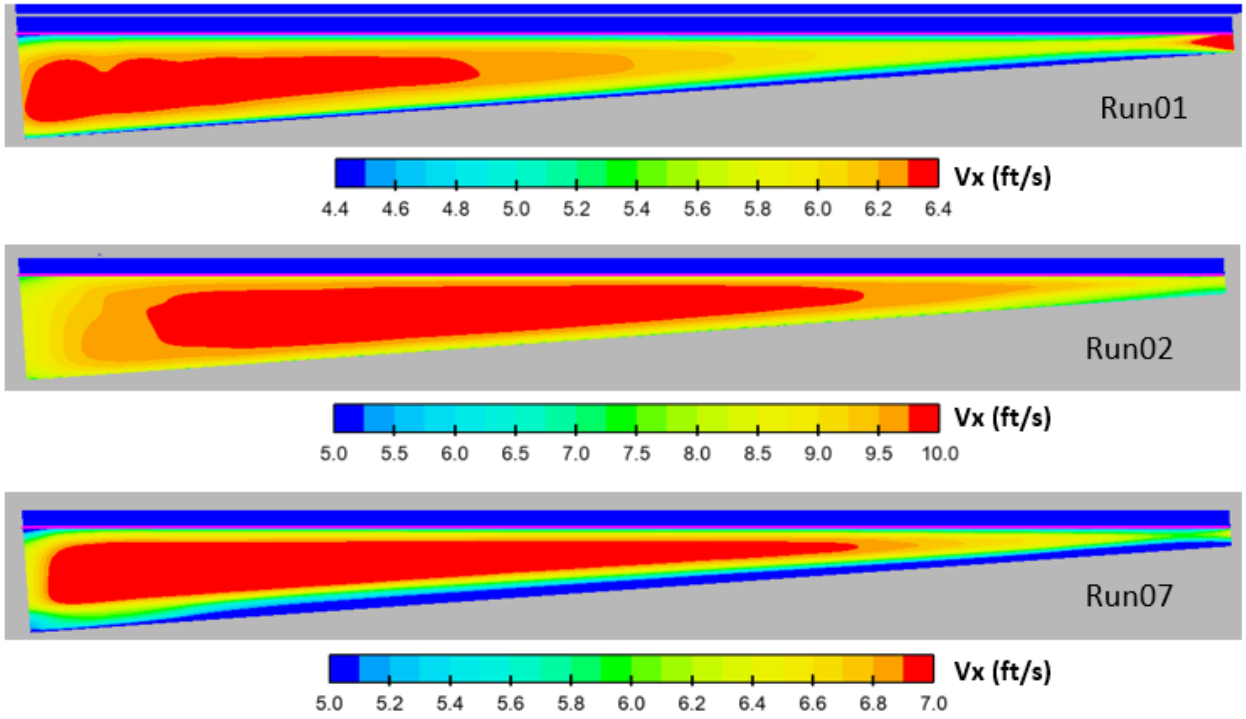

Figure 66 – Contours of sweeping velocity at 11.8 inches above the screen (i.e., approximately 60 percent depth for Run01)

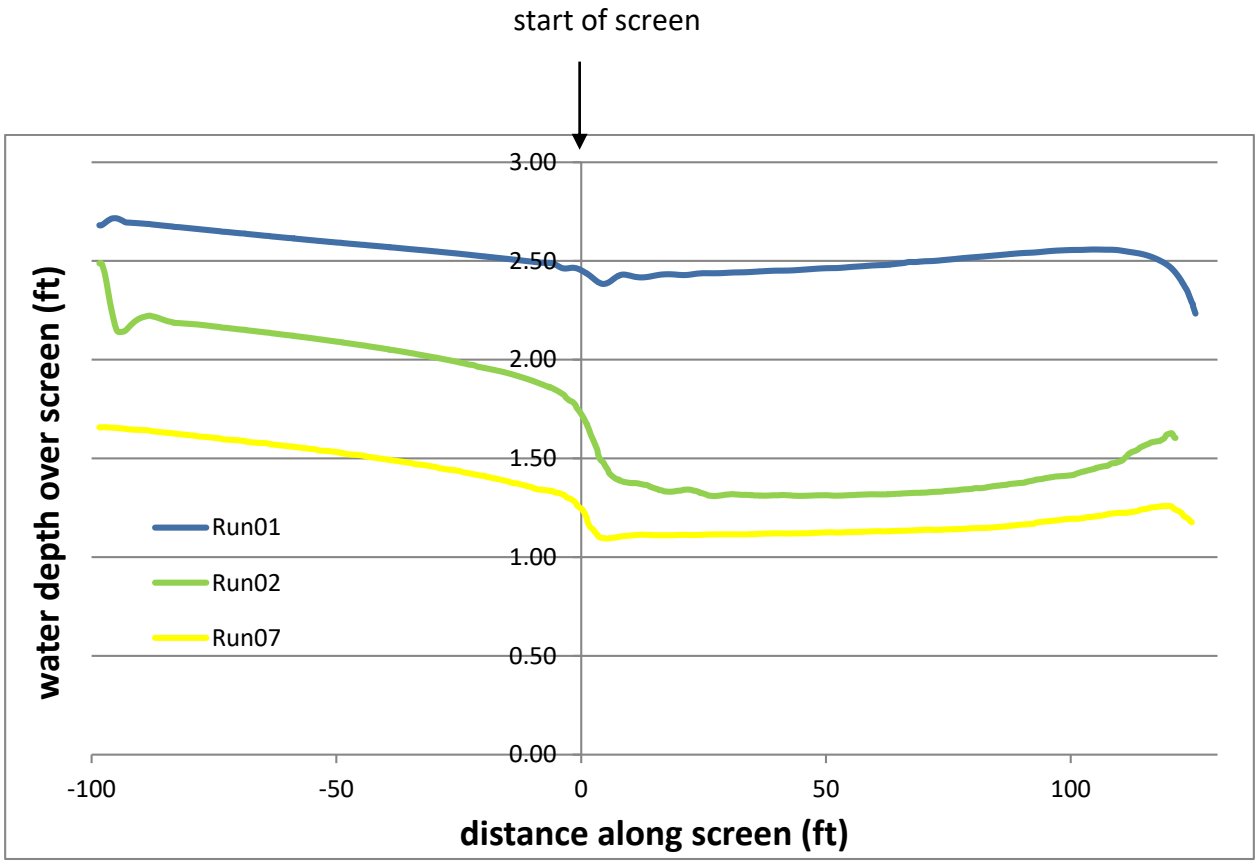

Figure 67 – Predicted water depth along the screen

3.4.2 Comparison to CFD Predictions from Davenport

Below, the results from the Derby Dam CFD simulations are compared to the results from the Davenport CFD simulations. Two comparisons are made; in backwatered conditions and in non-backwatered conditions. Comments on these results are given in *Section 3.4.3*.

Derby Dam Run01 (150 cfs, backwatered) versus Davenport OP1 (89 cfs, backwatered)

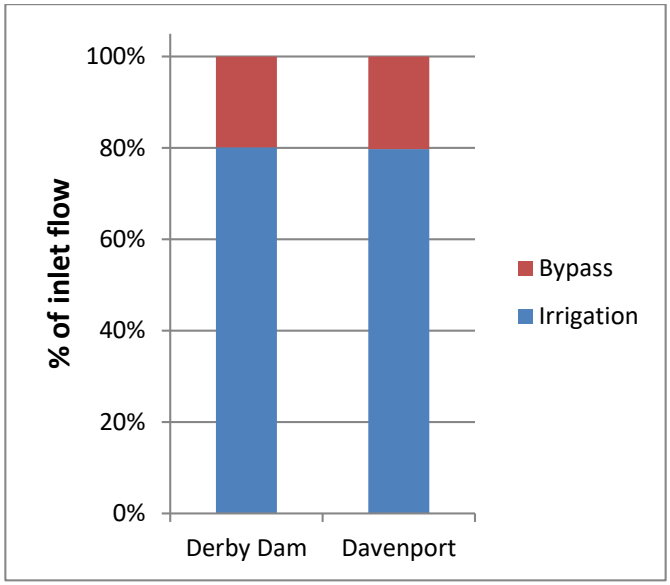

Figure 68 – Predicted flow balance as a percent of inlet flow

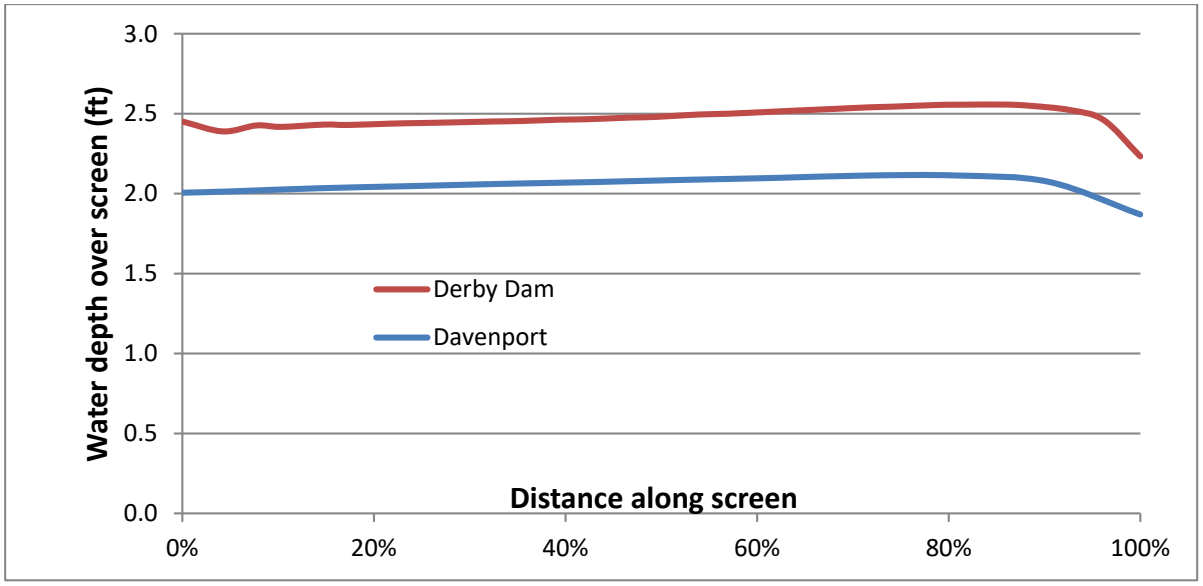

Figure 69 – Predicted water depth along the screen

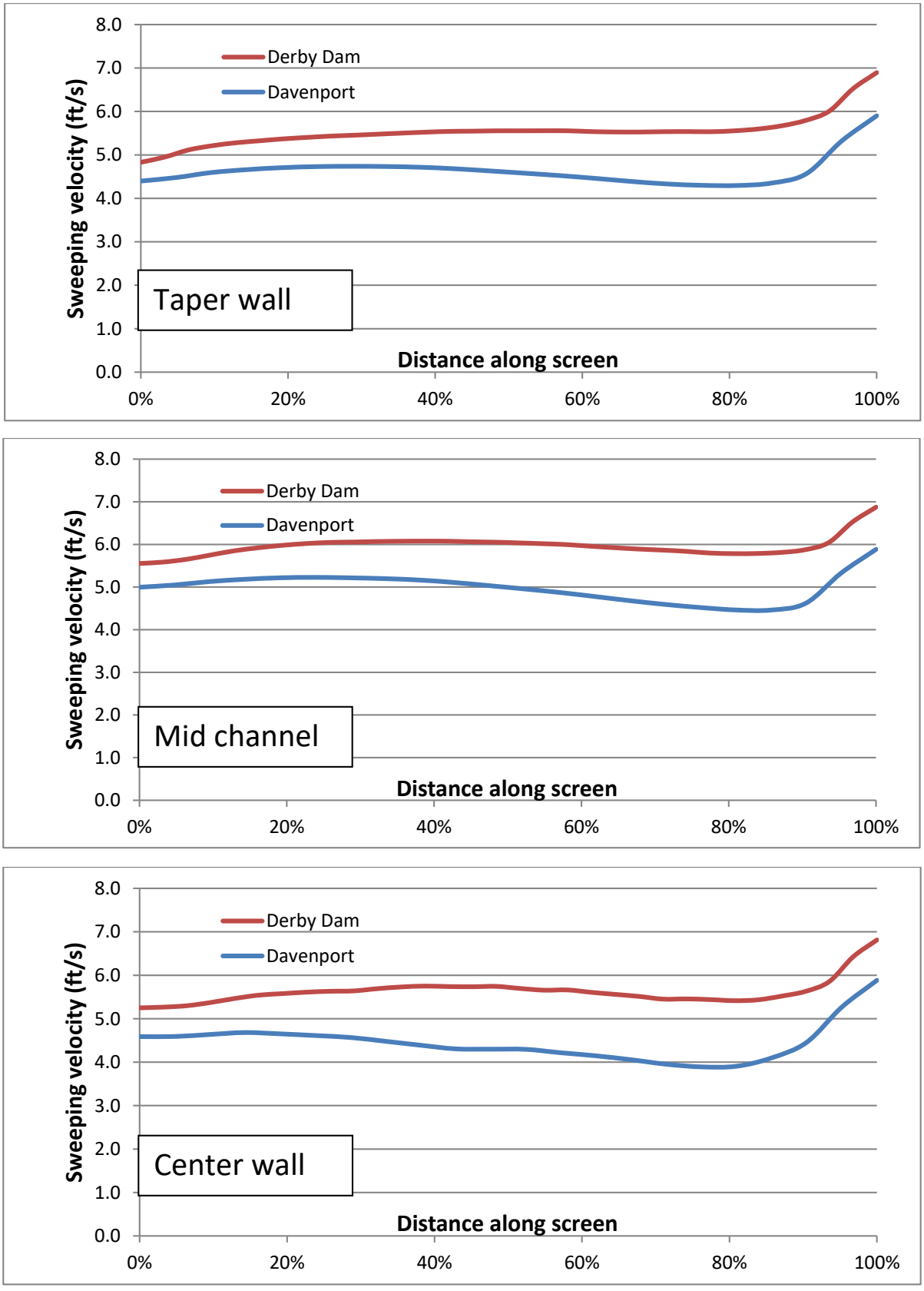

Figure 70 – Predicted sweeping velocity 4 inches above the surface of the screen

Derby Dam Run02 (150 cfs, non-backwatered) versus Davenport OP4 (84 cfs, non-backwatered)

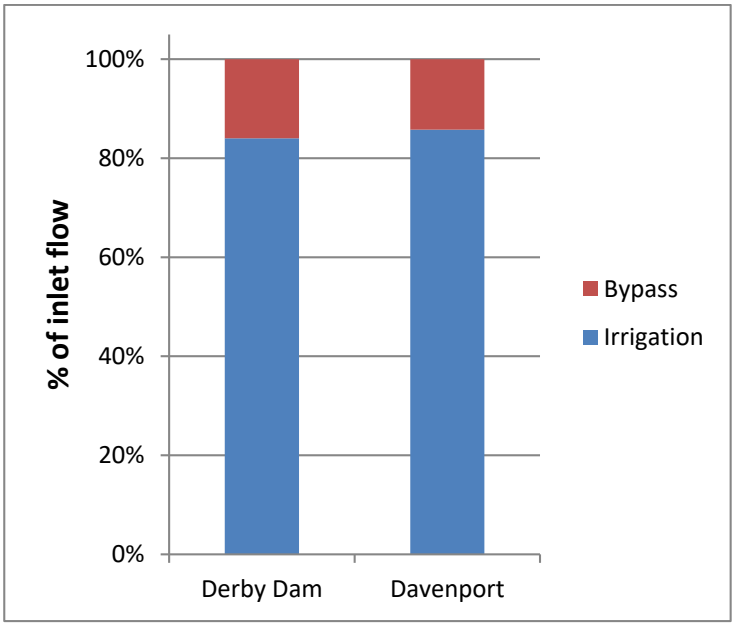

Figure 71 – Predicted flow balance as a percent of inlet flow

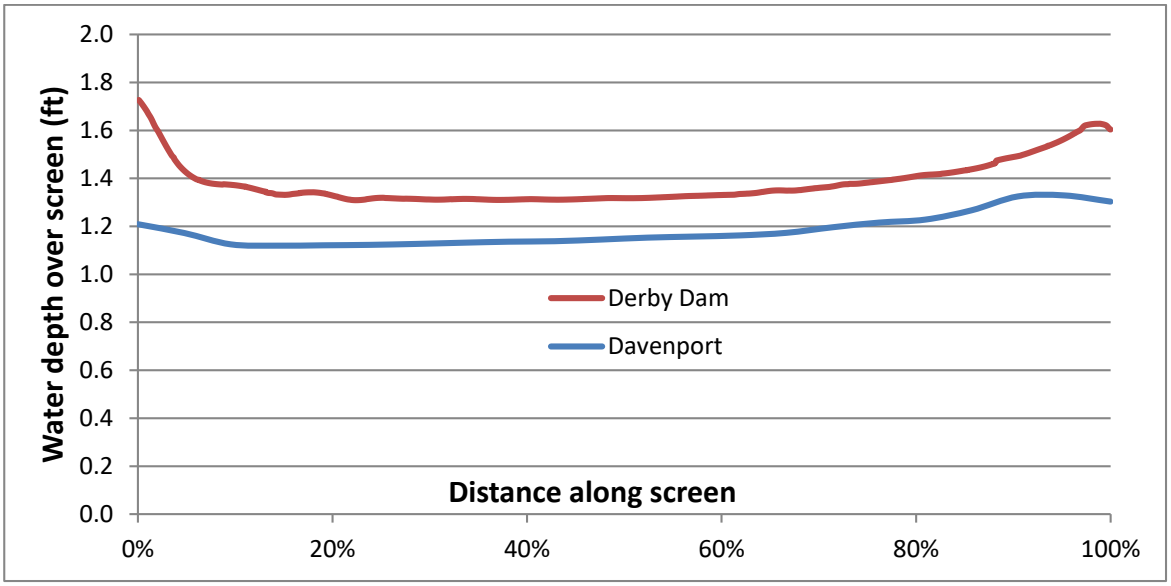

Figure 72 – Predicted water depth along the screen

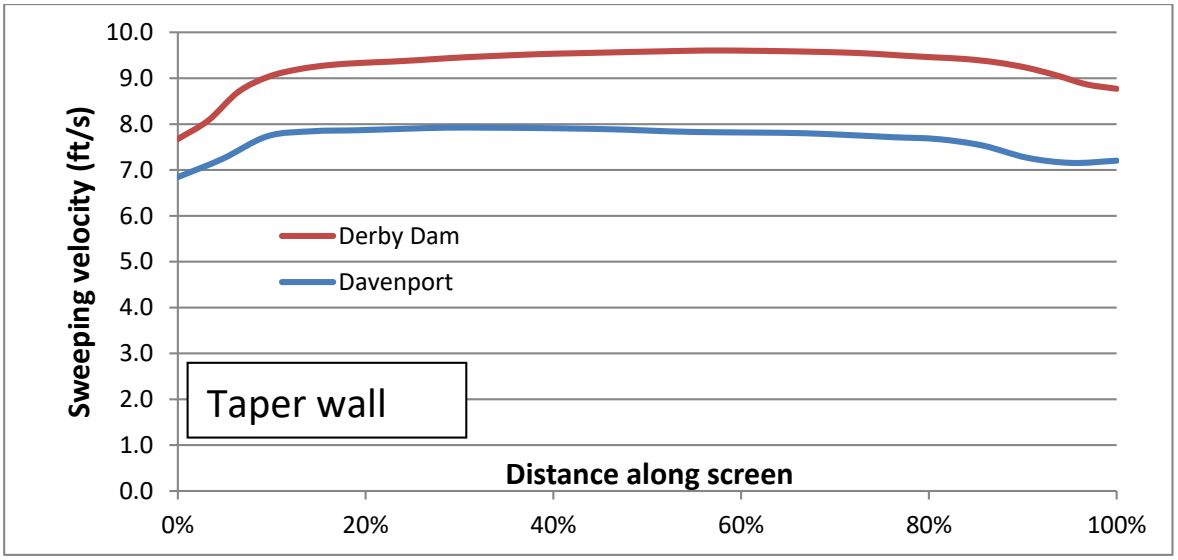

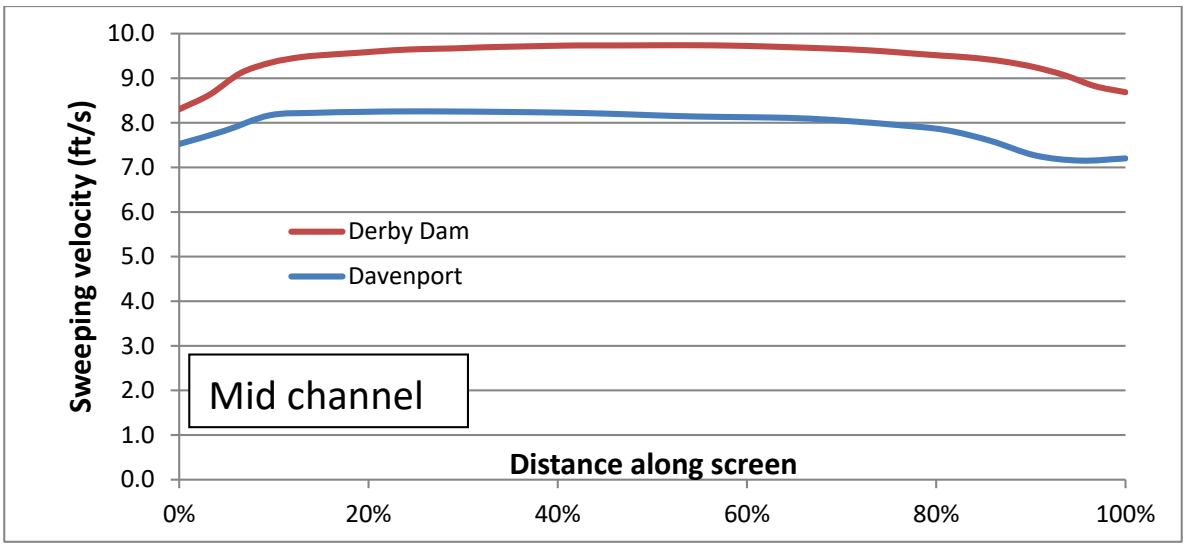

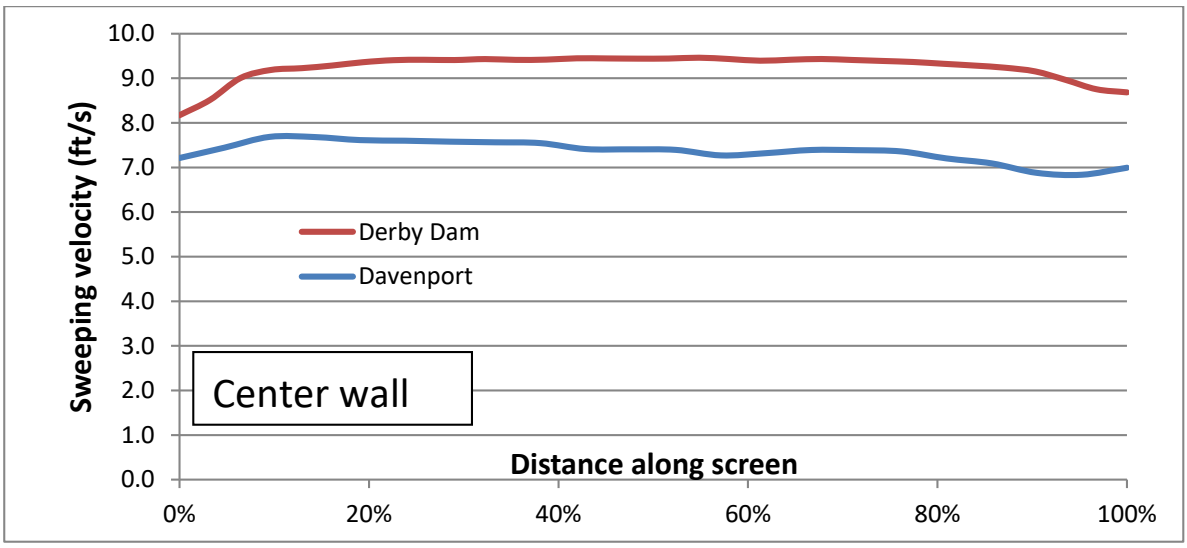

Figure 73 – Predicted sweeping velocity 4 inches above the surface of the screen

3.4.3 Review of Primary CFD Simulations of the Derby Dam

This section reviews the results of the primary CFD simulations of the Derby Dam presented in *Section 3.4.1* and *Section 3.4.2* above. The results are viewed in the light of the accuracy and limitations of the CFD model that were discussed in detail in *Section 2.4*.

Run01 – Maximum Flow, Backwatered Weir

Run01 is representative of the condition in which all five screens are operating at their maximum flow rate and the water depth in the canal is at full capacity. The inlet flow to the screen is fixed at 150 cfs and the weir wall is backwatered.

Comparison to CFD Model of the Davenport Screen at OP1

The Run01 CFD model of the Derby Dam shows identical flow balance to the CFD model of the Davenport screen at OP1 (see *Figure 68*) and very similar patterns of sweeping velocity and water depth (see *Figure 69* and *Figure 70*). It is therefore reasonable to assume that under these flow conditions, the real-world flow patterns at the Derby Dam will be very similar to the real-world flow patterns at the Davenport screen. In addition, it is likely that if the CFD model of the Davenport screen predicted a flow parameter to be 5 percent greater than the real-world measurement, then the CFD model of the Derby Dam will over-predict the same flow parameter by 5 percent. This logic is used to inform the comments below.

Flow Balance

From 150 cfs flow in the inlet flume, the CFD model predicts 120 cfs flow to irrigation, i.e., 80 percent of the total (see *Figure 60*). However, in similar flow conditions for the Davenport screen (OP1), the CFD model predicted 80 percent flow to irrigation when the actual measured value was 84 percent of the total (see *Figure 68* and *Figure 47*). Therefore, a best estimate is that given 150 cfs inlet flow at the Derby Dam, 84 percent (i.e., 126 cfs) will go to irrigation and 16 percent (i.e., 24 cfs) to bypass.

Streamlines

The streamline image (*Figure 62*) shows the complex patterns of recirculation around the taper wall, the weir wall, and in the attenuation bay. Two areas of interest stand out:

- A low-velocity recirculation beneath the screen against the center wall. Any sediment in this region would not be readily drawn towards the weir wall.
- A recirculating region against the downstream side of the taper wall. This appears to restrict the flow up and over the weir wall.

Flow Beneath the Screen

The effect of the recirculation beneath the screen is seen in *Figure 63*, which shows a dark blue region up against the center wall in which water is moving away from the weir wall rather than towards it.

Flow Through the Screen

Figure 64 shows a steadily increasing velocity through the screen, from beginning to end, with a final brief upwelling at the end of the screen. However, in similar flow conditions for the Davenport screen (OP1), a marked draw down in the water surface was measured in the first few feet of the screen (see *Figure 45*). This is a common observation on other installations of the Farmers Screen. The draw down is expected to be associated with a high downward velocity through the beginning of the screen. It is likely that a similar process will occur at the Derby Dam.

Sweeping Velocity

When the weir wall is backwatered, the water depth over the screen is very closely dependent on the water depth in the attenuation bay, and, hence, the expected water depth in the canal. For a given flow rate, as the water depth over the screen increases, the sweeping velocity must decrease. Run01 represents the condition of maximum flow and water depth in the canal (600 cfs), and, hence, is likely to represent the condition in which the sweeping velocity over the screen is lowest.

The predicted sweeping velocity for Run01 in *Figure 66* shows a gradual deceleration from the beginning of the wedge-wire screen to a minimum of approximately 15 feet from the end of the screen. Closer to the surface of the wedge wire (*Figure 65*), the minimum sweeping velocity is predicted to occur at the very beginning of the screen. In both cases, the minimum sweeping velocity is about 5 ft/s averaged across the width of the screen.

The predicted sweeping velocity, 4 inches above the surface of the screen at the Derby Dam, is higher than that at the Davenport screen, and shows somewhat less deceleration along the length of the screen (see *Figure 70*). Interpolating from the relationship between the Davenport CFD model and the measured data (*Figure 86*, *Figure 87*, and *Figure 88*), the minimum sweeping velocity at the Derby Dam in this flow condition is expected to be between 4.5 and 5.0 ft/s. This is well above the minimum required sweeping velocity of 2.5 ft/s specified in *Table 2*.

Water Depth

Figure 67 shows the water surface elevation throughout the CFD model. A gradual drop in elevation is seen along the length of the inlet flume. There is then a small draw down at the beginning of the screen before a steady increase in level along the screen. Finally, the water level drops sharply as the water accelerates towards the bypass outlet. As noted above, there is likely to be a more pronounced draw down than predicted.

The predicted water level at the Derby Dam is approximately 0.5 feet higher than the predicted water level at the Davenport screen (see *Figure 69*). The measured minimum water level at the Davenport screen in these conditions was >1.7 feet. The minimum real-world water level at the Derby Dam can therefore be expected to be approximately 2.2 feet (=1.7 feet + 0.5 feet). This is well above the minimum required water level of 1 foot specified in *Table 2*.

Run02 – Maximum Flow, Non-Backwatered Weir

Run02 is representative of the conditions in which one or more screens are expected to be operating the majority of the time. The inlet flow to the screen is fixed at 150 cfs, and the weir is not backwatered.

Comparison to CFD Model of the Davenport Screen at OP4

The Run02 CFD model of the Derby Dam predicts a similar flow balance and similar patterns of sweeping velocity and water depth to the CFD model of the Davenport screen at OP4 (see *Figure 71, Figure 72*, and *Figure 73*). The CFD simulation of the Davenport screen at similar conditions (OP4) significantly under-predicted the irrigation flow and significantly over-predicted the minimum sweeping velocity. It is expected that a similar relationship between CFD predictions and actual conditions will hold at the Derby Dam. However, the lower confidence in the CFD model at this flow condition does not warrant precise estimates to be made of the irrigation flow rate or the minimum sweeping velocity at the Derby Dam.

Flow Balance

From 150 cfs flow in the inlet flume, the CFD model predicts 126 cfs flow to irrigation, i.e., 84 percent of the total (see *Figure 60*). However, in similar flow conditions for the Davenport screen (OP1), the CFD model predicted 86 percent flow to irrigation, when the actual measured value was 93 percent of the total (see *Figure 52* and *Figure 71*). It is therefore very likely that the CFD model of the Derby Dam is also significantly under-predicting the irrigation flow rate at these conditions.

Streamlines

The streamline image (*Figure 62*) shows the same patterns of recirculation beneath the screen as was observed for Run01. Two areas of interest stand out:

- A low-velocity recirculation beneath the screen against the center wall. Any sediment in this region would not be readily drawn towards the weir wall.
- A recirculating region against the downstream side of the taper wall. This appears to restrict the flow up and over the weir wall.

Flow Beneath the Screen

In *Figure 63*, there are some regions of dark blue close to the center wall in which water is moving away from the weir wall rather than towards it. However, the areas are less widespread in Run02 compared to Run01.

Flow Through the Screen

The CFD simulation predicts a strong draw down of water through the first 5 feet of the wedge-wire screen, followed by a sharp decrease in the through-screen velocity, and then a steady increase along the rest of the screen (see *Figure 64*). This is a common observation on installations of the Farmers Screen. Comparison to the Davenport simulation at OP4 (*Figure 72*) suggests that the draw down may be more marked at the Derby Dam in these conditions.

Sweeping Velocity

Compared to the same flow rate in a backwatered condition (Run01), the CFD model predicts much higher sweeping velocities over the screen. Although there is less confidence in the accuracy of the predicted sweeping velocity at this operating condition, it is certain that the requirement of screen sweeping velocity >2.5 ft/s will be met.

Water Depth

The shape of the predicted water depth curve is similar to that of the simulation of the Davenport screen at OP4, but approximately 0.2 foot higher and with a more pronounced draw down at the start of the screen (see *Figure 72*). The real-world data from the Davenport screen showed a water depth of between 0.9 foot and 1.1 feet above the screen at these conditions (see *Figure 51*). Consequently, it is likely that the actual water depth at the Derby Dam will be approximately 0.2 foot higher than at the Davenport screen, and will therefore meet the minimum requirement of 1 foot of water depth.

Run07 – Minimum Flow, Non-Backwatered Weir

Run07 is representative of the minimum flow condition for a screen at the Derby Dam in which approximately 65 cfs goes to irrigation and the weir wall is not backwatered.

Comparison to CFD Predictions at Maximum Flow (Run02)

Qualitatively, the CFD predictions for Run07 show very similar trends in flow balance, flow patterns, sweeping velocity, and water depth to Run02. Quantitatively, everywhere, the flow velocities are lower than Run02 and the water depth is lower than Run02.

Flow Balance

The CFD model predicts that 78 cfs inlet flow is required to deliver 66 cfs to irrigation, i.e., 84 percent of the total (see *Figure 60*). This percentage of irrigation flow is the same as what is

predicted for Run02, and it is therefore likely that, as for Run02, the CFD model of the Derby Dam is significantly under-predicting the irrigation flow rate at the Run07 conditions.

Streamlines

The streamline image (*Figure 62*) shows the same patterns of recirculation beneath the screen and against the taper wall that were observed for Run01 and Run02.

Flow Beneath the Screen

Figure 63 shows similar regions of dark blue close to the center wall as in Run02. In these regions, water is predicted to be moving away from the weir wall rather than towards it.

Flow Through the Screen

The CFD simulation predicts a similar pattern of through-screen flow as in Run02. There is draw down of water through the first 5 feet of the wedge-wire screen, followed by a decrease in the through-screen velocity, and then a steady increase along the rest of the screen (see *Figure 64*).

Sweeping Velocity

The pattern of sweeping velocity predicted for Run07 is similar to that for Run02 (see *Figure 65* and *Figure 66*). There is an initial acceleration as the water comes onto the screen, followed by a steady decrease along the screen. The minimum sweeping velocity is predicted to occur in the last 10 feet of the screen. In general, the sweeping velocities are approximately 70 percent of those predicted at the maximum flow condition (Run02) and are likely to be above the 2.5 ft/s criterion.

Water Depth

The water surface is predicted to follow the same pattern as the high flow condition (Run02), but with about 0.2 foot reduced depth (see *Figure 67*). Comparison of Run07 to Run02 to the Davenport model of OP4 does not give certainty that the minimum water depth of 1 foot will be achieved throughout. However, the height of the weir wall can be tuned to meet the required minimum water depth at this minimum flow condition.

3.5 Results and Discussion of the Ancillary CFD Simulations of the Derby Dam

As well as the primary CFD simulations, a number of experimental simulations were performed to assess the impact of geometry changes on the bypass flow. Results from these ancillary CFD simulations of the Derby Dam, in the form of predicted flow measurements and flow visualizations, are presented below in *Section 3.5.1*. The results are compared to the CFD simulation of the baseline design in backwatered conditions (Run01). Comments on all results are given in *Section 3.5.2*.

3.5.1 Results of Ancillary CFD Simulations

Table 7 – Predicted flow balance for ancillary CFD simulations of the Derby Dam

	Flow rate (cfs)		
	Intake	Irrigation	Bypass
Run01	150	120	30
Run03	150	120	30
Run04	150	120	30
Run05	150	121	29
Run06	150	120	30

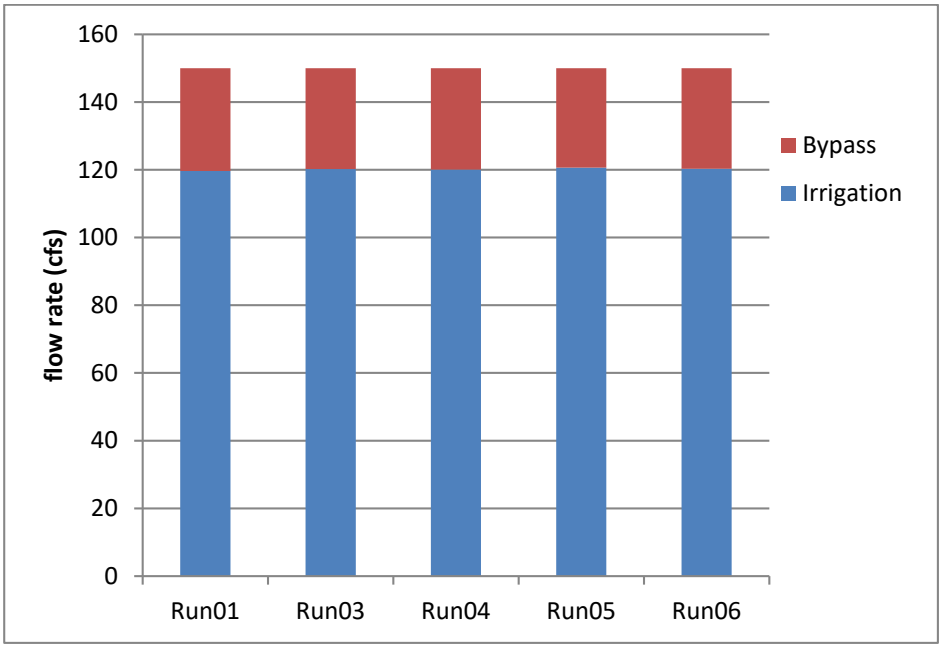

Figure 74 – Predicted flow balance for ancillary CFD simulations of the Derby Dam

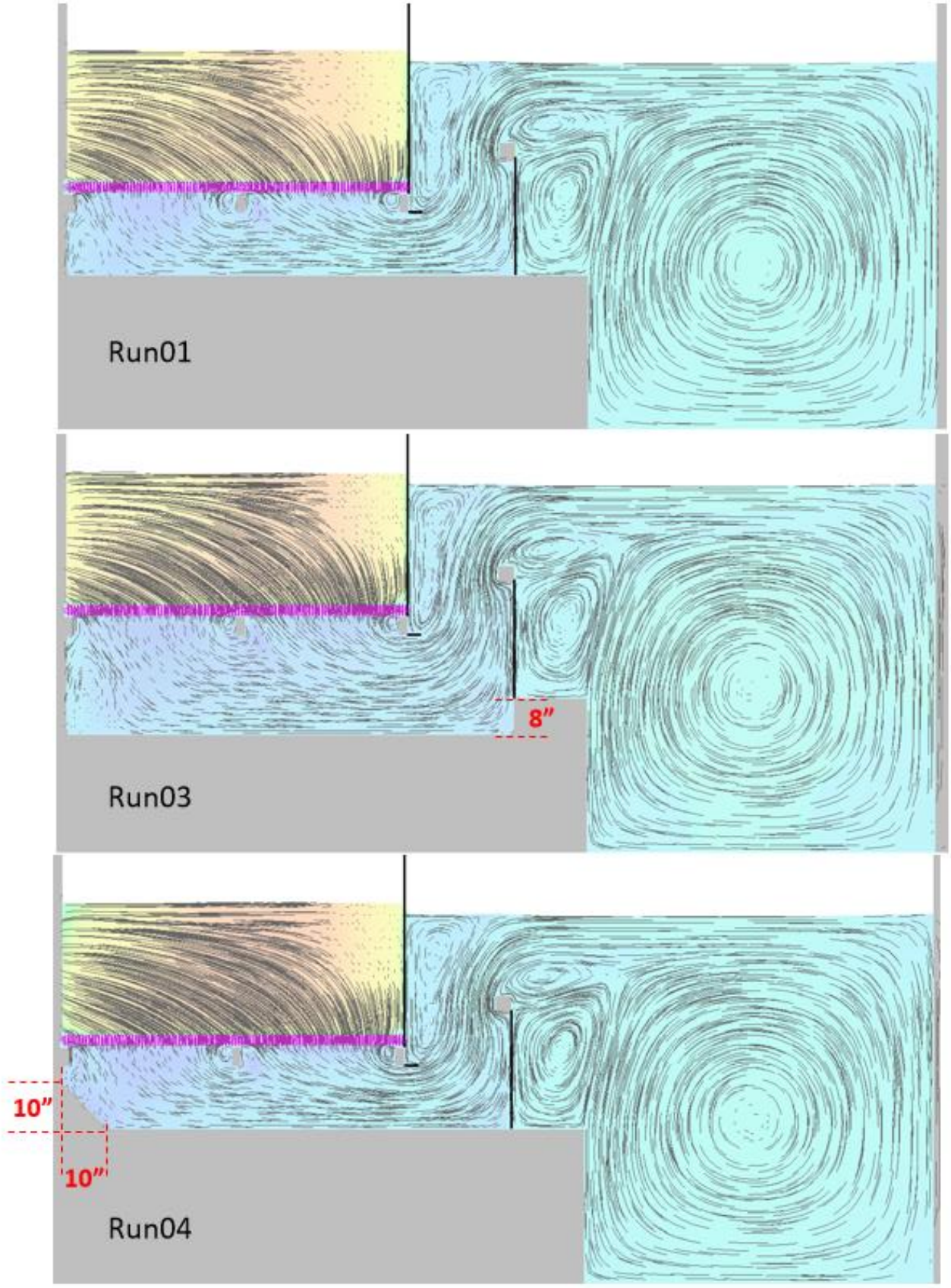
Run01
8”
Run03
10”
10”
Run04

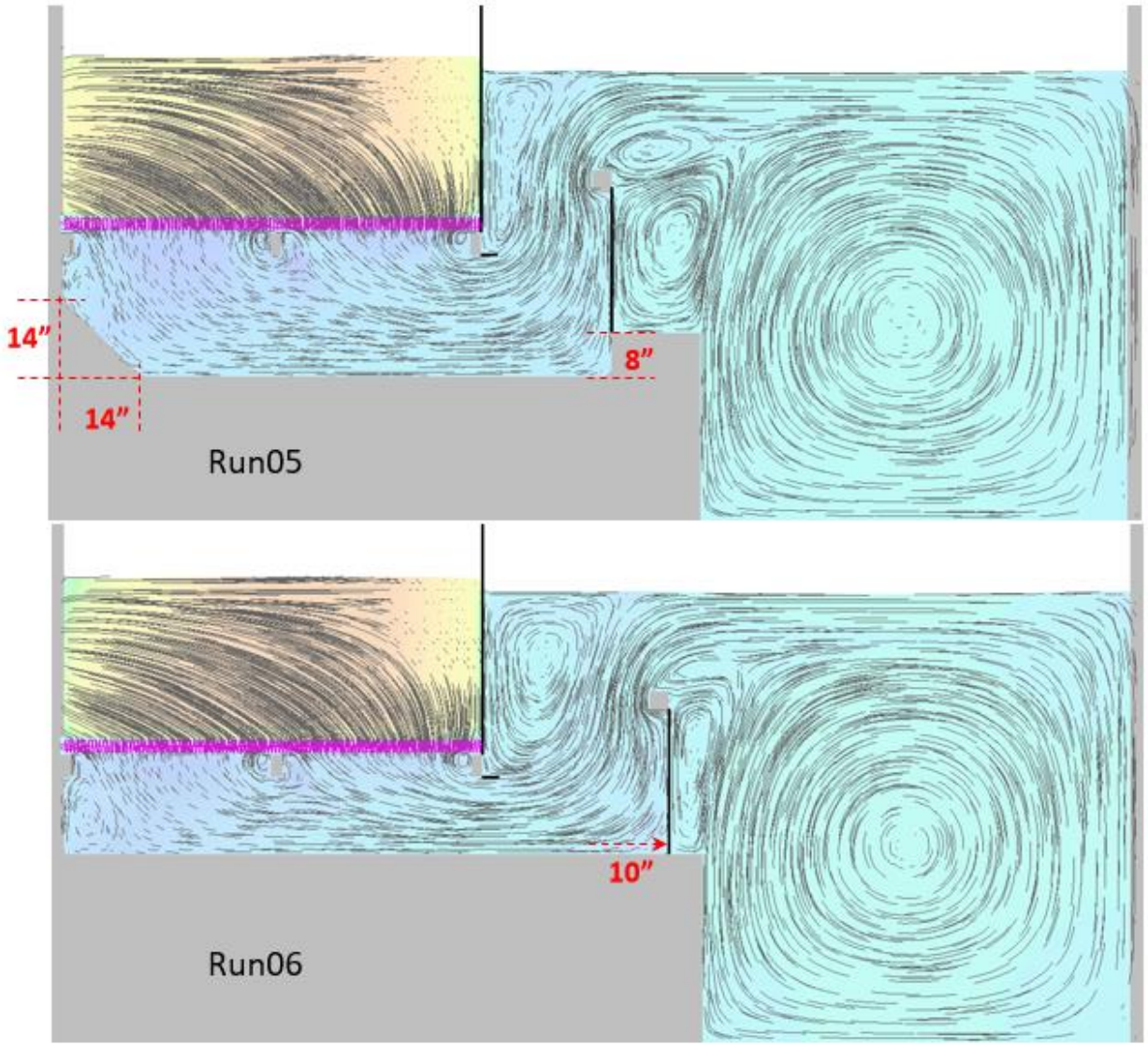

Figure 75 – Vertical slice through ancillary Derby Dam simulations showing streamlines in the plane of the slice (slice location as Figure 61)

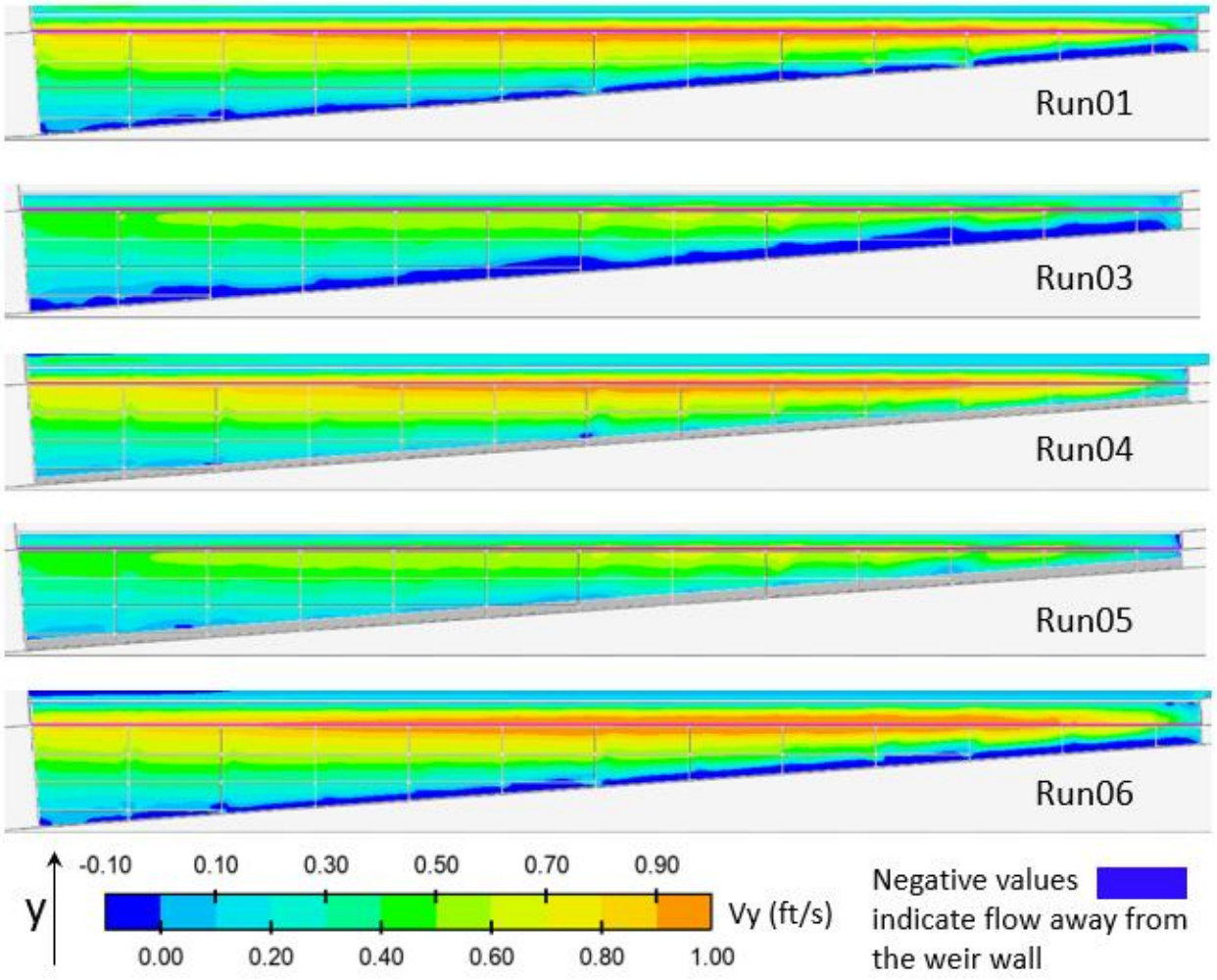

Figure 76 – Contours of y-velocity on a horizontal slice 0.2 inch above the floor of the underbay

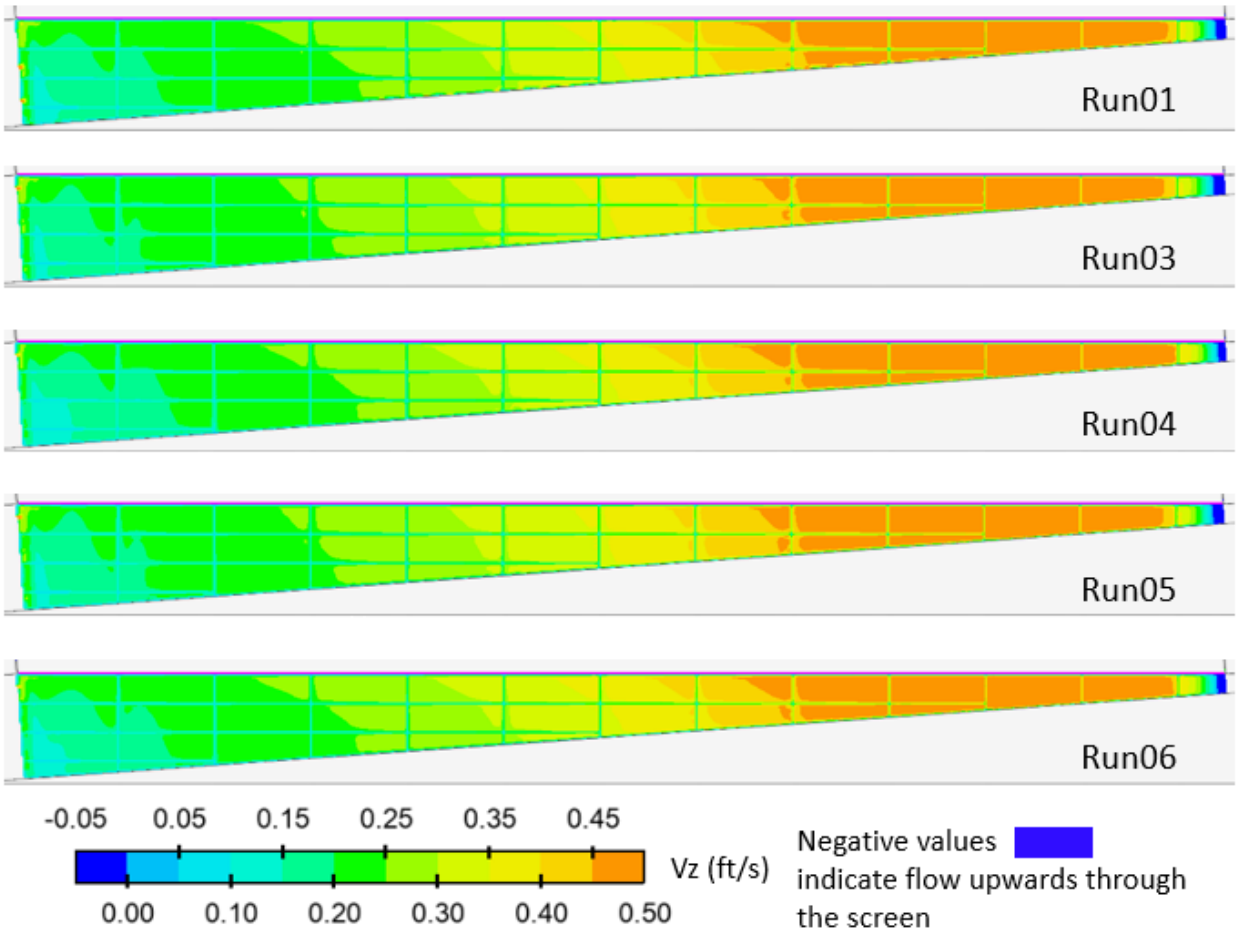

Figure 77 – Contours of downwards vertical velocity on a slice through the porous screen

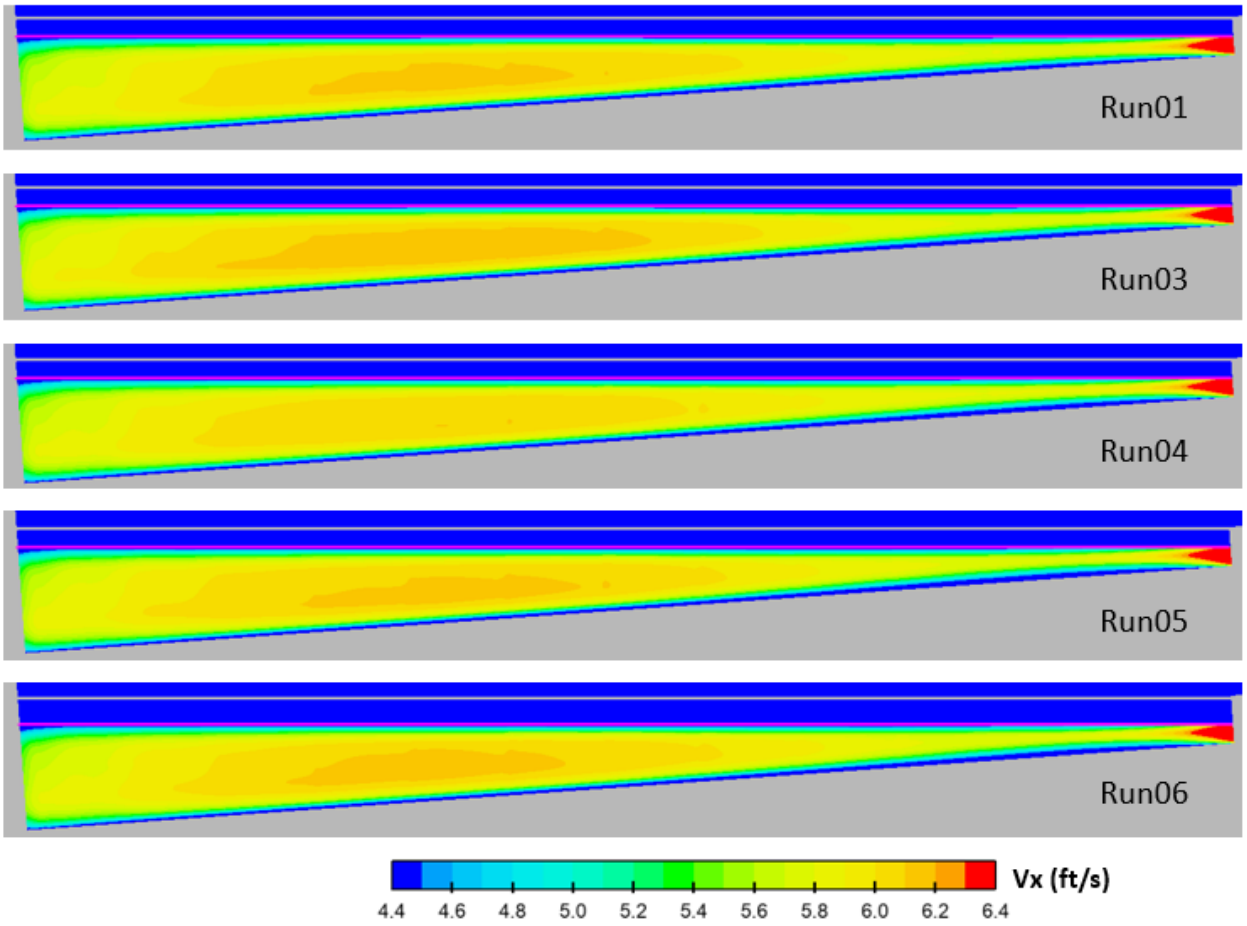

Figure 78 – Contours of sweeping velocity at 5.9 inches above the screen (i.e., approximately 80 percent depth)

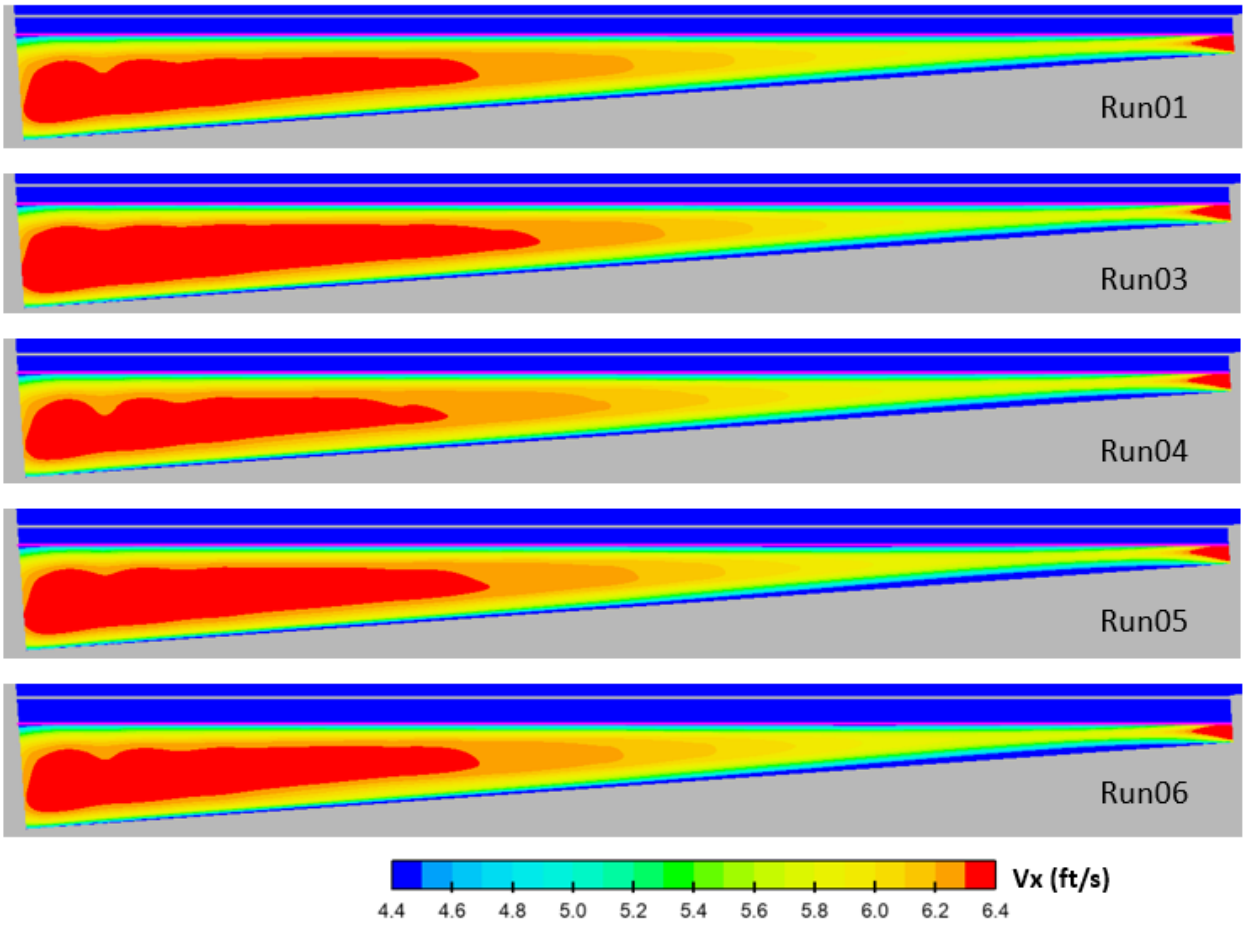

Figure 79 – Contours of sweeping velocity at 11.8 inches above the screen (i.e., approximately 60 percent depth)

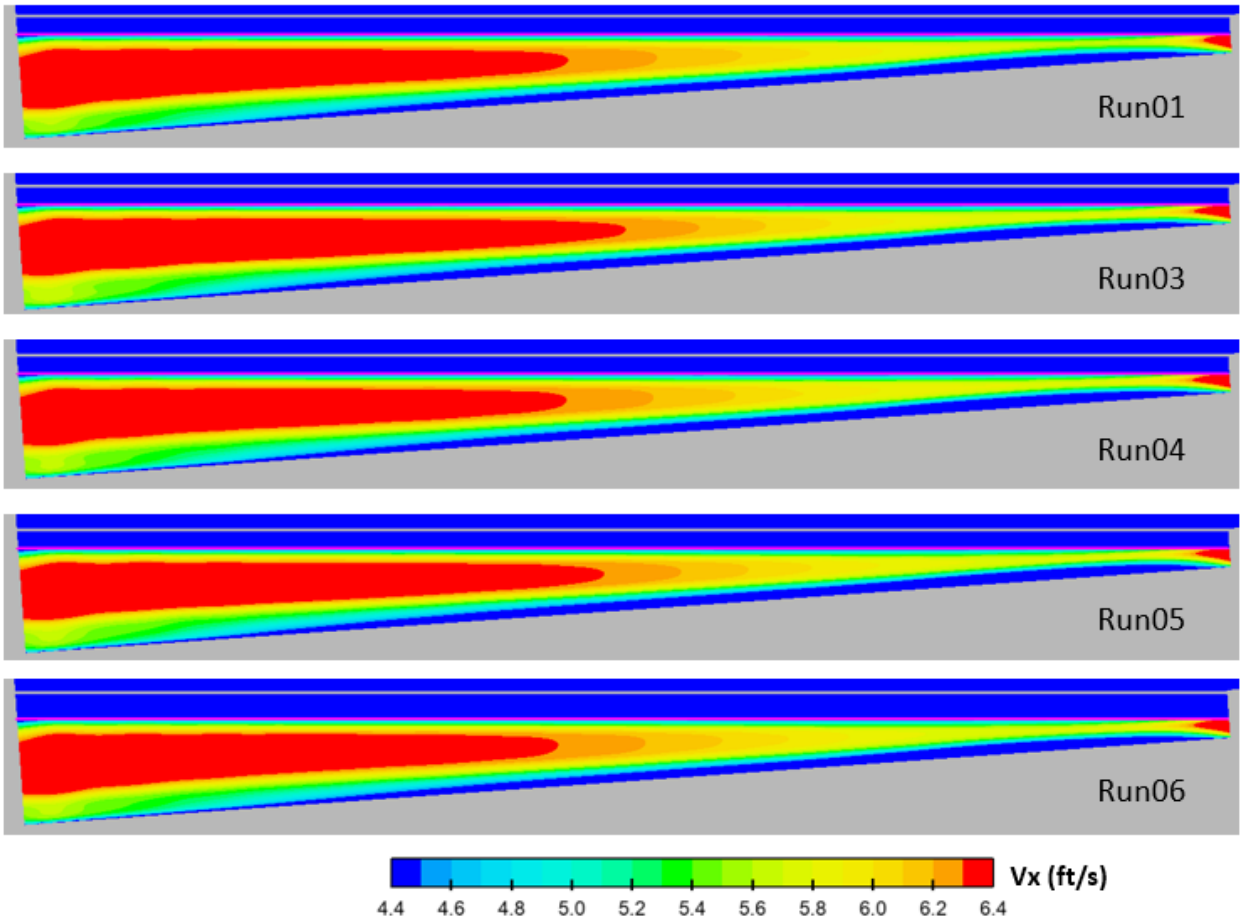

Figure 80 – Contours of sweeping velocity at 23.6 inches above the screen (i.e., approximately 20 percent depth)

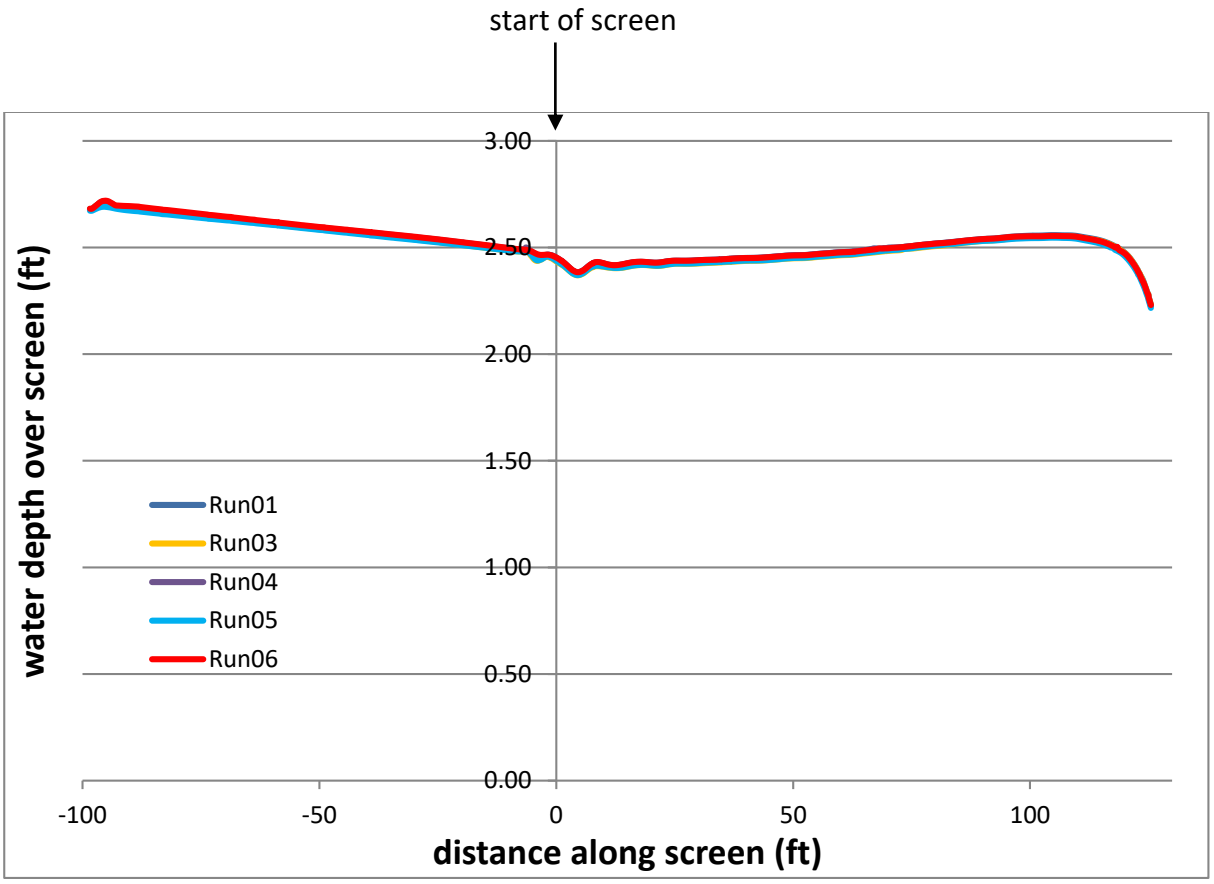

Figure 81 – Predicted water depth along the screen

3.5.2 Review of Ancillary CFD Simulations of the Derby Dam

This section reviews the results of the ancillary CFD simulations of the Derby Dam presented in *Section 3.5.1* above. The results are viewed in the light of the accuracy and limitations of the CFD model that were discussed in detail in *Section 2.4*.

Run03, Run06 – Effect of Increasing the Space Beneath the Screen

The modifications in Run03 and Run06 were both made in an attempt to increase the amount of flow to irrigation by increasing the space beneath the screen and reducing any restrictions.

Figure 74 shows no change in the predicted flow balance for either modification. This is reinforced by the contours of vertical velocity (*Figure 77*), which show minimal change in the flow through the wedge-wire screen compared to the baseline design (Run01). Only two differences from the results of the baseline simulation (Run01) stand out:

Run03 - Lowering the bed of the channel beneath the screen increases the size of the recirculation against the center wall (see *Figure 75)*. This in turn increases the amount of flow (dark blue) that is not drawn towards the weir wall (see *Figure 76*).

Run06 - Moving the weir wall away from the taper wall allows a greater region for upwelling but also increases the size of the recirculation against the taper wall (see *Figure 75*).

Overall, the CFD model gives confidence that neither the gap between the screen and the base of the channel, nor the gap between the taper wall and weir wall, are causing a restriction to the flow.

Run04, Run05 – Effect of Adding a Wedge Against the Center Wall

In modifications Run04 and Run05, a wedge was added beneath the screen against the center wall in an attempt remove the recirculation seen in this region in the baseline design (Run01).

Figure 75 shows that both modifications have the intended effect. The size of recirculation is greatly reduced and is moved away from the base of the channel. This change is reinforced by the y-velocity contours in *Figure 76*. These show water being drawn toward the weir wall in Run04 and Run05, with almost all negative velocities (dark blue) eliminated.

Modifications to Run04 and Run05 have minimal effect on other aspects of the flow compared to the baseline.

3.6 Overall Conclusions of the Derby Dam CFD Simulations

Based on the discussion above, the following overall conclusions are drawn from the CFD studies of the Farmers Screens at the Derby Dam:

3.6.1 Backwatered Weir, Maximum flow

With respect to the hydraulic design criteria in *Table 2*:

Sweeping velocity – The minimum sweeping velocity at the surface of the screen is expected to be 4.5 - 5.0 ft/s. This is well above the minimum required sweeping velocity of 2.5 ft/s specified in *Table 2*.

Minimum water depth – The minimum real-world water level at the Derby Dam is expected to be approximately 2.2 feet. This is well above the minimum required water depth of 1 foot specified in *Table 2.*

Irrigation flow – A best estimate is that given 150 cfs inlet flow at the Derby Dam, approximately 84 percent (i.e., 126 cfs) will go to irrigation and approximately 16 percent (i.e., 24 cfs) to bypass.

3.6.2 Weir Not Backwatered

With respect to the hydraulic design criteria in *Table 2*:

Sweeping velocity – At maximum flow rate, it is certain that the criteria of sweeping velocity >2.5 ft/s will be met. At minimum flow rate (65 cfs to irrigation), the sweeping velocities will be approximately 70 percent of those at the maximum flow rate and are also likely to be above the 2.5 ft/s criterion.

Minimum water depth – The water depth over the screen will be lowest at minimum flow conditions. The height of the weir wall can be tuned to ensure that this meets the minimum required water depth of 1 foot specified in *Table 2*. At maximum flow, non-backwatered conditions, the water depth is predicted to be approximately 0.2 foot higher throughout.

Irrigation flow – The CFD model predicts 84 percent of flow to irrigation in non-backwatered conditions. However, in similar flow conditions for the Davenport screen, the CFD model predicted 86 percent flow to irrigation when the actual measured value was 93 percent of the total. It is therefore very likely that the CFD model of the Derby Dam is significantly under-predicting the irrigation flow rate at these conditions.

3.6.3 All Operating Conditions

In general, the CFD studies showed that the Derby Dam screens are likely to perform in a very similar manner to the Davenport screen at all operating conditions. The power of this conclusion is that if the physical model at the Davenport screen operates successfully, then this gives confidence that the screens at the Derby Dam will likewise operate successfully. It also reinforces the benefit of the combined approach of using the physical test model and CFD studies to validate the screen performance at the Derby Dam.

Appendix A – Flow3D Settings for CFD Simulations of Davenport and Derby Dam

Software Version

Flow3D version 12.0

Physics

Gravity	Z = -9.81 m/s^2
Turbulence	RNG k-epsilon model turbulent mixing length = 0.035m

Fluids

Water at 20 deg. C	density	1000	kg/m^3
	viscosity	0.001	kg/m/s
Compressibility	5e-10 1/Pa		

Geometry

Porous screen	Porous properties		
	Porosity	0.5	
	X-direction porosity	0.5	
	Y-direction porosity	0.5	
	Z-direction porosity	0.5	
	Drag model	Forchheimer saturated drag	
	Drag coefficient A	1.82E+08	1/s
	Drag coefficient B	1	1/m
Surface roughness	Roughness height	0.5mm	screen support frame
		2.0mm	concrete intake channel, stop log

Boundary conditions

Inlet	Type = Velocity		
		Derby Dam Run01-06	Run07
	x-velocity	1.5689 m/s	1.3217 m/s
	y-velocity	0.1125 m/s	0.0947 m/s
	fluid elevation	0.81 m	0.5 m
Z max	Type = Pressure Stagnation pressure Fluid fraction = 0		
Irrigation outlet	Derby Dam Run01, 03-06	Run02, 07	
	Type = Pressure Stagnation pressure Fluid elevation = 0.671m	Type = outflow	
Bypass outlet	Type = Outflow		

Initial

Attenuation bay	stationary water to irrigation outlet level
Underbay	stationary water
Above screen	water moving at speed and depth of inlet to mid distance along screen

Numerics

Standard	Default values
If necessary	Implicit advection for velocity > 8m/s

Appendix B – Results of CFD Simulations of the Davenport Screen

This Appendix contains full results from the definitive CFD models of the Davenport screen in comparison with measured data. Two operating conditions were simulated as shown below.

Table 8 – Operating conditions simulated for the Davenport screen

Operating point	Inlet flow rate	Weir flow	Weir height
OP1	88.6 cfs	backwatered	11.25" above screen 3" gap under weir
OP4	83.7 cfs	no backwatering	8.25" above screen no gap

At each operating condition, the following results are presented:

- Predicted flow balance
- Streamlines on a vertical cross-section mid-distance along the screen
- Graph of water depth versus distance along the screen
- Graphs of sweeping velocity versus distance along the screen at various locations

Sweeping velocity is shown at a matrix of 9 lines; 3 water depths and 3 lateral positions as shown in *Figure* 82 below.

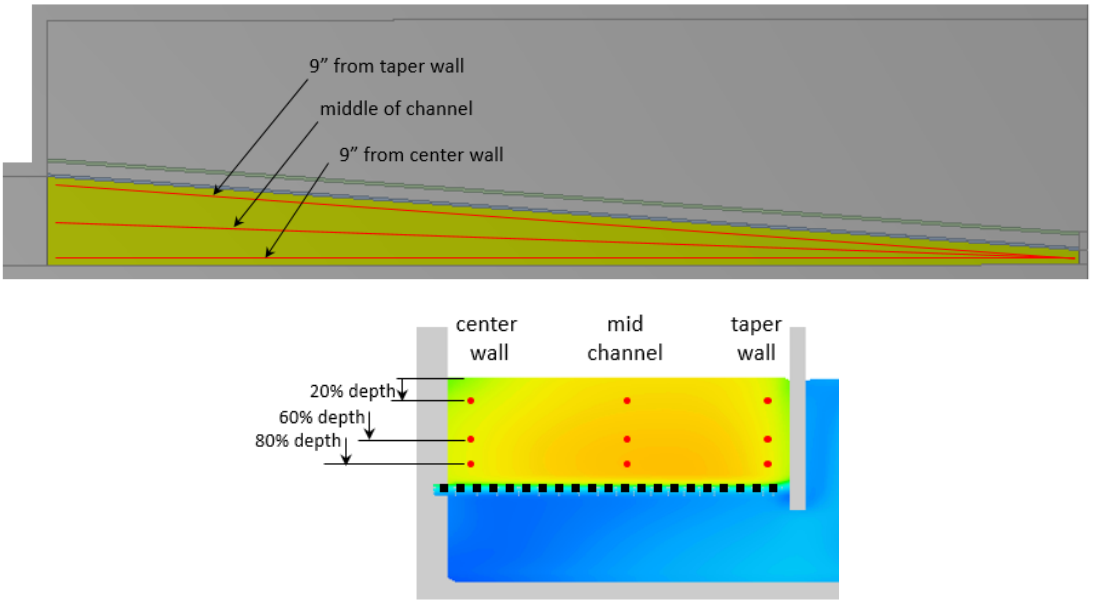

Figure 82 – Location of measurement lines for sweeping velocity

Operating Condition OP1

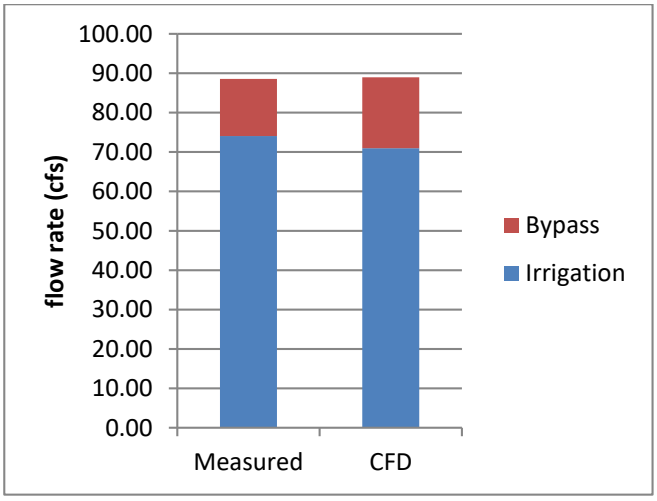

Figure 83 – Predicted flow balance

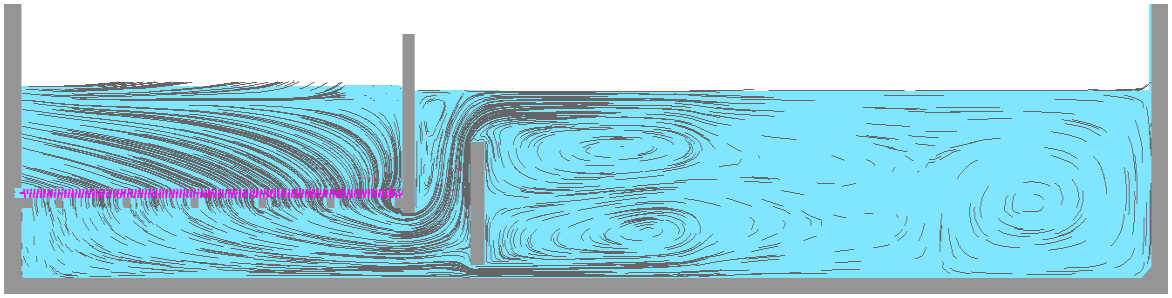

Figure 84 – In-plane streamlines on a vertical slice mid-distance along the screen

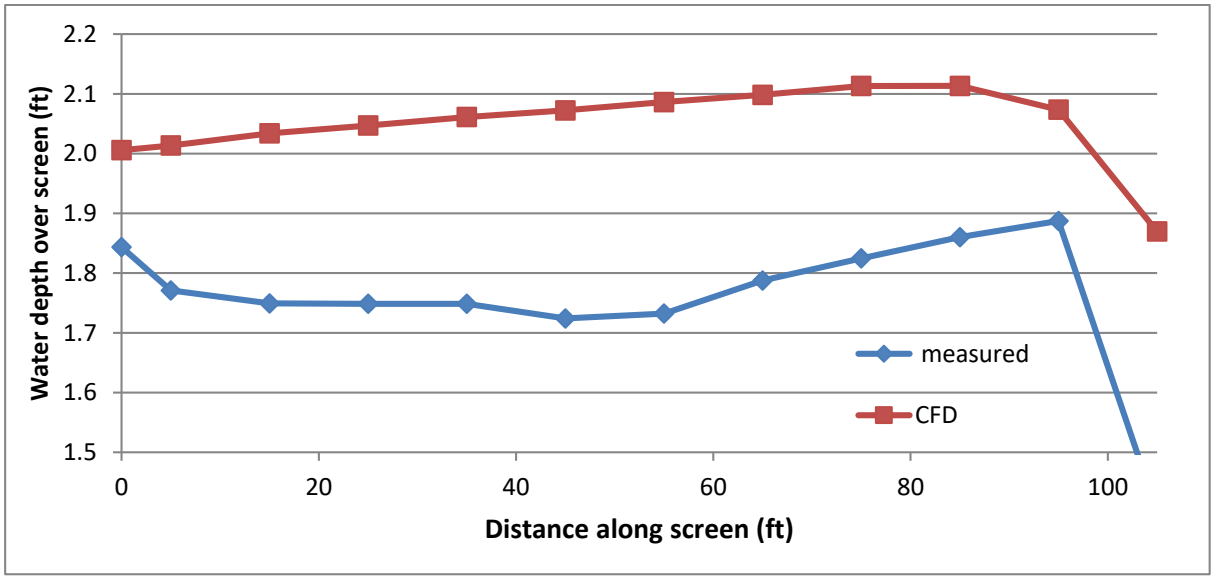

Figure 85 – Predicted water depth along the screen

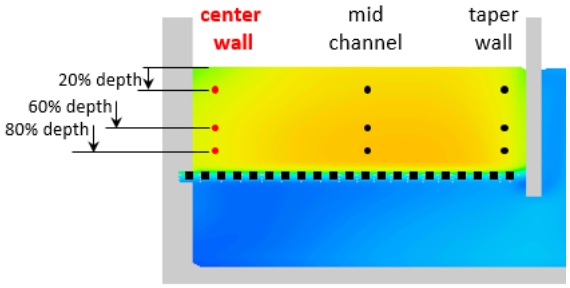

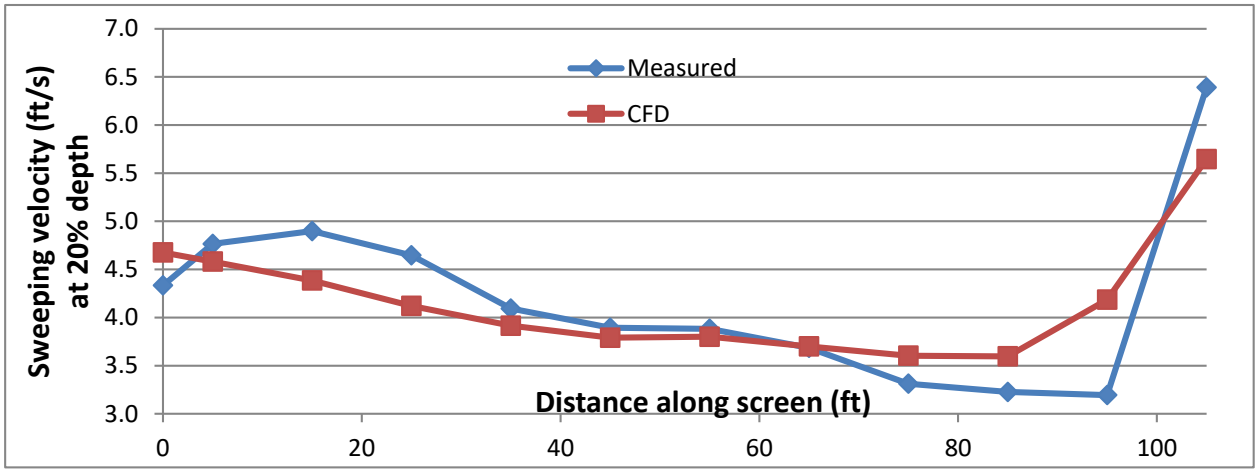

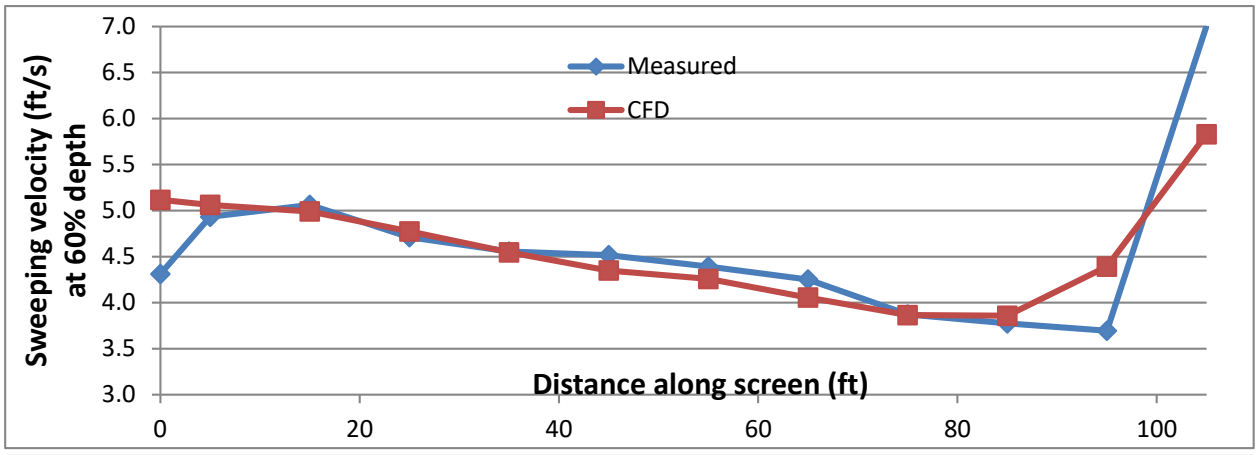

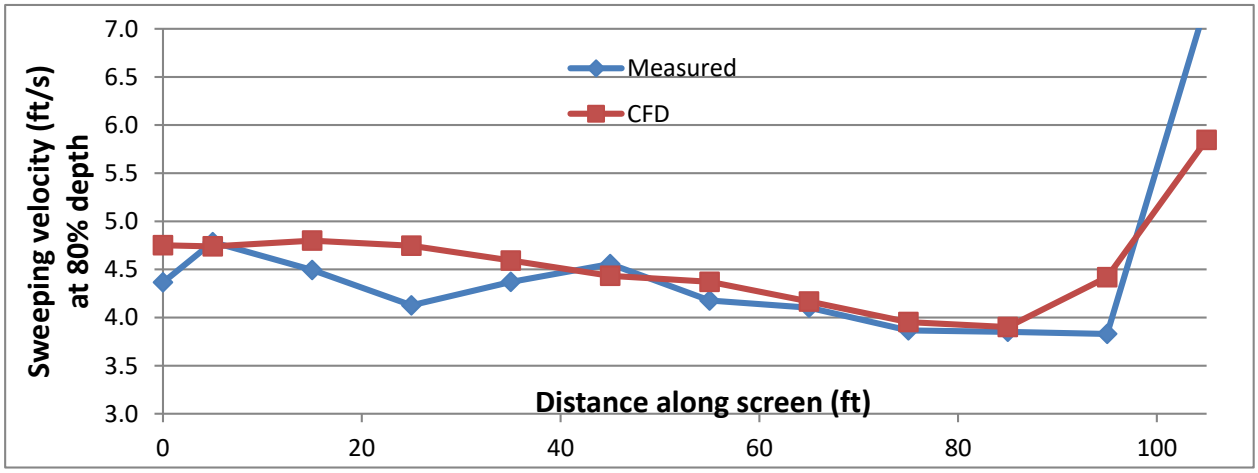

Figure 86 – Predicted sweeping velocity near the center wall

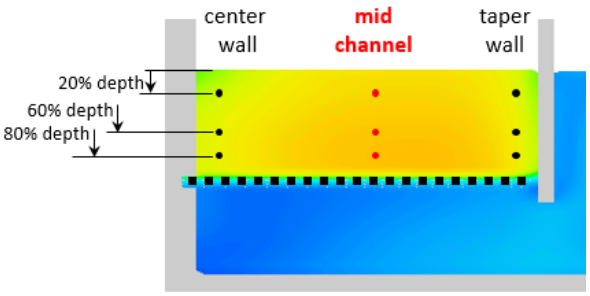

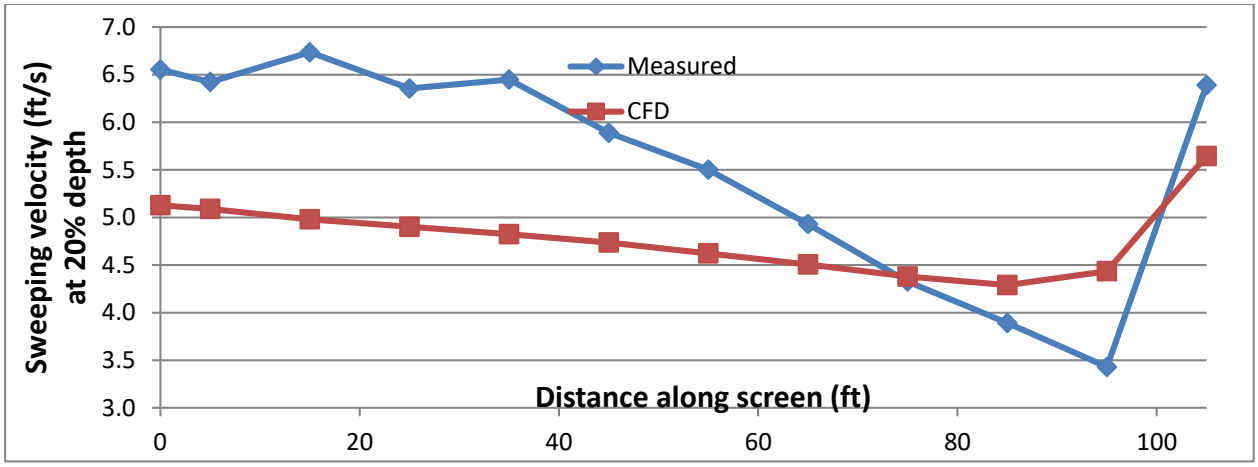

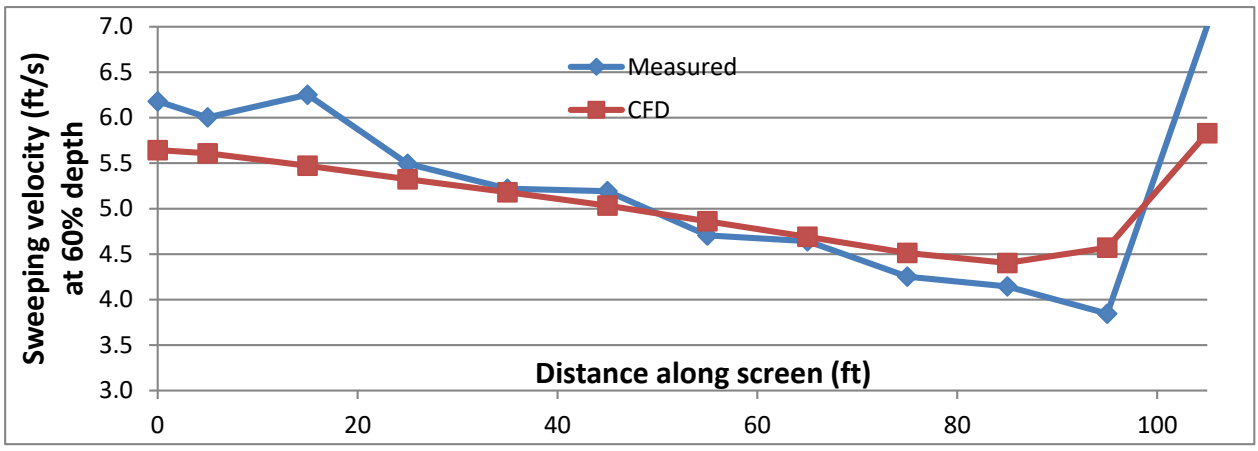

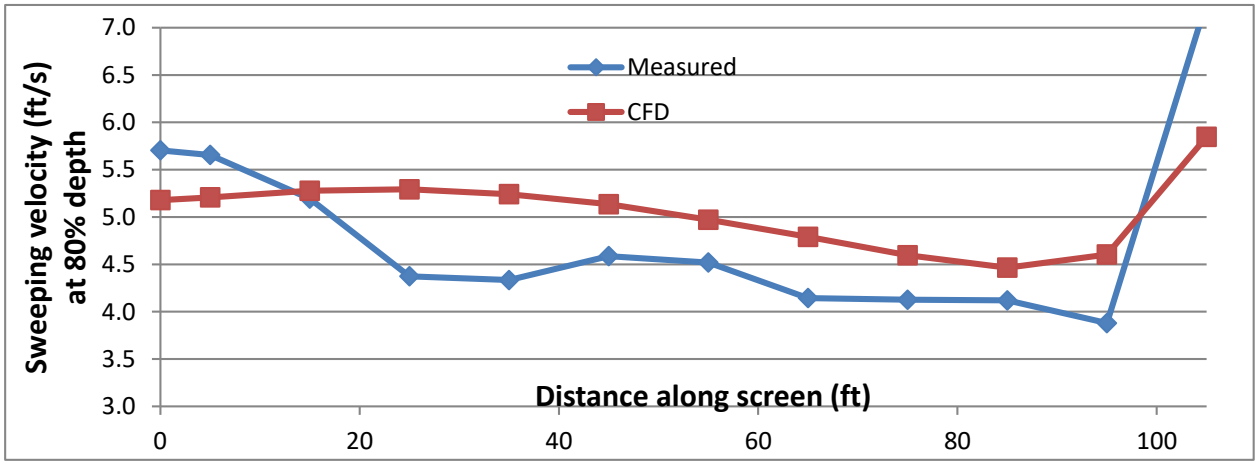

Figure 87 – Predicted sweeping velocity mid-channel

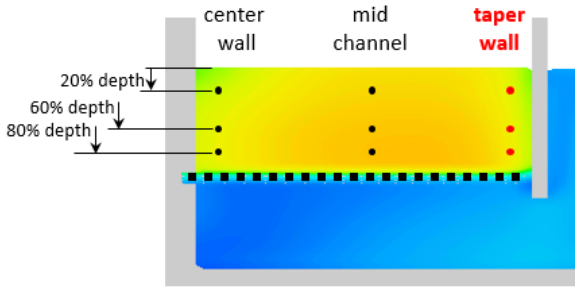

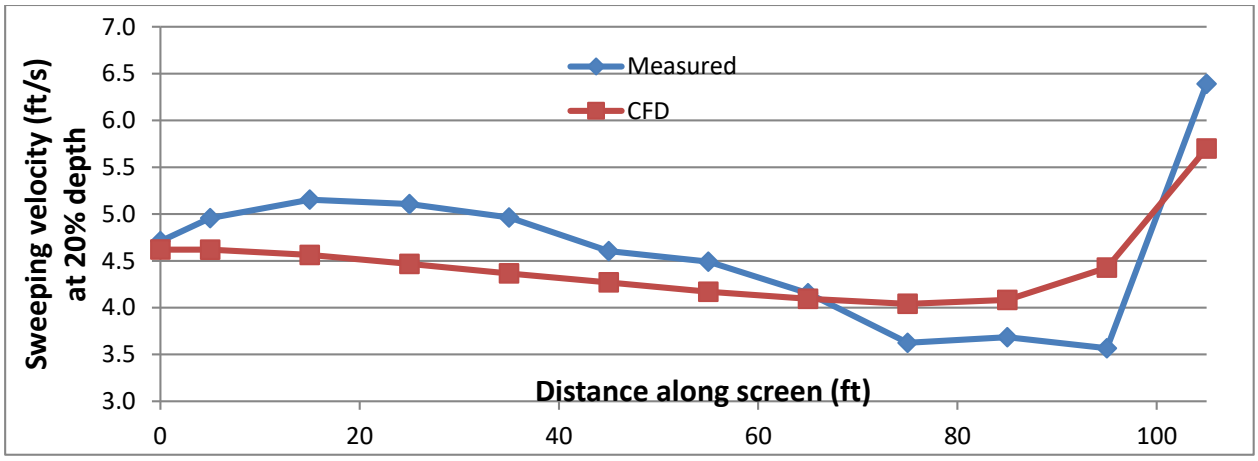

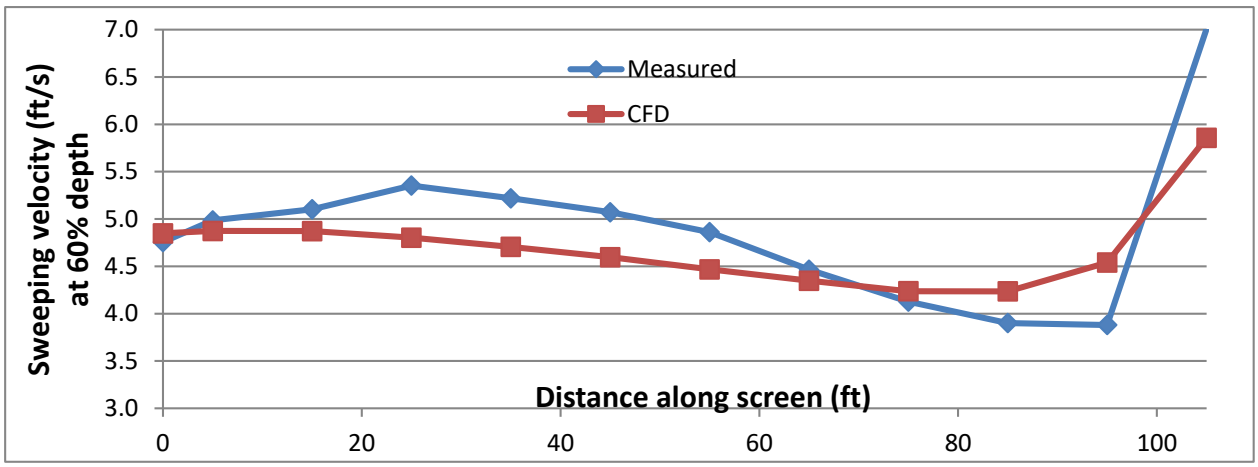

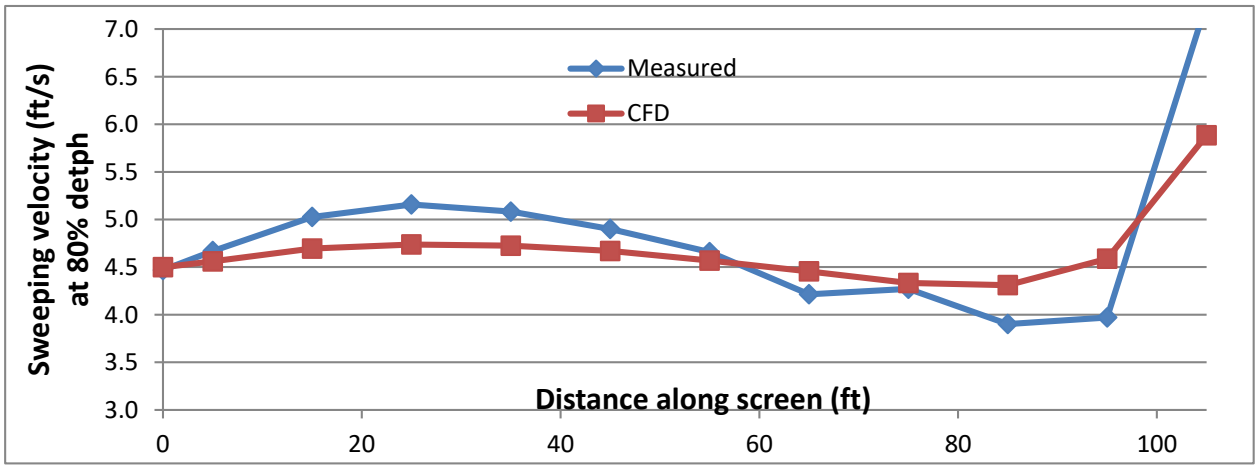

Figure 88 – Predicted sweeping velocity near the taper wall

Operating Condition OP4

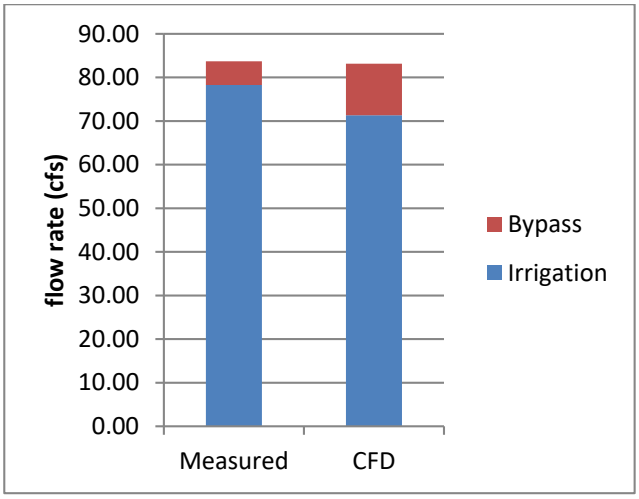

Figure 89 – Predicted flow balance

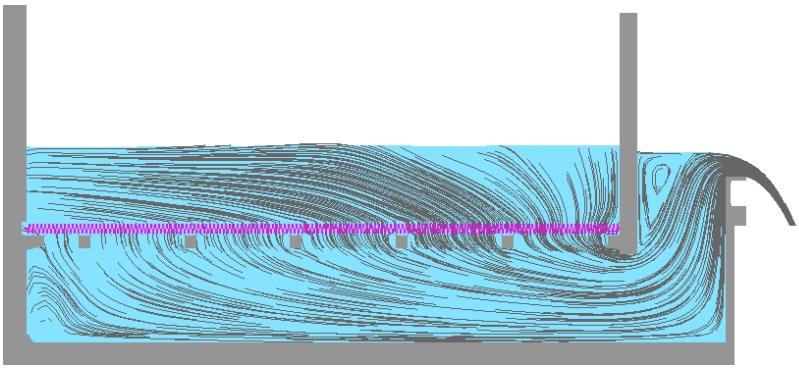

Figure 90 – In-plane streamlines on a vertical slice mid-distance along the screen

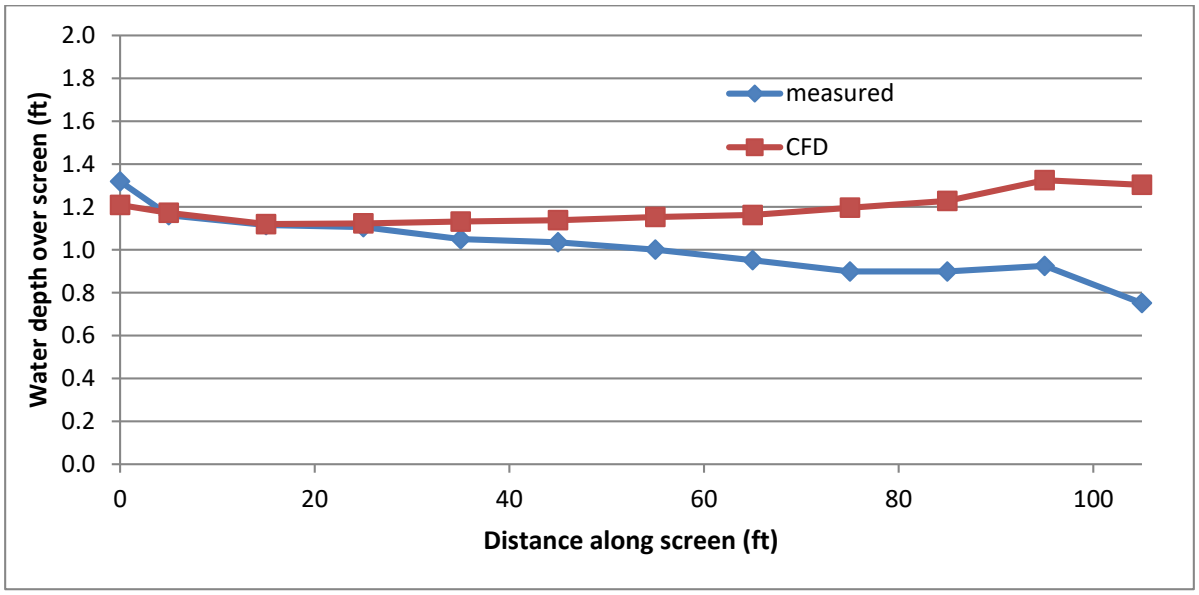

Figure 91 – Predicted water depth along the screen

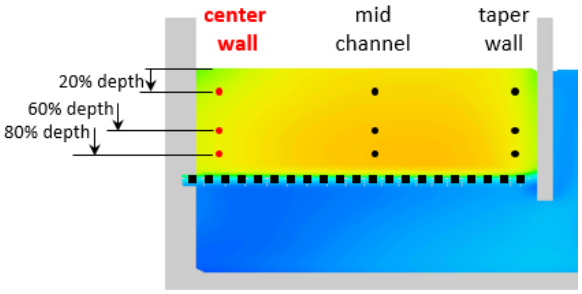

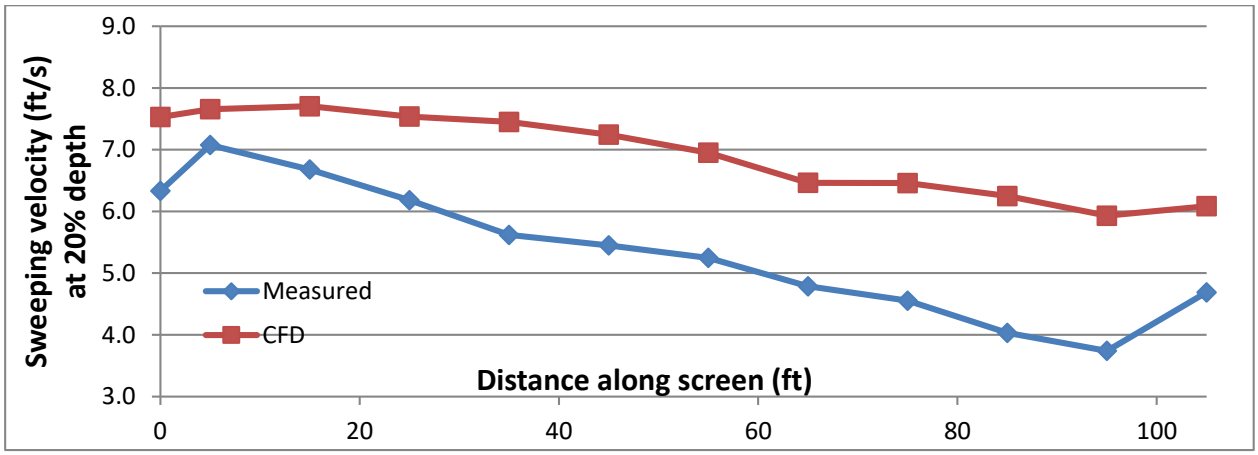

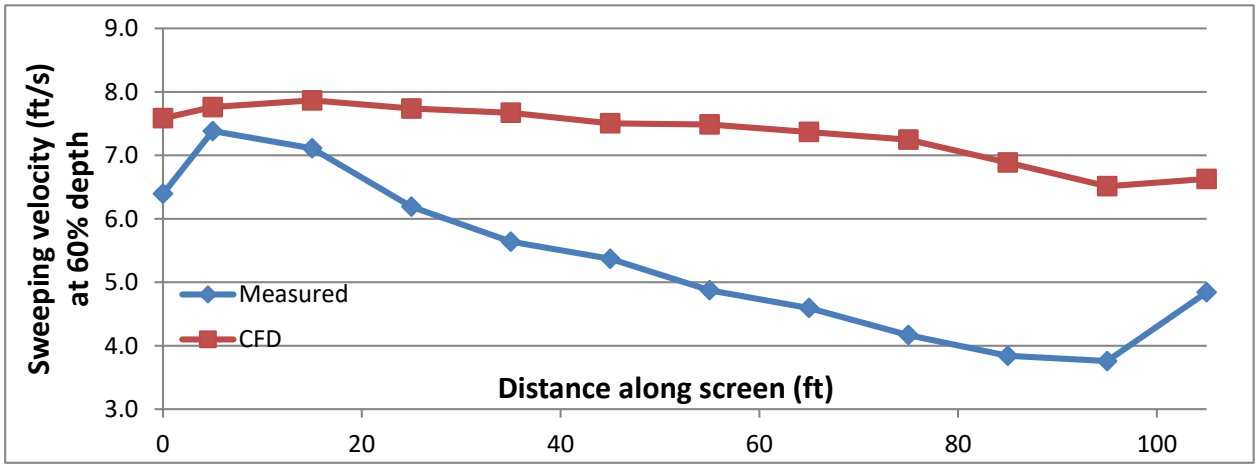

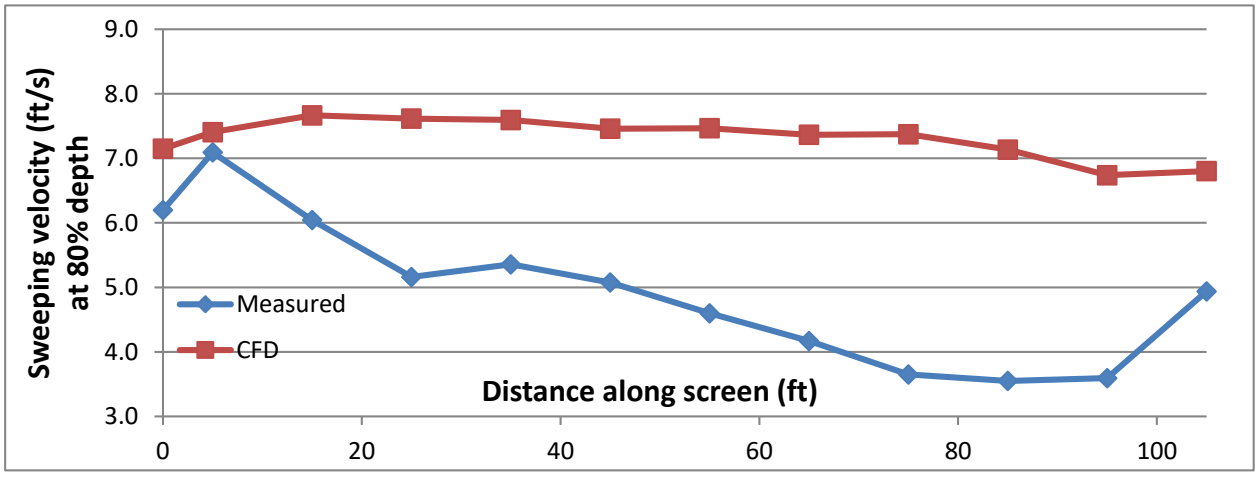

Figure 92 – Predicted sweeping velocity near the center wall

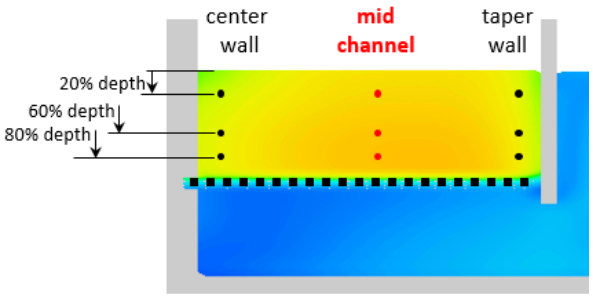

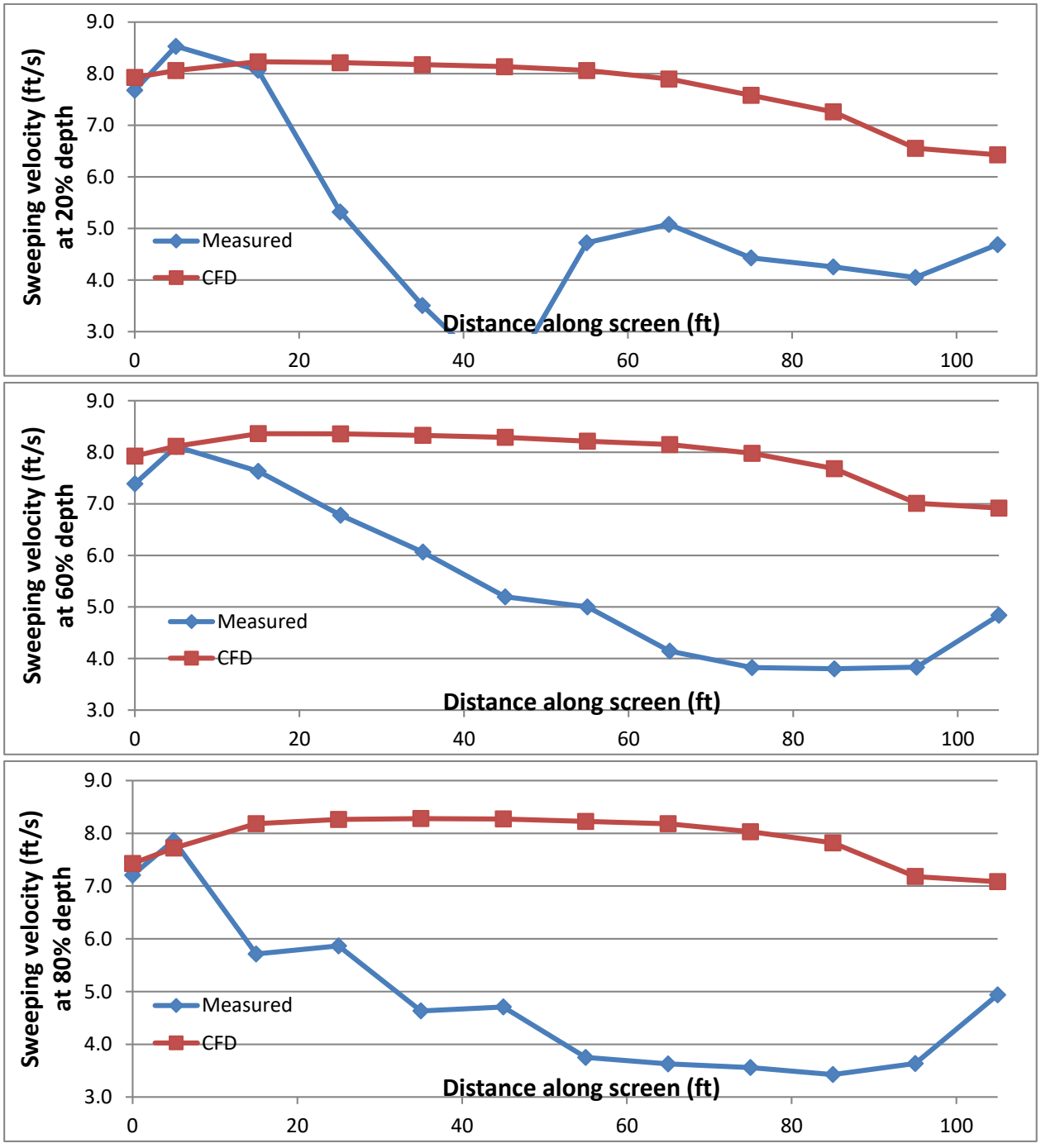

Figure 93 – Predicted sweeping velocity mid-channel

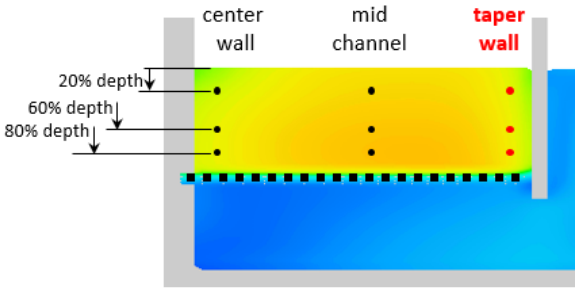

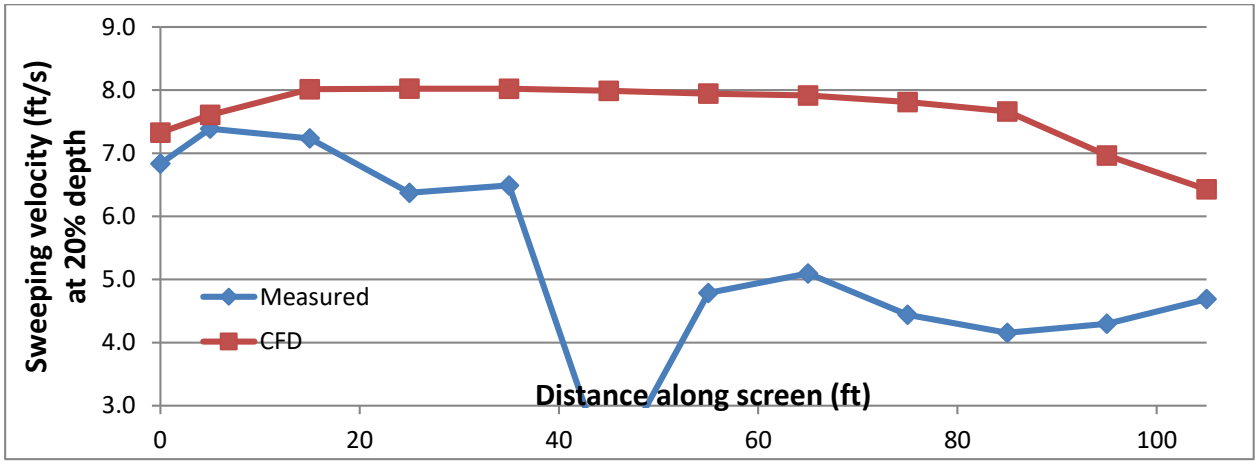

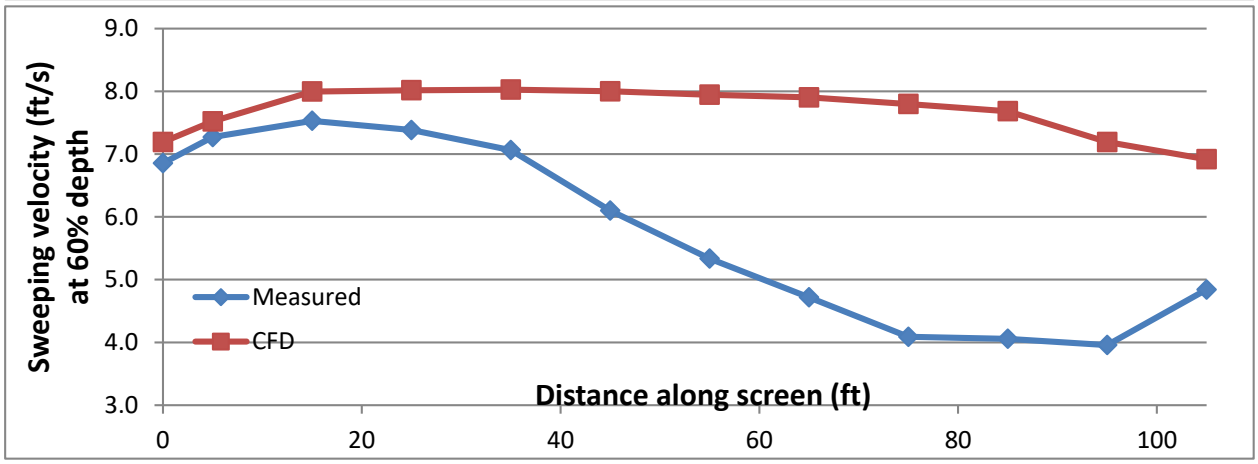

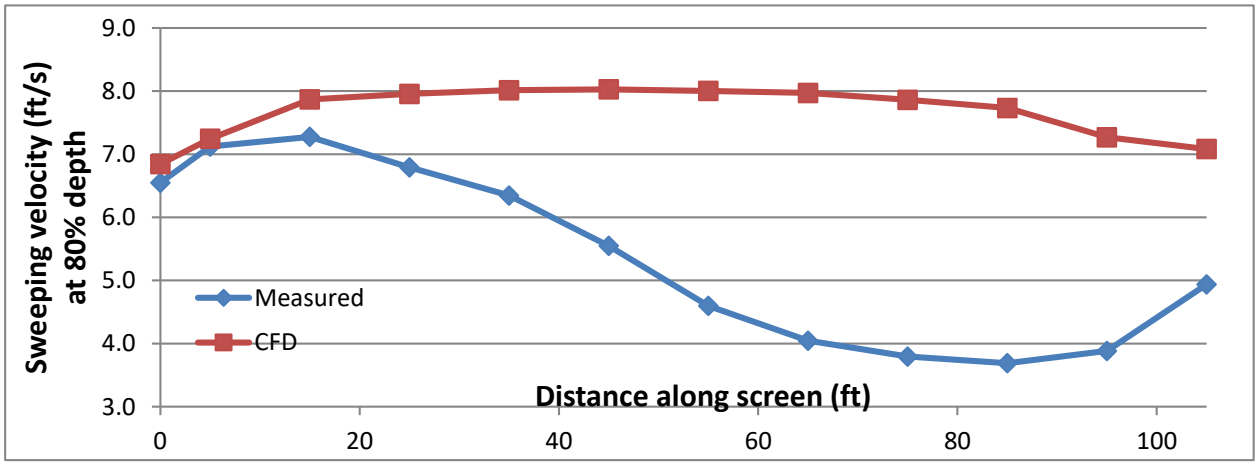

Figure 94 – Predicted sweeping velocity near the taper wall

USGS
science for a changing world

Biological Evaluations of an Off-Stream Channel, Horizontal Flat-Plate Fish Screen—The Farmers Screen

Open-File Report 2010–1042

U.S. Department of the Interior
U.S. Geological Survey

Biological Evaluations of an Off-Stream Channel, Horizontal Flat-Plate Fish Screen—The Farmers Screen

By Matthew G. Mesa, Brien P. Rose, and Elizabeth S. Copeland

Open-File Report 2010–1042

U.S. Department of the Interior
U.S. Geological Survey

U.S. Department of the Interior
KEN SALAZAR, Secretary

U.S. Geological Survey
Marcia K. McNutt, Director

U.S. Geological Survey, Reston, Virginia: 2010

Suggested citation:
Mesa, M.G., Rose, B.P., and Copeland, E.S., 2010, Biological evaluations of an off-stream channel, horizontal flat-plate fish screen—The Farmers Screen: U.S. Geological Survey Open-File Report 2010–1042, 18 p.

Contents

Abstract 1
Introduction 2
Study Methods 3
Results of Field Experiments 5
Biological Evaluation of Experimental Results 6
Conclusions 7
Acknowledgments 8
References 8

Figures

Figure 1. Photograph of the Herman Creek Screen, looking upstream, at the Oxbow Fish Hatchery, Cascade Locks, Oregon 9
Figure 2. Schematic of the modular screen apparatus used to evaluate the behavioral responses of juvenile salmonids encountering the leading edge of the Farmers Screen, 2010 10
Figure 3. Mean normal velocities (approach velocities corrected for the net open area of the screen) estimated for different sections of the Herman Creek screen relative to weir wall height and water depth, 2009 11
Figure 4. Distribution of the percent body surface area of large juvenile coho salmon injured when released over the Herman Creek screen (grey boxes) under different hydraulic conditions relative to control fish (white boxes).. 12
Figure 5. Distribution of the percent body surface area of small juvenile coho salmon injured when released over the Herman Creek screen (grey boxes) under different hydraulic conditions relative to control fish (white boxes).. 13

Tables

Table 1. Summary of hydraulic conditions at the Herman Creek screen and the numbers of two size groups of juvenile coho salmon used during injury assessments and delayed mortality tests 14
Table 2. General linear models describing the relation between hydraulic variables measured at the Herman Creek screen, 2009 15
Table 3. Mean number of fish contacts with the screen, their relative depth of travel during passage, and their general orientation to the water flow during passage for large juvenile coho salmon experimentally released over the Herman Creek screen, 2009 16
Table 4. Mean number of fish contacts with the screen, their relative depth of travel during passage, and their general orientation to the water flow during passage for small juvenile coho salmon experimentally released over the Herman Creek screen, 2009 17
Table 5. Summary of hydraulic conditions at the modular screen, the number and species of fish used for testing, and the percentage of fish that successfully passed over the screen during consecutive five minute periods, 2010 18

Conversion Factors and Abbreviations and Symbols

Conversion Factors

Multiply	By	To obtain
	Length	
inch (in.)	2.54	centimeter (cm)
inch (in.)	25.4	millimeter (mm)
	Flow rate	
foot per second (ft/s)	0.3048	meter per second (m/s)

Multiply	By	To obtain
	Length	
centimeter (cm)	0.3937	inch (in.)
millimeter (mm)	0.03937	inch (in.)
meter (m)	3.281	foot (ft)
	Flow rate	
centimeter per second (cm/s)	0.0328	feet per second
cubic meter per second (m^3/s)	35.31	Cubic feet per second

Abbreviations and Symbols

Abbreviation and Symbol	Meaning
AV	approach velocity
CRRL	Columbia River Research Laboratory
FID	Farmers Irrigation District
FL	fork length
h	hour
mg/L	milligram per liter
NMFS	National Marine Fisheries Service
NV	normal velocity
s	second
SV	sweeping velocity
UV	ultraviolet
Z	water depth
<	less than
>	greater than

Biological Evaluations of an Off-Stream Channel, Horizontal Flat-Plate Fish Screen—The Farmers Screen

By Matthew G. Mesa, Brien P. Rose, and Elizabeth S. Copeland

Abstract

Screens commonly are installed at water diversion sites to reduce entrainment of fish. Recently, the Farmers Irrigation District (Oregon) developed a flat-plate screen design (that is, the Farmers Screen) that operates passively and may offer reduced installation and operation costs to irrigators. To evaluate the performance of this type of screen (its biological effect on fish), we conducted two separate field experiments in consecutive years. First, in 2009, two size classes of juvenile coho salmon (*Oncorhynchus kistuch*) were released over a small working version of this screen at Herman Creek, Oregon. The screen was evaluated over a range of inflow [0.02–0.42 cubic meters per second (m^3/s)] and diversion flows (0.02–0.34 m^3/s) at different weir wall heights. The mean approach velocities ranged from 0 to 5 centimeters per second and mean sweeping velocities ranged from 36 to 178 centimeters per second. Water depths over the screen surface ranged from 1 to 25 centimeters and were directly related to weir wall height and inflow. Passage of juvenile coho salmon over the screen under various hydraulic conditions did not severely injure the fish or cause delayed mortality. Injury or mortality did not occur even though many fish contacted the screen surface during passage. No fish were observed becoming impinged on the screen surface. Second, in 2010, we constructed a modular screen apparatus that had 34 meters of wooden flume connected to a 3.5-meter long section of the Farmers Screen to determine whether fish would refuse to pass over the screen and swim back upstream after encountering the leading edge of the screen under various hydraulic conditions. For these tests, smolting coho salmon and steelhead trout (*O. mykiss*) were released at the upstream end of the flume and allowed to volitionally move downstream and pass over the screen. Overall, 81 and 91 percent of the fish moved downstream through the entire apparatus within 5 and 25 minutes from their release and only 1 of the 275 fish released swam back upstream after encountering the screen. Collectively, our results indicate that when operated within its design criteria, the Farmers Screen provided safe and efficient downstream passage of juvenile salmonids under various hydraulic conditions. However, we do not recommend operating the Herman Creek screen at inflows less than 0.14 m^3/s because water depth can be quite shallow and the screen can completely dewater, particularly at low flows.

Introduction

Diversions from natural or manmade waterways are common in the United States and the water is used for many purposes. Many diversion structures are fitted with screens meant to prevent fishes and other aquatic life from becoming entrained in the diversion, injured, or killed. However, many thousands of water diversions remain unscreened. Some screening technology (for example, submersible traveling screens or rotary drum screens) and design criteria meant to protect fishes [National Marine Fisheries Service (NMFS), 2008] are relatively expensive and require frequent maintenance to operate properly (McMichael and others, 2004), which can limit the installation of screens in areas where screens are needed. Recently, the development of unique horizontal flat-plate fish screens offer designs that may be less expensive to install, offer simpler, more passive operation, and may have fewer detrimental effects on aquatic communities. Research on the hydraulic characteristics and biological effects of some flat-plate screens has been promising (Beyers and Bestgen, 2001; Frizell and Mefford, 2001; and Rose and others, 2008), but more work is needed to fully evaluate the performance of flat-plate screens. Evaluating different designs and sizes of horizontal flat-plate screens in the laboratory and in the field would allow further verification of screen performance, provide data for comparison with criteria for more traditional fish screens, and perhaps facilitate screen installation.

We evaluated the hydraulic and biological performance of a newly developed, off-stream channel horizontal flat-plate fish screen, also known as the Farmers Screen. These screens, designed over a 10-year period by personnel from the Farmers Irrigation District in Hood River, Oregon, have a higher rate of horizontal movement of water across the screen (sweeping velocity, SV) relative to the rate of movement of water through the screen (approach velocity, AV), good self-cleaning characteristics, the potential for reduced impingement, injury, and entrainment of fish, and may reduce installation and maintenance costs. The screens are manufactured in various sizes—a large version, designed to accommodate flows as large as 2.27 m^3/s, was subjected to hydraulic, debris-loading, and biological tests to evaluate injury and mortality to juvenile salmonids, including Chinook salmon (*Oncorhynchus tshawytscha*) and steelhead (*O. mykiss*). The test results showed that the large Farmers Screen did not cause injury or mortality to fish when operated in accordance with its design parameters (Craven Consulting Group, 2003). However, smaller versions of this screen have not been tested. Such evaluations would help to more fully evaluate the performance of these alternative technology screens.

The U.S. Geological Survey's Columbia River Research Laboratory (CRRL) conducted field experiments to assess the performance of this screen type during 2009 and 2010. The objectives of the study were to assess the hydraulic performance of the Farmers Screen and determine the effects of downstream passage of fish over the screen on their injury, delayed mortality, and behavior under various hydraulic conditions. This paper describes the study methods and results of those experiments.

Study Methods

Screen hydraulics and biological performance (2009)—The screen evaluated for its hydraulic and biological performance was located at the Oxbow Fish Hatchery in Cascade Locks, Oregon (fig. 1). The screen is on a side-channel of Herman Creek, a tributary of the Columbia River, and is designed to divert 0.28 m^3/s of water. The installation is similar to other Farmers Screens that have already been installed in the Pacific Northwest. For a complete description of this screen and of the Farmers Screen in general, see Farmers Conservation Alliance, 2006, *http://www.farmerscreen.org/*. For purposes of this report, we refer to this screen as the Herman Creek screen.

To assess the hydraulic performance of the Herman Creek screen, we adjusted the inflow entering the screen, measured the inflow and water depth (Z), diversion discharge, and bypass discharge, and calculated mean SV, AV, and normal velocity (NV, which is the AV multiplied by the percentage of open area of the screen, or AV × 0.5) under different weir wall heights. After most of these hydraulic conditions were measured, we experimentally released fish over the screen. We evaluated the screen under four weir wall heights (that is, 4, 11, 13, and 20 cm) and at inflows ranging from 0.02 to 0.42 m^3/s. We used multiple linear regression analysis to evaluate the influence of several continuous and discrete variables (for example, streamflow, weir wall height) on water depth over the screen, diversion discharge, and sweeping velocity. All coefficients are significant at the $P < 0.05$ level unless noted.

To assess the biological performance of the Herman Creek screen, we experimentally released groups of juvenile coho salmon (*O. kistuch*) over the screen under various hydraulic conditions and quantified any injuries to the integument of the fish and documented short-term delayed mortality. Our test fish were from the Oxbow Hatchery and we evaluated two size groups, large [85–145 mm FL (fork length)] and small (54–78 mm FL)], in two separate sets of trials. Fish that passed over the screen (treatment fish) were released in groups of 10, at a distance of 1–2 m above the upper edge of the screen, and were recaptured in a net beneath the bypass outfall. Control fish were released into the bypass outfall and captured in a net and held for several minutes to simulate the time it took most treatment fish to pass over the screen. We used a fluorescein dye method described by Noga and Udomkusonsri (2002) to determine the extent of ulceration on the skin, eyes, and fins of each fish. After capture, both groups of fish were euthanized in a lethal dose of MS-222 (200 mg/L), rinsed in a freshwater bath for 1 minute, and then placed in a solution of fluorescein dye (fluorescein disodium salt at 20 mg/L). After 6 minutes, fish were removed from the dye and rinsed in three separate freshwater baths over 3 minutes to remove excess dye. Images were taken of both sides of each fish in a dark box under ultraviolet (UV) light using a digital camera with a 200-mm macro lens. The UV lights were placed at 45° angles to the side of the fish and a yellow barrier filter was used to eliminate the blue auto-fluorescence. Images were imported into Adobe© Photoshop CS3 and the body surface area and area of fluorescence was measured on each side of a fish. The percentage of body surface area of a fish that was injured was derived by dividing the total area of fluorescence by the total body surface area. This included the two sides and most, but not all, of the dorsal and ventral surfaces of the fish. For each release group, we compared the percentage of body surface area of the fish that was injured for control and treatment fish using two-sample, Mann-Whitney *U* tests. We were interested in whether the levels of injury in treatment fish were significantly different than those of control fish. The level of significance was set at $P < 0.05$.

To assess delayed mortality after passage, additional fish were released in the same manner as described above but were transported to holding tanks after being collected in the bypass outfall. Fish were monitored for 24–48 h after passage and handling and the number of fish that died was compared between treatment and control groups. Mortality tests were conducted for most, but not all, of the same hydraulic conditions as injury tests.

To document the behavior of fish passing over the screen, treatment fish were videotaped using three underwater cameras mounted to one edge of the screen. The system was not designed to cover the entire screen area, and each camera provided only a partial, upstream view of the screen. Video files were reviewed in slow motion, and the approximate number of times fish contacted the screen, their orientation to the current during passage, and their general depth of passage were recorded. Control fish were not videotaped.

Behavioral responses of fish encountering the leading edge of a screen (2010)—To evaluate whether fish would refuse to pass over the screen after encountering the leading edge (a question we did not answer in 2009), we constructed a modular screen apparatus that had 34 m of wooden flume (46-cm wide by 36-cm deep) connected to a 3.1-m (long section of the Farmers Screen (fig. 2). The purpose of the long flume was to provide fish with plenty of distance between their release point (at the upstream end of the flume) and the upstream edge of the screen so the fish could orient themselves and move downstream somewhat naturally. The flume received water from the outflow of the Herman Creek Screen and was designed so that water velocities were slower in the upstream one-half of the flume than in the downstream one-half. We installed a trap on the downstream end of the screen to capture the fish.

We used yearling coho salmon (113–161 mm FL) from the Oxbow State Fish Hatchery (Oregon) and Skamania-stock steelhead (134–260 mm FL) from the Bonneville Fish Hatchery (Oregon) for tests. We used fish presumably undergoing the process of smoltification to maximize the probability that the fish would have a strong desire to migrate downstream. All the test fish were large and silvery with faint or non-existent parr marks. These fish should have had a relatively strong swimming ability (compared to smaller fish) and thus would be most likely to reject the screen if conditions posed a behavioral obstacle. Normally, these fish would have been released from the hatcheries during mid-April to early May. Prior to testing, all fish were held in large tanks at the Oxbow State Fish Hatchery and water temperatures were monitored daily.

On the day of testing, we first established the hydraulic conditions for the test, including inflow volume, water depth, AV, and SV over the screen, and water velocity and depths at several locations throughout the flume. Our intent was to test fish under various hydraulic conditions over the screen. We then removed 10 fish from their holding tank, placed them in a 19-L bucket with water, transported them from the hatchery to the test facility (about 2 km), and gently released them at the upstream end of the flume. Fish were allowed 20 minutes to volitionally migrate down the flume and pass over the screen. After 20 minutes, we gently prodded any fish that remained in the upper 3 m of the flume until the fish moved downstream. We conducted three to four releases of about 10 fish each, for a total release of 20–40 fish for each species under the various hydraulic conditions.

An observer was stationed on an elevated platform slightly upstream of the fish screen to record the behavior and passage timing of fish as they approached the screen. For each of five consecutive 5-minute periods, we recorded the number of fish that encountered the screen and whether the fish passed over the screen or refused to (that is, the fish turned and swam back upstream). For our analysis, we pooled data from the release groups for each species and hydraulic condition and determined the proportion of fish that passed over or rejected the screen for each time period. We also tallied data from each time period and determined the proportion of fish that passed over the screen within 25 minutes of their release.

Results of Field Experiments

Screen hydraulics and biological performance (2009)—Hydraulic conditions measured at the Herman Creek screen and the numbers of coho salmon released for injury and delayed mortality assessments are summarized in table 1. Diversion discharges (the volume of water collected from the screen and sent to the hatchery) comprised from 65 to 100 percent of the inflow rates. Mean AVs estimated for the entire screen ranged from 0 to 5 cm/s and for individual sections of the screen, mean AVs never exceeded 6 cm/s. Mean NVs ranged from 0 to 10 cm/s and varied along the length of the screen (fig. 3). Mean SVs ranged from 36 to 178 cm/s and generally were faster at the upstream edge and slower at the downstream edge of the screening panels. Mean SVs usually were at least 32 times higher than AVs for all conditions tested. The mean Z ranged from 1 to 25 cm and generally was deeper at the upstream end of the screen than at the downstream end. Mean depths were directly related to weir wall height and inflow and were inversely related to diversion discharge (R^2= 0.84; table 2), mean SVs were inversely related to weir wall height and diversion discharge and were directly related to inflow (R^2= 0.81; table 2), and diversion discharge was related to several variables (R^2= 0.99; table 2). "Hot spots" or localized areas of high AV with spiraling flow were not observed during any of our tests.

Overall, the injury rates of fish after passage over the Herman Creek screen were low, and severe injuries to the skin, eyes, and fins of both size cohorts were not observed. For large fish, the mean percentage of body surface area that was injured varied by release group and ranged from about 0.5 to 2.5 percent (fig. 4). The mean percentage of body surface area that was injured in treatment fish was significantly different than that of control fish for all test conditions (Mann-Whitney *U* tests, $P < 0.05$; fig. 4), but the magnitude of these differences was small (< 1 percent). For small fish, the mean percentage of body surface area that was injured ranged from about 0.4 to 3.0 percent (fig. 5). The mean percentage of body surface area that was injured in treatment fish was significantly different than that in control fish for three test conditions (fig. 5), but again, the magnitude of this difference was small (< 1 percent). One small fish, shown as an outlier in figure 5 with about 60 percent of its body surface area injured, probably was injured by something other than passage over the screen. For delayed mortality after passage, we tested 849 fish in total and none died within 24–48 h of passage or handling and only one control fish died.

The results of our video analysis revealed that for large fish, the mean number of times fish contacted the screen surface ranged from 0.15 to 0.72 per fish observed (table 3). During passage, most fish remained low in the water column near the screen surface (table 3). Fish were oriented either upstream or downstream during passage, with no clear relation to the hydraulic conditions (table 3). For small fish, the mean number of times fish contacted the screen surface ranged from 0.26 to 0.62 per fish observed (table 4). Again, most fish remained low in the water column and near the screen surface during passage. Most fish were oriented upstream during passage.

Behavioral responses of fish encountering the leading edge of a screen (2010)—To evaluate the behavioral responses of juvenile salmonids approaching and passing over the screen, we released a total of 173 coho salmon and 102 steelhead trout in the modular screen apparatus under various hydraulic conditions (table 5). In general, the hydraulic conditions in the modular screen system were similar to those recorded in the Herman Creek screen. For example, mean AVs estimated for the entire screen ranged from 1 to 3 cm/s or 2 to 6 cm/s after correcting for net open area (50 percent) and Z ranged from 15 to 25 cm. Mean SVs ranged from 102 to 150 cm/s and were at least 32 times higher than AVs for all tests. In the flume, mean water velocities ranged from 60 to 79 cm/s in the upstream one-half of the flume and from 85 to 104 cm/s in the downstream one-half of the flume. Mean values of Z in the flume ranged from 23 to 31 cm. For coho salmon, from 75 to 95 percent of the fish approached and passed over the screen within 5 minutes of their release, depending on hydraulic conditions (table 5). Within 20

minutes, the percentages of fish that quickly passed over the screen increased to 82–98 percent. After 20 minutes, 12 fish remained upstream in the flume and were gently prodded to move downstream; all these fish passed over the screen without hesitation. For steelhead trout, from 47 to 90 percent of the fish approached and passed over the screen within 5 minutes of their release, depending on hydraulic conditions (table 5). Within 20 minutes, the percentages of fish that quickly passed over the screen increased to 79–95 percent. After 20 minutes, 11 fish (11 percent) were coerced downstream of the upper 3 m of the flume and one fish turned and swam back upstream after it encountered the screen. However, this fish returned to the screen within 10 minutes and successfully passed. Overall, 99.6 percent of the fish we observed passed over the screen without hesitation or delay.

Biological Evaluation of Experimental Results

The results of our experiments in 2009 indicate that passage of juvenile coho salmon over the Herman Creek screen under various hydraulic conditions did not severely injure the fish, cause delayed mortality, or delay fish migration. These results occurred even though most fish passed over the screen near the screen surface, many contacted the screen during passage, and fish were oriented to the current in various directions. However, we did not observe fish becoming impinged on the screen surface (that is, >1 second contact with the screen). The screen showed good self-cleaning performance and never had problems with debris loading. Our results are similar to those of Rose and others (2008), who also reported minimal injuries and low mortality of rainbow trout after passage over backwatered and inverted-weir horizontal flat-plate screens in Oregon. Other studies evaluated various designs of vertically oriented screens and reported results similar to ours (Danley and others, 2002; Zydlewski and Johnson, 2002).

The injuries observed in our fish—both treatment and control groups—were minor and indicate that fish had some trauma to the integument prior to testing and that our holding and handling procedures probably caused more trauma. The fluorescein dye method was effective for detecting injuries to the integument of fish and revealed that all fish had some level of injury after testing. As stated previously, however, all injuries were minor and any differences in mean injury rates between treatment and control groups were small, which makes it difficult to ascribe any biological significance to the injuries we observed. Furthermore, and perhaps more importantly, none of our test results would have exceeded the performance standards for safe passage of fish over conventional screen systems as established by NMFS. For example, performance standards set by NMFS include less than 0.5 percent mortality and 2 percent injury rate (that is, the percentage of a sample that is injured) for salmonid smolts, and that at least 90 percent of salmonids that encounter a screened water diversion are bypassed within 24 h (Bryan Nordlund, National Marine Fisheries Service, written commun., 2010). The agency defines injury as visual trauma (including but not limited to hemorrhaging, open wounds without fungus growth, gill damage, bruising greater than 0.5 cm in diameter), loss of equilibrium, or greater than 20 percent descaling on one side (Bryan Nordlund, National Marine Fisheries Service, written commun., 2009). Because none of our fish showed such injuries, mortality was less than 0.5 percent, and most fish traveled over the screen without hesitation or delay, the Herman Creek screen would surpass these NMFS standards. Although the performance standards discussed here are for other types of screens, the standards do indicate that screens like the one at Herman Creek probably would, at a minimum, meet federal regulatory standards.

The ability of the Herman Creek screen to safely and efficiently pass fish at water depths ranging from 7 to 25 cm was largely due to achieving a high ratio of SV to AV (30:1–60:1) under various diversion conditions. These ratios were substantially higher than the SV recommendations established by NMFS for horizontal screens, which only suggest that downstream SVs be higher than AVs for the

entire length of the screen (National Marine Fisheries Service, 2008). The combination of high SVs and low AVs facilitated quick downstream fish passage and eliminated impingements; results are similar to Beyers and Bestgen (2001). Because most fish passed over the screen near the screen surface—regardless of water depth—indicates that the 30 cm water depth recommendation established for horizontal screens (National Marine Fisheries Service, 2008) could be relaxed for smaller screens like the one at Herman Creek. Although fish safely passed over the screen at a depth of only 7 cm, the number of screen contacts per fish increased at this shallow depth for large, but not small, fish. Even though the screen contact rate was not related to the extent or severity of injuries, operating the screen at water depths near 7 cm seems too shallow, particularly under high-flow conditions. Thus, although our results suggest that the Herman Creek screen can be operated effectively at water depths less than 30 cm, we cannot unequivocally recommend a single, specific minimum depth for this screen. Rather, a range of minimum depths, perhaps from 15 to 20 cm, probably would provide safe passage of fish under most circumstances.

Despite the advantages of the Herman Creek screen for protecting fish populations, there are some things to consider when interpreting our results. First, we were unable to evaluate all possible hydraulic conditions on screen performance, fish injury, and mortality. Although we believe our evaluations were realistic because they encompassed typical diversion conditions, there may be other flow conditions we missed that are relevant to fish passage and safety. Second, only two species of fish were tested for the screen evaluations and our results may not be applicable to other species. The fishes used in our experiments probably were good surrogates for other salmonids of similar size. Extrapolation of our results to other fishes, such as juvenile lampreys or endangered suckers in the Klamath Basin, seems inappropriate and would require further testing. Next, our video analyses were not rigorous and our camera installation was meant to provide qualitative information on the behavior of fish as they passed over the screen. Even though we used three cameras, we had limited fields of view and it was often difficult to see because of water turbidity, sunlight, or other factors. Although we are confident that the data we did collect were representative of fish behavior during passage, more detailed analyses will require further work. Finally, we evaluated only the effects of downstream passage on juvenile fish. Further testing would be required to assess the effects of this screen type on fish migrating upstream across the screen surface.

The purpose of our testing in 2010 was to determine whether fish would reject or refuse to pass over the screen after encountering its leading edge—a notion that was a concern to fishery managers and something we did not evaluate in 2009. The concern was related to the changing hydraulic conditions at the flume-screen interface and whether fish would sense this change, turn around, and refuse to pass. Extended delays in passage over the screen could lead to excessive energy use in fish and violation of the NMFS standard that fish must be bypassed within 24 h. Our results, however, clearly indicate that the flume-screen interface was not an obstacle to passage for fish moving volitionally downstream, because high percentages of fish passed within 20 minutes. Even the small number of fish we had to manually coerce to move downstream readily passed over the flume-screen interface. We cannot state whether all fish encountering and passing through small versions of the Farmers Screen would be bypassed within 24 h because none of our tests were designed to answer this question. However, we think the possibility of fish not passing over these screens within 24 h would be remote.

Conclusions

When operated within its design criteria—diversion flows of about 0.28 m^3/s—the Herman Creek screen provided safe and effective downstream passage of juvenile coho salmon under various hydraulic conditions. We do not recommend operating the Herman Creek screen at inflows less than

about 0.14 m^3/s because water depth can be quite shallow due in part to a weir wall that was not sealed and the screen can completely dewater, particularly at low flows. If the screen is operated at inflows less than 0.14 m^3/s, caution must be used to avoid diverting an excessive amount of water, which can lead to shallow depths, insufficient bypass flow, and perhaps screen dewatering. Finally, we do not know the fate of fish that pass over the screen, enter the bypass channel, and are diverted back to the Columbia River. It is possible that passage through these areas is a stressful and disorienting event for fish, which could make them vulnerable to hazards that exist downstream, such as predation by fish or birds. This idea is not unique to the Herman Creek screen, but is relevant for many types of diversions and obstacles fish may encounter in the wild. Further research would be necessary to address this issue.

Acknowledgments

We thank Les Perkins, Julie Davies O'Shea, and Daniel Kleinsmith of The Farmers Conservation Alliance for financial and technical support; Jerry Bryan for his expertise and advice on the Farmers Screen; Duane Banks and his staff from the Oxbow Fish Hatchery for use of their facility and technical assistance; Bryan Nordlund, Michelle Day, and Larry Swenson of NMFS for early discussions and advice on our study; and staff from the Columbia River Research Laboratory for their assistance in the field.

References Cited

Beyers, D.W., and Bestgen, K.R., 2001, Bull trout performance in a horizontal flat plate screen: Final report to the Bureau of Reclamation, Water Resources Research Group, Denver, Colorado.

Craven Consulting Group, 2003, July 28, 2003 Memorandum and Draft Data Report—Evaluation of Overshot Horizontal Flat Plate Fish Screen: Farmers Canal, Hood River, Oregon. Prepared by Craven Consulting Group/Farmers Irrigation District.

Danley, M.L., Mayr, S.D., Young, P.S., and Cech, J.J., Jr., 2002, Swimming performance and physiological stress responses of split tail exposed to a fish screen: North American Journal of Fisheries Management, v. 22, p. 1241–1249.

Farmers Conservation Alliance, 2006, Resource solutions for rural communities: accessed November 12, 2010, at http://www.farmerscreen.org/.

Frizell, K., and Mefford, B., 2001, Hydraulic performance of a horizontal flat plate screen: Final report to the Bureau of Reclamation, Water Resources Research Group, Denver, Colorado.

McMichael, G.A., Vucelick, J.A., Albernathy, C.S., and Neitzel D.A., 2004, Comparing fish screen performance to physical design criteria: Fisheries, v. 29, chap. 7, p. 10–16.

National Marine Fisheries Service (NMFS), 2008, Anadromous salmonid passage facility design: NMFS, Northwest Region, Portland, Oregon.

Noga, E.J., and Udomkusonsri, P., 2002, Fluorescein: a rapid, sensitive, nonlethal method for detecting skin ulceration in fish: Veterinary Pathology, v. 39, p. 726–731.

Rose, B.P., Mesa M.G., and Zydlewski G.B., 2008, Field-base evaluations of horizontal flat plate fish screens: North American Journal of Fisheries Management, v. 28, p. 1702–1713.

Zydlewski, G.B., and Johnson, J.R., 2002, Response of bull trout fry to four types of water diversion screens: North American Journal of Fisheries Management, v. 22, p. 1276–1282.

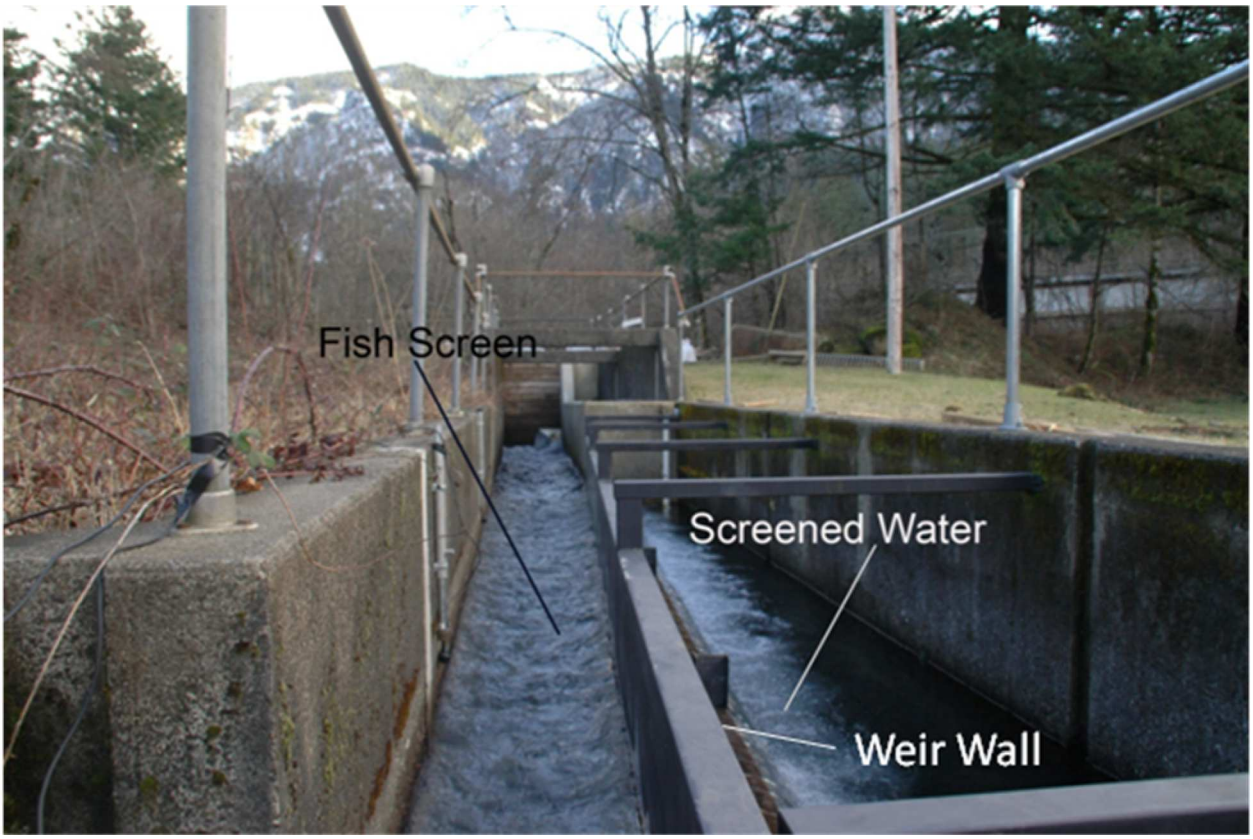

Figure 1. Photograph of the Herman Creek Screen, looking upstream, at the Oxbow Fish Hatchery, Cascade Locks, Oregon. Photograph taken by Brien P. Rose.

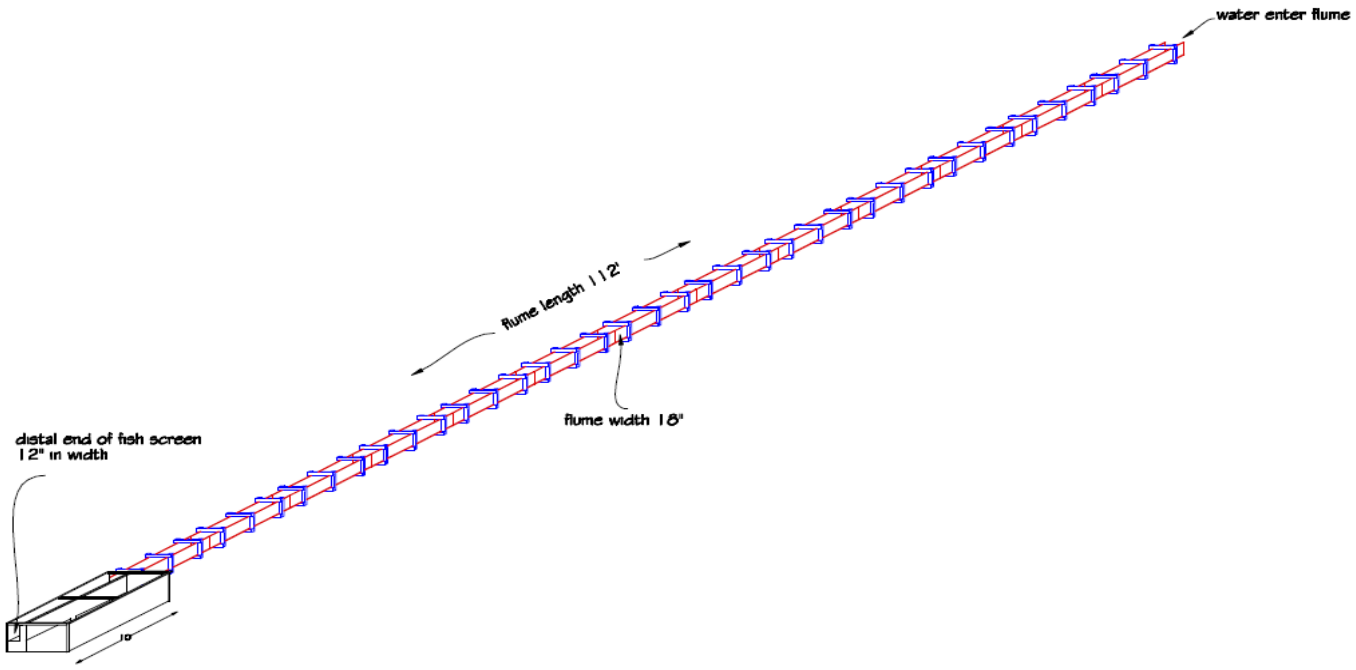

Figure 2. Schematic of the modular screen apparatus used to evaluate the behavioral responses of juvenile salmonids encountering the leading edge of the Farmers Screen, 2010. The modular screen apparatus consisted of a 34 m of wooden flume connected to a 3.1-m long section of the Farmers Screen.

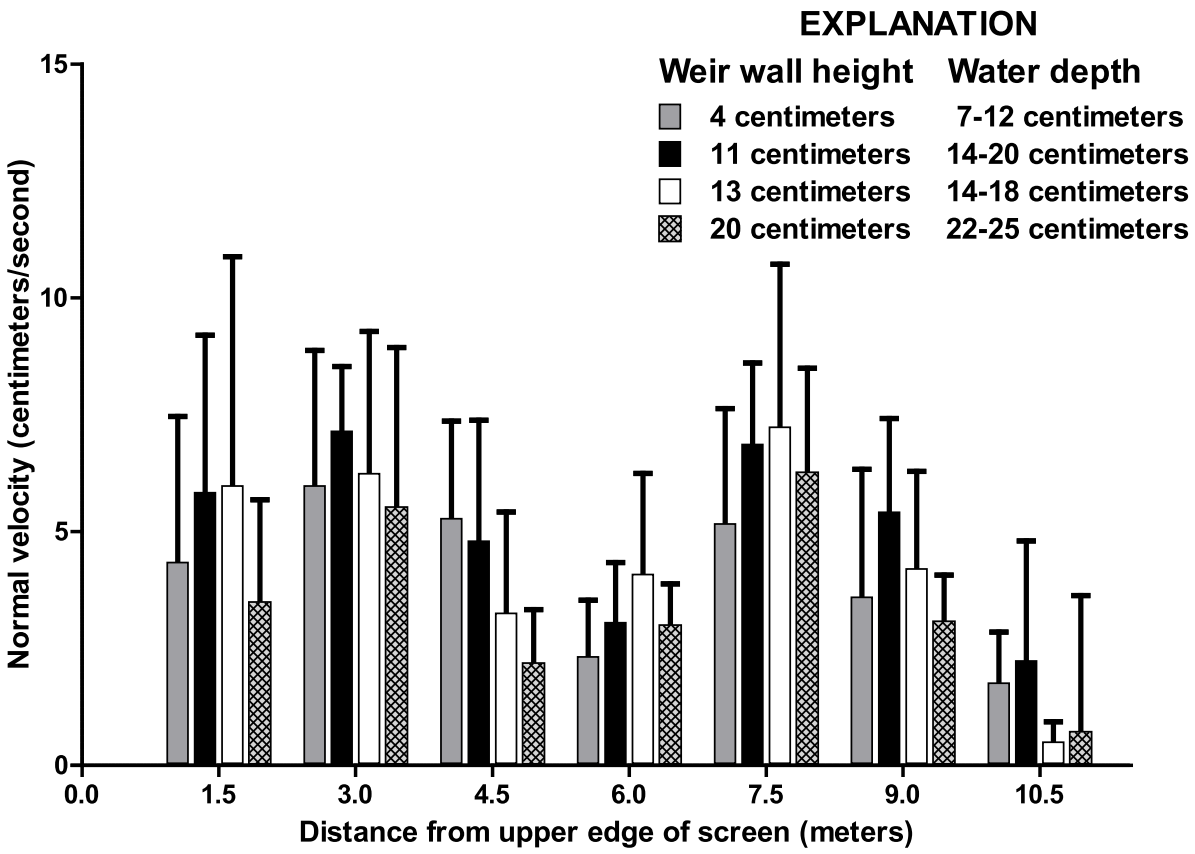

Figure 3. Mean normal velocities (approach velocities corrected for the net open area of the screen) estimated for different sections of the Herman Creek screen relative to weir wall height and water depth, 2009. The whiskers represent the standard deviations of the estimates.

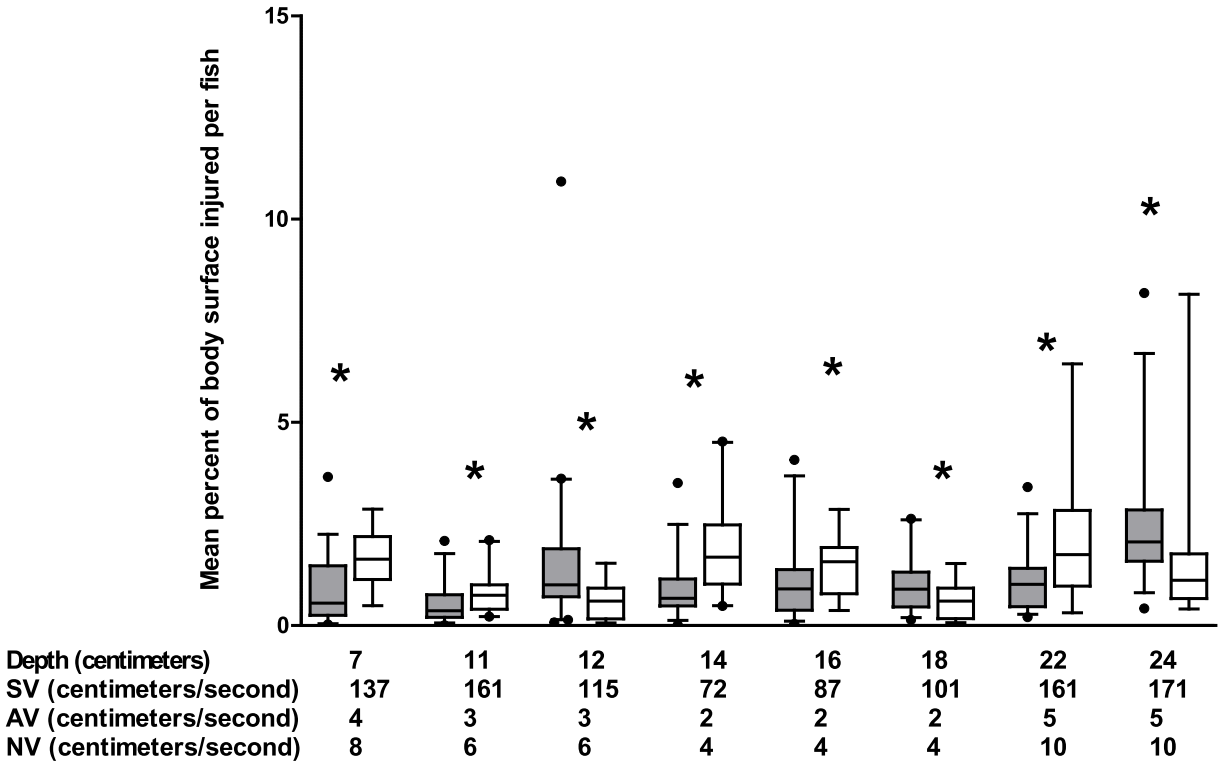

Figure 4. Distribution of the percentage of body surface area of large juvenile coho salmon injured when released over the Herman Creek screen (grey boxes) under various hydraulic conditions relative to control fish (white boxes). The upper and lower boundaries of the box represent the 25th and 75th quartiles, the line inside the box is the mean, the whiskers represent the 5- and 95-percent confidence intervals, and outliers are shown by solid points. The X-axis shows the water depth over the screen, the mean sweeping velocity (SV), the approach velocity (AV), and the normal velocity (NV) during each test. Asterisks denote a significant difference between medians within a group (Mann Whitney *U* test, $P < 0.05$).

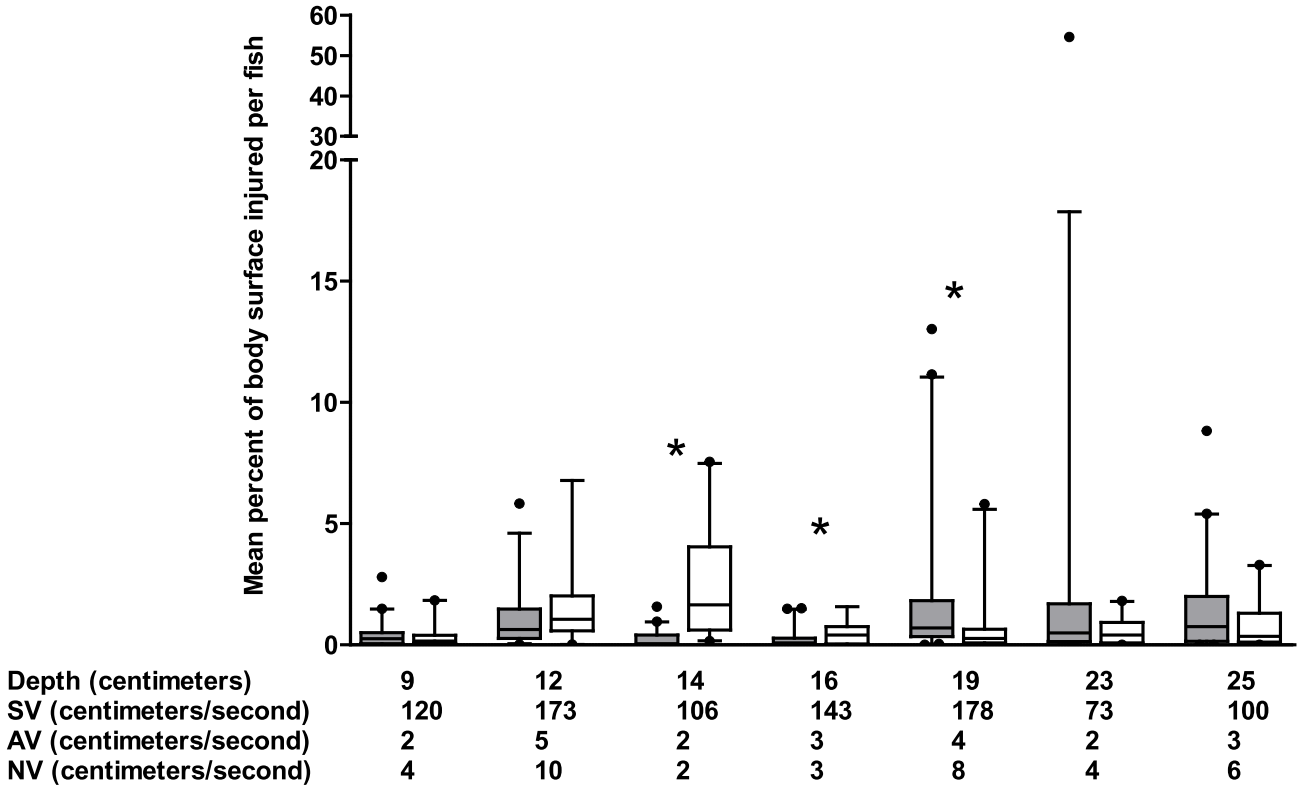

Figure 5. Distribution of the percentage of body surface area of small juvenile coho salmon injured when released over the Herman Creek screen (grey boxes) under different hydraulic conditions relative to control fish (white boxes). The upper and lower boundaries of the box represent the 25th and 75th quartiles, the line inside the box is the mean, the whiskers represent the 5- and 95-percent confidence intervals, and outliers are shown by solid points. The X-axis shows the water depth over the screen, the mean sweeping velocity (SV), the approach velocity (AV), and the normal velocity (NV) during each trial. Asterisks denote a significant difference between medians within a group (Mann Whitney *U* test, $P < 0.05$).

Table 1. Summary of hydraulic conditions at the Herman Creek screen and the numbers of two size groups of juvenile coho salmon used during injury and delayed mortality assessments.

[Trials were conducted on different days during February through May 2009. Q, discharge; SV, sweeping velocity; AV, approach velocity; Z, water depth over the screen; T, treatment fish; C, control fish. SD, standard deviation; cm, centimeters; cm/s, centimeters per second; m^3/s, cubic meters per second. Values in parentheses are data for delayed mortality tests. na, not available]

Inflow Q (m^3/s)	Diversion Q (m^3/s)	Bypass Q (m^3/s)	SV (cm/s; mean [SD])	AV (cm/s)	Z (cm; mean [SD])	Large fish		Small fish	
						T	C	T	C
4-cm weir wall height									
0.10	0.10	0.00	67 (34)	1	7 (1)				
0.14	0.13	0.01	87 (41)	2	7 (1)	37	17		
0.15	0.14	0.01	120 (50)	2	9 (1)			40 (44)	19 (15)
0.26	0.23	0.03	166 (52)	3	12 (1)				
0.27	0.25	0.02	137 (49)	4	11 (3)	38 (65)	20		
0.29	0.26	0.02	138 (73)	4	10 (1)				
0.31	0.28	0.02	130 (46)	4	12 (2)				
0.34	0.31	0.03	173 (45)	5	12 (1)			39 (51)	19 (17)
0.36	0.33	0.03	171 (41)	5	12 (1)	41 (60)	15 (30)		
11-cm weir wall height									
0.14	0.11	0.03	101 (30)	2	14 (1)	39	20		
0.15	0.12	0.03	106 (30)	2	14 (1)			40 (45)	20 (18)
0.29	0.23	0.05	161 (23)	3	16 (2)	40	20		
0.29	0.23	0.06	143 (30)	3	16 (1)			40 (45)	14 (15)
0.34	0.26	0.08	178 (32)	4	19 (1)			41 (36)	20 (15)
0.42	0.34	0.07	161 (30)	5	18 (1)	38 (61)	15 (42)		
13-cm weir wall height									
0.10	0.09	0.02	61 (20)	1	14 (0)				
0.20	0.13	0.07	170 (36)	2	16 (2)				
0.31	0.24	0.06	127 (25)	4	20 (1)				
20-cm weir wall height									
0.02	0.02	0.00	na	0	1 (1)				
0.04	0.03	0.01	36 (15)	0	8 (0)				
0.15	0.10	0.05	72 (12)	2	22 (1)	38	14		
0.15	0.10	0.05	73 (12)	2	23 (0)			36 (44)	20 (15)
0.27	0.20	0.07	100 (15)	3	25 (1)			35 (45)	20 (15)
0.28	0.22	0.06	115 (17)	3	24 (1)	39 (60)	15 (52)		
0.29	0.21	0.08	101 (25)	3	25 (1)				

Table 2. General linear models describing relation between hydraulic variables measured at the Herman Creek screen, 2009.

[All coefficients are significant (P < 0.05) unless noted. SV, sweeping velocity; Z, depth of water over screen; SQ, inflow discharge; DQ, diversion discharge; WW, weir wall height; *SEE*, standard error of estimate; cm, centimeters; m^3/s, cubic meters per second]

Dependent variable	Equation
Depth	$Z = 2.592^{1} + 0.572\ (WW) + 89.673\ (SQ) - 75.712\ (DQ)$
	$N = 24,\ R^2 = 0.84,\ SEE = 2.27$
Diversion discharge	$WQ = 0.056 - 0.003\ (WW) + 0.902\ (SQ) + 0.000\ (SV)$
	$N = 24,\ R^2 = 0.99,\ SEE = 0.01$
Sweeping velocity	$SV = 105.007 - 4.863\ (WW) + 1{,}166.178\ (SQ) - 1{,}063.394\ (DQ)$
	$N = 24\ R^2 = 0.81,\ SEE = 17.82$

[1] P=0.25

Table 3. Mean number of fish contacts with the screen, their relative depth of travel during passage, and their general orientation to the water flow during passage for large juvenile coho salmon experimentally released over the Herman Creek screen, 2009.

[AV, approach velocity; SV, sweeping velocity; SD, standard deviation; cm, centimeter; cm/s, centimeter per second]

Date	Water depth (cm; mean [SD]))	AV (cm/s)	SV (cm/s; mean [SD])	Mean (SD) number of screen contacts per fish	Depth in water column (percentage of observed)			Orientation (percentage of observed)		
					low	mid	high	up stream	down stream	other
2/27	7	2	87 (41)	0.72 (0.58)	69	25	6	44	56	0
2/17	11	4	137 (49)	0.45 (0.23)	41	54	5	36	60	4
3/4	12	5	171 (41)	0.47(0.24)	53	35	12	55	45	0
3/2	14	2	101 (30)	0.26 (0.18)	58	35	6	35	65	0
2/18	16	3	161 (23)	0.41(0.23)	44	43	13	58	42	0
3/3	18	5	161 (30)	0.15 (0.18)	66	28	5	33	67	0
2/24	22	2	72 (12)	0.41 (0.34)	69	25	5	53	47	0
2/19	24	3	115 (17)	0.41 (0.33)	60	32	8	46	54	0

Table 4. Mean number of fish contacts with the screen, their relative depth of travel during passage, and their general orientation to the water flow during passage for small juvenile coho salmon experimentally released over the Herman Creek screen, 2009.

[AV, approach velocity; SV, sweeping velocity; SD, standard deviation; cm, centimeter; cm/s, centimeter per second]

Date	Water depth (cm; mean [SD])	*AV* (cm/s)	*SV* (cm/s; mean [SD])	Mean (SD) number of contact per fish	Depth in water column (percentage of observed)			Orientation (percentage of observed)		
					low	mid	high	up stream	down stream	other
5/19	9 (1)	2	120 (50)	0.32 (0.14)	57	40	3	56	40	4
5/20	12 (1)	5	173 (45)	0.50 (0.30)	63	33	4	61	15	24
5/15	14 (1)	2	106 (30)	0.56 (0.26)	58	32	10	55	41	4
5/13	16 (1)	3	143 (30)	0.42 (0.25)	49	37	14	44	38	18
5/14	19 (1)	4	178 (32)	0.62 (0.35)	65	23	12	53	35	12
5/8	23 (0)	2	73 (12)	0.26 (0.22)	69	24	7	70	30	0
5/12	25 (1)	3	100 (15)	0.35 (0.21)	53	28	19	61	37	2

Table 5. Summary of hydraulic conditions at the modular screen, the number and species of fish used for testing, and the percentage of fish that successfully passed over the screen during consecutive 5-minute periods, 2010. Only one steelhead refused to pass over the screen initially, but eventually did so within 10 minutes.

[Q, discharge; AV, approach velocity; SV, sweeping velocity; SD, standard deviation; cm, centimeter; cm/s, centimeter per second;

Inflow *Q* (m^3/s)	Water depth (cm; mean [SD])	AV (cm/s)	SV (cm/s; mean [SD])	Number of fish released	Percentage of observations where fish passed over the screen				
					0 – 5 min	5 – 10 min	10 – 15 min	15 – 20 min	>20[1] min
Coho Salmon									
0.06	15 (1)	2	111 (6)	40	91	0	0	0	9
0.09	15 (1)	3	150 (8)	20	75	10	10	0	5
0.09	19 (1)	2	132 (7)	33	82	0	0	0	18
0.07	20 (0)	1	102 (10)	40	88	0	0	0	12
0.08	25 (1)	1	102 (13)	40	95	3	0	0	3
Steelhead Trout									
0.06	15 (1)	2	111 (6)	40	90	3	0	0	8
0.09	15 (1)	3	150 (8)	22	62	5	0	29	5
0.08	25 (1)	1	102 (13)	40	47	12	0	21	21

[1]Values include fish that were prodded from the upper 3 m of the flume.

Publishing support provided by the U.S. Geological Survey
Publishing Network, Tacoma Publishing Service Center

For more information concerning the research in this report, contact the
Director, Western Fisheries Research Center
U.S. Geological Survey, 6505 NE 65th Street
Seattle, Washington 98115
http://wfrc.usgs.gov/

North American Journal of Fisheries Management 32:604–612, 2012
American Fisheries Society 2012
ISSN: 0275-5947 print / 1548-8675 online
DOI: 10.1080/02755947.2012.678966

ARTICLE

Field-Based Evaluations of Horizontal Flat-Plate Fish Screens, II: Testing of a Unique Off-Stream Channel Device—the Farmers Screen

Matthew G. Mesa,* Brien P. Rose, and Elizabeth S. Copeland
U.S. Geological Survey, Western Fisheries Research Center, Columbia River Research Laboratory, 5501 Cook-Underwood Road, Cook, Washington 98605, USA

Abstract

Screens are installed at water diversion sites to reduce entrainment of fish. Recently, the Farmers Irrigation District (Oregon) developed a unique flat-plate screen (the "Farmers Screen") that operates passively and may offer reduced installation and operating costs. To evaluate the effectiveness of this screen on fish, we conducted two separate field experiments. First, juvenile coho salmon *Oncorhynchus kisutch* were released over a working version of this screen under a range of inflows (0.02–0.42 m^3/s) and diversion flows (0.02–0.34 m^3/s) at different water depths. Mean approach velocities ranged from 0 to 5 cm/s and sweeping velocities ranged from 36 to 178 cm/s. Water depths over the screen surface ranged from 1 to 25 cm and were directly related to inflow. Passage of fish over the screen under these conditions did not severely injure them or cause delayed mortality, and no fish were observed becoming impinged on the screen surface. Second, juvenile coho salmon and steelhead *O. mykiss* were released at the upstream end of a 34-m flume and allowed to volitionally move downstream and pass over a 3.5-m section of the Farmers Screen to determine whether fish would refuse to pass over the screen after encountering its leading edge. For coho salmon, 75–95% of the fish passed over the screen within 5 min and 82–98% passed within 20 min, depending on hydraulic conditions. For steelhead, 47–90% of the fish passed over the screen within 5 min and 79–95% passed within 20 min. Our results indicate that when operated within its design criteria, the Farmers Screen provides safe and efficient downstream passage of juvenile salmonids under a variety of hydraulic conditions.

There are many kinds of irrigation diversion screens in the USA, and all are designed to prevent fishes and other aquatic life from becoming entrained, injured, or killed by the diversion. The most common are vertically oriented screens, such as panel, traveling-belt, and rotary drum screens. Although these types of screens have been extensively studied and have design and operating criteria meant to protect fish (NMFS 2008), they can be relatively expensive and require frequent maintenance to operate properly (McMichael et al. 2004), which can limit the installation of screens in areas where they are needed. Recently, the development of unique horizontal flat-plate fish screens offer designs that may be less expensive to install and offer simpler, more passive (i.e., no moving parts) operation than other screens. Research on the hydraulic characteristics and biological effects of some flat-plate screens has resulted in a greater understanding of how they work (Frizell and Mefford 2001) and shown few negative effects (e.g., injury or mortality) on juvenile bull trout *Salvelinus confluentus* or rainbow trout *Oncorhynchus mykiss* that passed over such screens (Beyers and Bestgen 2001; Rose et al. 2008). However, more work is needed to fully evaluate their performance. Evaluating different designs and sizes of horizontal flat-plate screens in the laboratory and in the field would allow further verification of screen performance, provide data for comparison with more traditional fish screens, and perhaps facilitate screen installation.

For this work, we evaluated the hydraulic and biological performance of a newly developed horizontal flat-plate fish screen, also known as the Farmers Screen (Figures 1, 2), for use in an

*Corresponding author: mmesa@usgs.gov
Received November 17, 2011; accepted March 15, 2012
Published online June 18, 2012

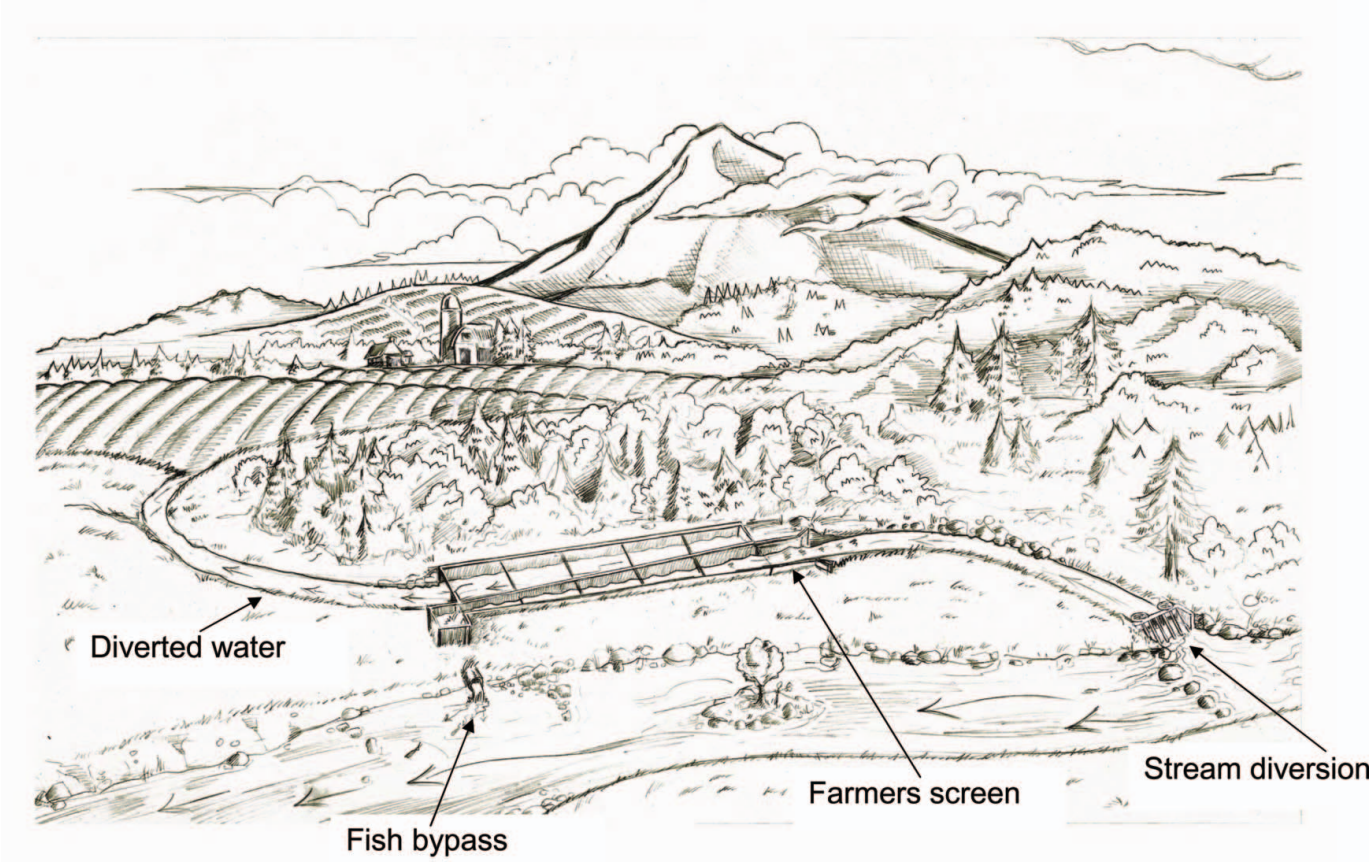

FIGURE 1. Conceptual drawing of a typical Farmers Screen installation (courtesy of the Farmers Conservation Alliance, Hood River, Oregon). [Figure available in color online.]

off-stream channel. These screens, designed over a 10-year period by personnel from the Farmers Irrigation District in Hood River, Oregon, have a high ratio of sweeping velocity (the velocity of water flowing parallel to the screen surface) to approach velocity (the velocity of water actually passing through the screen surface) and a 50% open surface area with relatively small screen pore sizes. These characteristics provide good self-cleaning; reduce the potential for fish impingement, injury, and entrainment; and may afford lower installation and maintenance costs (see www.farmerscreen.org for detailed information). The screens are manufactured in various sizes and can accommodate flows ranging from 0.01 to over 4.5 m^3/s (0.5–160 ft^3/s). There are many small unscreened or insufficiently screened diversions with flow less than 1.4 m^3/s (50 ft^3/s) in the western USA, and small diversions can take a high percentage of the flow from small streams; most larger diversions have already been screened (Moyle and Israel 2005; Rose et al. 2008). We therefore decided to test a small version of the Farmers Screen because of the great potential for installing these devices in many areas. Our objectives were to (1) assess the hydraulic performance of a Farmers Screen designed to divert only 0.28 m^3/s of water; (2) determine the extent of injury and delayed mortality in fish that have been experimentally released over the screen under various hydraulic conditions; and (3) evaluate whether fish would refuse to pass over the screen upon encountering its leading edge, again under a variety of hydraulic conditions.

METHODS

Study site and hydraulic assessments.—We evaluated a small Farmers Screen located at the Oxbow Fish Hatchery in Cascade Locks, Oregon (Figure 3). The screen is on a side-channel of Herman Creek, a tributary of the Columbia River, and was designed to divert 0.28 m^3/s of water. The screen was similar to other Farmers Screens that have already been installed in the Pacific Northwest. The Herman Creek screen site allowed us to create various test conditions.

For hydraulic assessments of the Herman Creek screen, we first adjusted the inflow entering the screen and measured it in the flume just upstream of the screen surface with a Marsh–McBirney electronic velocity meter following the protocol of Gallagher and Stevenson (1999). We also measured discharge at the very downstream end of the screen (i.e., the bypass flow) and estimated diversion discharge as the difference between the entrance and bypass flows. We then calculated mean approach velocity by dividing the effective screen surface area by the diversion discharge. Sweeping velocities and water depth were measured at 28 evenly spaced positions across seven transects

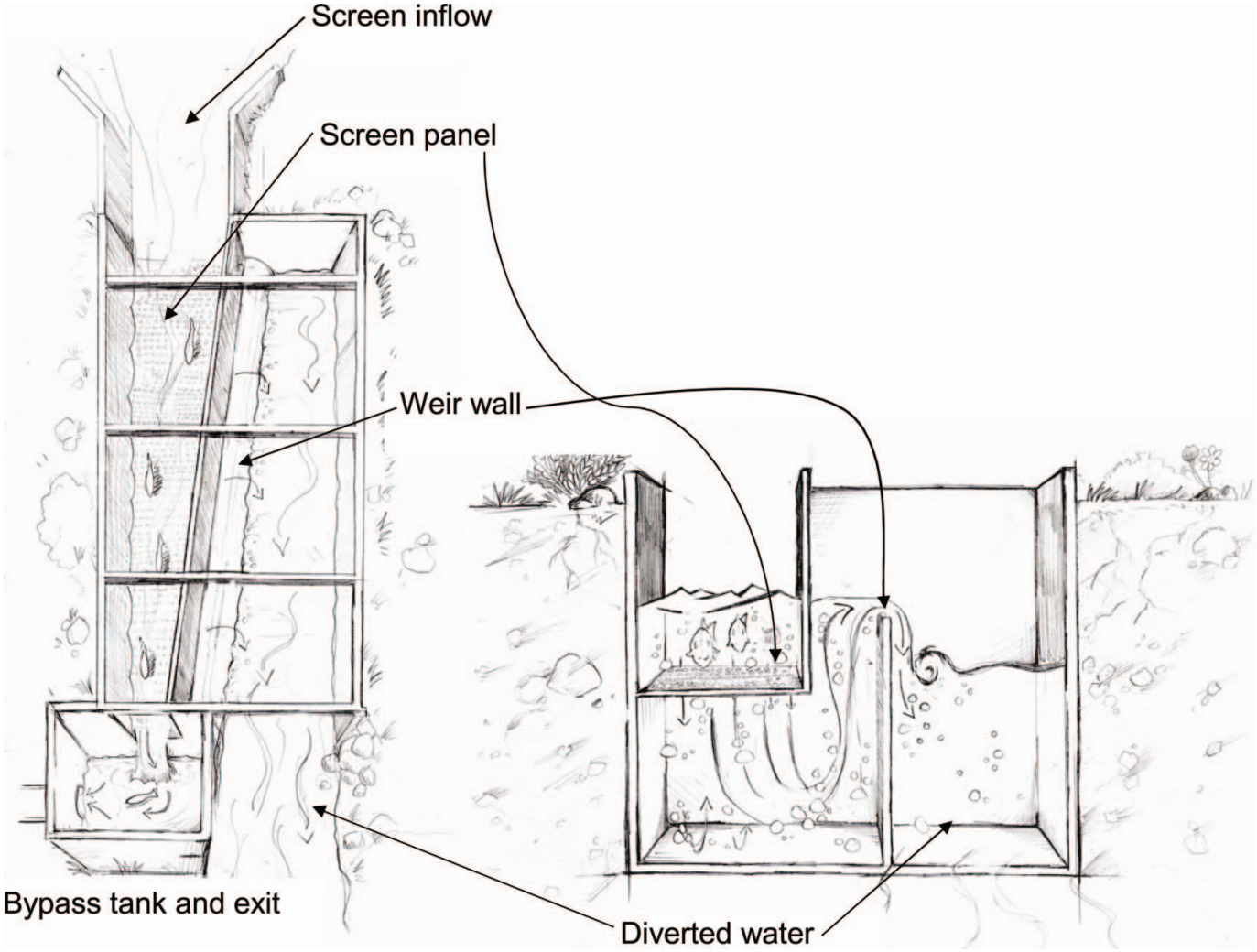

FIGURE 2. Conceptual overhead and frontal views of a typical Farmers Screen showing design details (courtesy of the Farmers Conservation Alliance, Hood River, Oregon). [Figure available in color online.]

on the fish screen perpendicular to the flow. Water velocities were measured at 7.6 cm above the screen surface or at 0.6 × water depth in shallow water. The diversion discharge was the volume of screened water going to the hatchery, and the bypass flow was the water returning fish and debris back to the stream. We recorded the diversion flow, and the sweeping velocity, approach velocity, and depth relative to the inflow and weir wall height.

Biological assessments.—To assess the biological performance of the Herman Creek screen, we experimentally released groups of juvenile coho salmon *O. kisutch* over the screen under various hydraulic conditions (as determined above) and quantified any injuries to the integument and documented short-term delayed mortality. Our test fish were from the Oxbow Hatchery, and we evaluated two size groups, large (85–145 mm fork length) and small (54–78 mm), in two separate sets of trials from 17 February to 20 May 2009. Prior to testing, fish were netted from their hatchery rearing ponds, examined for trauma or abnormalities (e.g., body deformities, missing fins, >20% descaling, etc.), and healthy fish were divided into groups that were held separately for up to a week in net pens placed within a large hatchery pond. On the day of testing, the hydraulic conditions for the screen were set, and several samples of 8–10 fish each were removed from the net pens and placed in 19-L buckets that received a constant inflow of river water. Groups impartially selected to pass over the screen (treatment fish) were released 1–2 m upstream of the upper edge of the screen and recaptured in a sanctuary net (45 cm wide, 35 cm long, and 100 cm deep with 0.3-cm nylon mesh) positioned beneath the bypass outfall. Groups selected as control fish were released directly into the sanctuary net and held for 2 min to simulate the time it took most groups of treatment fish to pass over the screen. After each test, the cod end of the sanctuary net containing the recaptured fish was quickly lifted and immersed in a bucket containing a lethal

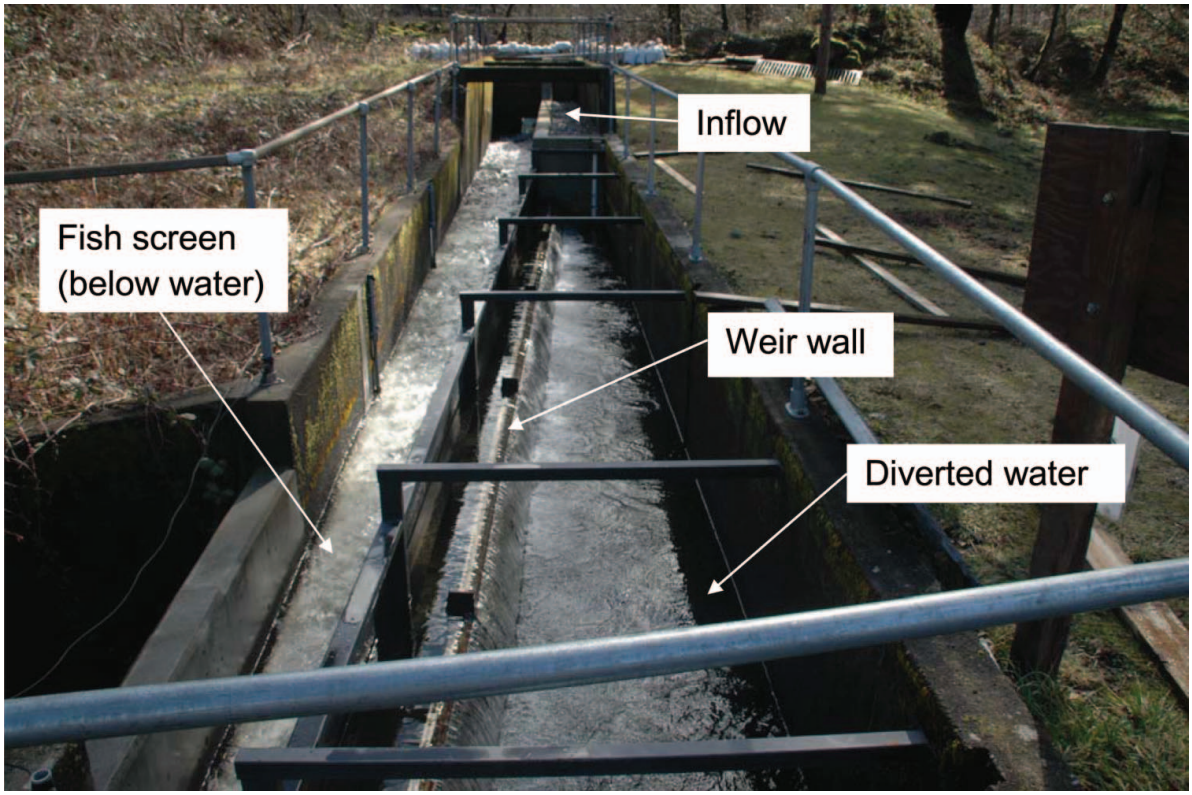

FIGURE 3. Photograph of the Herman Creek Screen, looking upstream, at the Oxbow Fish Hatchery, Cascade Locks, Oregon. Photograph by Brien P. Rose. [Figure available in color online.]

dose of MS-222 at 200 mg/L of water. Tests were conducted during daylight hours and water temperatures of 5–7°C.

We used a fluorescein dye method described by Noga and Udomkusonsri (2002) to determine the extent of ulceration on the skin, eyes, and fins of each fish. After fish were euthanized, they were rinsed in a freshwater bath for 1 min and then placed in a solution of fluorescein dye (fluorescein disodium salt at 200 mg/L). After 6 min, fish were removed from the dye and rinsed in three separate freshwater baths over 3 min to remove excess dye. Images were taken of both sides of each fish in a dark box under ultraviolet (UV) light using a digital camera with a 200-mm macro lens. The UV lights were placed at 45° angles to the side of the fish, and a yellow barrier filter was used to eliminate the blue auto-fluorescence. Images were imported into Adobe Photoshop CS3, and the body surface area and area of fluorescence were measured on each side of a fish. The percentage of body surface area of a fish that was injured was derived by dividing the total area of fluorescence by the total body surface area. This included the two sides and most, but not all, of the dorsal and ventral surfaces of the fish. For each release group, we compared the median percentage of body surface area that was injured between control and treatment fish using Mann–Whitney *U*-tests.

To assess delayed mortality after passage, additional fish were released in the same manner as described above but were transferred to 76-L holding tanks adjacent to the screen after being collected in the bypass outfall. The tanks received flow-through water from Herman Creek via a pump submerged in a nearby hatchery pond. Fish were monitored for 24–48 h after passage, and the number of fish that died was tallied for treatment and control groups. Mortality tests were conducted for most, but not all, of the same hydraulic conditions as injury tests.

Behavior of fish at the leading edge of a screen.—To evaluate whether fish would refuse to pass over a small Farmers Screen after encountering the leading edge, we constructed a 34-m wooden flume (46 cm wide × 36 cm deep) and connected it to a 3.1-m-long modular section of a Farmers Screen. The modular Farmers Screen is a prefabricated, 3.0-m-long section of screen designed for inflows ranging from 0.01 to 0.42 m^3/s (0.5–15 ft^3/s) that requires minimal site preparation, is easy to transport, and can be installed at remote locations. The purpose of the flume was to provide fish with plenty of distance between their release point (at the upstream end of the flume) and the upstream edge of the screen so they could orient themselves and move downstream somewhat naturally. The flume received water from the outflow of the Herman Creek screen and was designed so that water velocities were slower in the upstream half of the flume than in the downstream half. We installed a trap on the downstream end of the screen to capture the fish.

We used yearling coho salmon (113–161 mm) from the Oxbow Hatchery and Skamania steelhead (anadromous rainbow trout; 134–260 mm) from the Bonneville Fish Hatchery (Oregon) for these tests. All the fish were large and silvery with faint or nonexistent parr marks; they normally would have been released from the hatcheries during mid April to early May. Prior to testing, all fish were held in large tanks at the Oxbow Hatchery and water temperatures during holding and testing ranged from 6–9°C.

Prior to releasing fish, we first established the hydraulic conditions for the test, as described above, and also measured water velocities and depths at several locations throughout the flume. Our intent was to test fish under various hydraulic conditions over the screen, similar to those that we tested at the Herman Creek screen. We then removed 7–10 fish from their holding tank, placed them in a 19-L bucket with water, transported them from the hatchery to the test facility (about 2 km), and gently released them at the upstream end of the flume. Fish were allowed 20 min to volitionally migrate down the flume and pass over the screen. After 20 min, we gently prodded any fish that remained in the upper 3 m of the flume until they moved downstream. Under the various hydraulic conditions, we conducted three to four releases of 7–10 fish each, for a total release of 20–40 fish for each species.

An observer was stationed on an elevated platform slightly upstream of the fish screen to record the behavior and passage timing of fish as they approached the screen. For each of five consecutive 5-min periods, we recorded the number of fish that encountered the screen and whether the fish passed over the screen or refused to (e.g., the fish turned and swam back upstream). For analysis, we pooled data from the release groups for each species and hydraulic conditions and determined the cumulative proportions of fish that passed over or rejected the screen for each 5-min period.

RESULTS

Hydraulic Assessments

Inflows established at the Herman Creek screen ranged from 0.02 to 0.42 m^3/s, depending on water depth (Table 1). Diversion discharges ranged from 0.02 to 0.34 m^3/s, comprised 65–100% of the inflow rates, and were always higher than bypass flows. Mean approach velocities estimated for the entire screen ranged from 0 to 5 cm/s and never exceeded 6 cm/s for individual sections of the screen. Mean sweeping velocities ranged from 36 to 178 cm/s and were faster at the upstream edge and slower at the downstream edge of the screening panels. Mean sweeping velocities were at least 32 times higher than approach velocities for all conditions tested. The mean water depth ranged from 1 to 25 cm and generally was deeper at the upstream end of the screen than at the downstream end (Table 1). Hot spots (i.e., localized areas of high approach velocity with spiraling flow) were not observed during any of our tests.

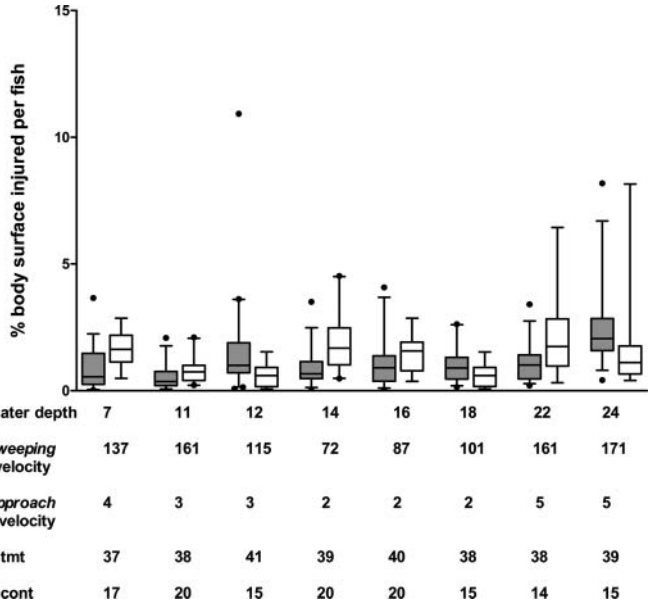

FIGURE 4. Box plots of percent body surface area injured for large (85–145 mm) juvenile coho salmon released over the Herman Creek screen (grey boxes) under different hydraulic conditions relative to control fish (white boxes). The upper and lower boundaries of the box represent the 25th and 75th quartiles, the horizontal line inside the box is the mean, the whiskers represent the 5% and 95% confidence intervals, and outliers are shown by solid points. The *x*-axis shows the water depth over the screen (cm), the mean sweeping velocity (cm/s), the approach velocity (cm/s), and the number of treatment (tmt) and control (cont) fish tested during each trial. Differences between medians within a group were significant for all tests (Mann–Whitney *U*-tests, $P < 0.05$).

Biological Assessments

Overall, the injury rates of fish after passage over the Herman Creek screen were low, and severe injuries to the skin, eyes, and fins of both size cohorts were not observed. For large fish, the percentage of body surface area that was injured varied by release group and ranged from about 0.5% to 2.5% (Figure 4). Median values were significantly different between treatment and control fish for all test conditions (Mann–Whitney *U*-tests: $P < 0.05$; Figure 4), but the magnitude of these differences was small (<1%). For small fish, the percentage of body surface area that was injured ranged from about 0.4% to 3.0% (Figure 5). The medians for treatment and control fish differed significantly for three test conditions (Figure 5), but again, the magnitude of these differences was small (<1%). For delayed mortality after passage, we tested 849 fish in total; no treatment fish died within 24–48 h of passage, and only one control fish died.

Behavior of Fish at the Leading Edge of a Screen

To evaluate the behavioral responses of juvenile salmonids approaching and passing over a modular Farmers Screen, we released a total of 173 coho salmon and 102 steelhead under various hydraulic conditions (Table 2). In the flume, mean water velocities ranged from 60 to 79 cm/s in the upstream half and from 85 to 104 cm/s in the downstream half. Mean water depths

TABLE 1. Summary of hydraulic conditions measured at the Herman Creek screen, February through May 2009. Single asterisks denote the hydraulic conditions under which fish were released for injury tests only, double asterisks those for injury and delayed mortality tests; NA = not available.

Inflow (m^3/s)	Diversion (m^3/s)	Bypass discharge (m^3/s)	Mean (SD) sweeping velocity (cm/s)	Approach velocity (cm/s)	Mean (SD) depth over screen (cm)
			Weir wall height: 4 cm		
0.10	0.10	0.00	67 (34)	1	7 (1)
0.14*	0.13	0.01	87 (41)	2	7 (1)
0.15**	0.14	0.01	120 (50)	2	9 (1)
0.26	0.23	0.03	166 (52)	3	12 (1)
0.27**	0.25	0.02	137 (49)	4	11 (3)
0.29	0.26	0.02	138 (73)	4	10 (1)
0.31	0.28	0.02	130 (46)	4	12 (2)
0.34**	0.31	0.03	173 (45)	5	12 (1)
0.36**	0.33	0.03	171 (41)	5	12 (1)
			Weir wall height: 11 cm		
0.14*	0.11	0.03	101 (30)	2	14 (1)
0.15**	0.12	0.03	106 (30)	2	14 (1)
0.29*	0.23	0.05	161 (23)	3	16 (2)
0.29**	0.23	0.06	143 (30)	3	16 (1)
0.34**	0.26	0.08	178 (32)	4	19 (1)
0.42**	0.34	0.07	161 (30)	5	18 (1)
			Weir wall height: 13 cm		
0.10	0.09	0.02	61 (20)	1	14 (0)
0.20	0.13	0.07	170 (36)	2	16 (2)
0.31	0.24	0.06	127 (25)	4	20 (1)
			Weir wall height: 20 cm		
0.02	0.02	0.00	NA	0	1 (1)
0.04	0.03	0.01	36 (15)	0	8 (0)
0.15*	0.10	0.05	72 (12)	2	22 (1)
0.15**	0.10	0.05	73 (12)	2	23 (0)
0.27**	0.20	0.07	100 (15)	3	25 (1)
0.28**	0.22	0.06	115 (17)	3	24 (1)
0.29	0.21	0.08	101 (25)	3	25 (1)

TABLE 2. The number of coho salmon and steelhead released (*N*) over the modular Farmers Screen in 2010, and the cumulative percentage of fish that successfully passed over the screen in consecutive 5-min periods. After 20 min had passed the remaining fish were coerced from the upper 3 m of the flume; only one steelhead refused to pass over the screen initially but eventually did so within 10 min.

					Percent of fish passing over screen				
Inflow discharge (m^3/s)	Depth (cm)	Approach velocity (cm/s)	Sweeping velocity (cm/s)	*N*	5 min	10 min	15 min	20 min	>20 min
			Coho salmon						
0.06	15 (1)	2	111 (6)	40	91	91	91	91	9
0.09	15 (1)	3	150 (8)	20	75	85	95	95	5
0.09	19 (1)	2	132 (7)	33	82	82	82	82	18
0.07	20 (0)	1	102 (10)	40	88	88	88	88	12
0.08	25 (1)	1	102 (13)	40	95	98	98	98	2
			Steelhead						
0.06	15 (1)	2	111 (6)	40	90	93	93	93	7
0.09	15 (1)	3	150 (8)	22	62	67	67	96	4
0.08	25 (1)	1	102 (13)	40	47	59	59	80	20

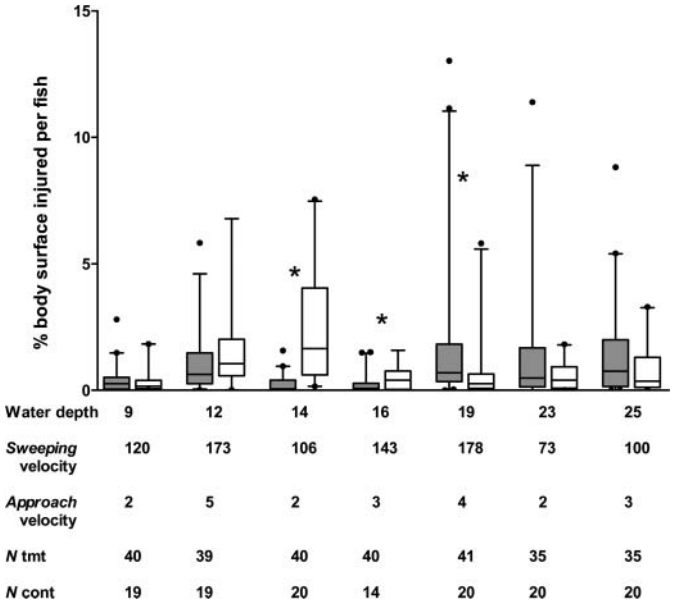

FIGURE 5. Box plots of percent body surface area injured for small (54–78 mm) juvenile coho salmon released over the Herman Creek screen (grey boxes) under different hydraulic conditions relative to control fish (white boxes). Box plot descriptions and *x*-axis labels are as defined in the caption for Figure 4. Differences between medians within a group are denoted by an asterisk (Mann–Whitney *U*-tests, $P < 0.05$).

in the flume ranged from 23 to 31 cm. For coho salmon, 75–95% of the fish approached and passed over the screen within 5 min of their release, depending on hydraulic conditions (Table 2). Within 20 min, the percentages of fish passing over the screen increased to 82–98%. After 20 min, 3–18% of the fish (12 total) remained upstream in the flume and were gently prodded to move downstream; all of these fish passed over the screen without delay.

For steelhead, 47–90% of the fish approached and passed over the screen within 5 min of their release, again depending on hydraulic conditions (Table 2). Within 20 min, the percentages of fish passing over the screen increased to 79–95%. After 20 min, 5–21% of the fish (11 total) were coerced downstream from the upper 3 m of the flume, and one fish turned and swam back upstream after it encountered the edge of the screen. However, this fish returned to the screen within 10 min and successfully passed. Overall, 99.6% of the fish we observed passed over the screen without delay.

DISCUSSION

The Farmers Screen is a unique type of horizontal flat-plate fish screen that may offer substantial benefits to irrigators and fish alike. Although there are several Farmers Screens currently operating in the Pacific Northwest, they have not received enough biological testing to evaluate their potential impacts on fish. As such, these screens are still considered experimental technology by the National Marine Fisheries Service (NMFS) and considerable debate has ensued regarding their hydraulic and biological criteria and operation. Our results indicate that passage of juvenile coho salmon over the Herman Creek screen under various hydraulic conditions did not severely injure them, cause delayed mortality, or delay migration. These results occurred even though most fish passed over the screen near the screen surface, many contacted the screen during passage, and fish were oriented to the current in various directions (based on video observations by us; data not shown here). However, we did not observe fish becoming impinged on the screen surface (i.e., >1 s contact with the screen). We also never had problems with debris loading on the screen, although our tests were done at times when the amount of debris was sparse. Our results were similar to those of Rose et al. (2008), who reported minimal injuries and low mortality of rainbow trout (45–250 mm) after passage over backwatered and inverted-weir horizontal flat-plate screens in Oregon. Rose et al. (2008) evaluated ranges of sweeping (15–143 cm/s) and approach (1–8 cm/s) velocities that were similar to ours. Other studies evaluated various designs of vertically oriented screens and reported results similar to ours for juvenile splittail *Pogonichthys macrolepidotus* (mean length of about 6 cm; Danley et al. 2002), bull trout (median length, 25 mm; Zydlewski and Johnson 2002), and juvenile Chinook salmon *O. tshawytscha* (4.4–7.9 cm; Swanson et al. 2004).

The injuries observed in our fish among both treatment and control groups were minor and indicate that fish had some trauma to the integument prior to testing and that our holding and handling procedures probably caused slightly more trauma. Compared with visual observations and quantification (see Rose et al. 2008), the fluorescein dye method was effective for detecting injuries to the integument of fish and revealed that all fish had some level of injury after testing. Again, however, all injuries were minor and any differences in injury rates between treatment and control groups were small, which makes it difficult to ascribe any biological significance to the injuries we observed. Further, and perhaps more importantly, none of our injury results would have exceeded the criteria for safe passage of fish over conventional screen systems, as established by NMFS (2008). For example, criteria specify a less than 0.5% mortality and 2% injury rate (i.e., the percentage of a sample that is injured) for salmonid smolts and that at least 90% of salmonids that encounter a screened water diversion should be bypassed within 24 h (Bryan Nordlund, NMFS, personal communication). The agency defines injury as visual trauma (including, but not limited to, hemorrhaging, open wounds without fungal growth, gill damage, bruising >0.5 cm in diameter), loss of equilibrium, or greater than 20% descaling on one side (Bryan Nordlund, NMFS, personal communication). Because none of our fish showed such injuries, mortality was less than 0.5% and most fish traveled over the screen without delay, the Herman Creek screen would easily surpass these NMFS standards. Although the criteria discussed here are for other types of screens, they do indicate that screens like the one at Herman Creek probably would, at a minimum, meet federal regulatory standards.

The ability of the Herman Creek screen to safely and efficiently pass fish at water depths ranging from 7 to 25 cm was largely due to achieving a high ratio of sweeping velocity to approach velocity (range = 30:1 to 54:1) under various hydraulic conditions. These ratios were substantially higher than initial recommendations for sweeping velocity established by NMFS for horizontal screens, which only suggest that downstream sweeping velocities be higher than approach velocities for the entire length of the screen (NMFS 2008). The combination of high sweeping velocities and low approach velocities facilitated quick downstream fish passage and eliminated impingements, which was similar to the results of Beyers and Bestgen (2001). That most fish passed over the screen near the screen surface, regardless of water depth, indicates that the 30-cm water depth recommendation established for horizontal screens (NMFS 2008) could be relaxed for smaller screens like the one at Herman Creek. Although fish safely passed over the screen at a depth of only 7 cm, the number of screen contacts per fish increased at this shallow depth for large (85–145 mm) but not small (54–78 mm) fish (based on video data not shown here). Even though the screen contact rate was not related to the extent or severity of injuries, operating the screen at water depths near 7 cm seems too shallow, particularly under high-flow conditions. Thus, although our results suggest that the Herman Creek screen can be operated effectively at water depths less than 30 cm, we cannot unequivocally recommend a single, specific minimum depth for this screen. Rather, a range of minimum depths, perhaps from 15 to 20 cm, would probably provide safe passage of fish under most circumstances.

Despite the success of the Herman Creek screen in safely and effectively passing fish, there are some things to consider when interpreting our results. First, we were unable to evaluate all possible hydraulic conditions on screen performance, fish injury, and mortality. Although we believe our evaluations were realistic because they encompassed typical diversion conditions, there may be other flow conditions we missed that are relevant to fish passage and safety. Second, we only tested two species of fish and our results may not be applicable to other species. The fishes used in our tests were probably good surrogates for other salmonids of similar size, but extrapolation of our results to other fishes, such as juvenile lampreys or endangered suckers in the Klamath Basin, seems inappropriate and would require further testing. Finally, we evaluated only the effects of downstream passage on juvenile fish. Further testing would be required to assess the effects of this screen type on fish migrating upstream across the screen surface, although such behavior would probably be rare.

The purpose of evaluating the reactions of fish approaching a Farmers Screen was to determine whether fish would reject or refuse to pass over the screen after encountering its leading edge, a notion that was a concern to fishery managers and something we did not evaluate specifically at the Herman Creek screen. The concern was related to the changing hydraulic conditions at the flume-screen interface and whether fish would sense this change, turn around, and refuse to pass. Extended delays in passage over the screen could lead to excessive energy use in fish and violation of the NMFS standard that fish must be bypassed within 24 h. Our results, however, clearly indicate that the flume–screen interface was not an obstacle to passage for fish moving volitionally downstream because high percentages of fish passed within 20 min. Even the small number of fish we had to manually coerce to move downstream readily passed over the flume–screen interface. We cannot state whether all fish encountering and passing through small versions of the Farmers Screen would be bypassed within 24 h because none of our tests were designed to answer this question. However, we think the possibility of fish not passing over these screens within 24 h is remote.

MANAGEMENT RECOMMENDATIONS

When provided with an adequate inflow and configured to maintain a water depth of near 10 cm, the Herman Creek screen provided safe and effective downstream passage of juvenile coho salmon under a variety of hydraulic conditions. As such, given proper site conditions, the Farmers Screen may offer a useful alternative to irrigators, fisheries agencies, and others contemplating a fish screen installation. With their off-channel installation, no moving parts, the potential for good self-cleaning ability, and safe and effective passage of juvenile salmonids under a variety of conditions, the Farmers Screen would appear to be a welcome addition to the arsenal of fish screening devices currently available. However, to achieve the full benefits of the Farmers Screen, they must be operated within their design criteria. This stipulation cannot be emphasized enough because these screens, like all horizontal flat-plate screens, can completely dewater under certain aberrant conditions, which could leave fish stranded on the screen surface. This is a problem unique to horizontal screens and requires that operators pay close attention to design criteria, particularly inflow rates, water depth over the screen, and sweeping velocity to approach velocity ratios. For example, we would not recommend operating the Herman Creek screen at inflows less than about 0.14 m^3/s (about half of what it was designed for) because water depth can become quite shallow if the weir wall is not fully sealed or the screen can completely dewater, particularly at very low flows. If the screen is operated at inflows near or slightly less than 0.14 m^3/s, caution must be used to avoid diverting an excessive amount of water, which can lead to shallow depths, insufficient bypass flow, and perhaps screen dewatering. In the end, however, a complete dewatering of the Farmers Screen would require significant deviations from design, installation, or operating criteria and can be easily avoided. Finally, for the Herman Creek screen, we do not know the fate of fish that pass over the screen, enter the bypass channel, and are diverted back to the Columbia River. It is possible that passage through these areas is a stressful and disorienting event for fish, which could make them vulnerable to hazards that exist downstream, such as predation by fish or birds. This idea is not unique to the Herman Creek screen, but is relevant for many

types of diversions and obstacles fish may encounter in the wild. Further research would be necessary to address this issue.

ACKNOWLEDGMENTS

We thank Julie Davies O'Shea, Daniel Kleinsmith, Les Perkins, and Roy Slayton of The Farmers Conservation Alliance for financial and technical support; Jerry Bryan for his expertise and advice on the Farmers Screen; Duane Banks and his staff from the Oxbow Fish Hatchery for use of their facility and technical assistance; Bryan Nordlund, Michelle Day, and Larry Swenson of NMFS for early discussions and advice on our study; and staff from the Columbia River Research Laboratory for their assistance in the field. Mention of trade names does not imply endorsement by the U. S. Government.

REFERENCES

Beyers, D. W., and K. R. Bestgen. 2001. Bull trout performance in a horizontal flat plate screen. Final report to the U. S. Bureau of Reclamation, Water Resources Research Group, Denver.

Danley, M. L., S. D. Mayr, P. S. Young, and J. J. Cech. 2002. Swimming performance and physiological stress responses of split tail exposed to a fish screen. North American Journal of Fisheries Management 22:1241–1249.

Frizell, K., and B. Mefford. 2001. Hydraulic performance of a horizontal flat plate screen. Final report to the U. S. Bureau of Reclamation, Water Resources Research Group, Denver.

Gallagher, A. S., and N. J. Stevenson. 1999. Streamflow. Pages 149–157 *in* M. B. Bain and N. J. Stevenson, editors. Aquatic habitat assessment: common methods. American Fisheries Society, Bethesda, Maryland.

McMichael, G. A., J. A. Vucelick, C. S. Albernathy, and D. A. Neitzel. 2004. Comparing fish screen performance to physical design criteria. Fisheries 29(7):10–16.

Moyle, P. B., and J. A. Israel. 2005. Untested assumptions: effectiveness of screening diversions for conservation of fish populations. Fisheries 30(5):20–28.

NMFS (National Marine Fisheries Service). 2008. Anadromous salmonid passage facility design. NMFS, Northwest Region, Portland, Oregon.

Noga, E. J., and P. Udomkusonsri. 2002. Fluorescein: a rapid, sensitive, nonlethal method for detecting skin ulceration in fish. Veterinary Pathology 39:726–731.

Rose, B. P., M. G. Mesa, and G. B. Zydlewski. 2008. Field-based evaluations of horizontal flat plate fish screens. North American Journal of Fisheries Management 28:1702–1713.

Swanson, C., P. S. Young, and J. J. Cech Jr. 2004. Swimming in two-vector flows: performance and behavior of juvenile Chinook salmon near a simulated screened water diversion. Transactions of the American Fisheries Society 133:265–278.

Zydlewski, G. B., and J. R. Johnson. 2002. Response of bull trout fry to four types of water diversion screens. North American Journal of Fisheries Management 22:1276–1282.

RECLAMATION

Managing Water in the West

Hydraulic Laboratory Report HL-2004-05

Hydraulic Performance of a Horizontal Flat-Plate Screen

U.S. Department of the Interior
Bureau of Reclamation
Technical Service Center
Water Resources Research Laboratory
Denver, Colorado

February 2005

REPORT DOCUMENTATION PAGE

Form Approved
OMB No. 0704-0188

PLEASE DO NOT RETURN YOUR FORM TO THE ABOVE ADDRESS.

1. REPORT DATE *(DD-MM-YYYY)*	2. REPORT TYPE	3. DATES COVERED *(From - To)*
02-22-2005	Technical	June 2000 - July 2001

4. TITLE AND SUBTITLE

Hydraulic Performance of a Horizontal Flat-Plate Screen

5a. CONTRACT NUMBER

5b. GRANT NUMBER

5c. PROGRAM ELEMENT NUMBER

6. AUTHOR(S)

Frizell, Kathleen H.
Mefford, Brent W.

5d. PROJECT NUMBER

5e. TASK NUMBER

5f. WORK UNIT NUMBER

7. PERFORMING ORGANIZATION NAME(S) AND ADDRESS(ES)

U.S. Department of the Interior, Bureau of Reclamation
Water Resources Research Laboratory
PO Box 25007
Denver, CO 80225

8. PERFORMING ORGANIZATION REPORT NUMBER

HL-2004-05

9. SPONSORING/MONITORING AGENCY NAME(S) AND ADDRESS(ES)

U.S. Department of the Interior
Bureau of Reclamation
Pacific Northwest Division
203 Collins Road
Boise, ID 83702-4520

U.S. Department of the Interior
Bureau of Reclamation
Science and Technology Research Program
PO Box 25007, D-9000
Denver, CO 80225

10. SPONSOR/MONITOR'S ACRONYM(S)

11. SPONSOR/MONITOR'S REPORT NUMBER(S)

12. DISTRIBUTION/AVAILABILITY STATEMENT

Available from:
National Technical Information Service, Operations Division, 5285 Port Royal Road, Springfield, Virginia 22161
http://www.ntis.gov

13. SUPPLEMENTARY NOTES

Prepared in cooperation with Colorado State University. The biological documentation is reported in "Bull Trout Performance During Passage Over A Horizontal Flat-plate Screen" by Beyers and Bestgen.

14. ABSTRACT

The Bureau of Reclamation with the assistance of the Colorado State University Larval Fish Laboratory has conducted hydraulic and biological tests of a horizontal flat-plate fish screen in the Water Resources Research Laboratory. Investigating the hydraulic characteristics of the screen will provide valuable information on how the screen operates and provide limitations on the zones of operation to ensure meeting biological needs. A laboratory-based biological assessment of the screening concept using bull trout will provide a pilot study that evaluates fish behavior and potential damage when exposed to the screen.

15. SUBJECT TERMS

horizontal flat-plate fish screen, hydraulic evaluation, sweeping velocity, approach velocity, diversion structure, bull trout fish passage, debris testing

16. SECURITY CLASSIFICATION OF:			17. LIMITATION OF ABSTRACT	18. NUMBER OF PAGES	19a. NAME OF RESPONSIBLE PERSON
a. REPORT	b. ABSTRACT	c. THIS PAGE			Clifford A. Pugh
UL	UL	UL	SAR	71	19b. TELEPHONE NUMBER *(Include area code)* 303-445-2151

Hydraulic Laboratory Report HL-2004-05

Hydraulic Performance of a Horizontal Flat-Plate Screen

Kathleen H. Frizell
Brent W. Mefford

U.S. Department of the Interior
Bureau of Reclamation
Technical Service Center
Water Resources Research Laboratory
Denver, Colorado

February 2005

Mission Statements

The mission of the Department of the Interior is to protect and provide access to our Nation's natural and cultural heritage and honor our trust responsibilities to Indian Tribes and our commitments to island communities.

The mission of the Bureau of Reclamation is to manage, develop, and protect water and related resources in an environmentally and economically sound manner in the interest of the American public.

Acknowledgments

Mr. Brian Hamilton of Reclamation's Pacific Northwest Region requested this work. Reclamation's Pacific Northwest Region and the Science and Technology Research Program supplied funding. The team formed by members of the National Marine Fisheries Service, Fish and Wildlife Service, and the Oregon Department of Fish and Wildlife provided invaluable guidance to the study.

Dr. Kevin Bestgen and Dr. Daniel Beyers from the Colorado State University Larval Fish Laboratory cultured the bull trout from eggs to the appropriate life stage. Their expertise in handling and performing the biological studies in the Water Resources Research Laboratory (WRRL) provided validity to the biological testing.

Thanks to WRRL technicians Jerry Fitzwater and Billy Baca for data collection assistance. The WRRL shop personnel expertly constructed the model and made changes to the model quickly, often with short notice.

Peer review was provided by Leslie Hanna, Hydraulic Engineer, in the Water Resources Research Laboratory.

Hydraulic Laboratory Reports

The Hydraulic Laboratory Report series is produced by the Bureau of Reclamation's Water Resources Research Laboratory (Mail Code D-8560), PO Box 25007, Denver, Colorado 80225-0007. At the time of publication, this report was also made available online at **http://www.usbr.gov/pmts/hydraulics_lab/pubs/HL/HL-2004-05.pdf**

Disclaimer

Table of Contents

Page

Introduction **1**

Objective **1**

Conclusions **2**

Similitude **4**

Physical Models of the Screen geometries tested **5**

Hydraulic Investigations **7**

Operations 7

Screen Sweeping Velocity Prediction Spreadsheet 8

Instrumentation 9

Sweeping Velocity 10

Diversion Weir Wall 11

Converging Wall Angle 12

Debris Testing 12

Rectangular Horizontal Flat-plate Screen Performance 13

Screen Performance with a Converging Side wall 27

Screen Performance with a Converging Side Wall and a Drop at the Downstream End of the Screen 38

Biological Testing – Flow Description **46**

Future Investigations **49**

Implementation Plan for Horizontal Fish Screen Technology **49**

References **50**

Appendix A **51**

Appendix B **52**

Rectangular Screen Data 52

Converging Side wall with 2.54-ft-wide Bypass Opening 57

Converging Wall with 1-ft-wide Bypass Entrance 65

Figures

Figure *Page*

1 Schematic of the physical fish screen model with the original design and the basic layout of the 15-degree wall convergence 6

2 Overall view of the horizontal screen model showing the flow channel designations and velocity 7

3 ADV probe close-up and instrument setup over screen 10

4 Locations where velocity data were gathered for the rectangular horizontal fish screen 14

Table of Contents—continued

Figures

Figure		*Page*
5	Test 1 with the rectangular screen geometry	15
6	Test 2 looking down onto the downstream end of the rectangular screen	16
7	Top and side view of test 3 with supercritical flow at the upstream end of the screen	17
8	Test 1. Rectangular 6-by-12 ft screen	18
9	Test 2. Rectangular 6-by-12 ft. screen	19
10	Test 3. Rectangular 6-by-12 ft screen	20
11	Test 4. Rectangular 6-by-12 ft screen	21
12	Test 5. Rectangular 6-by-12 ft screen	22
13	Test 6. Rectangular 6-by-12 ft screen	23
14	Test 6. Subcritical flow occurs across the rectangular screen with a jump downstream	24
15	Test 7. Rectangular 6-by-12 ft screen	25
16	Test 8. Rectangular 6-by-12 ft screen	26
17	Test 10. Converging side wall test with Q_c = 6.92 ft^3/s, Q_d/Q_c = 0.58	28
18	Test 13. Test of converging side wall Q_c=15 ft^3/s, Q_d/Q_c = 66 percent	29
19	Locations where velocity data were gathered for the 15° converging wall	30
20	Test 9. Converging wall with 15° angle	31
21	Test 10. Converging channel with 15° angle	32
22	Test 11. Converging walls with 15° angle	33
23	Test 12. Converging wall with 15° angle	34
24	Test 13. Converging wall with 15° angle	35
25	Test 14. Converging wall with 15° angle	36
26	Test 15. Converging wall with 15-degree angle and 2.54-ft-wide bypass opening	37
27	Test 20. Critical flow at the downstream end of the screen with Q_c=4.07 $^3/s$ and Q_d/Q_c= 67%	39
28	Test 18. Critical flow at the downstream end of the screen	39

Table of Contents—continued

Figures

Figure *Page*

29 Test 16 with 15-degree converging side wall to 1-ft wide bypass channel 41

30 Test 17 with 15-degree converging side wall to 1-ft-wide bypass....42

31 Test 18 with 15-degree converging side wall to 1-ft-wide bypass....43

32 Test 19 with 15-degree side wall to 1-ft-wide bypass....44

33 Test 20 with 15-degree converging side wall to 1-ft-wide bypass....45

34 Test 21 with 15-degree side wall with 1-ft-wide bypass....46

35 Bull trout testing with the 15-degree converging wall over the screen....48

36 Control test setup for bull trout testing with clear plastic over the screen and 2 ft/s sweeping velocity....48

37 Control test setup for bull trout testing with clear plastic over the screen and 4 ft/s sweeping velocity....48

Tables

Table *Page*

1 Flow rates tested with the rectangular screen geometry....13

3 Tests conducted with the 15-degree converging side wall to 2.54-ft-wide bypass with a flat, non-perforated bypass extension....27

4 Flow rates tested over the screen with a 1-ft-wide bypass and a drop at the downstream end 38

5 Hydraulic parameters used for the biological testing....48

INTRODUCTION

Reclamation's Pacific Northwest Region has a site where they have proposed using a horizontal flat-plate screen to divert water for irrigation. The site, located on the Powder River near Baker, Oregon, is in a potential bull trout habitat area. The proposed screen is considered experimental under current regulatory agency criteria for fish screen design because no method to automatically clean the screen is provided. In addition, there have been no statistically based biological studies performed on this type of screen. Initial field tests of several small screens have shown that horizontal flat-plate screens exhibit low fouling rates when operated at sweeping-to-approach-flow velocity ratios of greater than about 10:1. The low fouling attribute of the screening concept could reduce screen construction, operation and maintenance costs. Therefore, if the level of fish protection is comparable with accepted fish screening technology, the horizontal fish screen could potentially be used extensively.

The Bureau of Reclamation with the assistance of the Colorado State University Larval Fish Laboratory has conducted hydraulic and biological tests of a horizontal flat-plate fish screen in the Water Resources Research Laboratory. Investigating the hydraulic characteristics of the screen will provide valuable information on how the screen operates and provide limitations on the zones of operation to ensure meeting biological needs. A laboratory-based biological assessment of the screening concept using bull trout will provide a pilot study that evaluates fish behavior and potential damage when exposed to the screen.

This report presents the hydraulic assessment of the performance of the horizontal screen. The report of the biological assessment, "Bull Trout Performance in a Horizontal Flat-Plate Screen", prepared by Drs. Dan Beyers and Kevin Bestgen from the Colorado State University Larval Fish Laboratory, is available separately [1].

OBJECTIVE

The objective is to conduct laboratory hydraulic and biological testing of an experimental horizontal flat-plate fish screen. The screen will be evaluated to determine the effect of the following hydraulic parameters on screen performance:

- Approach and sweeping velocities,
- Depth over screen,
- Bypass flow control issues,
- Flow conditions including eddy zones,
- Diversion to bypass flow ranges,
- Approach channel conditions and,
- Debris.

The hydraulic aspects of the screen performance are discussed in this report. The biological aspects of bull trout passage over the screen are reported separately in a July 2002 report [1]. The draft hydraulic report was completed in June 2001. This final report is being published under this new report series for better distribution of the material and is dated accordingly.

CONCLUSIONS

The hydraulic modeling effort has resulted in a better understanding of how a horizontal flat-plate screen operates. The initial screen design had several very positive aspects that were discovered and other aspects that have been dealt with now that the screen operation is understood. A brief discussion of the final results of the screen testing is presented. The conclusions are general in nature and are given as guidance for future horizontal flat-plate screen designs.

- Uniform approach channel geometry of at least five depths in length upstream from the screen is recommended. A longer screen approach channel produces better flow conditions over the screen. A flat non-porous section upstream from the screen is ideal, as this will prevent a change in flow direction at the upstream edge of the screen.
- Depth is maintained over the screen by the use of a weir that must extend the entire length of the screen in the diversion channel. The diversion weir provides two important features. First, the weir wall ensures the screen will not dewater and maintains a minimum bypass flow. Second, the weir forces a nearly constant flow depth over the entire screen and therefore, a fairly uniform approach velocity field to the screen. Screen baffling is not required to maintain uniform approach velocity across the width and along the length of the screen.
- A flat non-perforated section with a length of at least two flow depths is recommended downstream from the screen section to alleviate possible non-uniformity in the approach flow near the end of the screen.
- Sweeping velocity will gradually decrease downstream along the length of the screen for all flows except those near the design flow.
- Depth will be constant over the screen when operating under the design condition, with the exception of surface waves across the width and length of the screen.
- Any approach velocity may be designed for and will be reasonably well maintained across and down the length of the screen with appropriate approach and bypass channel geometry.
- Head loss through the screen is minimal as expected with small screen approach velocities.

- Sweeping and approach velocities are generally consistent across the width of the screen section whether rectangular or with a converging side wall.
- As the depth increases over the screen the sweeping velocity decreases.
- Recirculation, ponded water, or the presence of a hydraulic jump over the screen increases the screen approach velocity and should be avoided during operation.
- Rectangular screen geometry is only appropriate for smaller diversion to channel flow ratios of about 25 percent or less.
- Debris handling issues were only briefly investigated with the following observations:
    - Higher sweeping velocities produce better debris handling performance.
    - Debris or gravel the size of the screen perforations is likely to become lodged in the screen.
    - Gravel smaller than the screen perforations will pass through the screen or remain suspended in the bypass flow and travel downstream. Gravel larger than the screen perforations will travel over the screen and out through the bypass.
    - Vegetation and algae were not fully tested in the laboratory, but initial tests revealed a tendency for waterlogged vegetation to stick to the screen and other types to pass downstream.
    - A sediment trap located upstream from the screen would be a wise design feature.
    - Dislodging gravel wedged in the screen perforations will be difficult.
    - Cleaning the area beneath the screen will be a difficult maintenance issue.
- Better overall screen performance exists with operation in the supercritical flow range.
- A change in flow condition over the screen, i.e. from supercritical to subcritical flow, is unacceptable.
- Downstream control of the bypass flow is not recommended, as it will likely produce an undesirable flow condition on the downstream end of the screen.
- A drop below the elevation of the screen structure is recommended, if possible, at a field installation. A solid or non-perforated section should be placed at the downstream end of the

screen before entering the drop to prevent excessive approach velocities or reverse flow at the bypass opening when operating with a drop at the end of the screen. The screen bypass discharge and bypass width will control the critical flow depth and control the sweeping velocity at the end of the screen. A drop below the elevation of the screen will generally produce increasing sweeping velocity into the bypass.

- NMFS screen exposure time criteria of 60 seconds would allow a very long screen with a reasonable sweeping velocity of 1 to 3 ft/s. Screen exposure time may be less critical depending upon the findings of the bull trout testing.
- For a given channel discharge and bypass flow, sweeping velocity and depth may be attained several ways. If larger flow depths are desired then a narrower channel is needed. However, larger flow depths decrease sweeping velocities and increase approach velocities. The best compromise that will attain both the highest sweeping velocity and most depth would be to optimize the screen geometry to produce a high length to width ratio.

A simple spreadsheet was developed in Microsoft Excel to help narrow down the range of operation in the model. This spreadsheet will allow a designer to hone in on a screen geometry option prior to making the final design computations using a backwater computation or software program.

These observations of the hydraulic performance of the screen should be interpreted with the results of the bull trout testing program. Studying both aspects of the screen performance will, hopefully, determine if a horizontal flat-plate screen is a viable alternative for water diversions where ESA listed species are located.

SIMILITUDE

The model testing was performed using Froude similitude where the geometric and kinematic parameters for a 1:3 scale are as follows:

$L_r = L_p/L_m = 3$
$A_r = (L_r)^2 = 9$
$V_r = (L_r)^{1/2} = 1.732$
$Q_r = (L_r)^{5/2} = 15.59$

Where: L_p = prototype characteristic length
L_m = model characteristic length
L_r = length ratio
A_r = area ratio
V_r = velocity ratio
Q_r = discharge ratio

The screen hole-size in the model is the same as the screen hole-size in the prototype with 3/32 in diameter holes and a 37 percent open area on the perforated plate. The Reynolds number was high enough in the model to eliminate scale effects; therefore, the model and prototype screen openings can be the same [2].

Various Froude model scales were used for the hydraulic testing. By using different model scales a larger range of flow conditions could be tested. Model results may be scaled to the prototype by using the above ratios or other ratios as needed to produce the desired prototype range of flows, velocities, or depths.

The biological investigations were performed as if the model were full field scale. The model was assumed to be of an actual prototype or field size for the biological testing. As a result, no scaling of discharge, velocities or depths is needed to interpret the biological results.

PHYSICAL MODELS OF THE SCREEN GEOMETRIES TESTED

A model of a water diversion containing a horizontal flat-plate screen was constructed in the Water Resources Research Laboratory (WRRL) in Denver, Colorado, figure 1. The model has a 6 ft wide rectangular channel approximately 40 ft long. A 10:1 (H:V) ramp slopes up to a 4-ft-long non-porous flat section, then to the screen about midway down the channel. The 6-ft-wide by 12-ft-long screen is supported 1 ft above the channel floor. The screen is composed of nine, 2-ft-wide by 4-ft-long punch plate screen panels supported on a metal frame. The screen has 3/32 in diameter holes on 3/16 in stagger. Flow passes from beneath the screen through a 12 ft long by 1 ft high rectangular opening in one side wall to the diversion channel. A 1-ft-high weir was placed across the diversion channel to ensure the screen cannot totally dewater channel flow. Slats were used in the downstream diversion channel to control diversion flow and depth over the weir. The downstream bypass channel consisted of a 2-ft-flat section immediately downstream of the screen leading to a 10:1 ramp down to the floor of the box. A flap gate was located downstream in the bypass channel to provide backwater or a control point, as needed.

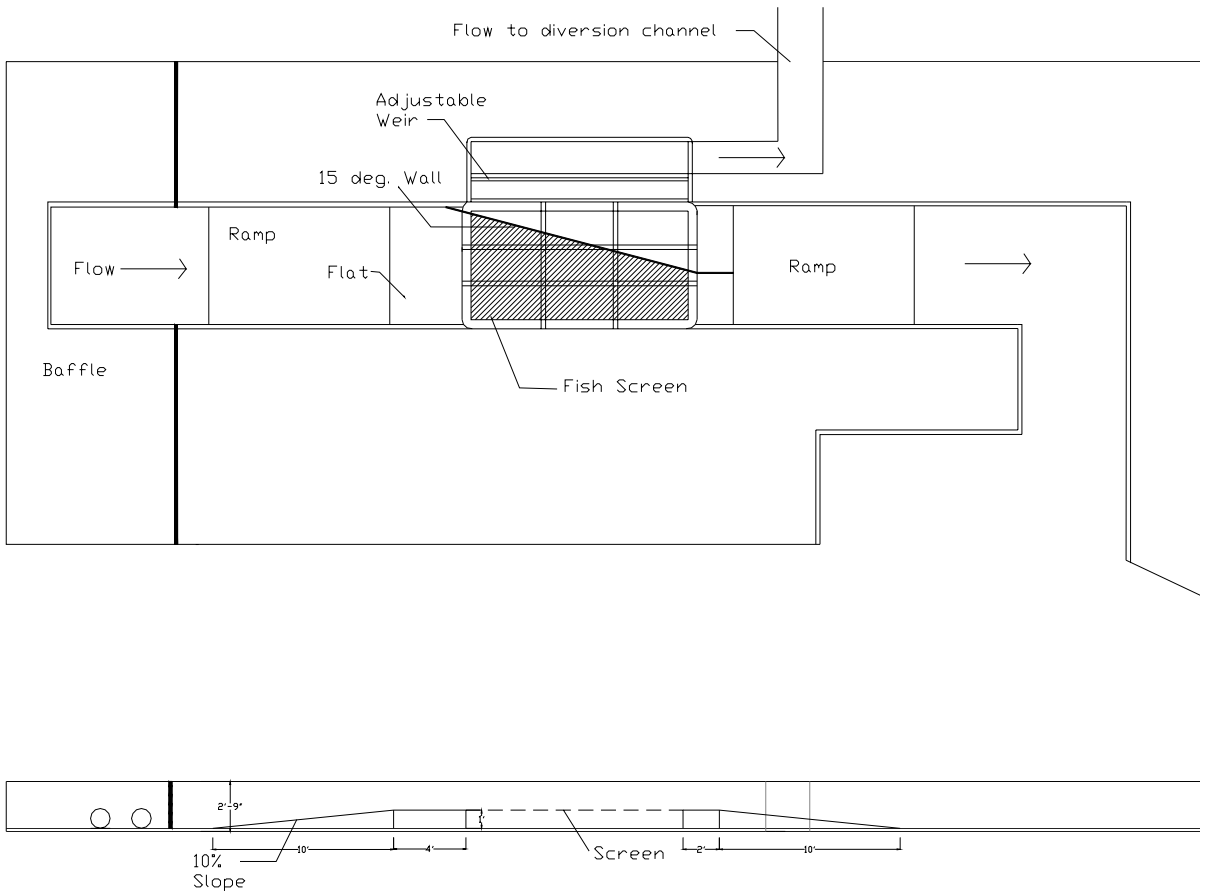

Figure 1.—Schematic of the physical fish screen model with the original design and the basic layout of the 15-degree wall convergence.

Flow was supplied to the model either using the permanent laboratory Venturi measurement system or a portable pump with an acoustic strap-on pipe flow meter for measurement. The bypass flow was measured using a contracted rectangular sharp-crested weir mounted in a box at the end of the bypass channel. The head on the weir was measured using a pressure cell in a stilling well and converted to flow using a continuous flow meter that updated and constantly displayed the flow rate. This allowed accurate setting of the flow volumes between the diversion and bypass flows.

A large compressor and heat exchanger was installed in the WRRL water storage channel to cool the water temperature to an acceptable range for the bull trout testing.

Initial model testing was conducted with a rectangular screen. The next tests were conducted with a converging wall on the left side. A portion of the screen was omitted and covered with a 15-degree sloping wall that began about 1 ft upstream from the screen, converged through the screen area, and continued straight through the flat section downstream from the screen producing a 2.54-ft-wide bypass opening. After completing testing on this geometry, the flat section in the

bypass channel was extended an additional 2 ft to make the bypass section 4 ft long before entering the downstream ramp.

Final testing was conducted with the model modified to produce a 1 ft wide bypass with a 15-degree wall producing a 4.22-ft-wide upstream channel width. The upstream channel width of 4.22 ft extended upstream to the beginning of the ramp to provide good approach conditions. The downstream flat section was removed to produce a drop at the downstream end of the screen. The gate in the downstream bypass channel was still available to provide control as necessary.

HYDRAULIC INVESTIGATIONS

Hydraulic investigations of the flow field near the screen were conducted for three screen and channel geometries. First, a rectangular screen with a constant width channel and a full width downstream bypass channel was tested. Second, a triangular screen with a converging wall from the same upstream width leading to a narrowed downstream bypass channel was tested. The third configuration consisted of a converging side wall from a narrower upstream channel leading to a 1 ft wide bypass channel. This configuration was tested using a Froude scale of 2:1 to provide a comparison to existing vertical screen and bypass technology. The model was operated over a range of diversion flow to channel flow ratios and flow depths. Tests were also conducted with and without downstream control in the bypass channel. For each flow tested three-dimensional point velocity measurements were measured three inches above the screen. These data were used to evaluate flow field uniformity, screen approach velocity, and screen sweeping velocity. Debris testing was also conducted to determine the self-cleaning characteristics of the screen. Testing covered sweeping to approach flow velocity ratios from 5:1 to about 30:1. The flow range tested included sweeping velocities in both the subcritical and supercritical range.

Operations

The channel discharge, Qc, approaches the screen with a 10:1 ramp and a 4-ft-long flat section leading up to the screen. The screen is mounted on a rack 1 ft off the floor of the model with the downstream end underneath closed off and the left side of the underneath area open for the diversion flow, Q_d. The bypass flow, Q_b, continues on over the screen and out to a laboratory return channel. These flow areas are shown on figure 2. Control of the diversion and bypass flows, for a given incoming channel flow, determines the flow ratios. A weir is set in the diversion channel along the entire length of the screen preventing the screen from dewatering either during operation or during shutdown of diversion operations.

There are innumerable ways to operate the screen based upon the importance of various parameters to the operator, owner, or agency. However, the range of acceptable operation of the screen is quite limited for a given diversion flow. The weir wall on the diversion must be set to keep the desired minimum water surface over the screen for the design diversion flow. The velocity of approach and the

area of the screen exposed determine the diversion flow amount. As the depth over the screen increases the sweeping velocity decreases. Depth and velocity are nearly uniform across the width of the screen.

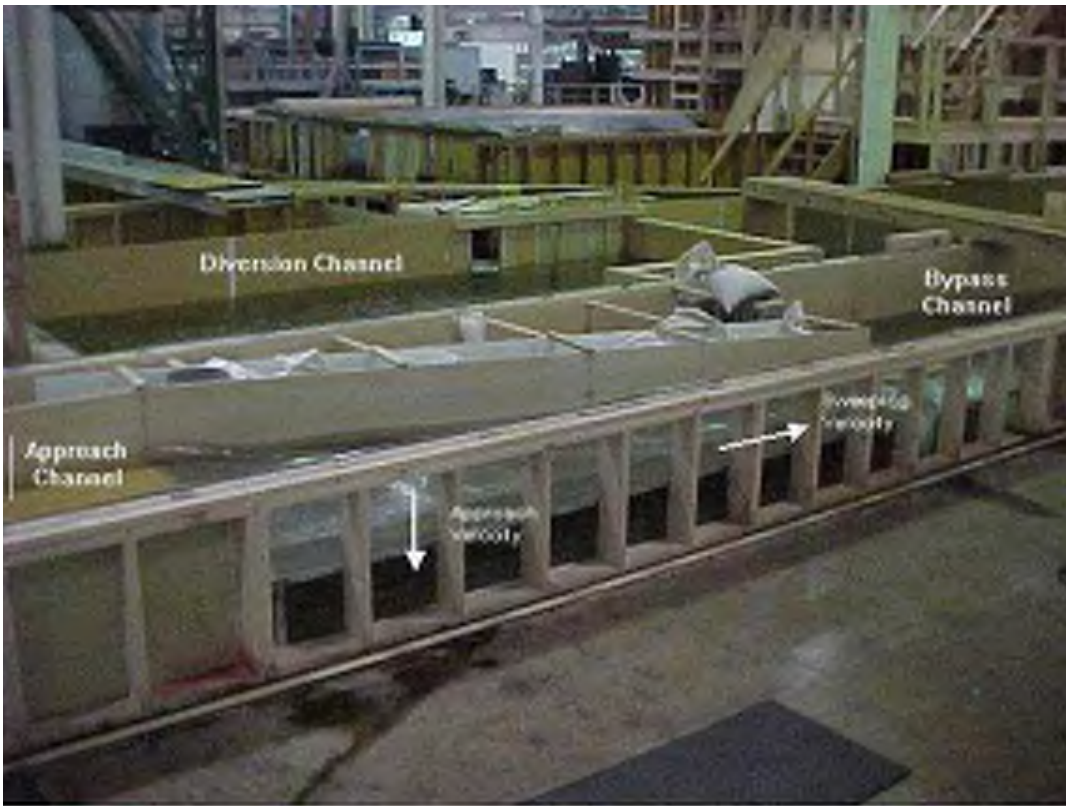

Figure 2.—Overall view of the horizontal screen model showing the flow channel designations and velocity orientations.

Screen Sweeping Velocity Prediction Spreadsheet

A spreadsheet was developed to help define parameters for design and testing of the horizontal screen. The spreadsheet computes discharge ratios and predicts sweeping velocity based upon variable screen dimensions and depths. The spreadsheet model assumes uniform approach velocity to the screen and a constant flow depth over the screen. It is also a one-dimensional simulation that assumes uniform flow across the width of the screen regardless of wall convergence. The program also does not discern where the control is for the depth over the screen. Control of the flow downstream of the bypass that causes backwater onto the screen is not characterized in the program. Also, a drop at the downstream end of the bypass producing critical depth and flow control is not modeled. With critical depth at the bypass entrance, the physical model shows that the bypass discharge is controlled by the depth at the end of the screen and not by just the channel discharge, the approach velocity, and the area of the screen, as computed by the program.

Originally, the program was developed for subcritical flow conditions. As testing continued, it became apparent that higher sweeping velocities were desirable. Therefore, the supercritical flow range was included in the acceptable range of flow.

Several conditions were determined to limit the range of operation for the screen. A minimum sweeping velocity, and a maximum change in sweeping velocity per ft of screen may be entered. A change in flow regime, i.e. from supercritical to subcritical, and violation of parameters entered is checked by the spreadsheet. When any of these conditions are violated, the screen would be operating in an unacceptable range.

The U.S. Geological Service Conte Anadromous Fish Laboratory has performed tests with accelerating flow over weirs that states that a velocity change of 1 ft/s per ft of distance will cause avoidance [3]. Agencies have expressed an interest in keeping the sweeping velocity as high as possible from a debris and fish passage point of view. The minimum acceptable sweeping velocity and percent acceleration or deceleration per foot of screen may be changed as necessary.

Irrigators will know the channel discharge or river discharge and how much water they would like diverted. Therefore, the spreadsheet evolved into entering the channel and diversion discharges, the flow depth and screen geometry and letting the spreadsheet compute the sweeping velocity, velocity of approach, and acceptable range of operation. The pivot table in the spreadsheet shows the acceptable ranges of operation for the geometry and hydraulic parameters entered. The desired design flow ratio or velocities may not be obtainable with the specified geometry. The geometry should then be modified until acceptable flow conditions occur. The desired and generally fairly small range of diversion to channel flow ratio is shaded for a range of approach velocities.

In addition to using the spreadsheet, with caution, to narrow down the acceptable screen geometry, a backwater computation must be performed using a program such as HEC-RAS. This will ensure that the downstream influence is appropriately accounted for in the design.

The spreadsheet is given in Appendix A with the equations shown in the cells should a designer wish to replicate the computations.

Instrumentation

A SonTek 19 MHz Micro Acoustic Doppler Velocimeter (ADV) was used to gather three-dimensional velocity data over the horizontal screen. The probe has 3 “arms” that receive the signal from the control volume located about 5 cm from the transmitter. The control volume is only 0.09 cm. The ADV measures all three velocity components simultaneously, providing a complete description of the flow field. Figure 3 shows the ADV mounted on a carriage with a motorized screw mechanism allowing travel up and down. The mount could also be moved

along the carriage to traverse both the length and width of the approach channel and the entire screen area.

Data were gathered at a rate of 10 Hz with 600 samples gathered at each data location and stored onto a PC. The data were input into the WinAdv software program that allowed filtering and reduction of the data and exporting into a format acceptable for spreadsheet use.

Initially, seeding was necessary to overcome the acoustic reflection off the screen surface. Eventually, the screen surface was sprayed with a very thin rubbery substance (Sure Grip) that minimized the reflection from the screen and increased the data quality without seeding.

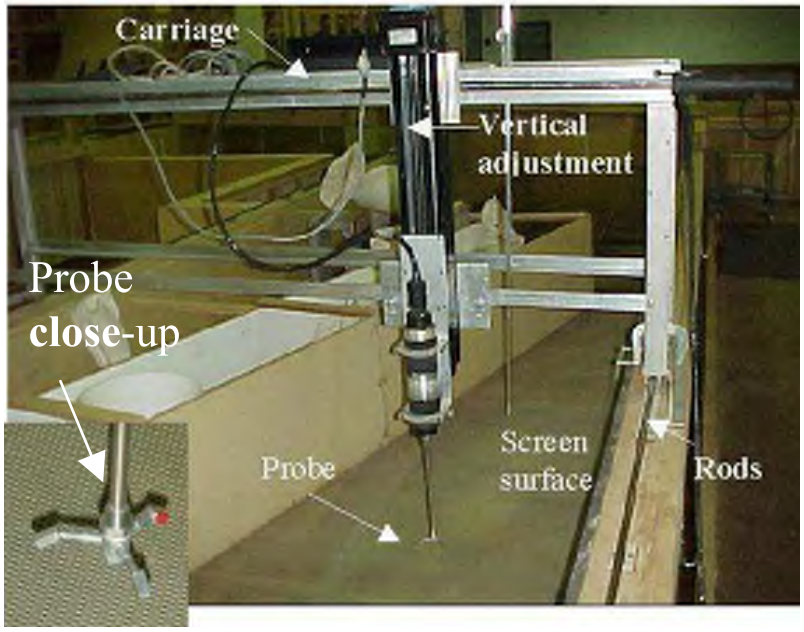

Figure 3.—ADV probe close-up and instrument setup over screen.

Data were collected 3 inches above the screen to correspond to the standard measurement distance in the prototype. Velocity measurements were obtained at grid points that were established for the screen geometry tested.

Flow depths were also gathered from a point gage mounted on the traversing system.

Sweeping Velocity

Investigation of the sweeping velocity provided very interesting results. Once the screen operation was determined, it was realized that sweeping velocity would typically decrease as a function of screen length. This occurs because with a constant inflow and depth, the volume of flow, thus velocity, passing over the screen decreases as the diversion flow leaves through the screen. The sweeping

velocity can be maintained by constructing a converging side wall, but for fairly limited operating range. Because setting the hydraulic model was quite tedious, the previously mentioned spreadsheet program that defines sweeping velocity conditions for any geometry was utilized and aided in defining the model test range.

Continuity of flow dictates that the sweeping velocity will decrease if the flow decreases and the depth remain constant for a given area [4]. This is seen by the equation: Q=VA where the area, A, is the width times the depth. Therefore, a converging wall will help to maintain sweeping velocity by decreasing the area at a rate that will offset the flow loss. Balancing the area with the flow withdrawn is the key to maintaining sweeping velocity.

It seems reasonable to define the bypass channel as the channel at the downstream end of the screen where the flow passing over the screen exits back to the river. Using this definition, unless there is a recirculation zone or eddy over the downstream end of the screen, it would usually be possible to maintain or have velocities increase into the bypass channel at the end of the screen to provide attraction flow for downstream migrants.

Diversion Weir Wall

Operation of the screen model soon showed the importance of the diversion weir wall. The diversion weir wall was set at the elevation of the screen with capability to adjust the level. Baffles were initially included in the model, but the effectiveness of the weir wall in controlling the depth and providing uniform approach velocities soon made it clear that the baffles were not needed. The elevation of the diversion wall will set the minimum depth on the screen for any given diversion flow. A downstream diversion gate may then be used to further increase depth over the diversion weir wall and the screen, if deemed necessary. The flow depth affects the sweeping velocity and higher flow depths for the same diversion rate produce lower sweeping velocities. The elevation of the diversion wall will prevent the screen from dewatering until the channel flow is stopped.

Depths were measured over the screen and in the basin formed by the weir wall leading to the diversion channel. There is very little head loss through the screen and through the opening to the weir wall. The head loss is a function of the approach velocity and since this is very small there is only a very slight difference in depth between that over the weir wall and over the screen.

The diversion weir wall is a valuable asset to the horizontal screen design, providing uniform depth and approach velocities over the screen and aiding in the prevention of surface irregularities. This may be seen in the screen approach velocity data shown later for each screen geometry tested.

Converging Wall Angle

The side wall angle improves the design of the horizontal screen by reducing the screen area as the channel flow is diverted, thus maintaining the sweeping velocity. The angle of the side wall; however, can produce some undesirable effects to water surface over the screen. Any angle will produce some buildup of flow depth along the wall that could lead to increased approach velocities. Given a severe enough angle this could be a problem. Also, cross-waves will form caused by the contraction. The height of the waves and the pattern is dependant upon the wall angle, Froude number, and depth [4]. The contraction or side wall angle may be designed to minimize flow disturbances. With this in mind, the maximum convergence angle should probably be 15 degrees. With high sweeping velocities, this angle should probably be minimized. The possible perturbations from the converging side wall will be minimized with a longer screen and smaller convergence angle.

Debris Testing

Debris is a big concern with the horizontal screen because in this experimental stage there is no plan to use a mechanical cleaning device. Eliminating the cleaning device makes the screen economical and more likely to be used, but riskier from a biological standpoint. Published vertical screen criteria require a minimum sweeping velocity of two times the approach velocity. Higher sweeping velocities are expected to produce optimal cleaning characteristics. Debris can be leaves, sand, fine sediment, evergreen needles, gravel, algae or trash.

Rigorous debris testing was not performed in this study. Various types of plants, and sand or gravel, were introduced upstream from both the rectangular and converging screen geometries and observed while traveling over the screen. Amounts passing through or bypassing the screen were not measured, but these tests did provide general information about the self-cleaning capability of the screen. Good self-cleaning characteristics were observed for various flow rates when the sand or gravel size exceeded or was smaller than the screen opening size. Particles larger than the screen hole-size would continue over the screen and into the bypass. Particles smaller than the screen hole-size would pass through the holes or remain suspended and be carried downstream. If smaller particles pass through the screen, a maintenance issue could develop if large amounts accumulate under the screen.

To investigate a predicted worse case, a test was performed with the majority of the test material graded to be about the size of the 3/32 or 0.0.0938 in screen openings. The material used was graded between a #8 and #4 sieve, or larger than very fine gravel (0.0925 in) and smaller than fine gravel (0.1811 in). The material was trickled into the channel on the flat section upstream from the screen geometry with a 15 degree wall convergence and a channel flow rate of 9.0 ft^3/s, $Q_d/Q_c = 0.82$ and subcritical flow conditions over the screen. A sweeping velocity, $V_s = 2.7$ ft/s, at the upstream end and about 1 ft/s at the downstream end

of the screen produced ratios of sweeping to approach velocity ratios of 18:1 and 6:1 at the upstream and downstream portions of the screen, respectively. The approach velocity averaged about 0.15 ft/s over the screen with a depth of 7 in. In addition, the bypass flow was being controlled by the weir gate downstream from the screen that caused a recirculation back up onto the end of the screen and a potentially poor flow condition for self-cleaning, figure 23. The fine gravel material wedged in the openings of the screen at the upstream end of the screen area and at the downstream end due to the backwater present on the screen. Particles lodged into the screen openings were difficult to remove. Sand and debris will clearly be less of an issue with the highest possible sweeping velocities over the screen.

Rectangular Horizontal Flat-plate Screen Performance

The initial hydraulic investigations were conducted with the full 6- by 12-ft rectangular screen. Data were gathered at the centerline of each of the three 2-ft by 4-ft screen sections throughout the length of the 12-ft-long screen section, figure 4. In the final tests, data were also gathered near the walls and further upstream and downstream from the screen to investigate flow conditions approaching and leaving the screen. Depth data were also gathered with a point gage along the length of the screen. Depth measurements were taken in the basin created by the weir wall to look at head loss through the screen to the diversion channel. The flow rates and diversion to channel flow ratios tested over the rectangular screen are shown in table 1.

Table 1.—Flow rates tested with the rectangular screen geometry

Test	Channel Discharge, Q_c (ft^3/s)	Diversion Discharge, Q_d (ft^3/s)	Bypass Discharge, Q_b (ft^3/s)	Q_d/Q_c (percent)	Theoretical Approach Velocity (ft/s)	Depth (ft)
1	10.04	8.30	1.74	83	0.115	0.5
2	11.76	8.25	3.51	70	0.115	0.5
3	15.25	8.35	6.90	55	0.116	0.5
4	10.01	5.78	4.23	58	0.115	0.67
5	10.00	3.92	6.08	40	0.054	0.5
6	10.01	2.08	7.93	21	0.03	0.583
7	17.36	14.29	3.07	82	0.2	0.5
8	20.4	14.35	6.05	70	0.2	0.67

Data are plotted on contour maps with the sweeping velocity forming the contours. The edges of the contours are the most outside locations where data were taken. The labels at the nodes show the approach velocity at that point, with negative values indicating flow into the screen. The accompanying tables show the actual distance along the screen that measurements were taken. At each

section, the sweeping velocities in the tables are averaged across the width and a Froude number computed to show the flow conditions that the screen is experiencing. Raw velocity data are shown in the appendix for test series 1-8.

Traditional screen flow conditions were initially investigated by operating the screen under specific sweeping to approach velocity ratios of 5, 10 and 20:1. The sweeping velocity ratios were computed at the downstream end of the screen using the bypass discharge, the screen width of 6 ft, and the depth over the screen. These flow conditions were tests 1, 2 and 3 with channel flows of 10, 11.76, and 15.25 ft^3/s with Q_d/Q_c=0.83, 0.70, and 0.55, respectively. The diversion flow, approach velocity, and depth were kept the same at 8.25 ft^3/s and 0.115 ft/s, and 0.5 ft, respectively. In all three cases, backwater was present on the downstream end of the screen under these flow divisions, figures 5, 6, and 7.

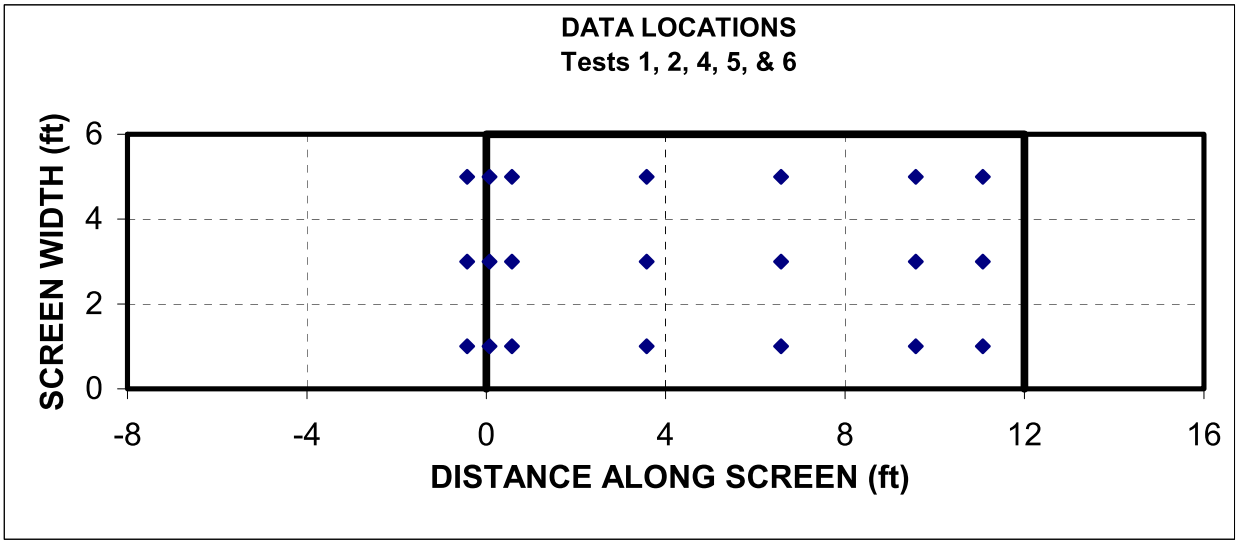

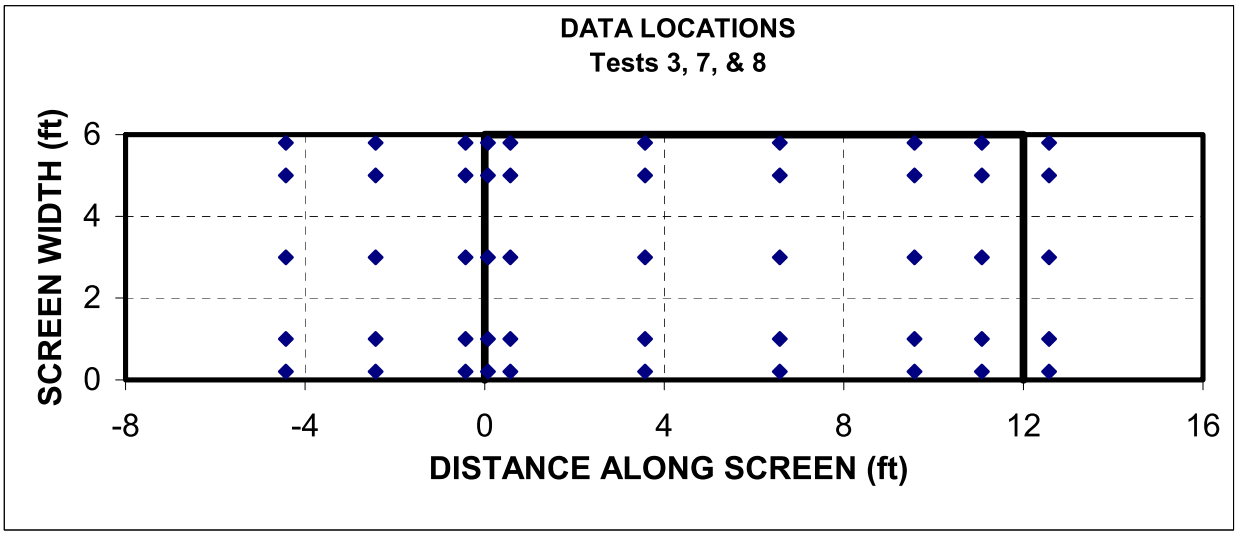

Figure 4.—Locations where velocity data were gathered for the rectangular horizontal fish screen. The 6 by 12 ft screen area is highlighted with the screen beginning at 0 ft. Data were gathered primarily along screen panel centerlines. For tests 3, 7, and 8, data were also gathered upstream from the screen and along the walls.

The first series shows a plan and side view of Test 1 with $Q_d/Q_c = 0.83$ and downstream control of the bypass flow, figure 5. Under this operating condition, recirculating eddies form over the downstream end of the screen caused pooled flow and an increase in the approach velocity above 0.2 ft/s. Figure 8 gives the velocity and Froude number data for this flow condition. The flow is subcritical throughout but would not be an acceptable operating condition with the eddy over the downstream end of the screen. Tests 2 and 3 are similar with the flow condition changing from subcritical to supercritical in test 3.

These tests showed higher sweeping velocities for increasing channel discharge and decreasing diversion ratios for the same diversion discharge and depth, figures 8, 9, and 10. The screen area is too large for high diversion ratios, and the sweeping velocities decreased down the length of the screen.

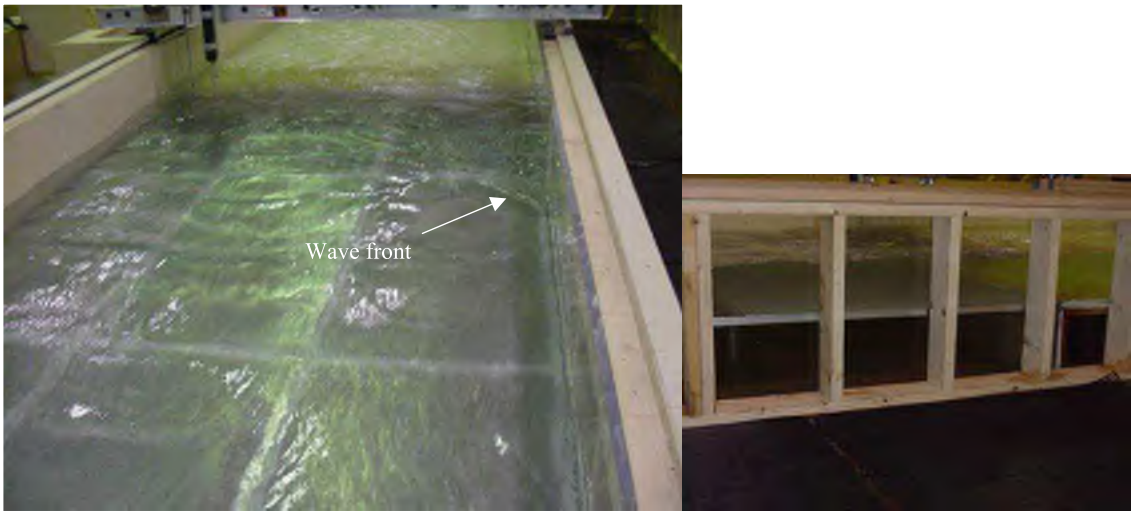

Figure 5.—Test 1 with the rectangular screen geometry, $Q_c = 10$ ft^3/s, and $Q_d/Q_c = 0.83$ and downstream control of the bypass. The flow over the screen is subcritical and downstream control is causing a recirculation pattern over the downstream portion of the screen. The wavy, higher water surface indicates the location of the recirculation. The velocity of approach increases above 0.2 ft/s in this area because of the ponded flow. This would be an unacceptable flow condition.

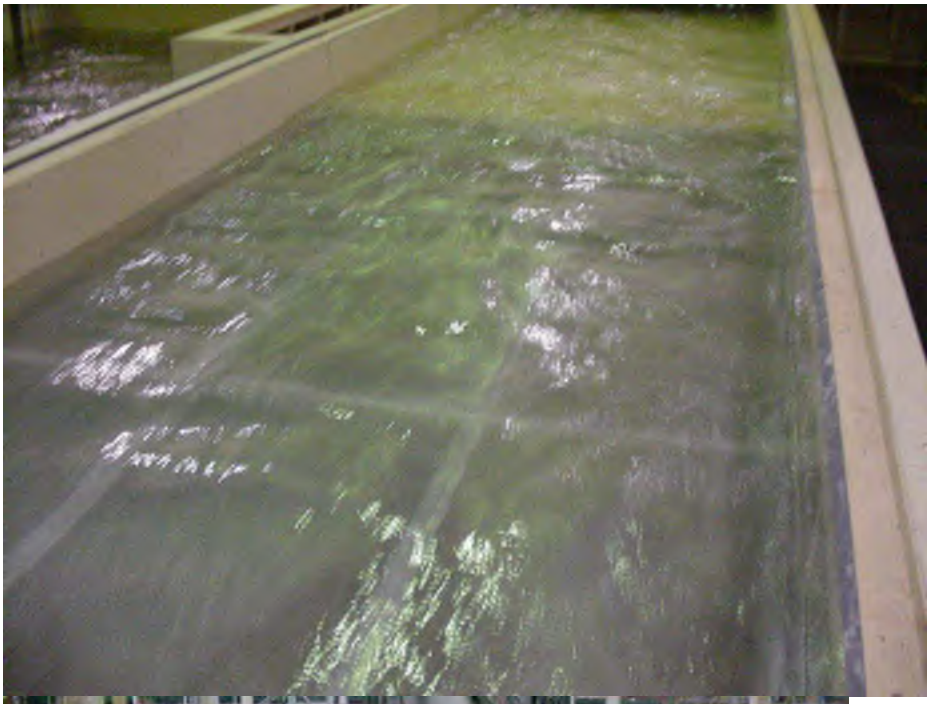

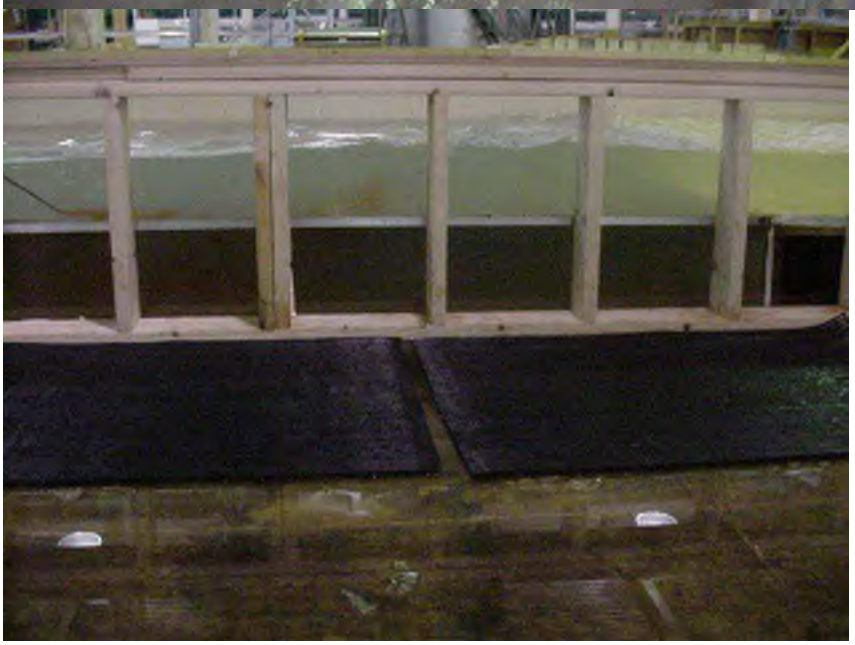

Figure 6.—Test 2 looking down onto the downstream end of the rectangular screen. Subcritical flow over the screen with Q_d/Q_c=0.70 and V_a= 0.115 ft/s. The upstream V_s/V_a = 34:1, and the downstream V_s/V_a =10:1 with the channel discharge, depth, and screen width used to compute the sweeping velocity. Compare to test 1 and test 3 with same approach velocity, depth and V_s/V_a=5 and 20 to 1.

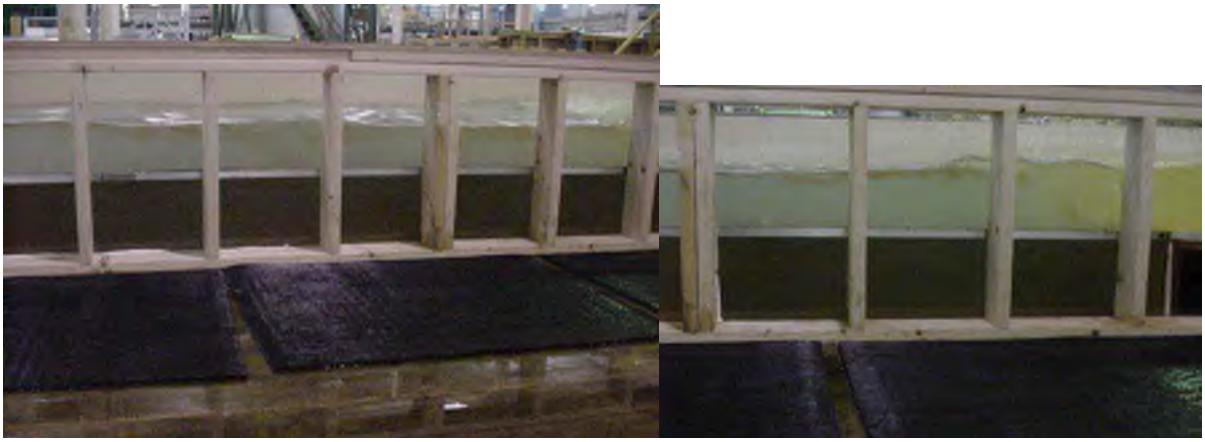

Figure 7.—Top and side views of test 3 with supercritical flow at the upstream end of the screen transitioning to subcritical with a jump over the downstream end of the screen. Q_d/Q_c=0.55 and V_a= 0.115 ft/s. The upstream V_s/V_a = 44:1, and the downstream V_s/V_a =20:1, with the channel discharge, depth, and screen width used to compute the sweeping velocity. Compare to test 1 and test 2 with same approach velocity, depth, and V_s/V_a=5 and 10 to 1.

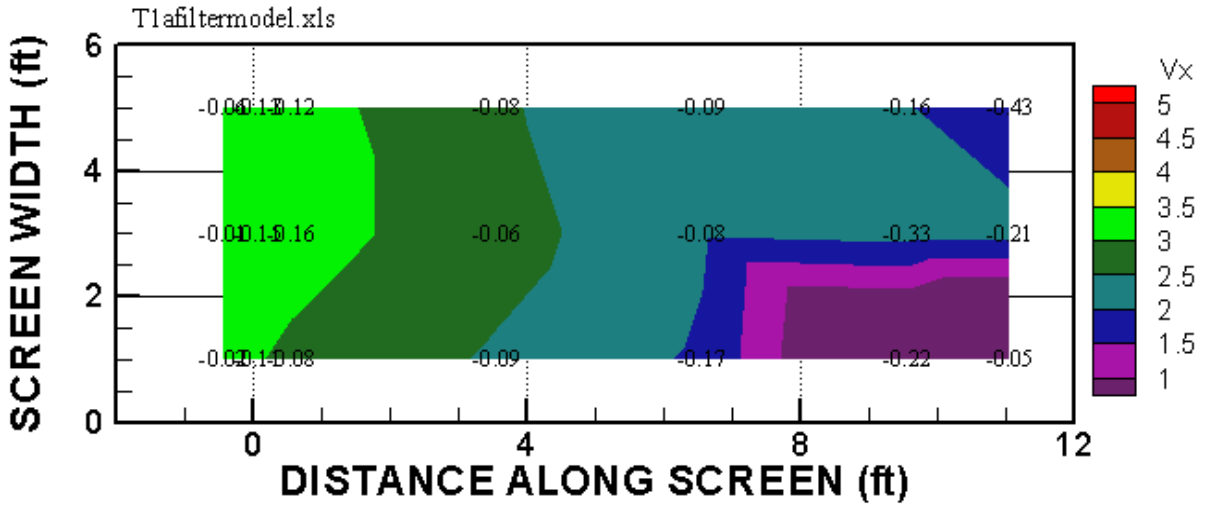

Qc=10.04 ft^3/s, Qb=1.74 ft^3/s, Qd=8.30 ft^3/s		
Depth = 0.5' or 6"		
Screen Distance (ft)	Average Sweeping Velocity Vs (ft/s)	Average Froude No. based on Vs
-0.4271	3.30	0.830
0.0729	3.113	0.776
0.5729	3.102	0.773
3.5729	2.569	0.640
6.5729	2.001	0.499
9.5729	1.241	0.393
11.0729	0.846	0.428

Figure 8.—Test 1. Rectangular 6-by-12 ft screen. Channel discharge, Q_c=10.04 ft^3/s, diversion discharge, Q_d=8.30 ft^3/s, bypass discharge, Q_b=1.74 ft^3/s. Diversion ratio, Q_d/Q_c = 0.83. Depth over screen=0.5 ft. Contours represent the sweeping velocity and indicate a wave front with some recirculating flow over the downstream right corner of the screen. Labels are the screen approach velocity values which increase under the influence of the pooled water over the screen. The theoretical average approach velocity of 0.115 ft/s produces 27:1 and 7:1 for sweeping to approach velocity ratios for the upstream and downstream portions of the screen, respectively. This screen flow condition is operating under the subcritical flow regime.

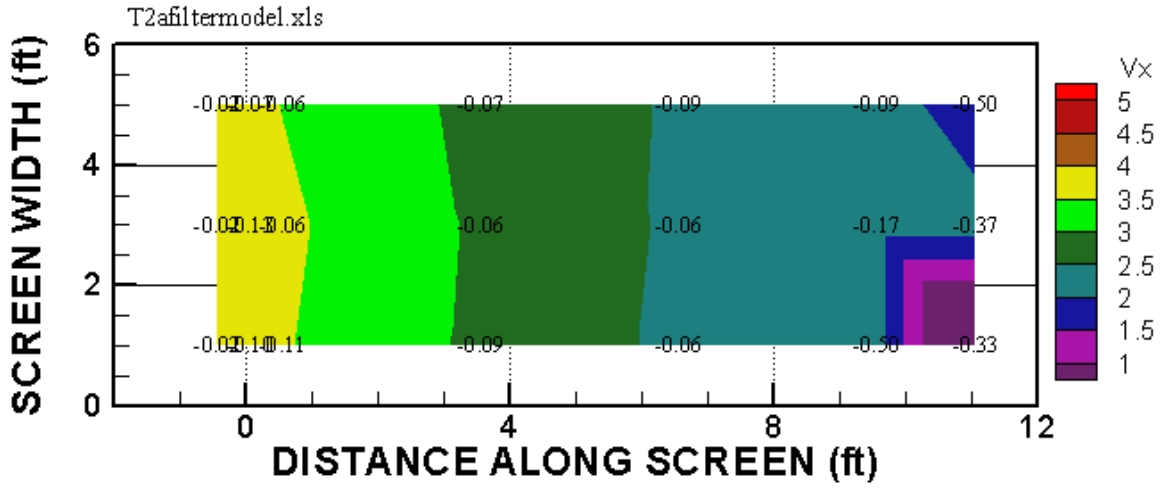

Qc=11.76 ft^3/s, Qb=3.51 ft^3/s, Qd=8.25 ft^3/s		
Depth = 0.5' or 6"		
Screen Distance (ft)	Average Sweeping Velocity Vs (ft/s)	Average Froude No. based on Vs
-0.4271	3.774	0.940
0.0729	3.629	0.904
0.5729	3.536	0.881
3.5729	2.895	0.721
6.5729	2.421	0.603
9.5729	2.272	0.566
11.0729	1.149	0.357

Figure 9.—Test 2. Rectangular 6-by-12 ft screen. Channel discharge, Q_c=11.76 ft^3/s, diversion discharge, Q_d=8.25 ft^3/s, bypass discharge, Q_b=3.51 ft^3/s. Diversion ratio, Q_d/Q_c = 0.7. Depth over screen=0.5 ft. Contours represent the sweeping velocity and indicate a wave front with some re-circulating flow over the downstream right corner of the screen. The screen approach velocity values increase under the influence of the pooled water over the screen. The theoretical average approach velocity of 0.115 ft/s produces 33:1 and 10:1 for sweeping to approach velocity ratios for the upstream and downstream portions of the screen, respectively. This screen flow condition is operating under the subcritical flow regime.

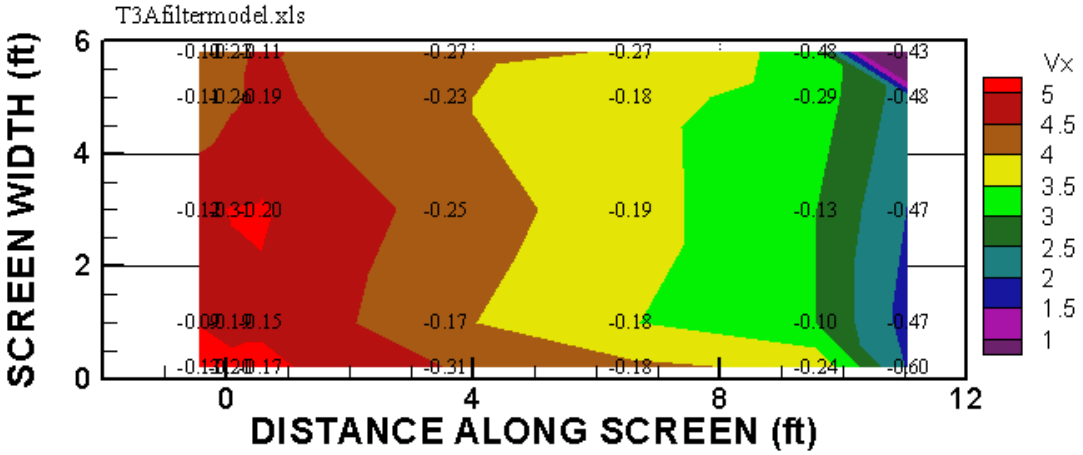

Qc=15.25 ft^3/s, Qb=6.90 ft^3/s, Qd=8.35 ft^3/s		
Depth = 0.5' or 6"		
Screen Distance (ft)	Average Sweeping Velocity Vs (ft/s)	Average Froude No. based on Vs
-0.4271	4.667	1.163
0.0729	4.767	1.188
0.5729	4.847	1.208
3.5729	4.211	1.050
6.5729	3.795	0.946
9.5729	3.293	0.821
11.0729	1.283	0.473

Figure 10.—Test 3. Rectangular 6-by-12 ft screen. Channel discharge, Q_c=15.25 ft^3/s, diversion discharge, Q_d=8.35 ft^3/s, bypass discharge, Q_b=6.90 ft^3/s. Diversion ratio, Q_d/Q_c = 0.55. Depth over screen=0.5 ft. Contours represent the sweeping velocity and indicate a hydraulic jump over the downstream end of the screen. The screen approach velocity values increase under the influence of the higher water surface and slower velocities associated with the jump. The theoretical average approach velocity of 0.116 ft/s produces 40:1 and 11:1 for sweeping to approach velocity ratios for the upstream and downstream portions of the screen, respectively. The flow was supercritical on the upstream portion of the screen and subcritical downstream of the jump.

The next series tested the same channel discharge with varying diversion flows, thus attempting to define the practical range of flow conditions possible with rectangular screen geometry while keeping one variable constant.

The next tests, 4, 5, and 6, were conducted with Q_d/Q_c =0.58 and 0.4 and 0.21, respectively, with the channel discharge constant and the diversion flow decreasing. The sweeping velocity contours are shown on figures 11, 12, and 13. Figure 14 shows a plan and side view of the rectangular screen for test 6 operating under Q_d/Q_c = 0.21. The diversion flow is only a small portion of the channel flow. The flow is subcritical across the screen and a jump occurs downstream

from the screen. The diversion flow is returning back up through the downstream portion of the screen as shown on figure 13 with a positive approach flow at the downstream end of the screen. Flow comes back up through the screen to provide a mass balance of the flow. This flow condition may not necessarily be a poor flow condition as there is no recirculation on the screen. This test series indicated that smaller diversion ratios are better suited for rectangular screens.

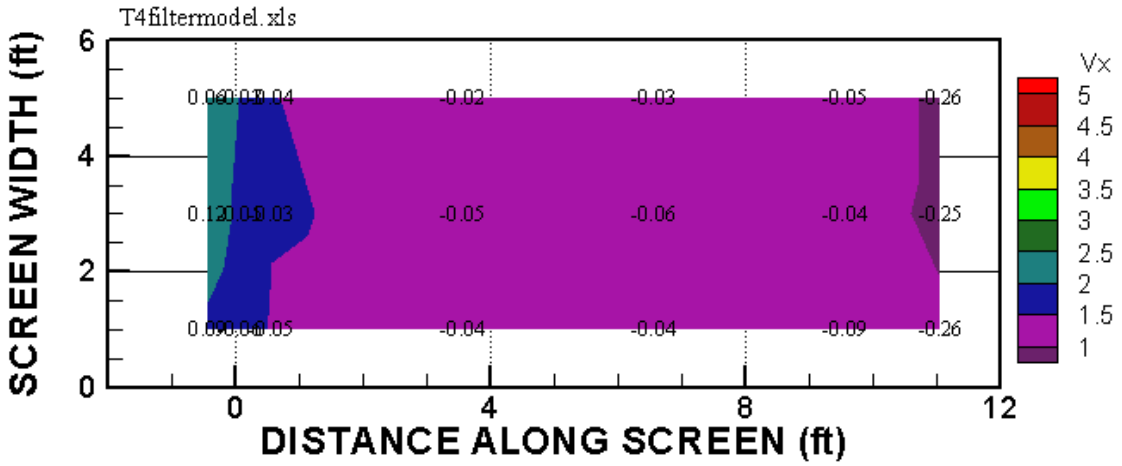

Qc=10.01 ft^3/s, Qb=4.23 ft^3/s, Qd=5.78 ft^3/s		
Depth = 0.667' or 8"		
Screen Distance (ft)	Average Sweeping Velocity Vs (ft/s)	Average Froude No. based on Vs
-0.4271	2.092	0.451
0.0729	1.914	0.413
0.5729	1.497	0.323
3.5729	1.308	0.282
6.5729	1.265	0.273
9.5729	1.185	0.256
11.0729	0.977	0.211

Figure 11.—Test 4. Rectangular 6-by-12 ft screen. Channel discharge, Q_c=10.01 ft^3/s, diversion discharge, Q_d=5.78 ft^3/s, bypass discharge, Q_b=4.23 ft^3/s. Diversion ratio, Q_d/Q_c = 0.58. Depth over screen=0.67 ft. Contours represent the sweeping velocity and indicate a wave front with some re-circulating flow over the downstream right corner of the screen. The screen approach velocity values increase under the influence of the pooled water over the screen. The theoretical average approach velocity of 0.115 ft/s produces 33:1 and 10:1 for sweeping to approach velocity ratios for the upstream and downstream portions of the screen, respectively. This screen flow condition is operating under the subcritical flow regime.

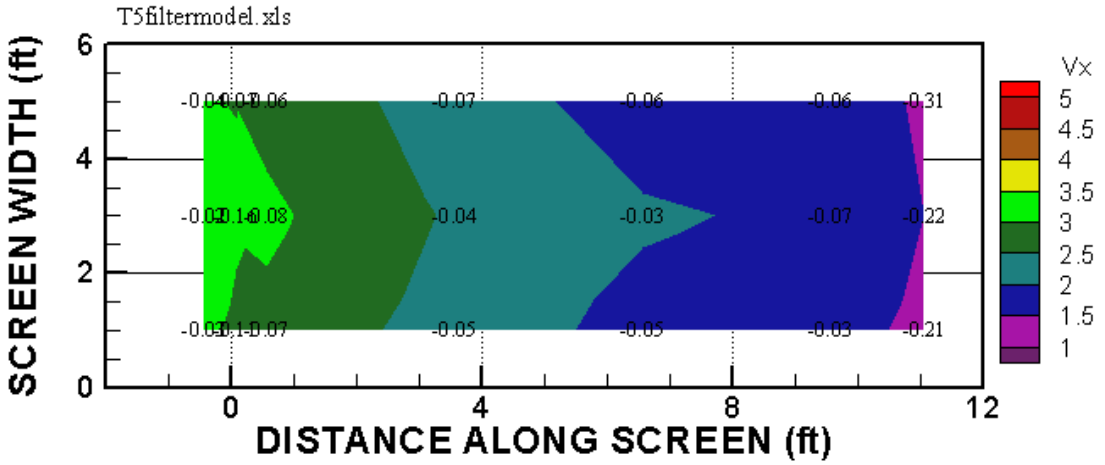

Qc=10.0 ft^3/s, Qb=6.08 ft^3/s, Qd=3.92 ft^3/s		
Depth = 0.5' or 6"		
Screen Distance (ft)	Average Sweeping Velocity Vs (ft/s)	Average Froude No. based on Vs
-0.4271	3.094	0.771
0.0729	2.995	0.746
0.5729	2.940	0.733
3.5729	2.318	0.578
6.5729	1.895	0.472
9.5729	1.830	0.456
11.0729	1.422	0.354

Figure 12.—Test 5. Rectangular 6-by-12 ft screen. Channel discharge, Q_c=10.0 ft^3/s, diversion discharge, Q_d=3.92 ft^3/s, bypass discharge, Q_b=6.08 ft^3/s. Diversion ratio, Q_d/Q_c = 0.4. Depth over screen=0.5 ft. Contours represent the sweeping velocity and indicate a weak wave front over the downstream end of the screen. The theoretical average approach velocity of 0.054 ft/s produces 57:1 and 26:1 for sweeping to approach velocity ratios for the upstream and downstream portions of the screen, respectively. This flow condition operated entirely under the subcritical flow regime.

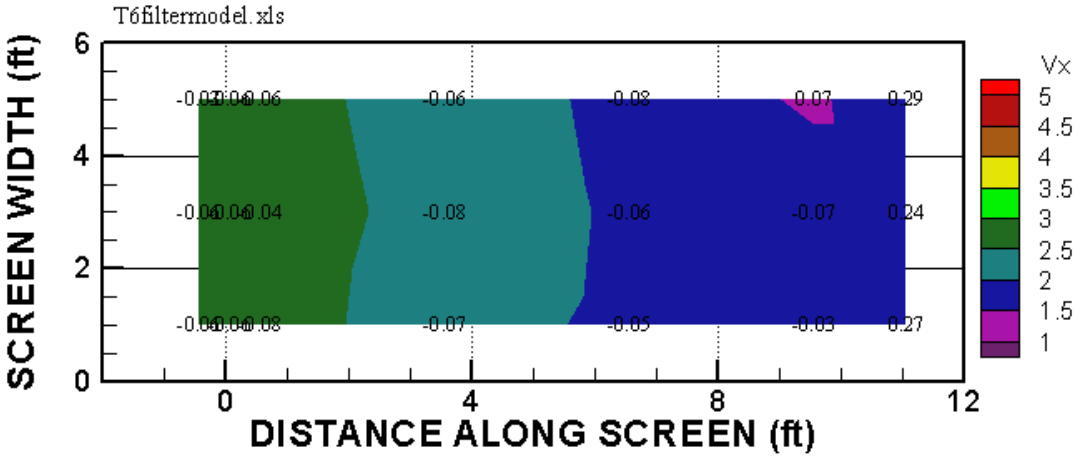

Qc=10.01 ft^3/s, Qb=7.93 ft^3/s, Qd=2.08 ft^3/s		
Depth = 0.583' or 7"		
Screen Distance (ft)	Average Sweeping Velocity Vs (ft/s)	Average Froude No. based on Vs
-0.4271	2.882	0.665
0.0729	2.822	0.651
0.5729	2.760	0.637
3.5729	2.240	0.517
6.5729	1.904	0.439
9.5729	1.616	0.373
11.0729	1.824	0.421

Figure 13.—Test 6. Rectangular 6-by-12 ft screen. Channel discharge, Q_c=10.01 ft^3/s, diversion discharge, Q_d=2.08 ft^3/s, bypass discharge, Q_b=7.93 ft^3/s. Diversion ratio, Q_d/Q_c = 0.21. Depth over screen=0.583 ft. Contours represent the sweeping velocity and indicate no downstream interference over the screen. The approach velocity still increases right at the end of the screen. The theoretical average approach velocity of 0.03 ft/s produces 96:1 and 60:1 for sweeping to approach velocity ratios for the upstream and downstream portions of the screen, respectively. This flow condition operated under the subcritical flow regime.

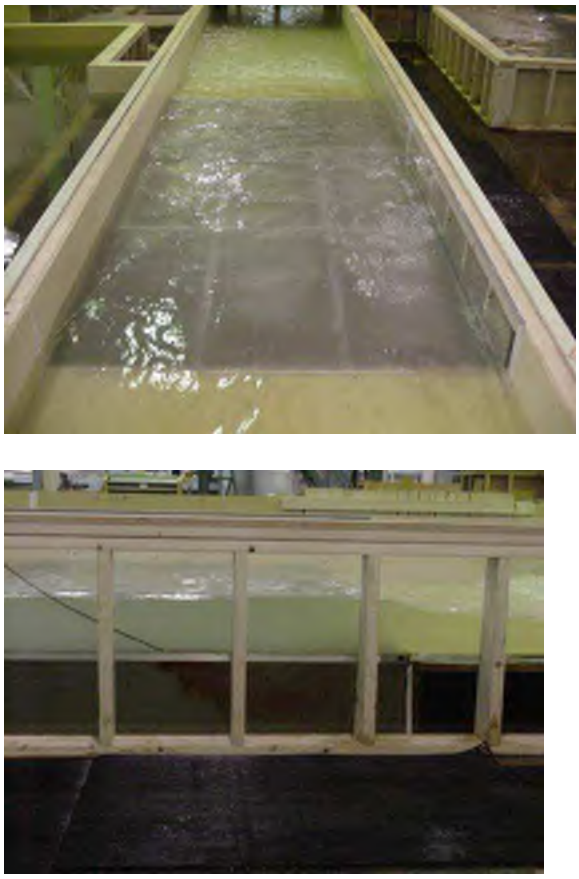

Figure 14.—Test 6. Subcritical flow occurs across the rectangular screen with a jump downstream of the screen forced by tailwater control. Q_c = 10 ft^3/s, and Q_d/Q_c = 0.21. The bypass flow is much greater than the diversion flow and flow is coming back up through the screen at the downstream end as indicated by positive V_a values and producing unacceptable flow conditions.

Additional data were recorded as tests 7 and 8 and are shown on figures 15 and 16. Both of these tests had high Q_d/Q_c ratios with the flow unacceptably transitioning from supercritical to subcritical over the screen.

Sweeping velocity is difficult to maintain on a rectangular screen because the continual loss of diversion flow over a constant area reduces the flow, thus velocity as the flow travels over the length of the screen. The depth is essentially constant over the screen except near the end depending upon whether there is control downstream or a transition on the screen or critical flow at the end of the screen. This arrangement might be used when the diversion flow rate is small compared to the channel flow rate.

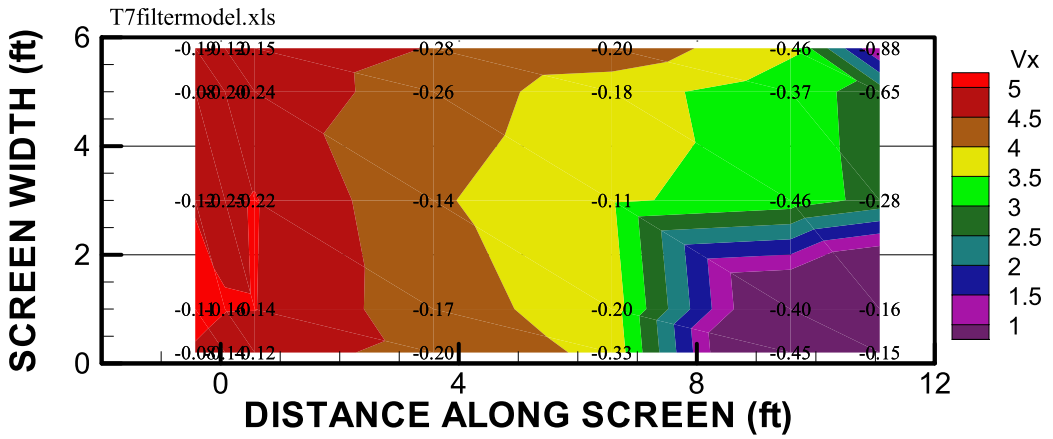

Qc=17.36 ft^3/s, Qb=3.07 ft^3/s, Qd=14.29 ft^3/s		
Depth = 0.5' or 6"		
Screen Distance (ft)	Average Sweeping Velocity Vs (ft/s)	Average Froude No. based on Vs
-0.4271	4.843	1.207
0.0729	4.841	1.207
0.5729	4.864	1.212
3.5729	4.264	1.063
6.5729	3.861	0.962
9.5729	1.684	0.585
11.0729	0.578	0.514

Figure 15.—Test 7. Rectangular 6-by-12 ft screen. Channel discharge, Q_c=17.36 ft^3/s, diversion discharge, Q_d=14.29 ft^3/s, bypass discharge, Q_b=3.07 ft^3/s. Diversion ratio, Q_d/Q_c = 0.82. Depth over screen=0.5 ft. Contours represent the sweeping velocity and indicate a wave front with re-circulating flow over the downstream right corner of the screen. The screen approach velocity values increase under the influence of the pooled water over the screen. The theoretical average approach velocity of 0.2 ft/s produces 24:1 and 3:1 for sweeping to approach velocity ratios for the upstream and downstream portions of the screen, respectively. The flow is supercritical over the upstream portion of the screen and transitions to subcritical about halfway down the screen.

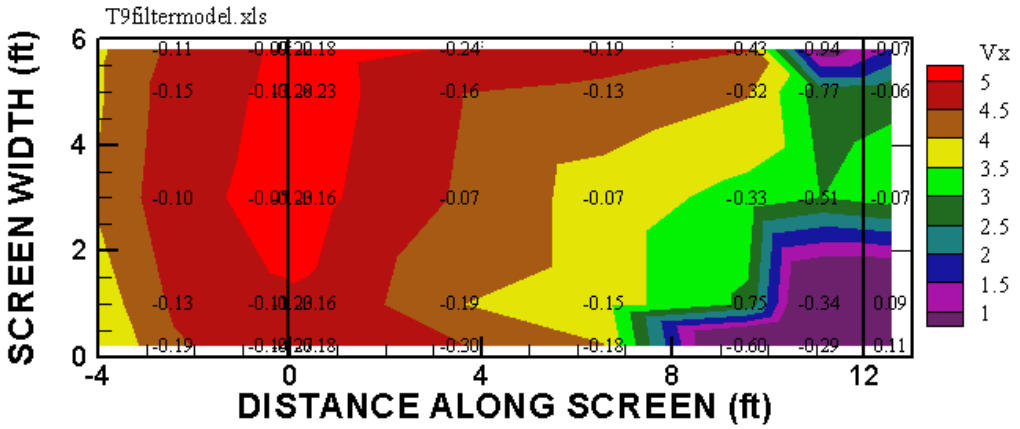

Qc=20.4 ft^3/s, Qb=6.05 ft^3/s, Qd=14.35 ft^3/s		
Depth = 0.667' or 8"		
Screen Distance (ft)	Average Sweeping Velocity Vs (ft/s)	Average Froude No. based on Vs
-4.4271	3.602	0.777
-2.4271	4.650	1.003
-0.4271	5.007	1.080
0.0729	5.069	1.094
0.5729	5.087	1.098
3.5729	4.488	0.968
6.5729	4.135	0.892
9.5729	2.818	0.668
11.0729	0.832	0.369
12.5729	1.030	0.444

Figure 16.—Test 8. Rectangular 6-by-12 ft screen. Channel discharge, Q_c=20.4 ft^3/s, diversion discharge, Q_d=14.35 ft^3/s, bypass discharge, Q_b=6.05 ft^3/s. Diversion ratio, Q_d/Q_c = 0.7. Depth over screen=0.67 ft. Contours represent the sweeping velocity and indicate a wave front with recirculating flow over the downstream corners of the screen. Recirculation is strong over the downstream right corner of the screen. The screen approach velocities increase under the influence of the pooled water over the screen. The theoretical average approach velocity of 0.2 ft/s produces 25:1 and 5:1 for sweeping to approach velocity ratios for the upstream and downstream portions of the screen, respectively. The flow is supercritical over the upstream portion of the screen and transitions to subcritical about halfway down the screen.

Screen Performance with a Converging Side wall

The concept of the converging side wall over a flat-plate screen is to decrease the exposed flow area to match the rate at which the channel flow is being diverted. This geometry will diminish or prevent a decrease in sweeping velocity along the screen.

Two wall convergences were tested in the model with the first discussed in this section. This geometry had the original 6 ft upstream width with the convergence beginning 1 ft upstream from the screen and ending at a bypass width of 2.54 ft. In addition, a non-perforated floor at the same elevation as the screen extended 2 to 4 ft downstream into the bypass. Table 2 shows the discharge conditions for the first series of converging side wall tests. The biological testing was also performed using this screen geometry.

Table 2.—Tests conducted with the 15-degree converging side wall to 2.54-ft-wide bypass with a flat, non-perforated bypass extension.

Test	Channel Discharge, Q_c (ft^3/s)	Diversion Discharge, Q_d (ft^3/s)	Bypass Discharge, Q_b (ft^3/s)	Q_d/Q_c (percent)	Theoretical Approach Velocity (ft/s)	Depth (ft)
9	7.38	5.70	1.68	77	0.115	0.42
10	6.92	4.00	2.92	58	0.10	0.42
11	7.00	4.95	2.05	71	0.10	0.42
12	9.08	7.45	1.63	82	0.15	0.58
13	15.00	9.89	5.11	66	0.2	0.58
14	12.00	9.89	2.11	82	0.2	0.58
15	11.5	7.42	4.08	64	0.15	0.42

Figures 17 and 18 show the flow conditions representing the opposite ends of the operating range with the converging side wall at 15-degrees, the 2.54-ft wide bypass, and a supported jet with downstream control. Figure 17, test 10, shows subcritical flow over the entire screen area. Figure 18, test 13, shows supercritical flow transitioning to subcritical flow over the screen. At the beginning of the study it was probably felt that the screen should operate in the subcritical range, however, observations of the flow conditions revealed that supercritical flow over the entire screen would be acceptable, if not preferable. The flow regime transition in figure 18 is, however, not acceptable as the wave front over the screen would cause fish to hold on the screen and a change in velocities over the screen.

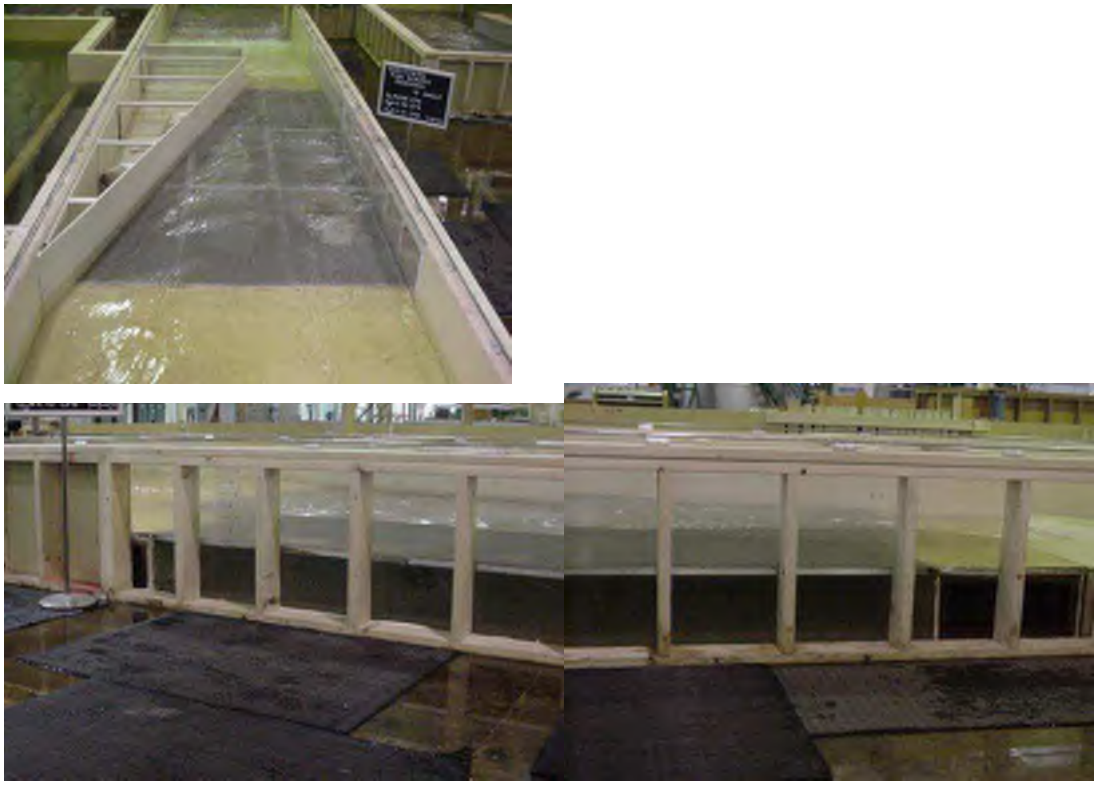

Figure 17.—Test 10. Converging side wall test with Q_c = 6.92 ft^3/s, Q_d/Q_c = 0.58 and no influence on the screen from downstream control. Flow is subcritical throughout and sweeping velocities are constant from upstream to downstream. This screen geometry and flow condition was used for the bull trout testing under a sweeping velocity of 2 ft/s.

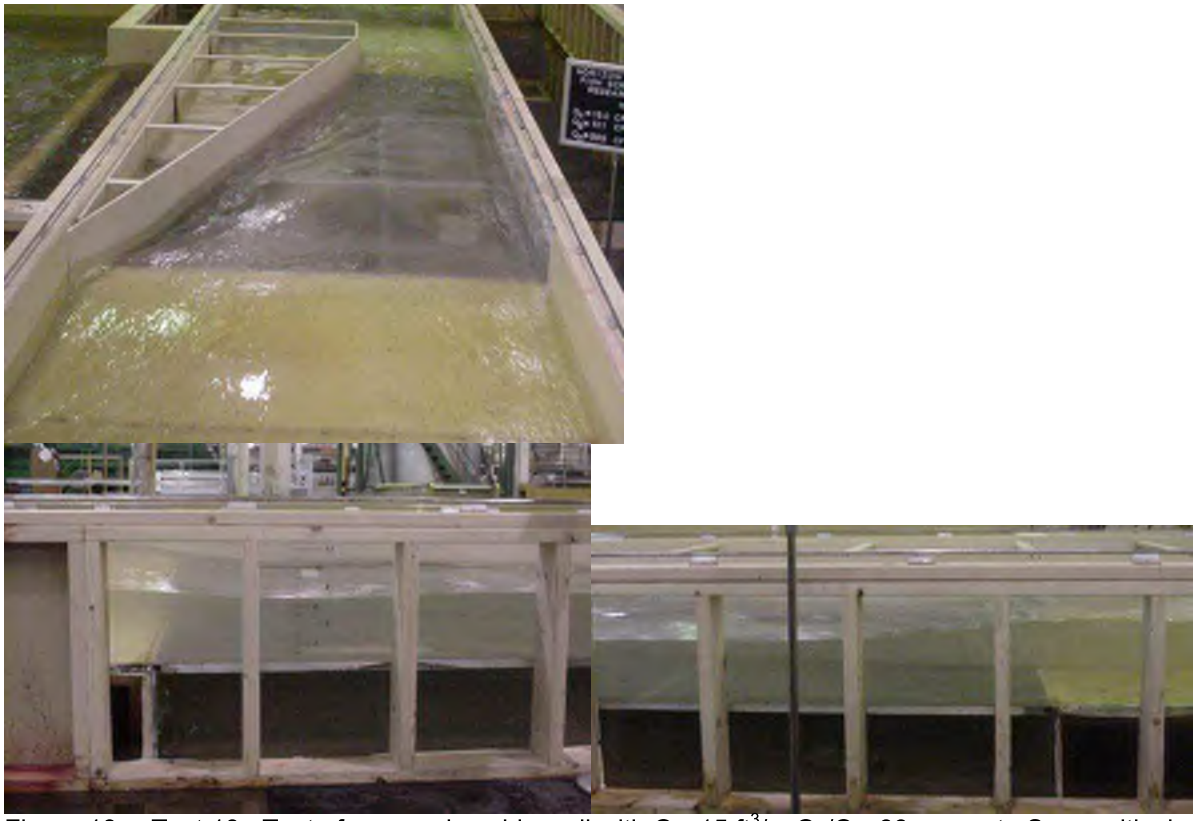

Figure 18.—Test 13. Test of converging side wall with Q_c=15 ft^3/s, Q_d/Q_c=66 percent. Supercritical flow at the upstream end of the screen transitioning to subcritical about 7 ft onto the screen.

Velocity data were recorded in the positions shown on figure 19 for tests 9-15 with the 15 degree converging side wall geometry. The sweeping velocity contour plots and longitudinal velocity and Froude number profiles are shown on figures 20-26. Velocity profiles were created by extracting data longitudinally along the screen from the data tables in the appendix at the centerline of the right screen 1 ft from the right wall, looking downstream. These data show the overall trends of the sweeping and approach velocities. The contour plots show that the sweeping velocities are very consistent across the width of the screen as with the rectangular screen. The approach velocities are slightly higher along the converging wall with the slight wave formed along the wall producing a slightly greater depth. The converging wall helps to keep the sweeping velocity deceleration rate less than with the rectangular screen. As the flow enters the bypass, the velocity does increase if there is no backwater present on the screen. Overall, the 15-degree converging side wall provided improved flow conditions and larger diversion to channel ratios than with the rectangular screen geometry.

In addition, the Froude number was plotted along the second y-axis to show sub or super-critical flow conditions. In test 13, shown on figure 18, the flow transitioned over the screen from supercritical to subcritical flow and would not be an acceptable condition for operation.

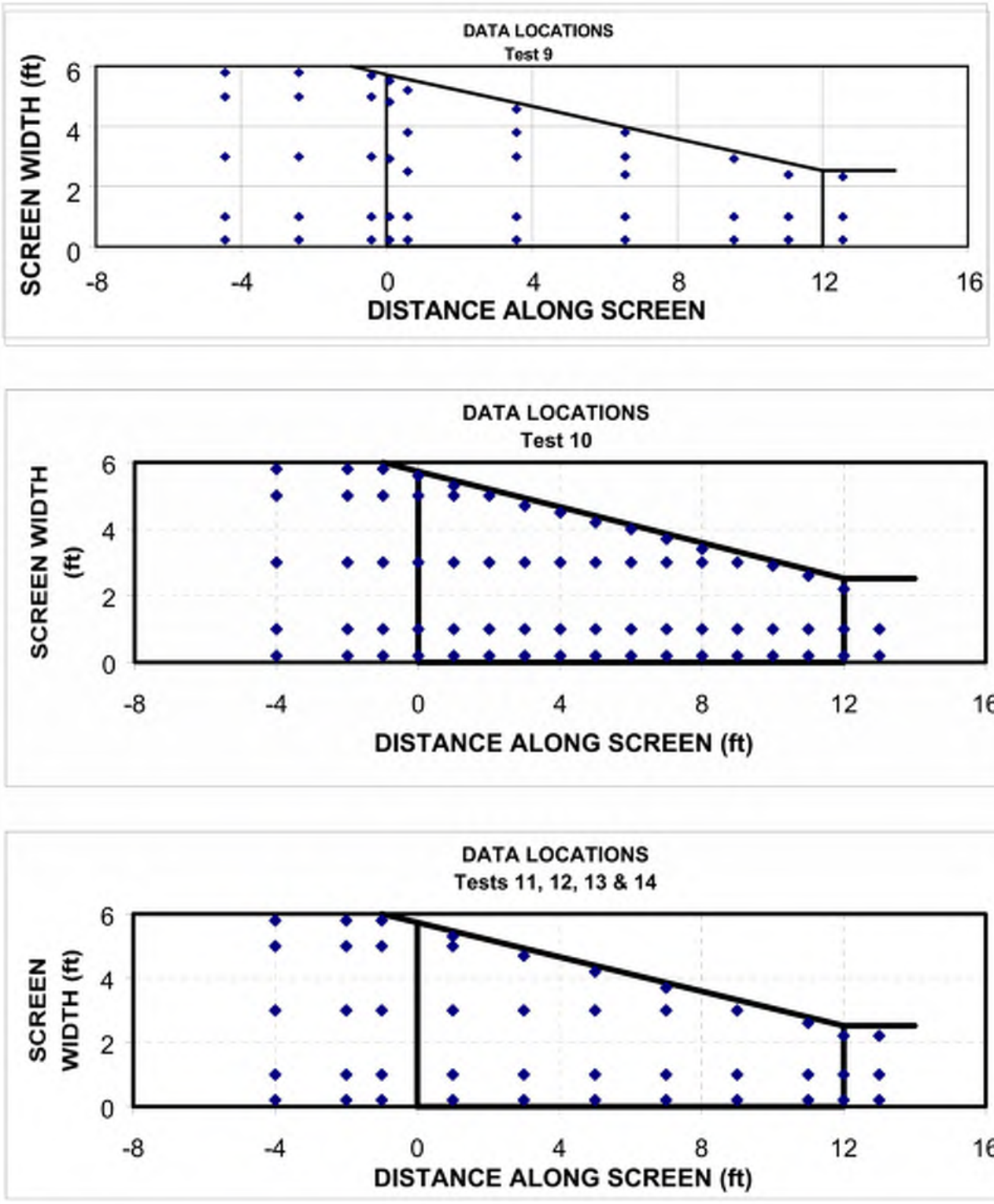

Figure 19.—Locations where velocity data were gathered for the 15° converging wall on the full-width horizontal fish screen. The exposed screen area is highlighted with the screen beginning at 0 ft. Data were gathered at various distances down the screen length primarily along screen panel centerlines and along the walls, including upstream and downstream from the screen. Test 15 data were only gathered along the screen length 1 ft from the right wall, looking downstream.

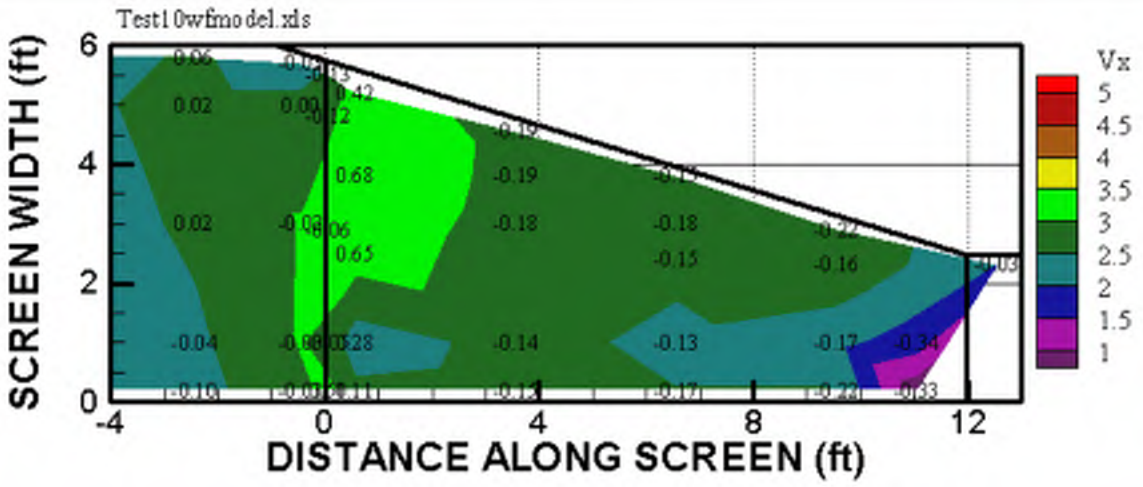

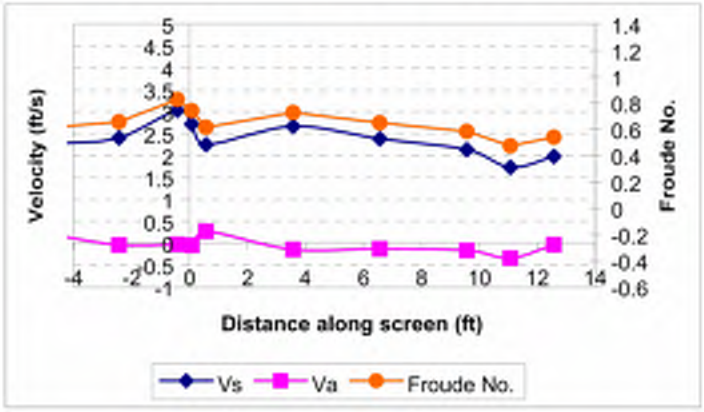

Qc=7.38 ft^3/s, Qb=1.68 ft^3/s, Qd=5.70 ft^3/s		
Depth = 0.42' or 5"		
Screen Distance (ft)	Average Sweeping Velocity Vs (ft/s)	Average Froude No. based on Vs
-4.4271	2.299	0.627
-2.4271	2.527	0.690
-0.4271	2.758	0.753
0.0729	2.908	0.794
0.5729	2.928	0.799
3.5729	2.791	0.762
6.5729	2.666	0.728
9.5729	2.629	0.718
11.0729	1.208	0.330
12.5729	1.981	0.541

Figure 20.—Test 9. Converging wall with 15° angle. Channel discharge, Q_c=7.38 ft^3/s, diversion discharge, Q_d=5.70 ft^3/s, bypass discharge, Q_b=1.68 ft^3/s. Diversion ratio, Q_d/Q_c = 0.77. Depth over screen=0.42 ft. Contours represent the sweeping velocity and indicate backwater from downstream control over the downstream corners of the screen. The screen approach velocities increase under the influence of the pooled water over the screen. The theoretical average approach velocity of 0.115 ft/s produces 25:1 and 16:1 for sweeping to approach velocity ratios for the upstream and downstream portions of the screen, respectively. The flow is subcritical across the screen.

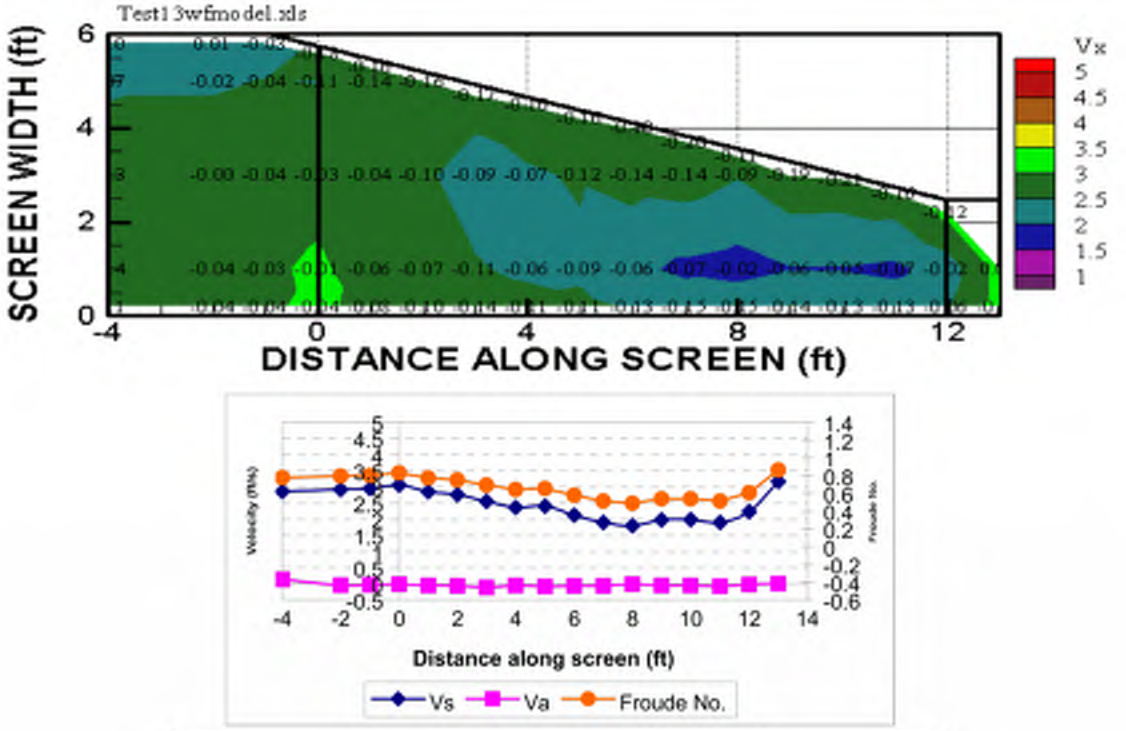

Qt=6.92 ft^3/s, Qb=2.92 ft^3/s, Qd=4.00 ft^3/s		
Depth = 0.42' or 5"		
Screen Distance (ft)	Average Sweeping Velocity Vs (ft/s)	Average Froude No. based on Vs
-4	2.6503	0.7207
-2	2.6744	0.7272
-1	2.6691	0.7258
0	2.8318	0.7700
1	2.8487	0.7746
2	2.7738	0.7543
3	2.5915	0.7047
4	2.5868	0.7034
5	2.6021	0.7076
6	2.4936	0.6781
7	2.4330	0.6616
8	2.3269	0.6327
9	2.4654	0.6704
10	2.3951	0.6513
11	2.3249	0.6322
12	2.6083	0.7093
13	3.1960	0.8691

Figure 21.—TEST 10. Converging channel with 15° angle. Channel discharge, Q_c=6.92 ft^3/s, diversion discharge, Q_d= 4.00 ft^3/s, bypass discharge, Q_b=2.92 ft^3/s. Diversion ratio, Q_d/Q_c = 0.58. Depth over screen=0.42 ft. Contours represent the sweeping velocity and indicate no influence from downstream control on the screen. The theoretical average approach velocity of 0.1 ft/s produces 28:1 and 26:1 for sweeping to approach velocity ratios for the upstream and downstream portions of the screen, respectively. The flow is subcritical across the entire screen with no decrease in sweeping velocity and a jump downstream from the screen. Bull trout tests were conducted with this screen geometry, flow rate, and sweeping velocity of about 2 ft/s.

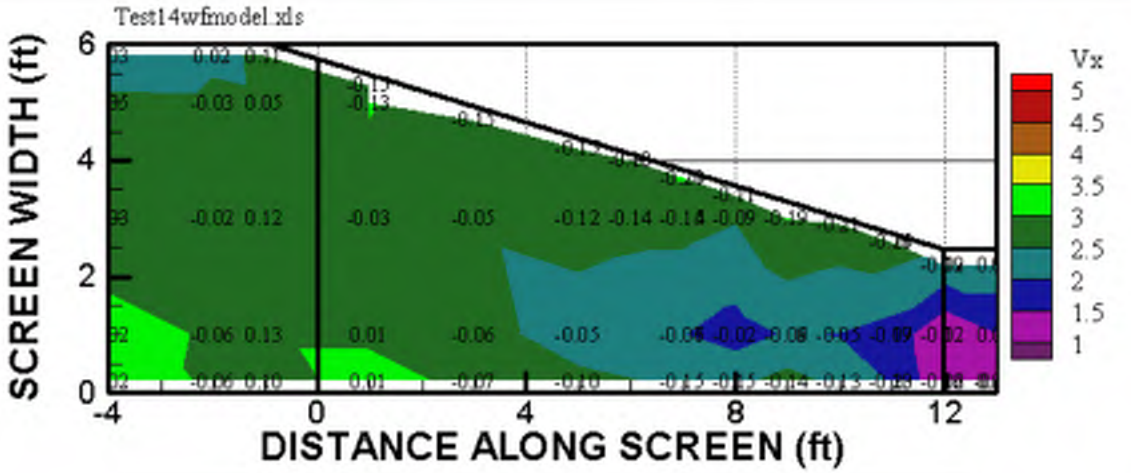

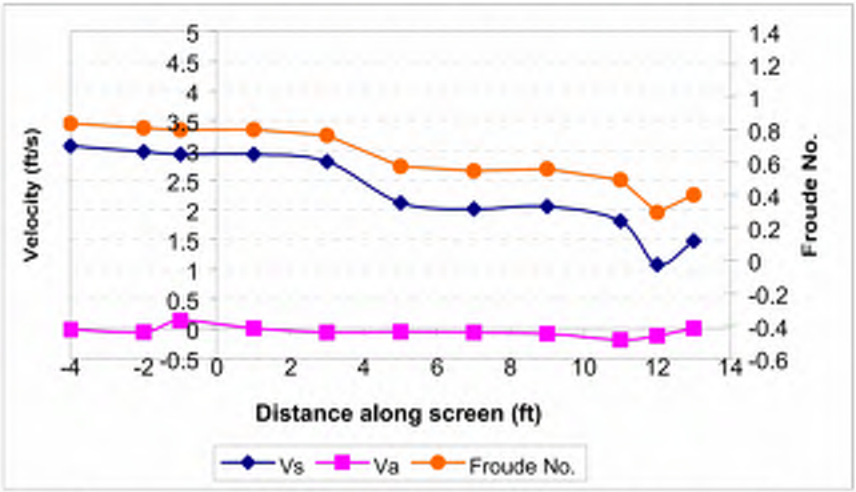

Qt=7.00 ft^3/s, Qb=2.05 ft^3/s, Qd=4.95 ft^3/s		
Depth = 0.42' or 5"		
Screen Distance (ft)	Average Sweeping Velocity Vs (ft/s)	Average Froude No. based on Vs
-4	2.774	0.754
-2	2.753	0.748
-1	2.705	0.736
1	2.990	0.813
3	2.805	0.763
5	2.591	0.704
7	2.527	0.687
9	2.582	0.702
11	2.181	0.593
12	1.496	0.407
13	1.748	0.475

Figure 22.—Test 11. Converging walls with 15° angle. Channel discharge, Q_c=7.00 ft^3/s, diversion discharge, Q_d=4.95 ft^3/s, bypass discharge, Q_b=2.05 ft^3/s. Diversion ratio, Q_d/Q_c = 0.71. Depth over screen=0.42 ft. Contours represent the sweeping velocity and indicate a weak wave from downstream backwater on the very end of the screen. The theoretical average approach velocity of 0.1 ft/s produces 30:1 and 15:1 for sweeping to approach velocity ratios for the upstream and downstream portions of the screen, respectively. The flow is subcritical across the screen.

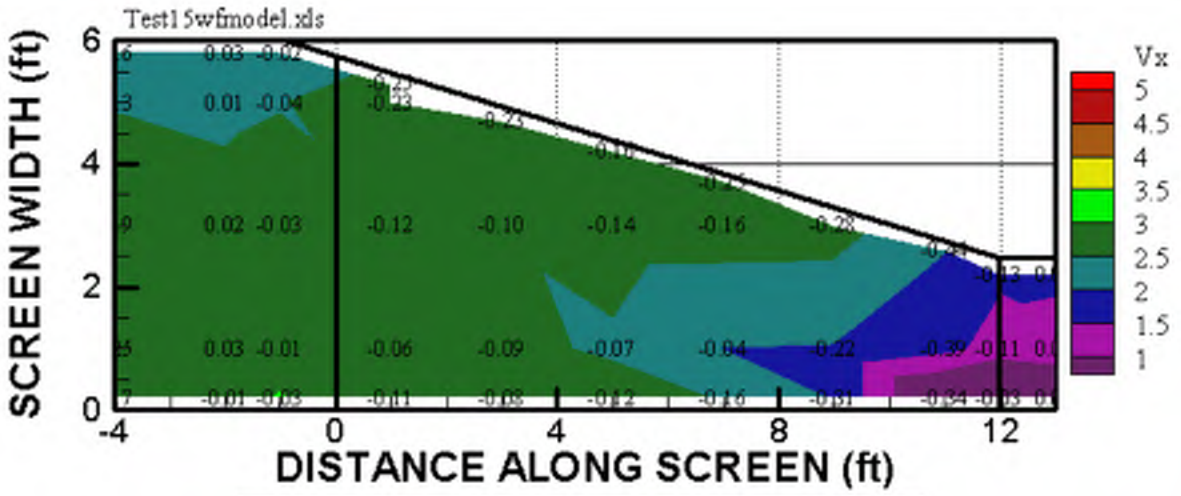

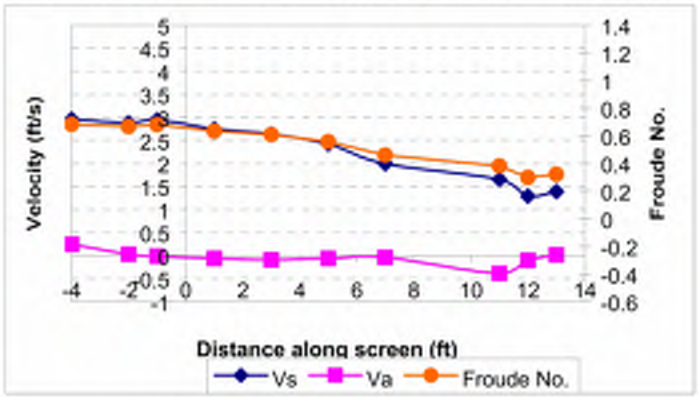

Qt=9.08 ft^3/s , Qb=1.63 ft^3/s , Qd=7.45 ft^3/s		
Depth = 0.58' or 7"		
Screen Distance (ft)	Average Sweeping Velocity Vs (ft/s)	Average Froude No. based on Vs
-4	2.707	0.625
-2	2.646	0.611
-1	2.654	0.613
1	2.698	0.623
3	2.587	0.597
5	2.631	0.607
7	2.465	0.569
9	2.216	0.511
11	1.296	0.299
12	0.882	0.203
13	1.018	0.235

Figure 23.—TEST 12. Converging wall with 15° angle. Channel discharge, Q_c=9.08 ft^3/s, diversion discharge, Q_d=7.45 ft^3/s, bypass discharge, Q_b=1.63 ft^3/s. Diversion ratio, Q_d/Q_c = 0.82. Depth over screen=0.58 ft. Contours represent the sweeping velocity and indicate backwater over the end of the screen from downstream control. The screen approach velocities increase under the influence of the pooled water over the screen. The theoretical average approach velocity of 0.15 ft/s produces 18:1 and 6:1 for sweeping to approach velocity ratios for the upstream and downstream portions of the screen, respectively. The flow is subcritical over the entire screen. Debris testing was performed with this screen geometry and flow condition.

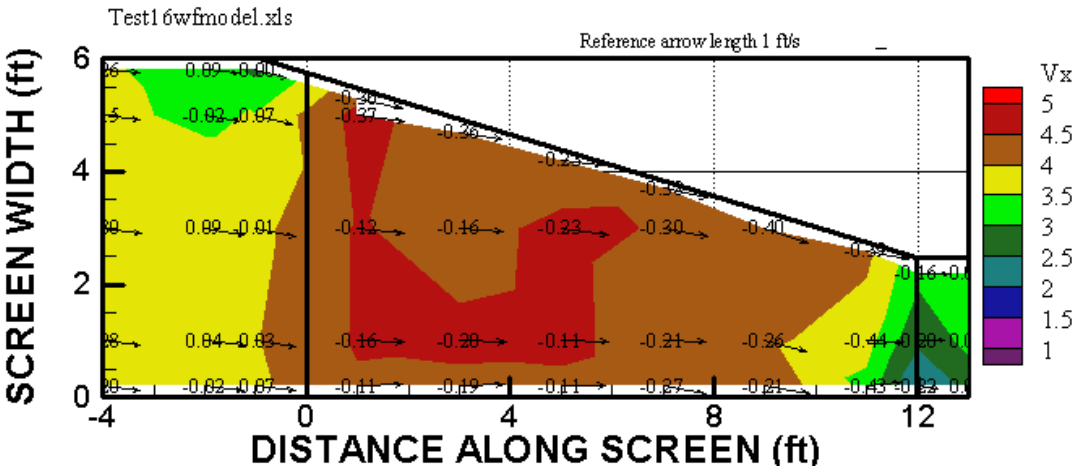

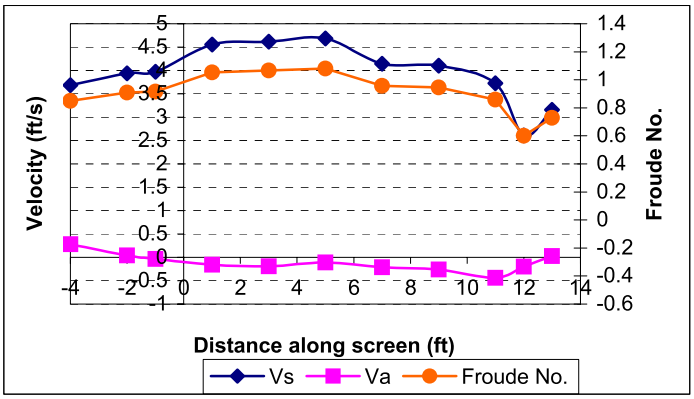

Qt=15.00 ft^3/s, Qb=5.11 ft^3/s , Qd=9.89 ft^3/s		
Depth = 0.58' or 7"		
Screen Distance (ft)	Average Sweeping Velocity Vs (ft/s)	Average Froude No. based on Vs
-4	3.646	0.841
-2	3.674	0.848
-1	3.634	0.839
1	4.519	1.043
3	4.378	1.011
5	4.447	1.026
7	4.277	0.987
9	4.250	0.981
11	3.733	0.862
12	2.587	0.597
13	3.054	0.705

Figure 24.—TEST 13. Converging wall with 15° angle. Channel discharge, Q_c=15.00 ft^3/s, diversion discharge, Q_d=9.89 ft^3/s, bypass discharge, Q_b=5.11 ft^3/s. Diversion ratio, Q_d/Q_c = 0.66. Depth over screen=0.58 ft. Contours represent the sweeping velocity and indicate backwater over the end of the screen from downstream control. The screen approach velocities increase under the influence of the pooled water over the screen. The theoretical average approach velocity of 0.2 ft/s produces 23:1 and 13:1 for sweeping to approach velocity ratios for the upstream and downstream portions of the screen, respectively. The flow is near critical over most of the screen and transitions to subcritical as the flow is backwatered onto the screen.

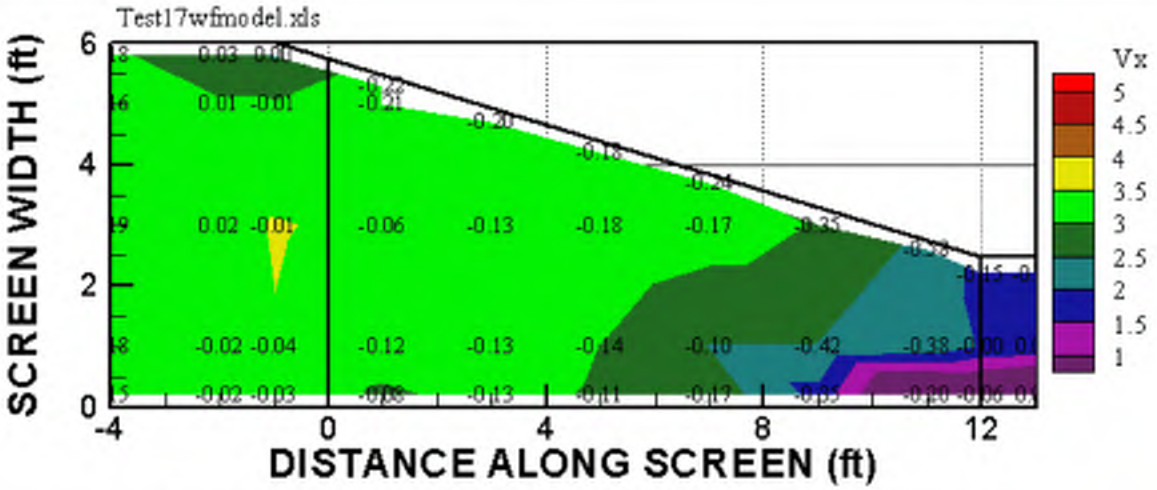

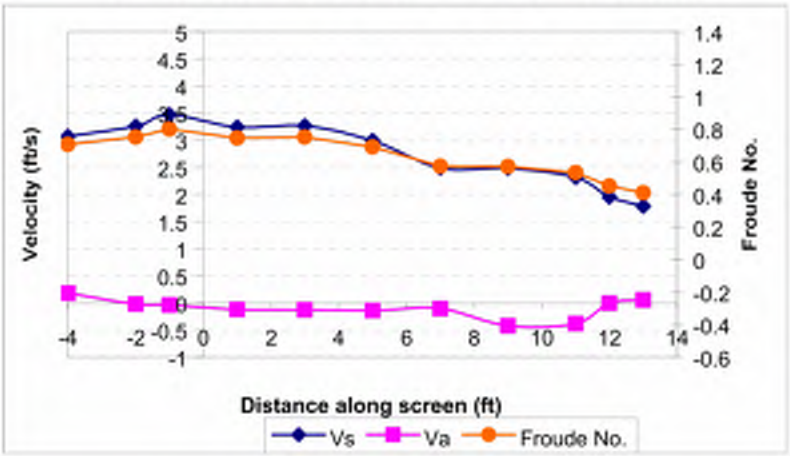

Qt=12.00 ft^3/s, Qb=2.11 ft^3/s, Qd=9.89 ft^3/s		
Depth = 0.58' or 7"		
Screen Distance (ft)	Average Sweeping Velocity Vs (ft/s)	Average Froude No. based on Vs
-4	3.128	0.722
-2	3.124	0.721
-1	3.182	0.734
1	3.274	0.756
3	3.175	0.733
5	3.180	0.734
7	2.909	0.671
9	2.426	0.560
11	1.440	0.332
12	1.262	0.291
13	1.161	0.268

Figure 25.—TEST 14. Converging wall with 15° angle. Channel discharge, Q_c=12.00 ft^3/s, diversion discharge, Q_d=9.89 ft^3/s, bypass discharge, Q_b=2.11 ft^3/s. Diversion ratio, Q_d/Q_c = 0.82. Depth over screen=0.58 ft. Contours represent the sweeping velocity and indicate a wave front with minor re-circulating flow over the downstream right corner of the screen. The screen approach velocities increase under the influence of the pooled water over the screen. The theoretical average approach velocity of 0.2 ft/s produces 16:1 and 6:1 for sweeping to approach velocity ratios for the upstream and downstream portions of the screen, respectively. The flow is subcritical across the entire screen.

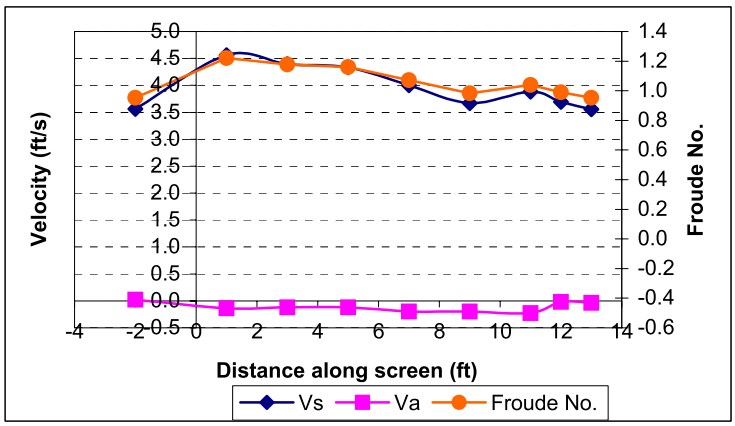

Screen Distance (ft)	Vs (ft/s)	Froude No.
-2.000	3.560	0.954
1.000	4.561	1.221
3.000	4.396	1.177
5.000	4.335	1.161
7.000	4.001	1.071
9.000	3.671	0.983
11.000	3.884	1.040
12.000	3.692	0.989
13.000	3.558	0.953

Figure 26. - Test 15. Converging wall with 15-degree angle and 2.54-ft-wide bypass opening. Channel discharge, Q_c=11.5 ft^3/s, diversion discharge, Q_d=7.42 ft^3/s, bypass discharge, Q_b=4.08 ft^3/s. Diversion ratio Q_d/Q_c=0.64. Depth over screen=0.42 ft. The profiles represent the sweeping and approach velocities measured over the screen 1 ft from the straight wall. Data were not gathered across the width; therefore, there is no contour plot. The flow is supercritical throughout the screen. Bull trout tests were conducted with this screen geometry, flow rate, and sweeping velocity of about 4 ft/s.

Screen Performance with a Converging Side Wall and a Drop at the Downstream End of the Screen

The second series of tests with a converging side wall were conducted with the model modified to form a 1-ft-wide bypass and a drop at the downstream end of the screen into the bypass. Constructing a 1-ft-bypass, while keeping the wall convergence at 15 degrees, meant reducing the upstream channel to a width of 4.22 ft. The Froude model scale that was used for these tests was 2:1. This allowed for deeper flow depths and investigation of a typical 2 ft bypass width normally used in vertical screen installations. In addition, adding a drop at the end of the screen into the bypass allowed investigation of the effects of flow depth control at the downstream end of the screen.

Critical depth occurred at the end of the screen and controlled the depth over the screen in addition to that provided by the diversion weir wall and control gate. With critical depth at the end of the screen (Froude number =1), the bypass flow is controlled for any given depth over the screen [4]. The flow conditions tested over the screen with the 15 degree wall convergence leading to the 1-ft-wide bypass with a drop at the downstream end are shown in table 3. After a few initial tests the channel flow was kept constant and the depth over the screen increased for comparison of flow conditions.

Table 3.—Flow rates tested over the screen with a 1-ft-wide bypass and a drop at the downstream end

Test	Channel Discharge, Q_c (ft^3/s)	Diversion Discharge, Q_d (ft^3/s)	Bypass Discharge, Q_b (ft^3/s)	Q_d/Q_c (percent)	Theoretical Approach Velocity (ft/s)	Depth (ft)
16	8	6.20	1.80	77	0.198	0.5
17	7	5.11	1.89	73	0.163	0.5
18	9	6.69	2.31	74	0.213	0.5
19	9	6.15	2.85	68	0.196	0.67
20	4.07	2.64	1.36	67	0.086	0.5
21	4.07	1.85	2.25	45	0.062	0.67

The flow characteristics at the end of the screen entering the bypass are complex. Two different flow conditions, represented by tests 20 and 18, are shown on figures 27 and 28. Test 20, shown on figure 27, has a fairly small channel flow and as a result the screen area is too large and flow returns back up through the screen at the downstream end. A necessary balance of flow causes flow to come up out of the screen for the given approach velocity, screen area, and depth. Test 18, shown on figure 28, has a large channel flow and cross-waves form due to the relatively short approach area causing build up of the flow at the downstream end of the screen and an increase in approach velocity at the downstream end of the screen.

Figure 27.—Test 20. Critical flow at the downstream end of the screen with Q_c= 4.07 ft^3/s and Q_d/Q_c= 67 percent. Flow depth of 0.5 ft. The sweeping velocity is increasing across the screen and particularly as the flow enters the bypass opening. The approach velocity in the last foot of the screen is positive indicating that flow is coming up through the screen.

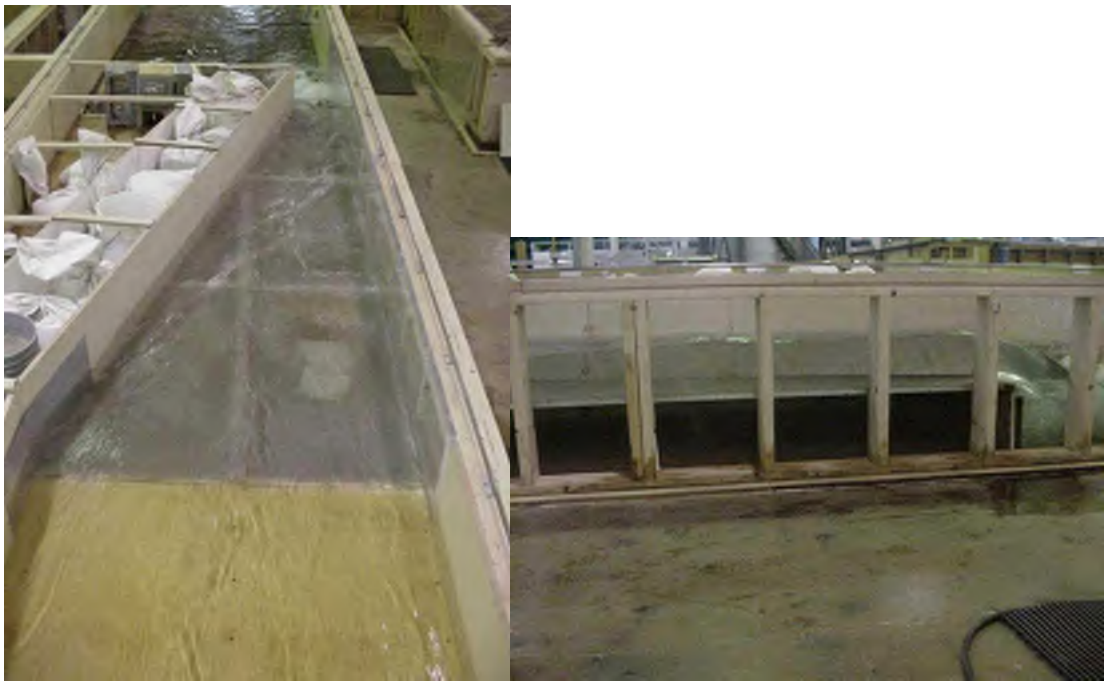

Figure 28.—Test 18. Critical flow at the downstream end of the screen with Q_c= 9 ft^3/s and Q_d/Q_c= 74 percent. Flow depth of 0.5 ft. The sweeping velocity is maintained across the screen and as the flow enters the bypass opening. The approach velocity over the last 2 feet of the screen exceeds the target of 0.2 ft/s indicating that the flow is deeper upstream from critical depth at the end of the screen. Notice the cross-waves extending the full width of the channel.

Velocity data were gathered along a profile located 0.5 ft from the straight right wall. Profiles of the depth at the end of the screen were measured to determine if the depth at the end of the screen was at, or above critical. In all cases depth measurements were equal to or greater than the computed critical depth for the bypass flow indicating subcritical flow conditions over the screen.

For all channel flow rates and Q_d/Q_c ratios tested the sweeping velocity increased or remained steady as the flow entered the bypass opening at the downstream end of the screen, figures 29-34. This is an improvement in sweeping velocity that should encourage fish passage and would be similar to bypass velocities with vertical screens.

The surface turbulence caused by the cross-waves from the wall convergence and the curvilinear flow at the drop produced some approach channel velocity anomalies at the end of the screen. In addition, the relatively short approach section to the screen section can also cause non-uniformity of the approach velocity. Approach conditions into the screen with higher sweeping velocities produced somewhat non-uniform approach velocities for every condition tested with small approach velocities at the upstream end of the screen that increased towards the downstream end of the screen.

For test 18, figure 31, and test 19, figure 32, with the same channel flow rate of 9 ft^3/s, the flow condition for test 18 produced increasing downward approach velocities along the screen, with the larger depth in test 19 following the same trend, but produced upwelling at the end of the screen. Figure 33, test 20, and figure 34, test 21, show the sweeping velocity increasing into the bypass and flow coming up out of the screen with positive approach velocities for Q_c=4.07 ft^3/s with Q_d/Q_c=0.67, D=0.5 ft and Q_d/Q_c=0.45, D=0.67 ft, respectively. The larger flow depth over the screen in test 21, compared to test 20, produced quite a large upwelling of velocity from the screen. This condition is not necessarily a problem hydraulically, but could cause fish avoidance at the bypass.

A solid or non-perforated section should perhaps be placed at the end of the screen to prevent excessive approach velocities or reverse flow at the bypass opening when operating with a drop at the end of the screen. In addition, a longer screen will reduce cross-waves by decreasing the side wall convergence for a given diversion design flow.

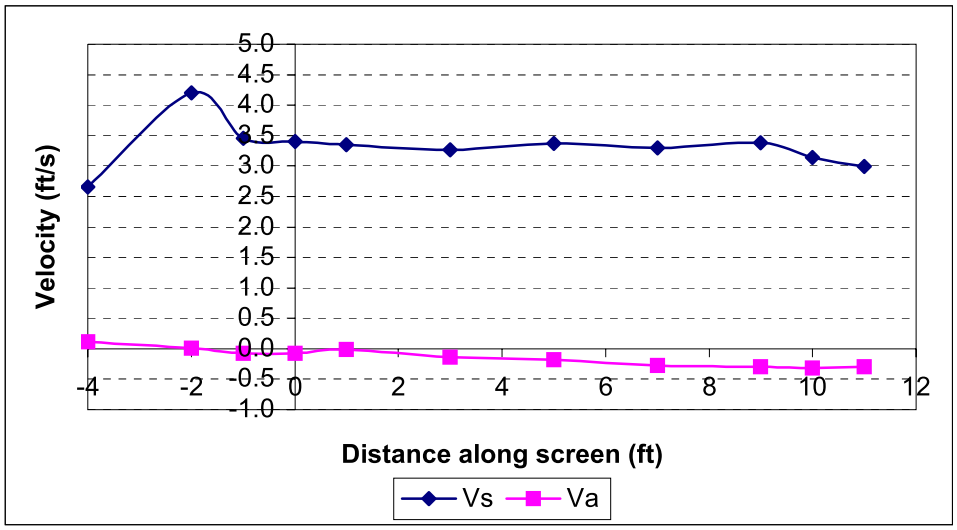

X	Vs (ft/s)	Vy (ft/s)	Va (ft/s)
-4	2.655	-0.024	0.113
-2	4.201	-0.082	0.012
-1	3.454	-0.065	-0.078
0	3.398	-0.022	-0.073
1	3.352	0.096	-0.010
3	3.269	-0.086	-0.135
5	3.374	0.040	-0.184
7	3.295	-0.504	-0.271
9	3.382	-0.342	-0.296
10	3.136	-0.523	-0.314
11	2.998	-0.504	-0.294

Figure 29.—Test 16 with 15-degree converging side wall to 1 ft wide bypass channel. Q_c=8 ft^3/s, Q_d=6.20 ft^3/s, and Q_d/Q_c=77.5 percent with a 0.5 ft depth. Approach velocities increase down the screen and sweeping velocities remain relatively constant, perhaps slightly decreasing.

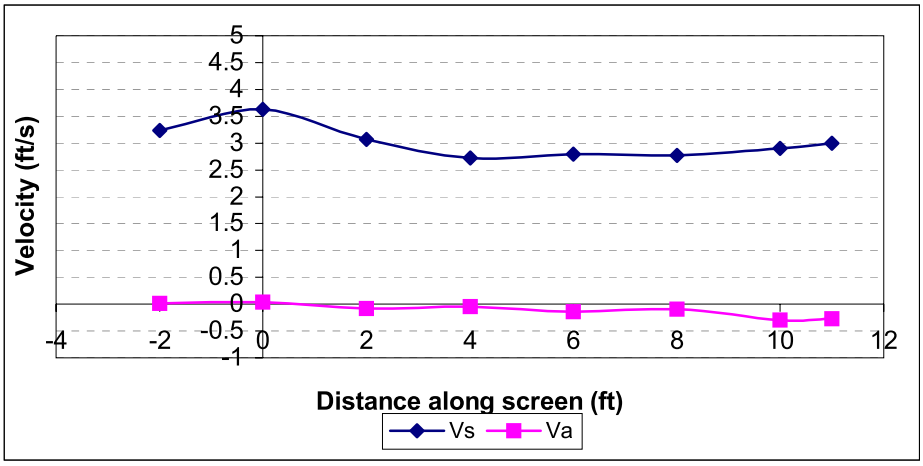

X distance (ft)	Vs (ft/s)	Vy (ft/s)	Va (ft/s)
-2	3.2365	-0.0231	0.0103
0	3.6254	-0.0447	0.0335
2	3.0673	-0.0458	-0.0847
4	2.7194	-0.1154	-0.0465
6	2.7903	-0.1694	-0.1365
8	2.7733	-0.2012	-0.0978
10	2.901	-0.3217	-0.2906
11	2.9947	-0.4747	-0.2701

Figure 30.—Test 17 with 15-degree converging side wall to 1-ft-wide bypass. Q_c=7 ft^3/s, Q_d=5.11 ft^3/s, and Q_d/Q_c=73 percent with a 0.5 ft depth. Approach velocities increase down the screen and sweeping velocities remain relatively constant once over the screen.

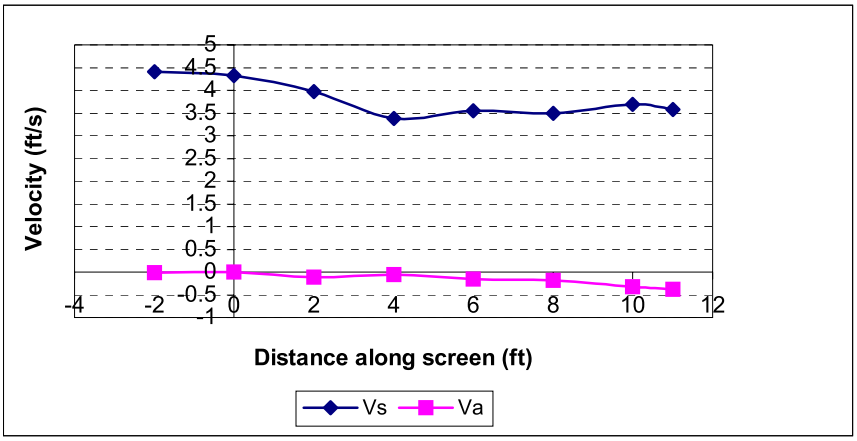

X Distance (ft)	Vs (ft/s)	Vy (ft/s)	Va (ft/s)
-2	4.4118	-0.0619	-0.0165
0	4.3276	-0.0555	-0.0006
2	3.9688	-0.0022	-0.1117
4	3.3786	-0.0721	-0.0633
6	3.5456	-0.1454	-0.1506
8	3.4904	-0.2494	-0.1771
10	3.6902	-0.2639	-0.3269
11	3.5782	-0.3731	-0.3825

Figure 31.—Test 18 with 15-degree converging side wall to 1-ft-wide bypass. Q_c=9 ft^3/s, Q_d=6.69 ft^3/s, and Q_d/Q_c=74 percent with a 0.5 ft depth. Approach velocities increase down the screen and sweeping velocities remain relatively constant once at a location 4 ft onto the screen.

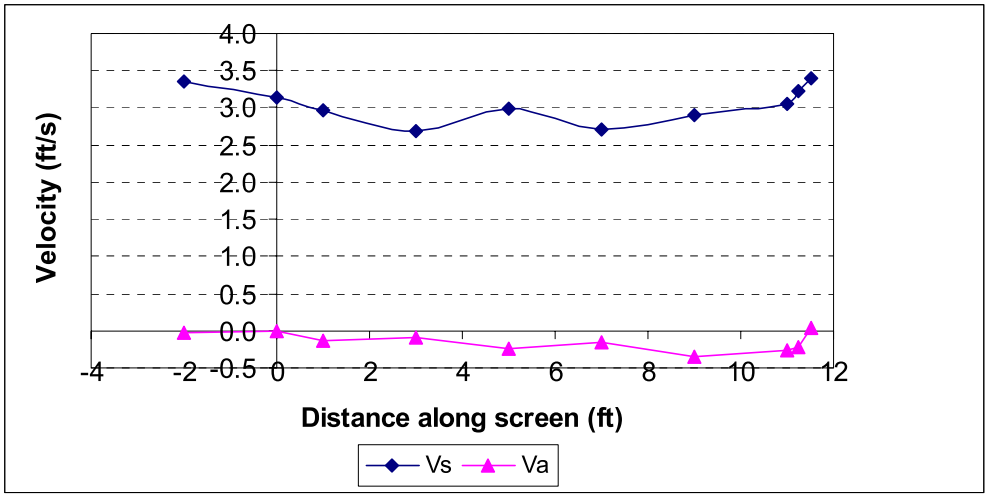

X	Vs (ft/s)	Vy (ft/s)	Va (ft/s)
-2	3.354	-0.129	-0.020
0	3.144	-0.167	0.000
1	2.976	-0.196	-0.138
3	2.687	-0.166	-0.098
5	2.994	-0.216	-0.247
7	2.718	-0.221	-0.147
9	2.912	-0.244	-0.353
11	3.056	-0.347	-0.256
11.25	3.223	-0.389	-0.212
11.5	3.404	-0.394	0.041

Figure 32.—Test 19 with 15-degree side wall to 1-ft-wide bypass. Q_c=9 ft^3/s, Q_d=6.15 ft^3/s, and Q_d/Q_c=68 percent with a 0.67 ft depth. Approach velocities increase down the screen and sweeping velocities increasing into the bypass.

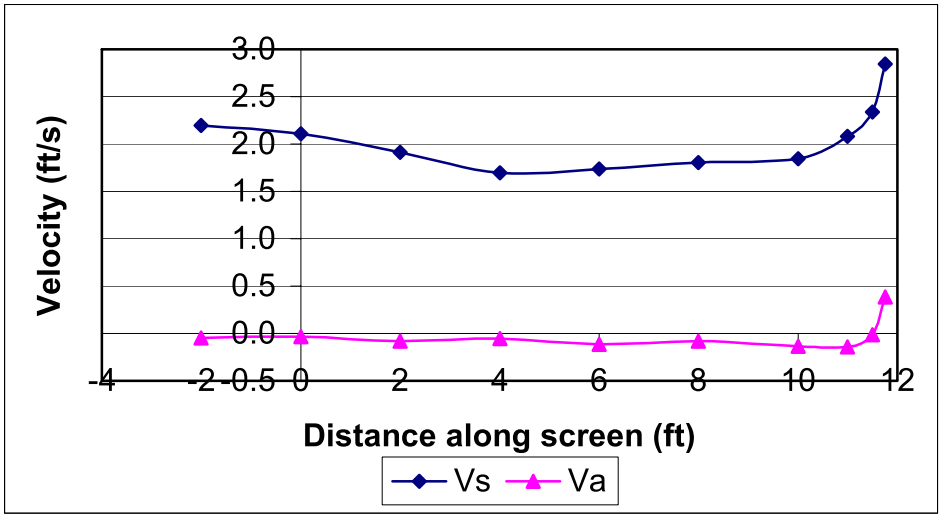

X	Vs (ft/s)	Vy (ft/s)	Va (ft/s)
-2	2.193	-0.046	-0.044
0	2.110	-0.109	-0.031
2	1.914	-0.002	-0.079
4	1.699	-0.021	-0.056
6	1.737	-0.093	-0.112
8	1.807	-0.083	-0.080
10	1.841	-0.131	-0.136
11	2.078	-0.269	-0.142
11.5	2.340	-0.306	-0.012
11.75	2.845	-0.379	0.383

Figure 33.—Test 20 with 15-degree converging side wall to 1-ft-wide bypass. Q_c=4.07 ft^3/s, Q_d=2.64 ft^3/s, and Q_d/Q_c=67 percent with a 0.67 ft depth. This flow condition indicates approach velocities coming up out of the screen and sweeping velocities increasing into the bypass.

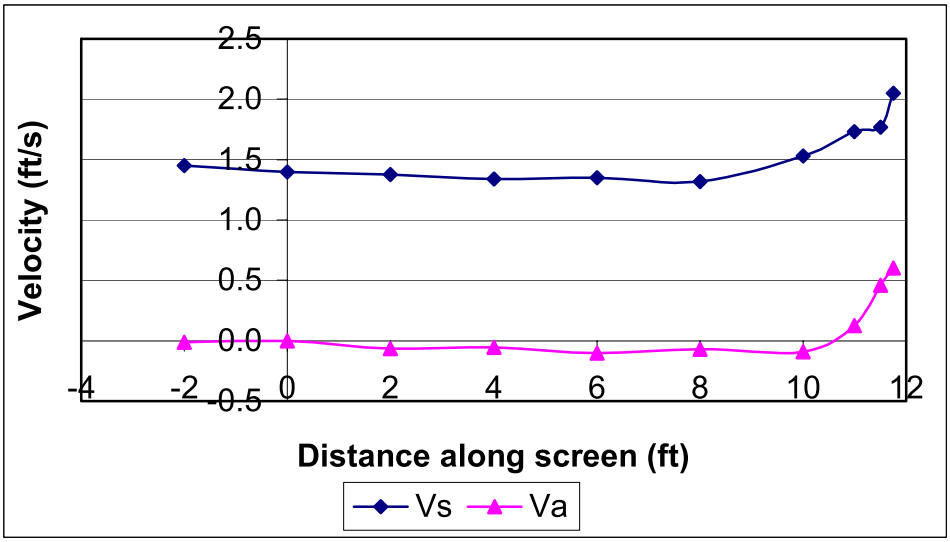

X	Vs (ft/s)	Vy (ft/s)	Va (ft/s)
-2	1.3995	-0.0291	-0.0145
0	1.3977	-0.0431	-0.0127
1	1.3796	-0.0439	-0.0618
3	1.3984	-0.073	-0.0341
5	1.3839	-0.1152	-0.1061
7	1.3715	-0.1353	-0.0468
9	1.5095	-0.175	-0.0941
11	1.5832	-0.2265	0.1052
11.5	1.9876	-0.2937	0.3614
11.75	1.8415	-0.5295	0.5617

Figure 34. - Test 21 with 15-degree side wall with 1-ft-wide bypass. Q_c=4.07 ft^3/s, Q_d=1.85 ft^3/s, and Q_d/Q_c=45 percent with 0.67 ft depth. This flow condition indicates approach velocities coming up out of the screen and sweeping velocities increasing into the bypass.

BIOLOGICAL TESTING – FLOW DESCRIPTION

The results of the biological testing of bull trout are attached under a separate report entitled "Bull Trout Performance in a Horizontal Flat-plate Screen" by Beyers and Bestgen [1]. The following is the Executive Summary from that comprehensive report.

"This investigation was conducted to the describe effects of passage of bull trout *Salvelinus confluentus* over a horizontal flat-plate screen. Experimental releases were conducted with three sizes of bull trout that averaged 28, 37, and 58 mm total length (TL). Fish were released individually and in batches to: (1) describe general behavior near and on the screen; (2) estimate physical condition and survival of fish after passage; and (3) estimate entrainment and impingement rates.

Consistent negative effects from passage of bull trout over a horizontal flat-plate screen were not observed. Potential entrainment was ≤ 3.5% for 28 mm fish, and was never observed for larger fish. Impingement never occurred. Passage times increased with fish size and ranged from 4 sec to more than 10 min. Physical damage to eyes, fins, and integument was either rare (eyes) or less frequent in fish that passed over the screen than in control fish. Fish that passed over the screen did contact the bottom more frequently than control fish, but no immediate mortality occurred from screen passage. Survival at 24 h was ≤ 1.5% lower for fish that passed over the screen compared to controls. At 96 h after passage, survival was reduced, but was not consistently lower for fish that passed over the screen compared to controls. Thus, physical effects of screen passage were at, or near the level of background effects induced by fish culture, handling, transport, and testing.

Water depth and orientation of bull trout changed with fish size and age despite the use of a standardized release methodology. Larger fish were more frequently observed near the bottom and more frequently oriented upstream than smaller fish. The tendency to occupy deeper water increased the likelihood that fish contacted the horizontal flat-plate screen. It also increased the likelihood that fish discovered attractive hydraulic properties of the screen. We observed several 58 mm fish that appeared to be maintaining position by using downward pressure generated by water approaching the screen. This behavior was the main factor responsible for increased passage time for larger fish. Thus, we did observe that certain hydraulic conditions of the horizontal flat-plate screen used in this investigation attracted fish and delayed their movement over the screen."

This section describes the flow conditions under which the biological testing was conducted. The testing was conducted with a 15-degree converging wall from the 6 ft wide channel to a 2.54 ft wide bypass. The wall convergence began 1 ft upstream from the 12 ft long screen section. The side wall in the downstream bypass area was extended to allow an acceptable area to net the fish below the screen.

Two sweeping velocities were selected for testing that represented large sweeping to approach velocity ratios and different flow conditions over the screen. Test 10 with subcritcal flow over the screen, V_s = 2 ft/s and Q_d/Q_c = 0.58, figures 17 and 21, were replicated for the bull trout tests. Supercritical flow, test 15, was used with V_s = 4 ft/s and Q_s/Q_c = 0.62, figure 26. Flow depths for both tests were about 0.42 feet over the length of the screen. The sweeping velocities were essentially constant over the screen and increased at the entrance to the bypass. Both control and screen exposure tests were performed. For the control tests, the screen was covered with a thin sheet of plastic and the wall geometry modified to produce the same sweeping velocity without diversion flow. The hydraulic information for the biological tests is given in table 4.

Figures 35- 37 show the geometry and flow conditions under which the bull trout testing was performed.

Table 4.—Hydraulic parameters used for the biological testing

	Q_c (ft^3/s)	Q_d (ft^3/s)	Q_b (ft^3/s)	Q_d/Q_c	V_s (ft/s)	V_a (ft/s)	V_s/V_a	Depth (ft)
Test 11	6.92	4.00	2.92	0.58	2	0.15	13:1	0.42
Control	2.05	0	2.05	0	2	N/A	N/A	0.42
Test 15	11.5	7.12	4.38	0.62	4	0.15	27:1	0.42
Control	4.08	0	4.08	0	4	N/A	N/A	0.42

Figure 35.—Bull trout testing with the 15-degree converging wall over the screen.

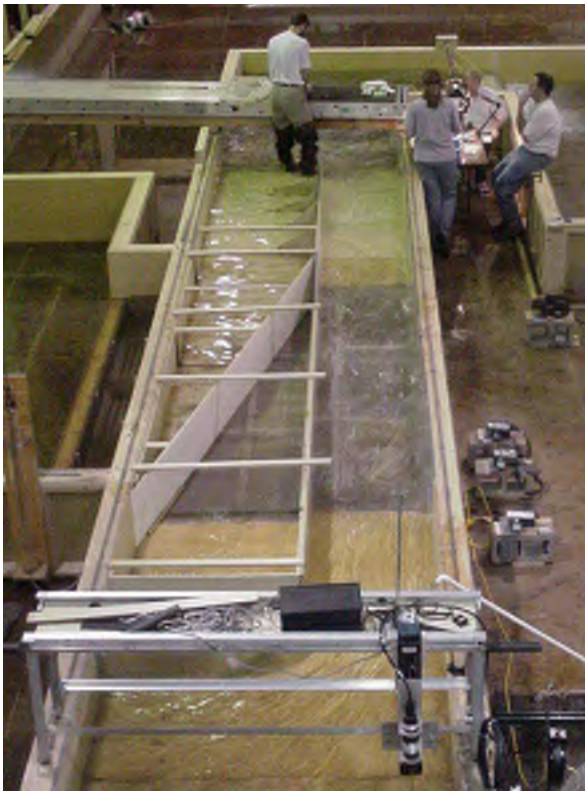

Figure 36.—Control test setup for bull trout testing with clear plastic over the screen and 2 ft/s sweeping velocity.

Figure 37.—Control test setup for bull trout testing with clear plastic over the screen and 4 ft/s sweeping velocity.

FUTURE INVESTIGATIONS

The hydraulic and biological investigations presented in this work will lead to discussions with Federal and State resource agencies regarding the feasibility of this technology. These agencies have been taking an active role in the investigations in order to resolve issues relating to requests from various irrigation districts to allow the use of the horizontal screen technology for flow diversion where ESA listed species are located.

Implementation of an experimental horizontal screen at a field site is, hopefully, the next step in these investigations. This site would require meeting the standards determined by the resource agencies and also require monitoring of hydraulic and possibly biological performance.

A few additional laboratory studies could be performed, should further research funding be available. These would include:

- Testing a wedge wire-type screen
- Testing various screen porosities
- More thorough debris tests
- Effectiveness of cleaning devices, if needed
- Further investigation of bypass exit conditions

IMPLEMENTATION PLAN FOR HORIZONTAL FISH SCREEN TECHNOLOGY

A meeting attended by Reclamation, the resource agencies, and members of the Baker Valley Irrigation District in July 2001 in Boise, ID to discuss what would be needed to utilize the horizontal flat-plate screen technology at a field site. The following items were determined to be necessary prior to use of the screen technology:

1. Obtain necessary permits and perform necessary biological assessments.
    a. Determine migration pattern for listed species during irrigation season.
2. Obtain the area hydrology.
    a. Hydrographs for all years.
    b. Q_{Design} and Q_{Ratio}.

3. Site parameters.
    a. Headwater control.
    b. Tailwater control or information.
    c. Modify site to meet optimal parameters.
    d. Downstream drop off screen if possible.
    e. Assess sediment issue with gradation information.
4. Evaluate debris type, i.e. leaves, needles, sand, etc. and quantity and design sediment traps, as needed.
5. Stay within recommended screen "criteria" (guidelines) for approach velocity and flow depth over 90 percent of the operational season.
    a. Use spreadsheet to develop initial design.
    b. Use a backwater program, such as HEC-RAS, for final design.
6. The diversion wall MUST be fixed.
7. Off-channel construction in diversion channels recommended.
8. Approach to design when outside of design with low flow.
    a. Construct 2 channels side-by-side and shut off 1 side.
    b. Use bypass control for low flows.
9. Evaluate hydraulic and biological performance throughout irrigation season.

REFERENCES

[1] Beyers, Daniel W., Bestgen, Kevin R., "Bull Trout Performance During Passage Over A Horizontal Flat-plate Screen", Contribution 128, Larval Fish Laboratory, Department of Fishery and Wildlife Biology, Colorado State University, Fort Collins, CO 80523, July 2001.

[2] Mefford, B., Kubitschek, J., "Physical Model Studies of the GCID Pumping Plant Fish Screen Structure Alternatives, Progress Report No. 1, 1:30 Scale Model Investigations, Alternative D", R-97-02, U.S. Bureau of Reclamation, Technical Services Center, March 1997.

[3] Odeh, Mufeed, "Advances in Fish Passage Technology: Engineering Design and Biological Evaluation", American Fisheries Society, Bethesda, Maryland, 2000.

[4] Chow, Ven Te, "Open-Channel Hydraulics", McGraw-Hill Book Company, 1959.

APPENDIX A

Flat-plate screen sweeping velocity prediction model. The computations are shown with the developed pivot table using cell K26.

Flat plate screen sweeping velocity prediction model

filename: flat plate screen worksheet sample.xls
Model assumes uniform approach velocity to the screen and a constant flow depth over the screen
Input parameters are shown in yellow
Spreadsheet computes discharges based upon variable screen dimensions and depths.

Table shows where velocity is outside specified limits or shows "Trans" where flow changes from subcritical to supercritical.
And includes supercritical flow range as acceptable.
Shaded areas in the table are for acceptable flow ratios given the specified input and approach velocity range.

Specific Case		
Qus =	10	
Va =	0.2	
Qdiv =	=+$G$26	
Qby=	=+$B$15-$B$17	
Screen length (L)	12	
channel width (Cw) =	5	
Wall angle (A)	15	
Bypass width (Bw) =	=+B30-(B29*TAN(B31*PI()/180))	12
Depth (D) =	1	13
%Acl/Dcl per ft	1	14
Vs (min), ft/s	2	15
		16
		Channel 17
		Flow, 18
		cfs 19
		20
		21
		22
		23
		24
		25
		26
Diversion ratio, Vr*		27
Vr>0.6		28
0.3<Vr<0.6		29

Screen length	Channel width	Area lost	Screen area	Qdiv	Qb	Flow area	Vs	
1 ft increments	Total u/s width-convergence angle*screen increment	Tan(A)*screen length*screen length/2	Width*length-area lost	Incremental Q thru screen	Total Q-Qdiv	Depth*channel width	Qb/flow area	
0	=($B$30)-(TAN(RADIANS($B$31))*C14)	0	0	0	=+$B$15-G14	=D14*$B$33	=H14/I14	
=+B29/12	=($B$30)-(TAN(RADIANS($B$31))*C15)	=TAN(RADIANS($B$31))*C15*C15/2	=$B$30*C15-E15	=+$B$16*F15	=+$B$15-G15	=D15*$B$33	=H15/I15	=IF((M15>J15),IF(
=+$C$15*2	=($B$30)-(TAN(RADIANS($B$31))*C16)	=TAN(RADIANS($B$31))*C16*C16/2	=$B$30*C16-E16	=+$B$16*F16	=+$B$15-G16	=D16*$B$33	=H16/I16	=IF((M16>J16),IF(
=+$C$15*3	=($B$30)-(TAN(RADIANS($B$31))*C17)	=TAN(RADIANS($B$31))*C17*C17/2	=$B$30*C17-E17	=+$B$16*F17	=+$B$15-G17	=D17*$B$33	=H17/I17	=IF((M17>J17),IF(
=+$C$15*4	=($B$30)-(TAN(RADIANS($B$31))*C18)	=TAN(RADIANS($B$31))*C18*C18/2	=$B$30*C18-E18	=+$B$16*F18	=+$B$15-G18	=D18*$B$33	=H18/I18	=IF((M18>J18),IF(
=+$C$15*5	=($B$30)-(TAN(RADIANS($B$31))*C19)	=TAN(RADIANS($B$31))*C19*C19/2	=$B$30*C19-E19	=+$B$16*F19	=+$B$15-G19	=D19*$B$33	=H19/I19	=IF((M19>J19),IF(
=+$C$15*6	=($B$30)-(TAN(RADIANS($B$31))*C20)	=TAN(RADIANS($B$31))*C20*C20/2	=$B$30*C20-E20	=+$B$16*F20	=+$B$15-G20	=D20*$B$33	=H20/I20	=IF((M20>J20),IF(
=+$C$15*7	=($B$30)-(TAN(RADIANS($B$31))*C21)	=TAN(RADIANS($B$31))*C21*C21/2	=$B$30*C21-E21	=+$B$16*F21	=+$B$15-G21	=D21*$B$33	=H21/I21	=IF((M21>J21),IF(
=+$C$15*8	=($B$30)-(TAN(RADIANS($B$31))*C22)	=TAN(RADIANS($B$31))*C22*C22/2	=$B$30*C22-E22	=+$B$16*F22	=+$B$15-G22	=D22*$B$33	=H22/I22	=IF((M22>J22),IF(
=+$C$15*9	=($B$30)-(TAN(RADIANS($B$31))*C23)	=TAN(RADIANS($B$31))*C23*C23/2	=$B$30*C23-E23	=+$B$16*F23	=+$B$15-G23	=D23*$B$33	=H23/I23	=IF((M23>J23),IF(
=+$C$15*10	=($B$30)-(TAN(RADIANS($B$31))*C24)	=TAN(RADIANS($B$31))*C24*C24/2	=$B$30*C24-E24	=+$B$16*F24	=+$B$15-G24	=D24*$B$33	=H24/I24	=IF((M24>J24),IF(
=+$C$15*11	=($B$30)-(TAN(RADIANS($B$31))*C25)	=TAN(RADIANS($B$31))*C25*C25/2	=$B$30*C25-E25	=+$B$16*F25	=+$B$15-G25	=D25*$B$33	=H25/I25	=IF((M25>J25),IF(
=+$C$15*12	=($B$30)-(TAN(RADIANS($B$31))*C26)	=TAN(RADIANS($B$31))*C26*C26/2	=$B$30*C26-E26	=+$B$16*F26	=+$B$15-G26	=D26*$B$33	=H26/I26	=IF((M26>J26),IF(
								=IF(AVERAGE(K1

Screen Approach Velocity, ft/s

0.15	=D31+0.025	=E31+0.025	=F31+0.025	=G31+0.025	=H31+0.025	=I31+0.025
Vs<Vmin	Vs<Vmin	Vs<Vmin	Vs<Vmin	>deltaVs	>deltaVs	>deltaVs
Vs<Vmin	Vs<Vmin	Vs<Vmin	Vs<Vmin	>deltaVs	>deltaVs	>deltaVs
Vs<Vmin	Vs<Vmin	Vs<Vmin	Vs<Vmin	>deltaVs	>deltaVs	>deltaVs
Vs<Vmin	Vs<Vmin	Vs<Vmin	Vs<Vmin	Vs<Vmin	>deltaVs	>deltaVs
0.494676581449592	Vs<Vmin	Vs<Vmin	Vs<Vmin	Vs<Vmin	>deltaVs	>deltaVs
0.412230484541326	0.61834572681199	Vs<Vmin	Vs<Vmin	Vs<Vmin	>deltaVs	>deltaVs
>deltaVs	0.530010622981706	0.70668083064227	Vs<Vmin	Vs<Vmin	>deltaVs	>deltaVs
>deltaVs	0.463759295108992	0.618345726811995	0.772932158514	Vs<Vmin	>deltaVs	>deltaVs
>deltaVs	>deltaVs	0.549640646055105	0.687050807568	0.82446096908	>deltaVs	>deltaVs
>deltaVs	>deltaVs	0.494676581449595	0.618345726811	0.74201487217	Vs<Vmin	>deltaVs
>deltaVs	>deltaVs	>deltaVs	0.562132478919	0.67455897470	0.786985470487	>deltaVs
TRANS	TRANS	>deltaVs	0.515288105676	0.61834572681	0.721403347947	0.824460969083
TRANS	TRANS	TRANS	TRANS	0.57078067090	0.665910782720	0.761040894531
TRANS	TRANS	TRANS	TRANS	0.530010622981	0.618345726811	0.706680830642
Vs>Vc	Vs>Vc	Vs>Vc	TRANS	TRANS	0.577122678357	0.659568775266
Vs>Vc	Vs>Vc	Vs>Vc	Vs>Vc	Vs>Vc	TRANS	TRANS
Vs>Vc	Vs>Vc	Vs>Vc	Vs>Vc	Vs>Vc	Vs>Vc	Vs>Vc
Vs>Vc	Vs>Vc	Vs>Vc	Vs>Vc	Vs>Vc	Vs>Vc	Vs>Vc

APPENDIX B

This appendix provides the actual three-dimensional velocity data as recorded by the SonTek ADV and analyzed with WinAdv. The "X" parameter is the distance down the screen in feet with 0 ft the beginning and 12 ft the end of the screen. The "Y" parameter is the distance across the screen in feet. Data were recorded for tests 16-21 only at one point 6 inches from the right or straight wall for each "X" distance when the "Y" distance is not shown.

Rectangular Screen Data

Test 1

X	Y	Vs	Vy	Va
-0.4271	1	3.196	-0.175	-0.017
-0.4271	3	3.498	-0.211	-0.014
-0.4271	5	3.295	-0.015	-0.057
0.0729	1	3.020	-0.196	-0.109
0.0729	3	3.169	-0.140	-0.152
0.0729	5	3.150	-0.010	-0.127
0.5729	1	2.903	-0.146	-0.082
0.5729	3	3.200	-0.064	-0.157
0.5729	5	3.204	0.018	-0.124
3.5729	1	2.435	-0.096	-0.091
3.5729	3	2.700	0.075	-0.059
3.5729	5	2.571	0.006	-0.085
6.5729	1	1.928	0.085	-0.170
6.5729	3	2.060	0.032	-0.084
6.5729	5	2.014	-0.075	-0.086
9.5729	1	-0.507	0.048	-0.224
9.5729	3	2.197	0.597	-0.327
9.5729	5	2.032	0.000	-0.159
11.0729	1	-1.309	-0.155	-0.055
11.0729	3	2.205	0.574	-0.214
11.0729	5	1.640	0.282	-0.428

Test 2

X	Y	Vs	Vy	Va
-0.4271	1	3.785	-0.392	-0.024
-0.4271	3	3.818	-0.568	-0.019
-0.4271	5	3.719	-0.331	-0.023
0.0729	1	3.555	-0.264	-0.101
0.0729	3	3.737	-0.369	-0.126
0.0729	5	3.595	-0.144	-0.070
0.5729	1	3.536	-0.259	-0.110
0.5729	3	3.588	-0.227	-0.061

X	Y	Vs	Vy	Va
0.5729	5	3.485	-0.157	-0.056
3.5729	1	2.896	-0.217	-0.092
3.5729	3	2.925	-0.226	-0.056
3.5729	5	2.863	-0.255	-0.069
6.5729	1	2.394	-0.223	-0.061
6.5729	3	2.427	-0.145	-0.060
6.5729	5	2.441	-0.203	-0.093
9.5729	1	2.206	0.647	-0.498
9.5729	3	2.245	-0.033	-0.168
9.5729	5	2.365	-0.147	-0.091
11.0729	1	-0.425	-0.148	-0.329
11.0729	3	2.278	0.560	-0.370
11.0729	5	1.594	0.033	-0.497

Test 3

X	Y	Vs	Vy	Va
-0.4271	0.2	5.157	0.085	-0.131
-0.4271	1	4.985	-0.074	-0.091
-0.4271	3	4.891	0.074	-0.124
-0.4271	5	4.134	0.007	-0.111
-0.4271	5.8	4.169	-0.050	-0.098
0.0729	0.2	5.078	0.236	-0.204
0.0729	1	4.907	-0.186	-0.187
0.0729	3	5.016	0.078	-0.312
0.0729	5	4.415	0.241	-0.260
0.0729	5.8	4.420	-0.021	-0.227
0.5729	0.2	5.110	0.122	-0.173
0.5729	1	4.920	-0.079	-0.152
0.5729	3	5.046	0.103	-0.203
0.5729	5	4.607	0.010	-0.189
0.5729	5.8	4.553	-0.004	-0.112
3.5729	0.2	4.504	0.135	-0.312
3.5729	1	4.092	0.081	-0.175
3.5729	3	4.295	0.256	-0.245
3.5729	5	4.052	0.117	-0.229
3.5729	5.8	4.116	-0.028	-0.274
6.5729	0.2	4.111	0.076	-0.181
6.5729	1	3.523	0.110	-0.176
6.5729	3	3.698	0.233	-0.193
6.5729	5	3.680	0.286	-0.184
6.5729	5.8	3.964	0.149	-0.274
9.5729	0.2	3.908	0.102	-0.239
9.5729	1	2.999	0.071	-0.099
9.5729	3	3.007	0.345	-0.131
9.5729	5	3.256	0.053	-0.290
9.5729	5.8	3.298	-0.267	-0.481
11.0729	0.2	1.950	0.430	-0.603

X	Y	Vs	Vy	Va
11.0729	1	1.789	0.340	-0.468
11.0729	3	1.978	0.045	-0.466
11.0729	5	2.238	-0.288	-0.477
11.0729	5.8	-1.541	-0.104	-0.425

Test 4

X	Y	Vs	Vy	Va
-0.4271	1	1.948	-0.082	0.091
-0.4271	3	2.173	-0.054	0.120
-0.4271	5	2.156	0.048	0.063
0.0729	1	1.802	-0.262	-0.058
0.0729	3	1.944	-0.302	-0.046
0.0729	5	1.995	-0.348	-0.033
0.5729	1	1.440	-0.186	-0.046
0.5729	3	1.543	-0.147	-0.027
0.5729	5	1.508	0.024	-0.035
3.5729	1	1.310	-0.036	-0.039
3.5729	3	1.352	0.061	-0.045
3.5729	5	1.262	0.017	-0.021
6.5729	1	1.238	-0.067	-0.041
6.5729	3	1.317	-0.020	-0.058
6.5729	5	1.239	-0.004	-0.031
9.5729	1	1.208	-0.008	-0.088
9.5729	3	1.146	0.023	-0.041
9.5729	5	1.201	0.051	-0.047
11.0729	1	1.055	0.010	-0.256
11.0729	3	0.933	0.032	-0.254
11.0729	5	0.945	-0.024	-0.264

Test 5

X	Y	Vs	Vy	Va
-0.4271	1	3.059	-0.241	-0.030
-0.4271	3	3.212	-0.278	-0.015
-0.4271	5	3.013	-0.208	-0.036
0.0729	1	2.944	-0.251	-0.113
0.0729	3	3.048	-0.232	-0.158
0.0729	5	2.992	-0.142	-0.069
0.5729	1	2.874	-0.173	-0.068
0.5729	3	3.095	-0.200	-0.076
0.5729	5	2.852	-0.112	-0.062
3.5729	1	2.265	-0.098	-0.048
3.5729	3	2.430	-0.140	-0.039
3.5729	5	2.259	-0.090	-0.068
6.5729	1	1.849	-0.094	-0.050
6.5729	3	2.055	-0.020	-0.033
6.5729	5	1.780	-0.086	-0.058

X	Y	Vs	Vy	Va
9.5729	1	1.719	-0.119	-0.031
9.5729	3	1.913	-0.028	-0.071
9.5729	5	1.858	-0.021	-0.060
11.0729	1	1.364	0.012	-0.210
11.0729	3	1.494	-0.022	-0.221
11.0729	5	1.408	-0.015	-0.308

Test 6

X	Y	Vs	Vy	Va
-0.4271	1	2.898	-0.180	-0.062
-0.4271	3	2.928	-0.199	-0.057
-0.4271	5	2.820	-0.227	-0.035
0.0729	1	2.816	-0.174	-0.060
0.0729	3	2.918	-0.213	-0.059
0.0729	5	2.733	-0.089	-0.057
0.5729	1	2.758	-0.125	-0.079
0.5729	3	2.798	-0.169	-0.040
0.5729	5	2.725	-0.064	-0.060
3.5729	1	2.193	-0.137	-0.070
3.5729	3	2.291	-0.185	-0.077
3.5729	5	2.235	-0.061	-0.057
6.5729	1	1.901	-0.071	-0.054
6.5729	3	1.925	-0.175	-0.064
6.5729	5	1.887	-0.057	-0.080
9.5729	1	1.643	-0.141	-0.032
9.5729	3	1.788	-0.155	-0.066
9.5729	5	1.417	-0.140	0.067
11.0729	1	1.805	-0.132	0.268
11.0729	3	1.793	-0.109	0.242
11.0729	5	1.874	-0.224	0.290

Test 7

X	Y	Vs	Vy	Va
-0.4271	0.2	5.157	0.085	-0.131
-0.4271	1	4.985	-0.074	-0.091
-0.4271	3	4.891	0.074	-0.124
-0.4271	5	4.134	0.007	-0.111
-0.4271	5.8	4.169	-0.050	-0.098
0.0729	0.2	5.078	0.236	-0.204
0.0729	1	4.907	-0.186	-0.187
0.0729	3	5.016	0.078	-0.312
0.0729	5	4.415	0.241	-0.260
0.0729	5.8	4.420	-0.021	-0.227
0.5729	0.2	5.110	0.122	-0.173
0.5729	1	4.920	-0.079	-0.152
0.5729	3	5.046	0.103	-0.203

X	Y	Vs	Vy	Va
0.5729	5	4.607	0.010	-0.189
0.5729	5.8	4.553	-0.004	-0.112
3.5729	0.2	4.504	0.135	-0.312
3.5729	1	4.092	0.081	-0.175
3.5729	3	4.295	0.256	-0.245
3.5729	5	4.052	0.117	-0.229
3.5729	5.8	4.116	-0.028	-0.274
6.5729	0.2	4.111	0.076	-0.181
6.5729	1	3.523	0.110	-0.176
6.5729	3	3.698	0.233	-0.193
6.5729	5	3.680	0.286	-0.184
6.5729	5.8	3.964	0.149	-0.274
9.5729	0.2	3.908	0.102	-0.239
9.5729	1	2.999	0.071	-0.099
9.5729	3	3.007	0.345	-0.131
9.5729	5	3.256	0.053	-0.290
9.5729	5.8	3.298	-0.267	-0.481
11.0729	0.2	1.950	0.430	-0.603
11.0729	1	1.789	0.340	-0.468
11.0729	3	1.978	0.045	-0.466
11.0729	5	2.238	-0.288	-0.477
11.0729	5.8	-1.541	-0.104	-0.425

Test 8

X	Y	Vs	Vy	Va
-4.4271	0.2	3.265	0.198	0.131
-4.4271	1.0	3.453	0.091	0.204
-4.4271	3.0	3.860	0.099	0.243
-4.4271	5.0	3.720	0.329	0.199
-4.4271	5.8	3.712	0.136	0.211
-2.4271	0.2	4.422	0.239	-0.186
-2.4271	1.0	4.591	0.126	-0.126
-2.4271	3.0	4.849	0.148	-0.100
-2.4271	5.0	4.759	0.264	-0.146
-2.4271	5.8	4.628	0.169	-0.113
-0.4271	0.2	4.871	0.176	-0.142
-0.4271	1.0	4.946	0.163	-0.110
-0.4271	3.0	5.126	0.031	-0.048
-0.4271	5.0	5.064	0.260	-0.132
-0.4271	5.8	5.029	-0.051	-0.092
0.0729	0.2	4.908	0.245	-0.271
0.0729	1.0	4.960	0.169	-0.234
0.0729	3.0	5.162	0.130	-0.226
0.0729	5.0	5.211	0.321	-0.280
0.0729	5.8	5.102	0.071	-0.224
0.5729	0.2	4.986	0.185	-0.183
0.5729	1.0	4.936	0.122	-0.156

X	Y	Vs	Vy	Va
0.5729	3.0	5.117	0.129	-0.163
0.5729	5.0	5.208	0.284	-0.226
0.5729	5.8	5.188	0.018	-0.182
3.5729	0.2	4.539	0.132	-0.302
3.5729	1.0	4.006	0.180	-0.185
3.5729	3.0	4.439	0.134	-0.074
3.5729	5.0	4.512	0.312	-0.156
3.5729	5.8	4.944	0.145	-0.240
6.5729	0.2	4.016	0.243	-0.181
6.5729	1.0	3.753	0.174	-0.151
6.5729	3.0	3.754	0.183	-0.072
6.5729	5.0	4.365	0.152	-0.129
6.5729	5.8	4.785	0.213	-0.187
9.5729	0.2	-0.696	0.136	-0.596
9.5729	1.0	2.907	0.973	-0.746
9.5729	3.0	3.325	0.605	-0.329
9.5729	5.0	4.044	0.215	-0.317
9.5729	5.8	4.510	0.068	-0.435
11.0729	0.2	-1.618	-0.119	-0.292
11.0729	1.0	-0.573	-0.368	-0.344
11.0729	3.0	2.989	1.170	-0.507
11.0729	5.0	2.748	0.328	-0.771
11.0729	5.8	0.614	-0.067	-0.936
12.5729	0.2	-1.902	-0.244	0.112
12.5729	1.0	-0.665	-0.586	0.087
12.5729	3.0	3.273	0.790	-0.071
12.5729	5.0	2.886	0.447	-0.062
12.5729	5.8	1.560	0.340	-0.070

Converging Side wall with 2.54-ft-wide Bypass Opening

Test 9

X	Y	Vs	Vy	Va
-4.427	0.2	2.272	-0.054	0.147
-4.427	1	2.276	-0.230	0.165
-4.427	3	2.275	-0.147	0.241
-4.427	5	2.409	-0.026	0.190
-4.427	5.8	2.264	-0.003	0.156
-2.427	0.2	2.308	-0.086	-0.098
-2.427	1	2.408	0.020	-0.040
-2.427	3	2.595	-0.211	0.020
-2.427	5	2.733	-0.062	0.016
-2.427	5.8	2.592	-0.093	0.061
-0.427	0.2	2.913	-0.050	-0.028
-0.427	1	3.037	-0.231	-0.027

X	Y	Vs	Vy	Va
-0.427	3	3.026	-0.324	-0.023
-0.427	5	2.747	-0.537	0.004
-0.427	5.7	2.065	-0.568	-0.029
0.073	0.2	3.120	-0.068	0.506
0.073	1	2.722	-0.148	-0.050
0.073	2.9	3.121	-0.335	-0.056
0.073	4.8	2.922	-0.373	-0.125
0.073	5.5	2.655	-0.704	-0.132
0.573	0.2	2.600	0.144	0.107
0.573	1	2.253	-0.068	0.275
0.573	2.5	3.234	-0.277	0.652
0.573	3.8	3.364	-0.354	0.683
0.573	5.2	3.192	-0.647	0.421
3.573	0.2	2.725	0.000	-0.149
3.573	1	2.670	-0.192	-0.142
3.573	3	2.819	-0.279	-0.180
3.573	3.8	2.865	-0.428	-0.195
3.573	4.55	2.878	-0.677	-0.188
6.573	0.2	2.509	-0.005	-0.170
6.573	1	2.381	-0.126	-0.131
6.573	2.4	2.623	-0.304	-0.152
6.573	3	2.981	-0.530	-0.176
6.573	3.8	2.838	-0.761	-0.149
9.573	0.2	2.509	0.022	-0.224
9.573	1	2.137	-0.110	-0.166
9.573	2.3	2.896	-0.486	-0.165
9.573	2.9	2.975	-0.664	-0.221
11.073	0.2	0.681	-0.031	-0.330
11.073	1	1.735	0.022	-0.340
12.573	2.3	1.981	-0.175	-0.033

Test 10

X	Y	Vs	Vy	Va
-4	0.2	2.847	0.013	0.107
-4	1	2.856	0.116	0.136
-4	3	2.626	0.009	0.129
-4	5	2.462	-0.034	0.066
-4	5.8	2.460	0.048	0.100
-2	0.2	2.920	0.029	-0.042
-2	1	2.923	0.031	-0.040
-2	3	2.718	-0.131	-0.001
-2	5	2.458	-0.062	-0.016
-2	5.8	2.352	0.029	0.012
-1	0.2	2.974	0.037	-0.038
-1	1	2.944	0.034	-0.031
-1	3	2.781	-0.174	-0.037
-1	5	2.512	-0.277	-0.041

X	Y	Vs	Vy	Va
-1	5.8	2.134	-0.256	-0.029
0	0.2	3.038	0.021	-0.037
0	1	3.056	0.027	-0.011
0	3	2.876	-0.257	-0.025
0	5	2.493	-0.431	-0.105
0	5.6	2.696	-0.539	-0.182
1	0.2	2.942	0.015	-0.079
1	1	2.845	0.045	-0.058
1	3	2.816	-0.235	-0.041
1	5	2.837	-0.482	-0.143
1	5.3	2.802	-0.556	-0.161
2	0.2	2.963	0.032	-0.103
2	1	2.759	0.012	-0.069
2	3	2.597	-0.229	-0.096
2	5	2.777	-0.569	-0.159
3	0.2	2.832	0.006	-0.139
3	1	2.552	-0.006	-0.110
3	3	2.237	-0.196	-0.089
3	4.7	2.745	-0.566	-0.167
4	0.2	2.744	0.030	-0.111
4	1	2.364	0.021	-0.057
4	3	2.435	-0.227	-0.067
4	4.5	2.804	-0.606	-0.099
5	0.2	2.611	0.035	-0.107
5	1	2.406	-0.005	-0.089
5	3	2.548	-0.274	-0.121
5	4.2	2.844	-0.594	-0.157
6	0.2	2.462	-0.043	-0.130
6	1	2.125	-0.002	-0.064
6	3	2.689	-0.415	-0.137
6	4	2.698	-0.540	-0.100
7	0.2	2.306	0.074	-0.148
7	1	1.894	0.022	-0.066
7	3	2.745	-0.471	-0.136
7	3.7	2.787	-0.593	-0.200
8	0.2	2.398	-0.040	-0.152
8	1	1.801	-0.024	-0.018
8	3	2.537	-0.507	-0.090
8	3.4	2.572	-0.553	-0.110
9	0.2	2.541	-0.003	-0.144
9	1	1.981	-0.059	-0.055
9	3	2.875	-0.639	-0.186
10	0.2	2.386	0.080	-0.127
10	1	1.983	-0.137	-0.053
10	2.9	2.816	-0.644	-0.212
11	0.2	2.295	0.042	-0.134
11	1	1.894	-0.206	-0.069
11	2.6	2.785	-0.554	-0.161

X	Y	Vs	Vy	Va
12	0.2	2.460	-0.040	-0.062
12	1	2.239	-0.198	-0.020
12	2.2	3.126	-0.601	-0.118
13	0.2	3.223	-0.001	-0.057
13	1	3.169	-0.057	0.003

Test 11

X	Y	Vs	Vy	Va
-4.00	0.2	3.133	0.048	-0.018
-4.00	1	3.076	0.021	-0.015
-4.00	3	2.864	-0.228	-0.031
-4.00	5	2.608	-0.250	-0.048
-4.00	5.8	2.188	-0.305	-0.030
-2.00	0.2	2.969	0.043	-0.057
-2.00	1	2.978	0.048	-0.059
-2.00	3	2.808	-0.117	-0.022
-2.00	5	2.565	-0.126	-0.026
-2.00	5.8	2.443	0.037	0.024
-1.00	0.2	2.856	0.015	0.095
-1.00	1	2.935	0.135	0.134
-1.00	3	2.664	0.009	0.123
-1.00	5	2.533	-0.008	0.052
-1.00	5.8	2.540	0.090	0.114
1.00	0.2	3.136	0.042	0.015
1.00	1	2.936	0.055	0.007
1.00	3	2.938	-0.244	-0.034
1.00	5	3.010	-0.505	-0.128
1.00	5.3	2.929	-0.578	-0.154
3.00	0.2	2.908	-0.037	-0.072
3.00	1	2.809	0.023	-0.064
3.00	3	2.631	-0.208	-0.048
3.00	4.7	2.872	-0.408	-0.151
5.00	0.2	2.685	0.175	-0.102
5.00	1	2.115	0.015	-0.051
5.00	3	2.830	-0.324	-0.123
5.00	4.2	2.733	-0.758	-0.150
7.00	0.2	2.386	0.194	-0.150
7.00	1	2.014	0.007	-0.063
7.00	3	2.672	-0.288	-0.148
7.00	3.7	3.035	-0.597	-0.209
9.00	0.2	2.676	0.146	-0.138
9.00	1	2.055	-0.003	-0.087
9.00	3	3.016	-0.617	-0.189
11.00	0.2	1.963	0.413	-0.202
11.00	1	1.809	-0.077	-0.186
11.00	2.6	2.771	-0.603	-0.210
12.00	0.2	1.086	-0.064	-0.120

X	Y	Vs	Vy	Va
12.00	1	1.078	-0.046	-0.117
12.00	2.2	2.325	-0.267	-0.087
13.00	0.2	1.406	-0.132	0.041
13.00	1	1.473	-0.051	0.006
13.00	2.2	2.365	-0.046	0.003
6.00	3	2.689	-0.415	-0.137
6.00	4	2.698	-0.540	-0.100
7.00	0.2	2.306	0.074	-0.148
7.00	1	1.894	0.022	-0.066
7.00	3	2.745	-0.471	-0.136
7.00	3.7	2.787	-0.593	-0.200
8.00	0.2	2.398	-0.040	-0.152
8.00	1	1.801	-0.024	-0.018
8.00	3	2.537	-0.507	-0.090
8.00	3.4	2.572	-0.553	-0.110
9.00	0.2	2.541	-0.003	-0.144
9.00	1	1.981	-0.059	-0.055
9.00	3	2.875	-0.639	-0.186
10.00	0.2	2.386	0.080	-0.127
10.00	1	1.983	-0.137	-0.053
10.00	2.9	2.816	-0.644	-0.212
11.00	0.2	2.295	0.042	-0.134
11.00	1	1.894	-0.206	-0.069
11.00	2.6	2.785	-0.554	-0.161
12.00	0.2	2.460	-0.040	-0.062
12.00	1	2.239	-0.198	-0.020
12.00	2.2	3.126	-0.601	-0.118
13.00	0.2	3.223	-0.001	-0.057
13.00	1	3.169	-0.057	0.003

Test 12

X	Y	Vs	Vy	Va
-4.0	0.2	2.957	-0.332	0.174
-4.0	1.0	2.958	-0.224	0.246
-4.0	3.0	2.637	-0.444	0.192
-4.0	5.0	2.487	-0.377	0.127
-4.0	5.8	2.495	-0.240	0.157
-2.0	0.2	2.949	-0.339	-0.014
-2.0	1.0	2.885	-0.292	0.030
-2.0	3.0	2.636	-0.512	0.019
-2.0	5.0	2.425	-0.418	0.010
-2.0	5.8	2.336	-0.314	0.031
-1.0	0.2	3.011	-0.380	-0.034
-1.0	1.0	2.947	-0.147	-0.011
-1.0	3.0	2.737	-0.437	-0.033
-1.0	5.0	2.479	-0.444	-0.043
-1.0	5.8	2.097	-0.422	-0.021

X	Y	Vs	Vy	Va
1.0	0.2	2.736	-0.135	-0.111
1.0	1.0	2.748	-0.107	-0.064
1.0	3.0	2.547	-0.372	-0.117
1.0	5.0	2.759	-0.585	-0.226
1.0	5.3	2.699	-0.694	-0.253
3.0	0.2	2.530	0.064	-0.079
3.0	1.0	2.640	0.014	-0.090
3.0	3.0	2.547	-0.323	-0.097
3.0	4.7	2.630	-0.519	-0.234
5.0	0.2	2.764	-0.001	-0.117
5.0	1.0	2.420	-0.048	-0.066
5.0	3.0	2.739	-0.432	-0.145
5.0	4.2	2.600	-0.424	-0.158
7.0	0.2	2.463	0.073	-0.157
7.0	1.0	1.994	-0.039	-0.044
7.0	3.0	2.728	-0.347	-0.155
7.0	3.7	2.676	-0.530	-0.254
9.0	0.2	1.972	0.253	-0.306
9.0	1.0	1.979	0.009	-0.220
9.0	3.0	2.696	-0.536	-0.280
11.0	0.2	0.216	0.139	-0.345
11.0	1.0	1.654	0.088	-0.392
11.0	2.6	2.017	-0.183	-0.435
12.0	0.2	-0.215	-0.337	-0.034
12.0	1.0	1.290	-0.076	-0.106
12.0	2.2	1.569	-0.136	-0.128
13.0	0.2	0.115	-0.104	0.020
13.0	1.0	1.391	-0.310	0.016
13.0	2.2	1.548	-0.063	0.007

Test 13

X	Y	Vs	Vy	Va
-4.00	0.2	3.598	-0.366	0.198
-4.00	1	3.683	-0.406	0.280
-4.00	3	3.798	-0.456	0.297
-4.00	5	3.588	-0.364	0.151
-4.00	5.8	3.562	-0.243	0.259
-2.00	0.2	3.825	-0.361	-0.021
-2.00	1	3.938	-0.393	0.039
-2.00	3	3.898	-0.630	0.091
-2.00	5	3.413	-0.545	-0.020
-2.00	5.8	3.298	-0.299	0.088
-1.00	0.2	3.912	-0.434	-0.069
-1.00	1	3.973	-0.498	-0.032
-1.00	3	3.869	-0.778	-0.006
-1.00	5	3.533	-0.782	-0.071
-1.00	5.8	2.884	-0.709	0.000

X	Y	Vs	Vy	Va
1.00	0.2	4.427	0.133	-0.113
1.00	1	4.558	-0.104	-0.157
1.00	3	4.541	-0.438	-0.120
1.00	5	4.661	-0.580	-0.369
1.00	5.3	4.410	-0.879	-0.363
3.00	0.2	4.398	0.173	-0.187
3.00	1	4.618	-0.069	-0.195
3.00	3	4.275	-0.334	-0.156
3.00	4.7	4.224	-0.592	-0.365
5.00	0.2	4.360	0.025	-0.113
5.00	1	4.685	-0.022	-0.113
5.00	3	4.659	-0.624	-0.226
5.00	4.2	4.083	-0.438	-0.227
7.00	0.2	4.138	-0.747	-0.268
7.00	1	4.144	-0.065	-0.212
7.00	3	4.451	-0.719	-0.297
7.00	3.7	4.375	-0.808	-0.384
9.00	0.2	4.399	-0.700	-0.212
9.00	1	4.101	-0.903	-0.262
9.00	3	4.249	-1.349	-0.396
11.00	0.2	3.347	0.340	-0.428
11.00	1	3.724	-0.159	-0.435
11.00	2.6	4.129	-0.721	-0.391
12.00	0.2	2.028	-0.188	-0.220
12.00	1	2.607	0.114	-0.198
12.00	2.2	3.127	-0.108	-0.165
13.00	0.2	2.640	-0.122	0.051
13.00	1	3.154	-0.036	0.030
13.00	2.2	3.367	0.001	0.022

Test 14

X	Y	Vs	Vy	Va
-4.00	0.2	3.104	-0.010	0.154
-4.00	1	3.070	-0.025	0.177
-4.00	3	3.246	-0.031	0.187
-4.00	5	3.174	0.126	0.159
-4.00	5.8	3.046	0.096	0.178
-2.00	0.2	3.196	-0.001	-0.020
-2.00	1	3.262	-0.006	-0.020
-2.00	3	3.301	-0.152	0.023
-2.00	5	3.027	0.008	0.011
-2.00	5.8	2.835	0.038	0.030
-1.00	0.2	3.397	0.032	-0.033
-1.00	1	3.472	0.007	-0.036
-1.00	3	3.537	-0.244	-0.007
-1.00	5	3.042	-0.187	-0.013
-1.00	5.8	2.462	-0.281	0.003

X	Y	Vs	Vy	Va
1.00	0.2	2.909	0.181	-0.084
1.00	1	3.240	0.033	-0.122
1.00	3	3.366	-0.167	-0.056
1.00	5	3.485	-0.576	-0.205
1.00	5.3	3.368	-0.563	-0.221
3.00	0.2	3.155	0.067	-0.129
3.00	1	3.267	-0.002	-0.127
3.00	3	3.276	-0.318	-0.130
3.00	4.7	3.001	-0.470	-0.196
5.00	0.2	2.946	0.035	-0.113
5.00	1	2.996	-0.026	-0.139
5.00	3	3.467	-0.518	-0.179
5.00	4.2	3.310	-0.566	-0.176
7.00	0.2	2.828	-0.056	-0.173
7.00	1	2.488	-0.151	-0.103
7.00	3	3.253	-0.367	-0.172
7.00	3.7	3.067	-0.408	-0.243
9.00	0.2	1.832	0.254	-0.345
9.00	1	2.478	0.211	-0.421
9.00	3	2.967	-0.424	-0.348
11.00	0.2	-0.355	0.053	-0.197
11.00	1	2.317	0.175	-0.378
11.00	2.6	2.356	-0.365	-0.577
12.00	0.2	-0.018	-0.549	-0.057
12.00	1	1.957	-0.363	-0.005
12.00	2.2	1.846	-0.157	-0.148
13.00	0.2	-0.223	-0.042	0.074
13.00	1	1.782	-0.589	0.057
13.00	2.2	1.925	-0.152	0.000

Test 15

X	Y	Vs	Vy	Va
-2	1	3.560	-0.025	0.026
1	1	4.561	-0.003	-0.137
3	1	4.396	0.072	-0.123
5	1	4.335	-0.057	-0.121
7	1	4.001	-0.098	-0.196
9	1	3.671	-0.282	-0.196
11	1	3.884	-0.344	-0.226
12	1	3.692	-0.336	-0.020
13	1	3.558	-0.061	-0.036

Converging Wall with 1-ft-wide Bypass Entrance

Test 16

X	Vs	Vy	Va
-4	2.655	-0.024	0.113
-2	4.201	-0.082	0.012
-1	3.454	-0.065	-0.078
0	3.398	-0.022	-0.073
1	3.352	0.096	-0.010
3	3.269	-0.086	-0.135
5	3.374	0.040	-0.184
7	3.295	-0.504	-0.271
9	3.382	-0.342	-0.296
10	3.136	-0.523	-0.314
11	2.998	-0.504	-0.294

Test 17

X distance (ft)	Vs	Vy	Va
-2	3.2365	-0.0231	0.0103
0	3.6254	-0.0447	0.0335
2	3.0673	-0.0458	-0.0847
4	2.7194	-0.1154	-0.0465
6	2.7903	-0.1694	-0.1365
8	2.7733	-0.2012	-0.0978
10	2.901	-0.3217	-0.2906
11	2.9947	-0.4747	-0.2701

Test 18

X Distance (ft)	Vs	Vy	Va
-2	4.4118	-0.0619	-0.0165
0	4.3276	-0.0555	-0.0006
2	3.9688	-0.0022	-0.1117
4	3.3786	-0.0721	-0.0633
6	3.5456	-0.1454	-0.1506
8	3.4904	-0.2494	-0.1771
10	3.6902	-0.2639	-0.3269
11	3.5782	-0.3731	-0.3825

Test 19

X	Vs	Vy	Va
-2	3.354	-0.1286	-0.0204
0	3.144	-0.167	0.0001
1	2.9758	-0.1962	-0.1375
3	2.6868	-0.1663	-0.0984
5	2.9937	-0.2155	-0.2466
7	2.7179	-0.2205	-0.1472

X	Vs	Vy	Va
9	2.9123	-0.2442	-0.3532
11	3.0562	-0.3474	-0.2561
11.25	3.2229	-0.3886	-0.2118
11.5	3.4039	-0.3942	0.041

Test 20

X	Vs	Vy	Va
-2	2.193	-0.046	-0.044
0	2.110	-0.109	-0.031
2	1.914	-0.002	-0.079
4	1.699	-0.021	-0.056
6	1.737	-0.093	-0.112
8	1.807	-0.083	-0.080
10	1.841	-0.131	-0.136
11	2.078	-0.269	-0.142
11.5	2.340	-0.306	-0.012
11.75	2.845	-0.379	0.383

Test 21

X	Vs	Vy	Va
-2	1.453	0.009	-0.014
0	1.400	-0.074	-0.003
2	1.378	-0.058	-0.064
4	1.337	-0.082	-0.056
6	1.351	-0.044	-0.103
8	1.318	-0.155	-0.071
10	1.530	-0.150	-0.090
11	1.731	-0.209	0.125
11.5	1.769	-0.458	0.457
11.75	2.048	-0.475	0.601